A comparative study of physiological and modulators of Aquaporin ion channels in diverse phyla

A thesis submitted for the degree of

DOCTOR OF PHILOSOPHY

THE UNIVERSITY of ADELAIDE

by

Mohamad Kourghi, B.Sc. (Hons)

Discipline of Physiology

School of Medicine

The University of Adelaide

August 2017

Table of Contents

Declaration and Published Works

This work contains no material which has been accepted for the award of any other degree or diploma in any university or other tertiary institution to Mohamad Kourghi and, to the best of my knowledge and belief, contains no material previously published or written by another person, except where due reference has been made in the text. I give consent to this copy of my thesis when deposited in the University Library, being made available for loan and photocopying, subject to the provisions of the Copyright Act 1968. The author acknowledges that copyright of published works contained within this thesis (as listed below*) resides with the copyright holder(s) of those works. I also give permission for the digital version of my thesis to be made available on the web, via the University's digital research repository, the Library catalogue, the Australasian Digital Theses Program (ADTP) and also through web search engines, unless permission has been granted by the University to restrict access for a period of time.

.....

Mohamad Kourghi

.....

Date

*Work in this thesis has appeared in the following publications:

Kourghi M, Pei JV, De Ieso ML, Flynn G, and Yool AJ (2016) Bumetanide derivatives AqB007 and AqB011 selectively block the aquaporin-1 ion channel conductance and slow cancer cell migration. Mol Pharmacol 89:133–140.

Pei JV, Ameliorate JL, Kourghi M, De Ieso ML, and Yool AJ (2016) Drug discovery and therapeutic targets for pharmacological modulators of aquaporin channels, in Aquaporins in Health and Disease: New Molecular Targets For Drug Discovery (Soveral G, Casinin A, and Nielsen S, eds) pp 275–297, CRC Press, Oxfordshire, United Kingdom.

Byrt, C. S., M. Zhao, M. Kourghi, J. Bose, S. W. Henderson, J. Qiu, M. Gilliham, C. Schultz, M. Schwarz, S. A. Ramesh, A. Yool and S. Tyerman (2016). "Non-selective cation channel activity of aquaporin AtPIP2;1 regulated by Ca^{2+} and pH." Plant Cell Environ.

Acknowledgements

My first and endless gratitude is for Allah for gifting me with the priceless gift of faith. This faith has given me comfort and hope in difficult times. He has helped me to stand up whenever I have fallen in life. In times where I was surrounded in darkness and I felt there was no escape, He has lightened my way and has guided my steps through the darkness. Faith in God has ensured that all material I have included in this thesis is true and accurate to best of knowledge.

This research was supported by the Faculty of Medicine at the University of Adelaide. I would like to take this opportunity and thank the tireless commitment, patience and scientific rigorousness of my principal supervisor Professor Andrea Yool. Her support and commitment allowed me to cope and overcome the magnitude of my project, and see the light at the end of the tunnel. I will always feel privileged and honoured to have been supervised by Professor Andrea Yool. Furthermore I would like to thank my co-supervisors Dr, Ian Musgrave and Professor Stephen Tyerman for their ongoing support and interest which has helped me in continuing my journey. I would like to specially thank Professor Tyerman for his collaboration work on plant Aquaporins, which was very helpful in increasing my experience and expanding my knowledge in the field.

Thereafter I would like to thank my lab mate Jinxin (Victor) Pei for his support in helping me with learning micro-injection, swelling assay and data analysing techniques. His support is much appreciated.

I want to extent my gratitude to the security services and all the friendly stuff members for their tireless effort and commitment, for keeping the university

environment safe and friendly. They did not deprive me of their help whenever it was needed.

I would like to thank the Australian government for accepting me and my family as Kurdish refugees in Turkey in the year 2003. Upon our arrival to date this country has nurtured and nourished us. It has provided us with priceless gift of education. The gift of enjoying freedom to be ourselves, to know God, and the values of humanity. I will ensure the skills I have enquired is to serve the betterment of this country and this nation. My gratitude is endless.

I want to take this valuable opportunity to express my endless gratitude towards my Parents Mustafa Kourghi and Masumeh Karimi. My success has been possible due to the value they have given to education and attaining knowledge. I want to remind myself of the times we were refuges in Turkey. My dad would come from work sometimes 1am at night in winter. His hands and face frozen on the bike while riding back home from work. But despite all that difficulty he send us to school, never for one day did he let us miss school without a valid excuse. Despite life being difficult as refugees, it was made comfortable for us because of their sacrifices. My mother Masumeh has always been the corner stone of the house, the light and the comfort of the family. Of all the gifts that life offers, I think mother is the greatest of them all. My gratitude for both of my parents is beyond any words.

I want to thank my wife Van Truong for the support and comfort she has given me throughout my Journey. This saying is very true, behind every successful man, there is a woman. My success would not have been possible without her support.

I express my gratitude for my sister in law Shiva Zardehnalous, for during the times my mother has not been here, she has lightened our house, and has filled her absence. She has made our dinner tables colourful with the delicious dishes she puts on the table. Her sacrifices and efforts are greatly appreciated.

Expressing my gratitude towards those special people who have helped me in my program would not be complete without thanking my brother Hasan Kourghi. We grew up together not just as two brothers, but as two close friends throughout the journey we have been together. He has helped me physically and spiritually during my journey. I consider myself fortunate for having him as my brother.

From among my friends I want to thank Beverly and Jason dearly for their help and support during difficult times when it was most needed. Their help and support are greatly appreciated.

Chapter 1. Statement of Authorship

Statement of Authorship

Title of Paper	Chapter 1-Literature Review: Fundamental structural and functional properties of Aquaporin ion channels found across the kingdoms of life
Publication Status	☐ Published ☐ Accepted for Publication ☐ Submitted for Publication ☑ Unpublished and Unsubmitted w ork w ritten in manuscript style
Publication Details	

Principal Author

Name of Principal Author (Candidate)	Mohamad Kourghi
Contribution to the Paper	Served as the corresponding author. Put the manuscript together, review and edited the article. Generated the figures and wrote Abstract, introduction, AtPIP2;1 and summary.
Overall percentage (%)	55%
Certification:	This paper reports on original research I conducted during the period of my Higher Degree by Research candidature and is not subject to any obligations or contractual agreements with a third party that would constrain its inclusion in this thesis. I am the primary author of this paper.
Signature	Date 6/09/2017

Co-Author Contributions

By signing the Statement of Authorship, each author certifies that:

i. the candidate's stated contribution to the publication is accurate (as detailed above);
ii. permission is granted for the candidate in include the publication in the thesis; and
iii. the sum of all co-author contributions is equal to 100% less the candidate's stated contribution.

Name of Co-Author	Jinxin Pei
Contribution to the Paper	Contributed with writing the "Drosophila Bib Brain" part of the manuscript.
Signature	Date 6/9/17

Name of Co-Author	Michael De Ieso
Contribution to the Paper	Contributed with writing the "AQP0" and "AQP6" part of the manuscript
Signature	Date 6/9/17

Name of Co-Author	Pak Hin Chow
Contribution to the Paper	Contributed with writing "the role of AQP1 ion channel in cerebrospinal fluid (CSF) production" part of the manuscript.
Signature	Date 5/9/2017

Name of Co-Author	Saeed Nourmohammadi
Contribution to the Paper	Contributed with writing "the role of AQP1 in cancer cell migration"
Signature	Date 6/9/2017

Name of Co-Author	Andrea J. Yool
Contribution to the Paper	Contributed with reviewing and editing the manuscript.
Signature	Date 5/9/2017

Chapter 1-Literature Review: Fundamental structural and functional properties of Aquaporin ion channels found across the kingdoms of life.

Mohamad Kourghi*, Jinxin V Pei, Michael L De Ieso, Saeed Nourmohammadi, Pak Hin Chow, and Andrea J Yool

*corresponding author

Abstract

Aquaporin (AQPs) are membrane-spanning proteins belonging to the large family of Major Intrinsic Proteins (MIP) found across all forms of life from prokaryotes to eukaryotes. AQP channels form as tetramers. Some classes allow the transport not only of water but other small molecules such as urea, ammonia, boric acid, glycerol, CO_2, nitric oxide and ions. AQPs are responsible for diverse functions such as maintaining osmotic water homeostasis, enabling flow across barrier tissues, supporting metabolic demands, as well as cell and matrix adhesions, cellular structure, and volume regulation for enhanced cellular migration. Ion channel function has been demonstrated for mammalian AQPs 0, 1, 6, Drosophila big brain (BIB), soybean nodulin 26 and Arabidopsis thaliana AtPIP2;1. The dual function of AQPs as water and ion channels is being investigated for physiological relevance using pharmacological agents that differentially modulate AQP channel functions. Wound closure experiments revealed that AqB011 (a specific blocker of the central ion channel in mammalian AQP1 but not the parallel intrasubunit water pores) was able to impair migration of the HT29 colon cancer cells, indicating that the central ion

pore of AQP1 possesses a physiological role in promoting cancer cell migration. Lens MIP (AQP0) is an anion selective channel which has an important role in maintaining the normal structure, integrity and transparency of the eye lens; but its role as an ion channel remains to be defined. Drosophila big brain (BIB) channel is a monovalent cation channel which acts in parallel with Notch and Delta signalling to determine the development fate of fly neuroblast cells via processes of lateral inhibition. More recently plant AQP AtPIP2;1, highly expressed in plasma membrane of root epidermal cells has been shown to allow ionic permeation, which is inhibited by calcium and protons and could be an important mechanism in responding to environmental stress. Understanding dual water and ion channel role of AQPs could open new windows in developing pharmacological agents in conditions such as cerebral ischemia, congestive heart failure, hypertension, angiogenesis, metastasis, sickle cell anaemia, reducing cerebrospinal fluid production following traumatic injury, and more.

Introduction

Maintaining water homeostasis is vital to every living organism. Aquaporins (AQPs) from the Major Intrinsic Protein (MIP) family form membrane-spanning tetrameric pores which allow the transport of water molecules down osmotic or hydrostatic pressure gradients. To date 15 different aquaporin genes have been identified in mammals (AQP0- AQP14) (Ishibashi 2009, Finn, Chauvigne et al. 2014). AQPs 3, 7, 9 and 10 are classified as aquaglyceroporins because of their ability to allow permeation of small uncharged molecules such as glycerol in addition to water.

Numerous MIP channels are expressed in plants. More than 100 different plant-AQP loci have been identified and characterised from genomic sequencing analysis (Zhang, Ali et al. 2013, Shivaraj, Deshmukh et al. 2017)

AQPs organize as conserved tetrameric pores in cell membranes that are found across all forms of life from prokaryotes and eukaryotes (Agre 2004, Benga 2009, Gomes, Agasse et al. 2009). AQPs consist of six membrane spanning helices and five loops (loops A to E). N- and C-terminals reside on the cytosolic side (Jung, Preston et al. 1994). Loops A and C are extracellular and loop D is intracellular. Loops B and E from the inner and the extracellular sides respectively fold back into the membrane to form two short half-helices penetrating the membrane as an hourglass shape with a highly conserved asparagine-proline-alanine (NPA) signature motif (Jung, Preston et al. 1994).

As shown in figure 2, mammalian aquaporins -0, -1, and -6, fly *Drosphila* Big Brain, plant AtPIP2;1 and Nodulin-26 have been shown to acquire ion channel activity (Modesto, Barcellos et al. 1990, Weaver, Shomer et al. 1994, Anthony, Brooks et al. 2000, Hazama, Kozono et al. 2002, Yanochko and Yool 2002, Byrt, Zhao et al. 2016). In AQP1 and AtPIP2;1 channels, the central pore of the tetramer has been hypothesized as the pathway for cation conductance (Yool and Weinstein 2002, Yu, Yool et al. 2006, Byrt, Zhao et al. 2016). The intrasubunit pores have been proposed as possible pathways for ion transport in BIB, AQP0 and AQP6 channel (Yasui, Hazama et al. 1999, Ikeda, Beitz et al. 2002, Yool 2007). Evidence for intra-subunit ion pores in BIB comes from mutational studies in which the mutation of glutamic acid at position 71 to aspargine (E71N) in BIB diminished ionic conductance,

whereas the equivalent mutation in AQP1 E17N did not prevent ion channel activity, but blocked AQP1 water channel function (Yool 2007). In AQP6 the key residues that affect ion channel properties are located in loop B, a domain that is associated with water channel function in other AQPs (Yasui, Hazama et al. 1999, Ikeda, Beitz et al. 2002).

1.Mammalian Aquaporin-1 ion channels functional properties

The ion channel activity of AQP1 has been the most comprehensively studied to date in terms of physiology, pharmacology, and functional roles. It is likely that understanding of the potentially diverse roles of aquaporin ion channels will continue to expand as the initially disputed concept (Agre, Lee et al. 1997) gains acceptance, and work in the field expands. Several lines of research have addressed the potential roles of AQP1 ion channels in pathological conditions such as cancer metastasis and brain oedema. The responsiveness of mammalian AQP1 ionic conductance to cGMP is modulated in part by tyrosine phosphorylation at position 253 (Y253) in carboxyl terminal domain of AQP1 channel (Campbell, Birdsell et al. 2012). The role of the C-terminus in activation was further supported by work from Boassa and colleagues who showed that AQP1 ionic current activation was disrupted when two key residues aspartate (D237) and lysine (K243) at the carboxyl terminal domain were mutated (Boassa and Yool 2003).

Another line of evidence supporting the proposed ion channel function of AQP1 comes from studies of the physiological importance of AQP1 in cancer cell migration. A bumetanide derivative AqB011 is a specific blocker of the AQP1 central ion pore

but not the water pores. When tested in HT29 cancer cells with high levels of AQP1-expression, AqB011 significantly blocked migration as compared to the untreated cancer cells (Kourghi, Pei et al. 2016), indicating that the AQP1 ion channel can enhance cell motility. Moreover, the ion channel property is not unique to AQP1; other members of the MIP family such as lens MIP26 and AQP6 also have been shown to have ion conductance properties (Zampighi, Hall et al. 1985) (Yasui, Hazama et al. 1999, Ikeda, Beitz et al. 2002).

1.1 The role of AQP1 ion conductance in cancer cell migration

The characteristics of uncontrolled malignant transformation in cancers include proliferation, aberrant apoptosis, angiogenesis, migration and invasion, all processes that are influenced by ion channels (Stringer, Cooper et al. 2001, Wang H, Zhang Y et al. 2002, Orrenius, Zhivotovsky et al. 2003, Ge, Tai et al. 2009, Flourakis, Lehen'kyi et al. 2010, Li, Cubbon et al. 2011, Prevarskaya, Skryma et al. 2011, Bose, Cieślar-Pobuda et al. 2015). Moreover a subtype of aquaporins (AQPs) have empirically been shown to contribute to cancer cell migration and metastasis (Hu and Verkman 2006, Li, Lu et al. 2013, Kang, Kim et al. 2015).

The ion channels such as K^+ channels play a crucial role in cell migration by regulating the cell volume and membrane potential. (Schwab, Hanley et al. 2008). Blocking of K^+ permeability reduces cancer cell migration and metastatic potential (Girault, Haelters et al. 2011). Second messenger Ca^{2+} signalling mediated pathways influence cellular processes such as facilitating cancer cell migration and proliferation (Parekh and Penner 1997, Roderick and Cook 2008, Prevarskaya,

Skryma et al. 2011, Monteith, Davis et al. 2012). Stores-operated Ca^{2+} entry (SOCE) is a major source of cellular Ca^{2+} (Barritt, Litjens et al. 2009). The calcium release-activated calcium channel protein 1 (Orai1) and stromal interaction molecule 1 (STIM1), two major components of SOCE, are sensitive to the blockers, SKF96365 and 2-APB (2-Aminoethyl diphenylborinate), which have been demonstrated to decrease cancer cell migration and proliferation in clear cell renal cell carcinoma (Kim, Lkhagvadorj et al. 2014). In addition, transient receptor potential (TRP) channels are implicated in Ca^{2+} signalling in cell migration by enabling the entry of Ca^{2+}; *TRPM7* knockdown abolished the transport of Ca^{2+} in migrating fibroblasts resulting in significant reduction of cell migration (Wei, Wang et al. 2009). Results on Ca^{2+} regulation in normal fibroblasts may provide insight into mechanisms relevant in cancer cells (Prevarskaya, Skryma et al. 2011). Furthermore, the epithelial sodium channel (ENaC) and acid sensitive ionic channel (ASIC) play important roles in cancer invasion and migration (Del Mónaco, Marino et al. 2009, Wang, He et al. 2013, Yang, He et al. 2015). Knockdown of sodium channels, ASIC1, and epithelial sodium channel subunits resulted in inhibition of glioblastoma cell migration (Kapoor, Bartoszewski et al. 2009). These evidences suggest the importance of ion channels in cell migration and cancer. AQP1 expression is also associated with tumour angiogenesis, and AQP1 knockdown or inhibition is correlated with reduced growth and angiogenesis (Saadoun, Papadopoulos et al. 2005, Nicchia, Stigliano et al. 2013) .

AQP1 is also recognized as a dual water and ion channel protein which carries an ionic conductance gated by cyclic GMP (cGMP) (Anthony, Brooks et al. 2000,

Boassa, Stamer et al. 2006, Campbell, Birdsell et al. 2012). AQPs have four identical subunits, forming as tetramers. The central pore in AQP1 channels follows a structural pattern of organization generally similar to that of other ion channels such as cyclic nucleotide-gated (CNG) channels and K^+ channels (Jan and Jan 1992, Yool and Weinstein 2002). The AQP1 ion channel mediates currents carried by Na^+, K^+, and Cs^+, but is not appreciably permeant to divalent cations or protons (Yool, Stamer et al. 1996, Anthony, Brooks et al. 2000). Evidence from molecular dynamic modelling and site-directed mutagenesis have converged on the idea that the ion permeation pathway in AQP1 is the central pore at the 4-fold axis of symmetry (Yu, Yool et al. 2006, Campbell, Birdsell et al. 2012). The gating of the AQP1 ion channel depends on cyclic GMP (Anthony, Brooks et al. 2000) which is thought to interact with an arginine-rich region of cytoplasmic loop D to open a gate resulting in central pore hydration, and subsequent permeation of water and cations (Yu, Yool et al. 2006). The responsiveness of mammalian AQP1 ionic conductance to cGMP is modulated by tyrosine phosphorylation at position 253 (Y253) in carboxyl terminal domain of AQP1 channel (Campbell, Birdsell et al. 2012). Boassa and colleagues showed that AQP1 ionic current activation was disrupted when two key residues aspartate (D237) and lysine (K243) at the carboxyl terminal domain were mutated (Boassa and Yool 2003). Therefore, single amino acids in the C-terminal domain of AQP1 do not directly gate the channel but appear to influence the efficacy of cGMP-mediated activation of ion conductance in AQP1 channels. A bumetanide derivative AqB011 acts as a specific blocker of the AQP1 ion channel, but not the water channels. The compound binds to the loop D domain of the channel and prevents

ion permeation (Kourghi et al., 2017, in preparation). Studies conducted on AQP1 expressing HT29 colon cancer cells showed that AqB011 impairs cell migration, with a dose dependent relationship that matches predicted efficacy based on the dose-dependent block of the ion channel conductance (Kourghi, Pei et al. 2016). AQP1 expression is also linked with tumour angiogenesis; AQP1 inhibition or siRNA knockdown (75% reduction) is correlated with reduced growth (Nicchia, Stigliano et al. 2013).

The Na^+/H^+ exchanger (NHE1) is an additional player in cell migration, proliferation and volume regulation (Grinstein, Rotin et al. 1989, Lang, Busch et al. 1998, Shi, Yuan et al. 2013). Inhibition of NHE1 leads to decreased motility (Stock and Schwab 2009, Stock, Ludwig et al. 2012). It was suggested that NHE1 and AQP1 facilitated ions and osmotic water uptake at the leading edge of the cell and help the lamellipodium, a cytoskeleton protein actin projection, to be extended, thereby contributing to cell migration (Saadoun, Papadopoulos et al. 2005, Schwab, Rossmann et al. 2005). AQP1 is involved in the process of lamellipodium extension in which it accelerates cancer cell migration (Saadoun, Papadopoulos et al. 2005).
The ability of AQP1 to function as an ion channel depends on cyclic GMP interaction with an arginine- rich region located on loop D of the AQP1 channel (Yu, Yool et al. 2006). The responsiveness of AQP1 ionic conductance to cGMP is modulated by tyrosine phosphorylation at position 253 in carboxyl terminal domain of human AQP1,(Campbell, Birdsell et al. 2012) and protein- kinase- C mediated phosphorylation at threonine residues 157 and 239 (Zhang, Zitron et al. 2007).

Knocking down of AQP1 dissociated cadherin/β-catenin/Lin-7/F-actin complexes and reduced migration and invasion of tumour cells (Monzani, Bazzotti et al. 2009). Moreover, AQP1 promoted migration and metastasis in bone marrow mesenchymal stem cells by regulating FAK through PI3K/Akt signalling pathway (Meng, Rui et al. 2013, Tai, Chen et al. 2015).

Judging from the breadth of findings gathered thus far, AQP1 might be a critical target to slow down the migration and metastasis during cancer progression. Therefore, the contribution of AQP1 as ion channel in cancer cell migration might have therapeutic significance for anti-cancer treatment in which AQP1 serves a key role in metastasis and angiogenesis.

1.2 The role of AQP1 ion conductance in cerebrospinal fluid (CSF) production

Choroid plexus is located in the ventricles in the brain and it consists of a single layer of cuboidal epithelial cells that interface with the blood capillary system and stromal space (Dziegielewska, Ek et al. 2001). The principal role of choroid plexus is secreting cerebrospinal fluid (CSF). CSF is found in the brain and spine; it provides physical support for the brain and a specialized extracellular environment facilitating the transport of nutrients, peptides, and hormones throughout the brain (Pollay 1977, Redzic, Preston et al. 2005). The mechanism of CSF production involves bulk ion movement from the blood to the ventricle across the choroid plexus though transcellular transporters (Segal and Pollay 1977). In choroid plexus, transporters and ion pumps are located on the apical and basal membranes to create an apico-basolateral polarity. Studies using inhibitors have

suggested that volume regulation in choroid plexus is also mediated by a combination of Na^+-H^+ exchange (NHE) and Cl^- - $HCO3^-$ exchange (Hughes, Pakhomova et al. 2010).

AQP1 is highly expressed in choroid plexus, specifically on the apical side (Nielsen, Smith et al. 1993, Speake, Freeman et al. 2003). The major function of AQP1 in choroid plexus is to facilitate water movement from the intracellular side to apical side of the barrier (Johansson, Dziegielewska et al. 2005), following the gradient created by active transport of sodium ions (Miyajima and Arai 2015). Interestingly, Boassa and colleagues in 2006 proposed that the ion channel function of AQP1 also regulated CSF flow rate in choroid plexus (Boassa, Stamer et al. 2006). Their results showed that AQP1 ion channel was activated and CSF production was stimulated when atrial natriuretic peptide (ANP) was added. ANP peptide binds to an endogenous guanylate cyclase receptor, producing cGMP (Boassa, Stamer et al. 2006). When AQP1 ion channels were blocked by Cd^{2+}, CSF production was slowed in a primary cell culture model (Boassa, Stamer et al. 2006). Further work in vivo is needed to evaluate whether the AQP1 ion channel function is one of the many factors regulating CSF secretion in physiological conditions.

Possible functions of AQP1 dual water and ion channels in other tissues and cells remain to be tested, but could be potentially relevant in a variety of processes such as angiogenesis, (Saadoun, Papadopoulos et al. 2005), fluid transport in renal proximal tubule as was proposed based on computational modelling (Yool and

Weinstein 2002), red blood cell adaptation to stressors, and a host of other conditions involving AQP1-expressing cells.

2. Other classes of aquaporins with ion channel activity

2.1 Mammalian Aquaporin 0

AQP0, previously known as lens MIP or MIP26, is an intrinsic membrane protein in ocular lens fibres (Bloemendal and Hockwin 1982), and is the major protein component of isolated lens junctions. AQP0 has been shown to function as a water channel when expressed exogenously in Xenopus oocytes (Kushmerick, Rice et al. 1995, Chandy, Zampighi et al. 1997) and endogenously in membrane vesicles generated from freshly isolated preparations of mouse, frog and rabbit lens fibres (Varadaraj, Kushmerick et al. 1999, Varadaraj, Kumari et al. 2005, Varadaraj, Kumari et al. 2007). However, AQP0 has the lowest water permeability of mammalian AQPs 1 to 5 (Yang and Verkman 1997), with single channel water permeability about 1/40th that of AQP1 (Chandy, Zampighi et al. 1997). The primary functions of AQP0 in the lens may include more than just increasing membrane water permeability. AQP0 in the lens could function in cell-cell adhesion of lens fibres, and regulation of gap junction channels (Liu, Tsujimoto et al. 2011). It is also proposed that AQP0 is required for maintaining the transparency and optical accommodation of the ocular lens (Chepelinsky 2009). Humans and mice lacking AQP0 developed congenital cataracts (Berry, Francis et al. 2000, Chepelinsky 2009).

When reconstituted in bilayers, AQP0 showed ion channel activity (Zampighi, Hall et al. 1985, Ehring and Hall 1988, Modesto, Barcellos et al. 1989, Ehring, Zampighi et

al. 1990, Shen, Shrager et al. 1991). Bovine AQP0 had a conductance of 200 pS in unilamellar vesicles with 100 mM saline. The ion channel was voltage- and pH-sensitive, open at high H^+ concentration, and generally closed at neutral pH showing a current amplitude similar to control bilayers (Zampighi, Hall et al. 1985). AQP0 channels reconstituted in bi-layers exhibit a large single-channel conductance In KCl and are permeable to both potassium and sodium ions (Zampighi, Hall et al. 1985). (0.1M). AQP0 channel openings had two main conductance states with amplitudes of 380 and 160 pS. AQP0 displayed a slight anionic selectivity, symmetrical voltage dependence, and rapid opening and slow closing rates (Zampighi, Hall et al. 1985). The water channel activity of AQP0 was subsequently shown to be dependent upon pH and calcium regulation (Németh-Cahalan and Hall 2000), suggesting regulatory mechanisms modulated both the water flux and ion conductance of AQP0. Maintaining optimal lens transparency of the eye lens might be in part inked with the dual water and ion channel function of AQP0 (Ehring, Zampighi et al. 1990). Noting that light scattering contributes to a reduction in transparency, Ehring and colleagues postulated that regulating fluid balance and minimizing extracellular space in the lens, via ion and water flow into the lens fibres, could reduce light scattering, and in turn, assist in maintaining optimal transparency.

2.2 Mammalian Aquaporin 6

Aquaporin-6 (AQP6) is a dual anion channel and water channel that is unusual among AQPs because atypically it is activated rather than blocked by mercuric chloride ($HgCl_2$) (Hazama, Kozono et al. 2002), unlike AQP1 (Preston, Jung et al. 1993) and other AQPs. AQP6 assembles as a tetramer, possessing monomeric

pores for water as well as anions, with a permeability series of NO_3>I>>Br>Cl>>F (Yasui, Hazama et al. 1999, Ikeda, Beitz et al. 2002). Interestingly, when expressed in *Xenopus* laevis oocytes, AQP6 showed low water permeability. However, when AQP6-expressing oocytes were exposed to $HgCl_2$ at concentrations up to 300μM, AQP6 water permeability increased over five-fold, and the ion conductance increased more than six-fold (Yasui, Hazama et al. 1999, Hazama, Kozono et al. 2002). This observation contrasts with other AQPs such as AQP1, -2, and -5 that are blocked by $HgCl_2$. Yasui et al. (1999a) discovered that two cysteine residues, C155 and C190, are important for the $HgCl_2$ gating of AQP6. Moreover, AQP6 water and anion conductance was reversibly potentiated by low pH, suggesting a mechanism of activation with some potential physiological relevance (Yasui, Hazama et al. 1999).

AQP6 is expressed in intracellular vesicles of renal collecting duct intercalated cells in mammals (Yasui, Kwon et al. 1999, Kwon, Hager et al. 2001). In α-intercalated cells, AQP6 was colocalized with H^+/ATPases in intracellular vesicles, but not in plasma membrane (Yasui, Hazama et al. 1999), and was suggested to contribute to urinary acid secretion and acid/base regulation (Carbrey and Agre 2009). Significant upregulation of AQP6 expression was observed in rats exposed to chronic alkalosis or water loading, but not chronic acidosis (Promeneur, Kwon et al. 2000). AQP6 similarly might function as a pH-sensitive chloride channel in kidney endosomes (Verkman 2002). Expression of AQP6 in rat gastrointestinal epithelium, near tight junctions and secretory granule membranes in rat parotid acinar cells, and

in some ovarian cancers (Matsuki-Fukushima, Hashimoto et al. 2008, Laforenza, Gastaldi et al. 2009, Ma, Zhou et al. 2016) has suggested other possible roles in tissues involving acid-base regulation, although the physiological significance of AQP6 in these systems is not yet understood.

AQP6 has been proposed to contribute a protective role against certain viral pathologies (Molinas, Mirazimi et al. 2016), based on studies showing AQP6 expression levels were inversely correlated with susceptibility to viral infection in host cell lines. Molinas and colleagues introduced GFP-tagged AQP6 into mouse fibroblast cells, infected with Hazara virus as a model for Crimean–Congo hemorrhagic fever. Overexpression of AQP6 reduced infectivity of the Hazara virus, cells infected with Hazara virus showed altered cell morphology and a reduced level of AQP6 expression at both protein and mRNA levels (Molinas, Mirazimi et al. 2016).

2.3 Arabidopsis thaliana PIP2;1

The plant aquaporin AtPIP2;1 is a plasma membrane protein highly expressed in *Arabidopsis* roots that is involved in maintaining plant water homeostasis (Alexandersson, Fraysse et al. 2005). Water transport studies conducted on proteoliposomes showed that the osmotic water permeability of AtPIP2;1 channels was impaired by divalent cations, with the highest inhibitory efficacies shown by Ca^{2+}, Cd^{2+} and Mn^{2}. Protons also blocked the water flux, with half-maximal inhibition at pH 7.15 (Verdoucq, Grondin et al. 2008). Calcium plays an important role in signal

transduction in plants, particularly under stress conditions (Sanders, Pelloux et al. 2002).

AtPIP2;1 channels expressed in *Xenopus* laevis oocytes and analyzed by two-electrode voltage clamp also mediate cation currents that are sensitive to block by divalent cations and pH (Byrt, Zhao et al. 2016) confirming this channel is another example of the expanding list of dual water and ion channel aquaporins. The ionic current in AtPIP2;1-expressing oocytes cannot be explained as an indirect result of native oocyte channels activating in response to swelling, since the co-expression of another related channel (AtPIP1;2) with AtPIP2;1 increased water permeability but removed the ionic conductance. Furthermore, the mutation of glycine at position 103 to tryptophan (G103W) in AtPIP2;1 similarly impaired ion channel but not water channel activity, demonstrating the ion channel function is property that is intrinsic to the AtPIP2;1 channel. AtPIP2:1 ion currents are blocked by extracellular Ca^{2+} and Cd^{2+} (Byrt, Zhao et al. 2016). The dose-response curve for conductance as a function of EGTA-buffered free Ca^{2+} levels generated an IC_{50} value of 0.32 mM, in agreement with prior reports of non-selective cation channels in Arabidopsis root protoplasts that were blocked by Ca^{2+}. Low external pH also inhibited the ionic conductance (IC_{50} pH 6.8). These data suggest that the AtPIP2;1 might be the molecular basis of a cationic conductance in roots that is important for plant responses to environmental conditions, but not previously defined at the molecular level.

Based on patterns of expression, AtPIP2;1 ion channels might contribute to coupled ion and water transport to facilitate rapid shrinking responses as well as in guard cell closing (MacRobbie 2006, Grondin, Rodrigues et al. 2015), and regulating hypoosmotic turgor in plants in the absence of water potential differences (Wegner 2014). Water permeability through AtPIP2;1 channels is regulated via phosphorylation (Prado, Boursiac et al. 2013, Grondin, Rodrigues et al. 2015). It will be of interest to analyze consensus phosphorylation sites of AtPIP2;1 to study the relationship between phosphorylation state and ionic conductance in AtPIP2;1 channels. Precedent for the regulation of aquaporin ion channels by phosphorylation has been established for mammalian AQP1, in which the phosphorylation of tyrosine 253 in the carboxyl terminal domain of AQP1 has been shows to govern the responsiveness of the central ion channel pore to cGMP (Campbell, Birdsell et al. 2012). The probability of AQP1 being available to be gated as an ion channel is enhanced when the tyrosine phosphorylated state of the channel is favored via treatment with a tyrosine phosphatase inhibitor, bisperoxo (1,10-phenanthroline) oxovanadate-(V) (Campbell, Birdsell et al. 2012). Testing whether similar second messenger candidate sites influence dual water and ion transport through AtPIP2;1 in plants is merited, since prior work also suggested connections between cyclic nucleotide levels in roots and phosphorylation of proteins, including AQPs (Maurel, Kado et al. 1995, Isner, Nuhse et al. 2012).

2.4 Drosophila Big Brain

The transmembrane protein Big Brain (BIB), encoded by a Drosophila neurogenic gene, belongs to the MIP channel family (Rao, Bodmer et al. 1992). During neurogenesis in the early development of Drosophila, a loss-of-function mutation of the big brain gene (*bib)* causes the overproduction of neuroblasts (Lehmann, Jimenez et al. 1983). Similar to other neurogenic genes such as *Notch* and *Delta*, BIB is involved in the process of lateral inhibition, and its absence leads to the pathological phenotype (Lehmann, Jimenez et al. 1983, Rao, Bodmer et al. 1992). Unlike most AQPs in the MIP family, BIB has not been found to be permeable for water. When expressed in *Xenopus* oocytes, BIB functions as a monovalent cation channel activated by membrane pricking or pharmacological modulation of tyrosine kinase signalling pathways. Results from Yanochko and colleagues showed BIB is a voltage-insensitive cation channel that was inhibited downstream of insulin-like receptor activation of a tyrosine kinase pathway; conversely application of a tyrosine kinase inhibitor, lavendustin A, increased the net conductance of BIB-expressing oocyte. The involvement of tyrosine was validated by western blot showing tyrosine phosphorylation at consensus sites in the carboxyl terminal domain (Yanochko and Yool 2002). The BIB ion channel showed voltage-sensitive block by divalent cations such as Ca^{2+} and Ba^{2+}, suggesting the binding site is within the electrical field. A glutamate residue in the first transmembrane domain Glu^{71}, a position that is highly conserved in the MIP family, was defined as essential for divalent cation binding in BIB (Yanochko and Yool 2004).

3. Summary and future directions

Acquiring a full perspective on the functional roles and regulatory controls for aquaporin dual water and ion channels will be critical for understanding the spectrum of potentially important physiological roles that these channels might serve, as well as their potential value as targets in an impressively diverse array of applications. AQP modulators have promise for future therapeutic interventions in clinical disorders including cancer metastasis, renal failure, and brain pathophysiology; for enhancing agricultural productivity in challenging environments; for managing vectors of transmitted diseases, and much more.

Evolutionary relationships have been evaluated for the broad MIP family of channels based on analyses of amino acid sequences, as summarised in review articles published by (Reizer, Reizer et al. 1993). Statistical analysis suggest the two halves of the MIP protein have evolved to possess distinct functions, the first half of the protein provides a general or similar function of these proteins, while the second, structurally divergent half provides the specific function of the protein. The patterns from sequence analyses of polygenic tree of members of the MIP family suggest that a primordial gene emerged in prokaryotes before the appearance of eukaryotic cells, and this gene was vertically transmitted into primitive eukaryotes. Therefore the following gene multiplication and division gave rise to kingdom-related subfamilies of the MIP family (Reizer, Reizer et al. 1993).

The development of AQP ion channel selective blockers such as AqB011, a first-in-class compound, has allowed characterization of the AQP1 ionic conductance as a key component in HT29 cancer cell migration (Kourghi et al., 2016), and provides strong evidence for physiological relevance of AQP1 ionic function. The continuing discovery of medicinal blockers of AQP1 that selectively inhibit water permeability such as bacopaside II, or that block both the water and ion channel pores (such as bacopaside I) are promising tools for manipulating cell processes that rely on AQP1 expression (Pei et al., 2016). Value in limiting cancer metastasis awaits validation in vivo and potentially in clinical trials. Work in progress (Kourghi et al., unpublished) suggests that selective inhibitors of AQP1 also could be a useful in protecting red blood cells from pathological changes in cell morphology in sickle cell anaemia.

Initial studies with AQP6 could open new opportunities to study the roles of AQPs in cellular vulnerability to certain viral pathologies such as Hazara virus (Molinas, Mirazimi et al. 2016)

Dual water and ion channel AQPs appear to be important for modulation of transmembrane fluid gradients, volume regulation, signal transduction, and adaptation to environment for many different types of organisms. Exploring the multifunctional role of aquaporins offer exciting challenges and opportunities for basic research and translational advances, and allows us to appreciate the diversity and complexity of AQPs in physiology and pathology across all forms of life.

References

Agre, P. (2004). "Aquaporin water channels (Nobel Lecture)." Angew Chem Int Ed Engl **43**(33): 4278-4290.

Agre, P., M. D. Lee, S. Devidas and W. B. Guggino (1997). "Aquaporins and ion conductance." Science **275**(5305): 1490-1490.

Alexandersson, E., L. Fraysse, S. Sjovall-Larsen, S. Gustavsson, M. Fellert, M. Karlsson, U. Johanson and P. Kjellbom (2005). "Whole gene family expression and drought stress regulation of aquaporins." Plant Mol Biol **59**(3): 469-484.

Anthony, T. L., H. L. Brooks, D. Boassa, S. Leonov, G. M. Yanochko, J. W. Regan and A. J. Yool (2000). "Cloned human aquaporin-1 is a cyclic GMP-gated ion channel." Molecular Pharmacology **57**(3): 576-588.

Anthony, T. L., H. L. Brooks, D. Boassa, S. Leonov, G. M. Yanochko, J. W. Regan and A. J. Yool (2000). "Cloned human aquaporin-1 is a cyclic GMP-gated ion channel." Mol Pharmacol **57**(3): 576-588.

Barritt, G. J., T. L. Litjens, J. Castro, E. Aromataris and G. Y. Rychkov (2009). "Store-operated Ca^{2+} channels and microdomains of Ca^{2+} in liver cells." Clinical and Experimental Pharmacology and Physiology **36**(1): 77-83.

Benga, G. (2009). "Water channel proteins (later called aquaporins) and relatives: past, present, and future." IUBMB Life **61**(2): 112-133.

Berry, V., P. Francis, S. Kaushal, A. Moore and S. Bhattacharya (2000). "Missense mutations in MIP underlie autosomal dominant'polymorphic'and lamellar cataracts linked to 12q." Nature genetics **25**(1): 15.

Bloemendal, H. and O. Hockwin (1982). "Lens protein." Critical Reviews in Biochemistry **12**(1): 1-38.

Boassa, D., W. D. Stamer and A. J. Yool (2006). "Ion channel function of aquaporin-1 natively expressed in choroid plexus." Journal of Neuroscience **26**(30): 7811-7819.

Boassa, D., W. D. Stamer and A. J. Yool (2006). "Ion channel function of aquaporin-1 natively expressed in choroid plexus." J Neurosci **26**(30): 7811-7819.

Boassa, D. and A. J. Yool (2003). "Single amino acids in the carboxyl terminal domain of aquaporin-1 contribute to cGMP-dependent ion channel activation." BMC Physiol **3**: 12.

Bose, T., A. Cieślar-Pobuda and E. Wiechec (2015). "Role of ion channels in regulating Ca^{2+} homeostasis during the interplay between immune and cancer cells." Cell death & disease **6**(2): e1648.

Brooks, H. L., J. W. Regan and A. J. Yool (2000). "Inhibition of aquaporin-1 water permeability by tetraethylammonium: involvement of the loop E pore region." Mol Pharmacol **57**(5): 1021-1026.

Byrt, C. S., M. Zhao, M. Kourghi, J. Bose, S. W. Henderson, J. Qiu, M. Gilliham, C. Schultz, M. Schwarz, S. A. Ramesh, A. Yool and S. Tyerman (2016). "Non-selective cation channel activity of aquaporin AtPIP2;1 regulated by Ca^{2+} and pH." Plant Cell Environ.

Campbell, E. M., D. N. Birdsell and A. J. Yool (2012). "The activity of human aquaporin 1 as a cGMP-gated cation channel is regulated by tyrosine phosphorylation in the carboxyl-terminal domain." Mol Pharmacol **81**(1): 97-105.

Campbell, E. M., D. N. Birdsell and A. J. Yool (2012). "The activity of human aquaporin 1 as a cGMP-gated cation channel is regulated by tyrosine phosphorylation in the carboxyl-terminal domain." Molecular pharmacology **81**(1): 97-105.

Carbrey, J. M. and P. Agre (2009). Discovery of the aquaporins and development of the field. Aquaporins. E. Beitz, Springer Berlin Heidelberg. **190:** 3-28.

Cardone, R. A., A. Bellizzi, G. Busco, E. J. Weinman, M. E. Dell'Aquila, V. Casavola, A. Azzariti, A. Mangia, A. Paradiso and S. J. Reshkin (2007). "The NHERF1 PDZ2 domain regulates PKA–RhoA–p38-mediated NHE1 activation and invasion in breast tumor cells." Molecular biology of the cell **18**(5): 1768-1780.

Chandy, G., G. Zampighi, M. Kreman and J. Hall (1997). "Comparison of the water transporting properties of MIP and AQP1." Journal of Membrane Biology **159**(1): 29-39.

Chepelinsky, A. B. (2009). Structural function of MIP/aquaporin 0 in the eye lens; genetic defects lead to congenital inherited cataracts. Aquaporins, Springer**:** 265-297.

Chepelinsky, A. B. (2009). "Structural function of MIP/aquaporin 0 in the eye lens; genetic defects lead to congenital inherited cataracts." Handb Exp Pharmacol(190): 265-297.

Chiang, Y., C. Y. Chou, K. F. Hsu, Y. F. Huang and M. R. Shen (2008). "EGF upregulates Na^+/H^+ exchanger NHE1 by post-translational regulation that is

important for cervical cancer cell invasiveness." Journal of cellular physiology **214**(3): 810-819.

Del Mónaco, S. M., G. I. Marino, Y. A. Assef, A. E. Damiano and B. A. Kotsias (2009). "Cell migration in BeWo cells and the role of epithelial sodium channels." Journal of Membrane Biology **232**(1-3): 1-13.

Dorward, H. S., A. Du, M. A. Bruhn, J. Wrin, J. V. Pei, A. Evdokiou, T. J. Price, A. J. Yool and J. E. Hardingham (2016). "Pharmacological blockade of aquaporin-1 water channel by AqB013 restricts migration and invasiveness of colon cancer cells and prevents endothelial tube formation in vitro." Journal of Experimental & Clinical Cancer Research **35**(1): 36.

Dziegielewska, K. M., J. Ek, M. D. Habgood and N. R. Saunders (2001). "Development of the choroid plexus." Microsc Res Tech **52**(1): 5-20.

Ehring, G. and J. Hall (1988). Single channel properties of lens MIP 28 reconstituted into planar lipid bilayers. Proceedings of the Western Pharmacology Society.

Ehring, G. R., G. Zampighi, J. Horwitz, D. Bok and J. E. Hall (1990). "Properties of channels reconstituted from the major intrinsic protein of lens fiber membranes." J Gen Physiol **96**(3): 631-664.

Ehring, G. R., G. Zampighi, J. Horwitz, D. Bok and J. E. Hall (1990). "Properties of channels reconstituted from the major intrinsic protein of lens fiber membranes." The Journal of General Physiology **96**(3): 631-664.

Finn, R. N., F. Chauvigne, J. B. Hlidberg, C. P. Cutler and J. Cerda (2014). "The lineage-specific evolution of aquaporin gene clusters facilitated tetrapod terrestrial adaptation." PLoS One **9**(11): e113686.

Flourakis, M., V. Lehen'kyi, B. Beck, M. Raphael, M. Vandenberghe, F. V. Abeele, M. Roudbaraki, G. Lepage, B. Mauroy and C. Romanin (2010). "Orai1 contributes to the establishment of an apoptosis-resistant phenotype in prostate cancer cells." Cell death & disease **1**(9): e75.

Ge, R., Y. Tai, Y. Sun, K. Zhou, S. Yang, T. Cheng, Q. Zou, F. Shen and Y. Wang (2009). "Critical role of TRPC6 channels in VEGF-mediated angiogenesis." Cancer letters **283**(1): 43-51.

Girault, A., J.-P. Haelters, M. Potier-Cartereau, A. Chantôme, M. Pinault, S. Marionneau-Lambot, T. Oullier, G. Simon, H. Couthon-Gourves and P.-A. Jaffres (2011). "New alkyl-lipid blockers of SK3 channels reduce cancer cell migration and occurrence of metastasis." Current cancer drug targets **11**(9): 1111-1125.

Gomes, D., A. Agasse, P. Thiebaud, S. Delrot, H. Geros and F. Chaumont (2009). "Aquaporins are multifunctional water and solute transporters highly divergent in living organisms." Biochim Biophys Acta **1788**(6): 1213-1228.

Grondin, A., O. Rodrigues, L. Verdoucq, S. Merlot, N. Leonhardt and C. Maurel (2015). "Aquaporins Contribute to ABA-Triggered Stomatal Closure through OST1-Mediated Phosphorylation." Plant Cell **27**(7): 1945-1954.

Han, Z. and R. V. Patil (2000). "Protein kinase A-dependent phosphorylation of aquaporin-1." Biochemical and biophysical research communications **273**(1): 328-332.

Hazama, A., D. Kozono, W. B. Guggino, P. Agre and M. Yasui (2002). "Ion permeation of AQP6 water channel protein single-channel recordings after Hg^{2+} activation." Journal of Biological Chemistry **277**(32): 29224-29230.

Hoffmann, E. K., N. B. Holm and I. H. Lambert (2014). "Functions of volume-sensitive and calcium-activated chloride channels." IUBMB life **66**(4): 257-267.

Hu, J. and A. Verkman (2006). "Increased migration and metastatic potential of tumor cells expressing aquaporin water channels." The FASEB Journal **20**(11): 1892-1894.

Hughes, A. L., A. Pakhomova and P. D. Brown (2010). "Regulatory volume increase in epithelial cells isolated from the mouse fourth ventricle choroid plexus involves Na^+-H^+ exchange but not Na^+-K^+-$2Cl^-$ cotransport." Brain Res **1323**: 1-10.

Ikeda, M., E. Beitz, D. Kozono, W. B. Guggino, P. Agre and M. Yasui (2002). "Characterization of aquaporin-6 as a nitrate channel in mammalian cells - Requirement of pore-lining residue threonine 63." Journal of Biological Chemistry **277**(42): 39873-39879.

Ishibashi, K. (2009). "New members of mammalian aquaporins: AQP10-AQP12." Handb Exp Pharmacol(190): 251-262.

Isner, J. C., T. Nuhse and F. J. Maathuis (2012). "The cyclic nucleotide cGMP is involved in plant hormone signalling and alters phosphorylation of Arabidopsis thaliana root proteins." J Exp Bot **63**(8): 3199-3205.

Jan, L. Y. and Y. N. Jan (1992). "Structural elements involved in specific K^+ channel functions." Annual review of physiology **54**(1): 537-555.

Johansson, P. A., K. M. Dziegielewska, C. J. Ek, M. D. Habgood, K. Mollgard, A. Potter, M. Schuliga and N. R. Saunders (2005). "Aquaporin-1 in the choroid plexuses of developing mammalian brain." Cell Tissue Res **322**(3): 353-364.

Jung, J. S., G. M. Preston, B. L. Smith, W. B. Guggino and P. Agre (1994). "Molecular-Structure of the Water Channel through Aquaporin Chip - the Hourglass Model." Journal of Biological Chemistry **269**(20): 14648-14654.

Kapoor, N., R. Bartoszewski, Y. J. Qadri, Z. Bebok, J. K. Bubien, C. M. Fuller and D. J. Benos (2009). "Knockdown of ASIC1 and epithelial sodium channel subunits inhibits glioblastoma whole cell current and cell migration." Journal of Biological Chemistry **284**(36): 24526-24541.

Kim, J.-H., S. Lkhagvadorj, M.-R. Lee, K.-H. Hwang, H. C. Chung, J. H. Jung, S.-K. Cha and M. Eom (2014). "Orai1 and STIM1 are critical for cell migration and proliferation of clear cell renal cell carcinoma." Biochemical and biophysical research communications **448**(1): 76-82.

Klein, M., P. Seeger, B. Schuricht, S. L. Alper and A. Schwab (2000). "Polarization of Na^+/H^+ and $Cl^-/HCO\ 3^-$ exchangers in migrating renal epithelial cells." The Journal of general physiology **115**(5): 599-608.

Kondratskyi, A., K. Kondratska, R. Skryma and N. Prevarskaya (2015). "Ion channels in the regulation of apoptosis." Biochimica et Biophysica Acta (BBA)-Biomembranes **1848**(10): 2532-2546.

Kourghi, M., J. V. Pei, M. L. De Ieso, G. Flynn and A. J. Yool (2016). "Bumetanide Derivatives AqB007 and AqB011 Selectively Block the Aquaporin-1 Ion Channel Conductance and Slow Cancer Cell Migration." Mol Pharmacol **89**(1): 133-140.

Kushmerick, C., S. Rice, G. Baldo, H. Haspel and R. Mathias (1995). "Ion, water and neutral solute transport in Xenopus oocytes expressing frog lens MIP." Experimental eye research **61**(3): 351-362.

Kwon, T.-H., H. Hager, L. N. Nejsum, M. Andersen, J. Frøkiaer and S. Nielsen (2001). Physiology and pathophysiology of renal aquaporins. Seminars in nephrology.

Laforenza, U., G. Gastaldi, M. Polimeni, S. Tritto, M. Tosco, U. Ventura, M. F. Scaffino and M. Yasui (2009). "Aquaporin-6 is expressed along the rat gastrointestinal tract and upregulated by feeding in the small intestine." BMC Physiology **9**(1): 18.

Lehmann, R., F. Jimenez, U. Dietrich and J. A. Campos-Ortega (1983). "On the phenotype and development of mutants of early neurogenesis inDrosophila melanogaster." Wilehm Roux Arch Dev Biol **192**(2): 62-74.

Li, J., R. M. Cubbon, L. A. Wilson, M. S. Amer, L. McKeown, B. Hou, Y. Majeed, S. Tumova, V. A. Seymour and H. Taylor (2011). "Orai1 and CRAC channel

dependence of VEGF-activated Ca^{2+} entry and endothelial tube formation." Circulation research: CIRCRESAHA. 111.243352.

Liu, K., H. Tsujimoto, S. J. Cha, P. Agre and J. L. Rasgon (2011). "Aquaporin water channel AgAQP1 in the malaria vector mosquito Anopheles gambiae during blood feeding and humidity adaptation." Proceedings of the National Academy of Sciences of the United States of America **108**(15): 6062-6066.

Ma, J., C. Zhou, J. Yang, X. Ding, Y. Zhu and X. Chen (2016). "Expression of AQP6 and AQP8 in epithelial ovarian tumor." Journal of molecular histology **47**(2): 129-134.

MacRobbie, E. A. (2006). "Control of volume and turgor in stomatal guard cells." J Membr Biol **210**(2): 131-142.

Matsuki-Fukushima, M., S. Hashimoto, M. Shimono, K. Satoh, J. Fujita-Yoshigaki and H. Sugiya (2008). "Presence and localization of aquaporin-6 in rat parotid acinar cells." Cell and Tissue Research **332**(1): 73-80.

Maurel, C., R. T. Kado, J. Guern and M. J. Chrispeels (1995). "Phosphorylation regulates the water channel activity of the seed-specific aquaporin alpha-TIP." EMBO J **14**(13): 3028-3035.

Meng, F., Y. Rui, L. Xu, C. Wan, X. Jiang and G. Li (2013). "Aqp1 enhances migration of bone marrow mesenchymal stem cells through regulation of FAK and β-catenin." Stem cells and development **23**(1): 66-75.

Miyajima, M. and H. Arai (2015). "Evaluation of the Production and Absorption of Cerebrospinal Fluid." Neurol Med Chir (Tokyo) **55**(8): 647-656.

Modesto, E., L. Barcellos and A. Campos-de-Carvalho (1989). "MIP 28 forms channels in planar lipid bilayers." Brazilian journal of medical and biological research= Revista brasileira de pesquisas medicas e biologicas/Sociedade Brasileira de Biofisica...[et al.] **23**(10): 1029-1032.

Molinas, A., A. Mirazimi, A. Holm, V. M. Loitto, K.-E. Magnusson and E. Vikström (2016). "Protective role of host aquaporin 6 against Hazara virus, a model for Crimean–Congo hemorrhagic fever virus infection." FEMS microbiology letters **363**(8): fnw058.

Monzani, E., R. Bazzotti, C. Perego and C. A. La Porta (2009). "AQP1 is not only a water channel: it contributes to cell migration through Lin7/beta-catenin." PLoS One **4**(7): e6167.

Németh-Cahalan, K. L. and J. E. Hall (2000). "pH and calcium regulate the water permeability of aquaporin 0." Journal of Biological Chemistry **275**(10): 6777-6782.

Orrenius, S., B. Zhivotovsky and P. Nicotera (2003). "Regulation of cell death: the calcium-apoptosis link." Nature reviews. Molecular cell biology **4**(7): 552.

Nielsen, S., B. L. Smith, E. I. Christensen and P. Agre (1993). "Distribution of the aquaporin CHIP in secretory and resorptive epithelia and capillary endothelia." Proc Natl Acad Sci U S A **90**(15): 7275-7279.

Pei, J. V., M. Kourghi, M. L. De Ieso, E. M. Campbell, H. S. Dorward, J. E. Hardingham and A. J. Yool (2016). "Differential Inhibition of Water and Ion Channel Activities of Mammalian Aquaporin-1 by Two Structurally Related Bacopaside Compounds Derived from the Medicinal Plant Bacopa monnieri." Mol Pharmacol **90**(4): 496-507.

Pollay, M. (1977). "Capillary permeability in cold induced cerebral edema." Acta Neurol Scand Suppl **64**: 396-397.

Prado, K., Y. Boursiac, C. Tournaire-Roux, J. M. Monneuse, O. Postaire, O. Da Ines, A. R. Schaffner, S. Hem, V. Santoni and C. Maurel (2013). "Regulation of Arabidopsis leaf hydraulics involves light-dependent phosphorylation of aquaporins in veins." Plant Cell **25**(3): 1029-1039.

Preston, G. M., J. S. Jung, W. B. Guggino and P. Agre (1993). "The Mercury-Sensitive Residue at Cysteine-189 in the Chip28 Water Channel." Journal of Biological Chemistry **268**(1): 17-20.

Preston, G. M., J. S. Jung, W. B. Guggino and P. Agre (1994). "Membrane topology of aquaporin CHIP. Analysis of functional epitope-scanning mutants by vectorial proteolysis." J Biol Chem **269**(3): 1668-1673.

Prevarskaya, N., R. Skryma and Y. Shuba (2011). "Calcium in tumour metastasis: new roles for known actors." Nature Reviews Cancer **11**(8): 609-618.

Promeneur, D., T.-H. Kwon, M. Yasui, G.-H. Kim, J. Frøkiær, M. A. Knepper, P. Agre and S. Nielsen (2000). "Regulation of AQP6 mRNA and protein expression in rats in response to altered acid-base or water balance." American Journal of Physiology-Renal Physiology **279**(6): F1014-F1026.

Rao, Y., R. Bodmer, L. Y. Jan and Y. N. Jan (1992). "The big brain gene of Drosophila functions to control the number of neuronal precursors in the peripheral nervous system." Development **116**(1): 31-40.

Redzic, Z. B., J. E. Preston, J. A. Duncan, A. Chodobski and J. Szmydynger-Chodobska (2005). "The choroid plexus-cerebrospinal fluid system: from development to aging." Curr Top Dev Biol **71**: 1-52.

Saadoun, S., M. C. Papadopoulos, M. Hara-Chikuma and A. Verkman (2005). "Impairment of angiogenesis and cell migration by targeted aquaporin-1 gene disruption." Nature **434**(7034): 786-792.

Sanders, D., J. Pelloux, C. Brownlee and J. F. Harper (2002). "Calcium at the crossroads of signaling." Plant Cell **14**: S401-S417.

Schwab, A., P. Hanley, A. Fabian and C. Stock (2008). "Potassium channels keep mobile cells on the go." Physiology **23**(4): 212-220.

Schwab, A., H. Rossmann, M. Klein, P. Dieterich, B. Gassner, C. Neff, C. Stock and U. Seidler (2005). "Functional role of Na^+–$HCO3^-$ cotransport in migration of transformed renal epithelial cells." The Journal of physiology **568**(2): 445-458.

Schwab, A. and C. Stock (2014). "Ion channels and transporters in tumour cell migration and invasion." Phil. Trans. R. Soc. B **369**(1638): 20130102.

Segal, M. B. and M. Pollay (1977). "The secretion of cerebrospinal fluid." Exp Eye Res **25 Suppl**: 127-148.

Shen, L., P. Shrager, S. J. Girsch, P. J. Donaldson and C. Peracchia (1991). "Channel reconstitution in liposomes and planar bilayers with HPLC-purified MIP26 of bovine lens." Journal of Membrane Biology **124**(1): 21-32.

Shivaraj, S. M., R. K. Deshmukh, R. Rai, R. Belanger, P. K. Agrawal and P. K. Dash (2017). "Genome-wide identification, characterization, and expression profile of aquaporin gene family in flax (Linum usitatissimum)." Sci Rep **7**: 46137.

Speake, T., L. J. Freeman and P. D. Brown (2003). "Expression of aquaporin 1 and aquaporin 4 water channels in rat choroid plexus." Biochim Biophys Acta **1609**(1): 80-86.

Steinberg, M. H. (1999). "Management of sickle cell disease." N Engl J Med **340**(13): 1021-1030.

Stock, C., F. Ludwig and A. Schwab (2012). "Is the multifunctional Na^+/H^+ exchanger isoform 1 a potential therapeutic target in cancer?" Current medicinal chemistry **19**(5): 647-660.

Stock, C. and A. Schwab (2006). "Role of the Na^+/H^+ exchanger NHE1 in cell migration." Acta physiologica **187**(1-2): 149-157.

Stock, C. and A. Schwab (2009). "Protons make tumor cells move like clockwork." Pflügers Archiv-European Journal of Physiology **458**(5): 981-992.

Stringer, B. K., A. G. Cooper and S. B. Shepard (2001). "Overexpression of the G-protein inwardly rectifying potassium channel 1 (GIRK1) in primary breast carcinomas correlates with axillary lymph node metastasis." Cancer research **61**(2): 582-588.

Tai, Y.-L., L.-C. Chen and T.-L. Shen (2015). "Emerging roles of focal adhesion kinase in cancer." BioMed research international **2015**.

Umenishi, F. and R. W. Schrier (2003). "Hypertonicity-induced aquaporin-1 (AQP1) expression is mediated by the activation of MAPK pathways and hypertonicity-responsive element in the AQP1 gene." Journal of Biological Chemistry **278**(18): 15765-15770.

Varadaraj, K., S. Kumari, A. Shiels and R. T. Mathias (2005). "Regulation of aquaporin water permeability in the lens." Investigative ophthalmology & visual science **46**(4): 1393-1402.

Varadaraj, K., S. S. Kumari and R. T. Mathias (2007). "Functional expression of aquaporins in embryonic, postnatal, and adult mouse lenses." Developmental Dynamics **236**(5): 1319-1328.

Varadaraj, K., C. Kushmerick, G. Baldo, S. Bassnett, A. Shiels and R. Mathias (1999). "The role of MIP in lens fiber cell membrane transport." Journal of Membrane Biology **170**(3): 191-203.

Verdoucq, L., A. Grondin and C. Maurel (2008). "Structure-function analysis of plant aquaporin AtPIP2;1 gating by divalent cations and protons." Biochemical Journal **415**: 409-416.

Verkman, A. (2002). "Aquaporin water channels and endothelial cell function." Journal of anatomy **200**(6): 617-627.

Wang H, Zhang Y, Cao L, Han H, Wang J and Y. B. e. al. (2002). "HERG K^+ channel, a regulator of tumor cell apoptosis and proliferation. ." Cancer Res **62 : 4843 – 4848.**

Wang, S., G. He, Y. Yang, Y. Liu, R. Diao, K. Sheng, X. Liu and W. Xu (2013). "Reduced expression of Enac in Placenta tissues of patients with severe preeclampsia is related to compromised trophoblastic cell migration and invasion during pregnancy." PloS one **8**(8): e72153.

Weaver, C. D., N. H. Shomer, C. F. Louis and D. M. Roberts (1994). "Nodulin 26, a nodule-specific symbiosome membrane protein from soybean, is an ion channel." J Biol Chem **269**(27): 17858-17862.

Wegner, L. H. (2014). "Root pressure and beyond: energetically uphill water transport into xylem vessels?" J Exp Bot **65**(2): 381-393.

Wei, C., X. Wang, M. Chen, K. Ouyang, L.-S. Song and H. Cheng (2009). "Calcium flickers steer cell migration." Nature **457**(7231): 901-905.

Yang, B. and A. Verkman (1997). "Water and glycerol permeabilities of aquaporins 1–5 and MIP determined quantitatively by expression of epitope-tagged constructs inXenopus oocytes." Journal of Biological Chemistry **272**(26): 16140-16146.

Yang, Y., G. He, W. Xu and X. Liu (2015). "ENaC mediates human extravillous trophblast cell line (HTR8/SVneo) invasion by regulating levels of matrix metalloproteinase 2 (MMP2)." Placenta **36**(5): 587-593.

Yanochko, G. M. and A. J. Yool (2002). "Regulated cationic channel function in Xenopus oocytes expressing Drosophila big brain." J Neurosci **22**(7): 2530-2540.

Yanochko, G. M. and A. J. Yool (2004). "Block by extracellular divalent cations of Drosophila big brain channels expressed in Xenopus oocytes." Biophys J **86**(3): 1470-1478.

Yasui, M., A. Hazama, T.-H. Kwon, S. Nielsen, W. B. Guggino and P. Agre (1999). "Rapid gating and anion permeability of an intracellular aquaporin." Nature **402**(6758): 184-187.

Yasui, M., T.-H. Kwon, M. A. Knepper, S. Nielsen and P. Agre (1999). "Aquaporin-6: An intracellular vesicle water channel protein in renal epithelia." Proceedings of the National Academy of Sciences **96**(10): 5808-5813.

Yool, A. J. (2007). "Dominant-negative suppression of big brain ion channel activity by mutation of a conserved glutamate in the first transmembrane domain." Gene Expr **13**(6): 329-337.

Yool, A. J., W. D. Stamer and J. W. Regan (1996). "Forskolin stimulation of water and cation permeability in aquaporin 1 water channels." Science **273**(5279): 1216-1218.

Yool, A. J. and A. M. Weinstein (2002). "New roles for old holes: ion channel function in aquaporin-1." News Physiol Sci **17**: 68-72.

Yool, A. J. and A. M. Weinstein (2002). "New roles for old holes: ion channel function in aquaporin-1." Physiology **17**(2): 68-72.

Yool, A. J. and A. M. Weinstein (2002). "New roles for old holes: Ion channel function in aquaporin-1." News in Physiological Sciences **17**: 68-72.

Yu, J., A. J. Yool, K. Schulten and E. Tajkhorshid (2006). "Mechanism of gating and ion conductivity of a possible tetrameric pore in aquaporin-1." Structure **14**(9): 1411-1423.

Zampighi, G. A., J. E. Hall and M. Kreman (1985). "Purified lens junctional protein forms channels in planar lipid films." Proceedings of the National Academy of Sciences **82**(24): 8468-8472.

Zhang, D. Y., Z. Ali, C. B. Wang, L. Xu, J. X. Yi, Z. L. Xu, X. Q. Liu, X. L. He, Y. H. Huang, I. A. Khan, R. M. Trethowan and H. X. Ma (2013). "Genome-wide sequence characterization and expression analysis of major intrinsic proteins in soybean (Glycine max L.)." PLoS One **8**(2): e56312.

Zhang, W., E. Zitron, M. Homme, L. Kihm, C. Morath, D. Scherer, S. Hegge, D. Thomas, C. P. Schmitt, M. Zeier, H. Katus, C. Karle and V. Schwenger (2007). "Aquaporin-1 channel function is positively regulated by protein kinase C." J Biol Chem **282**(29): 20933-20940.

Figure legends

Figure 1A: Crystal structure of an AQP1 monomer. Highlighted in blue is the loop D domain, in red is the double arginine residues at positions 159 and 160 (R159+R160) located within the loop D domain. The R159+R160 is the cGMP binding site, and the predicted AqB011, bacopaside I interaction sites (Yu, Yool et al. 2006, Kourghi, Pei et al. 2016, Pei, Kourghi et al. 2016). In cyan is Cysteine at position 189, which is the Mercury binding site (Preston, Jung et al. 1993). In magenta is the Tyrosine at position 186, serving as the TEA binding site (Brooks, Regan et al. 2000). In Yellow is the Threonine amino acids at position 157, and 239, acting as the PKC regulatory site (Zhang, Zitron et al. 2007), and in green is the N-terminal. Figure1B presents the membrane topology of AQP1 consisting of 5 membrane spanning helices, connected by 5 intracellular and extracellular loops (A and E extracellular, B, C, and D intracellular). The Asn-Pro-Ala (NPA) signature motif is located on loops B and E. The key regulatory sites presented in A is also highlighted in this figure with the addition of Tyrosine 259 (Y259), functioning as the Tyrosine phosphorylation site.

Figure 2: Two models for the proposed pathway for ion flow for AQP1, AtPIP2;1, BIB, AQP0 and AQP6 channels. The ion permeation for AQP1 and AtPIP2;1 channels is likely to be through the central pore, located at the middle of the tetramer subunits (Yool and Weinstein 2002, Yu, Yool et al. 2006, Byrt, Zhao et al. 2016), and water transport through the individual monomers (Jung, Preston et al. 1994, Preston, Jung et al. 1994). Whereas for BIB, AQP 0 and AQP6 ion permeation is predicted to be mediated through the individual intrasubunit pores (Yasui, Hazama et al. 1999,

Ikeda, Beitz et al. 2002, Yool 2007). Water permeation in all aquaporin channels is thought to occur primarily through the individual intrasubunit pores, with exceptions of the Big Brain channel which shows no appreciable water permeability (Yanochko and Yool 2004).

Figure 3: AqB011 is a specific blocker of AQP1 ion channel and impairs cancer cell migration in HT29 cancer cells (Kourghi, Pei et al. 2016). AqB011 is predicted to bind with loop D domain of the channel. Bottom panel: view of the putative binding of the ligand indicating interaction with two conserved arginine residues in the loop D gating domain.

Figure 4: Live cell-imaging assay showing the effects of AQP1 water channel blocker bacopaside II on HT29 colon cancer cells motility and migration. Circular wounds were created on confluent monolayers of HT29 cancer cells. Single cells at the edge of the wounds were tracked with time lapse images taken over 24 hour periods for cells treated with and without 15 μM bacopaside II. For clarity only images at 8 hour intervals are shown. White arrows indicate a single cell for each treatment at 0 hours, and follow the same cell in each subsequent frame. It is clear that cells treated with bacopaside II exhibit a reduced level of migration and movement as compared to untreated cells.

Figure 5: Amino acid alignment comparing the loop D region between BIB, hAQP1, AtPIP2;1 AtPIP2;2 and AtPIP2;7. The predicted interaction site of AqB011 in the

preserved poly Arginine box present in hAQP1, is absent in BIB, AtPIP2;1 AtPIP2;2 and AtPIP2;7 Aquaporins.

Figures

Figure 1

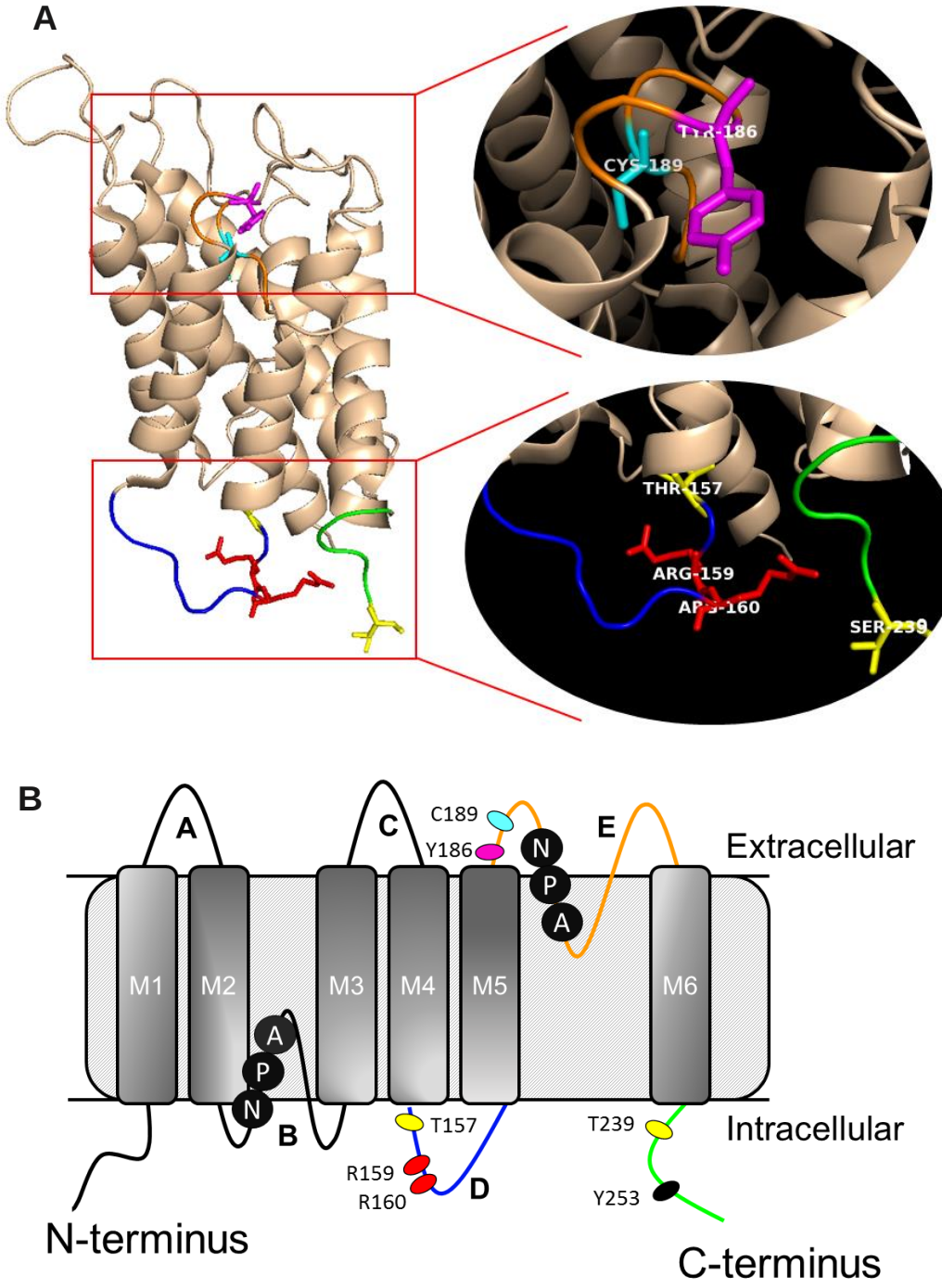

Figure 2

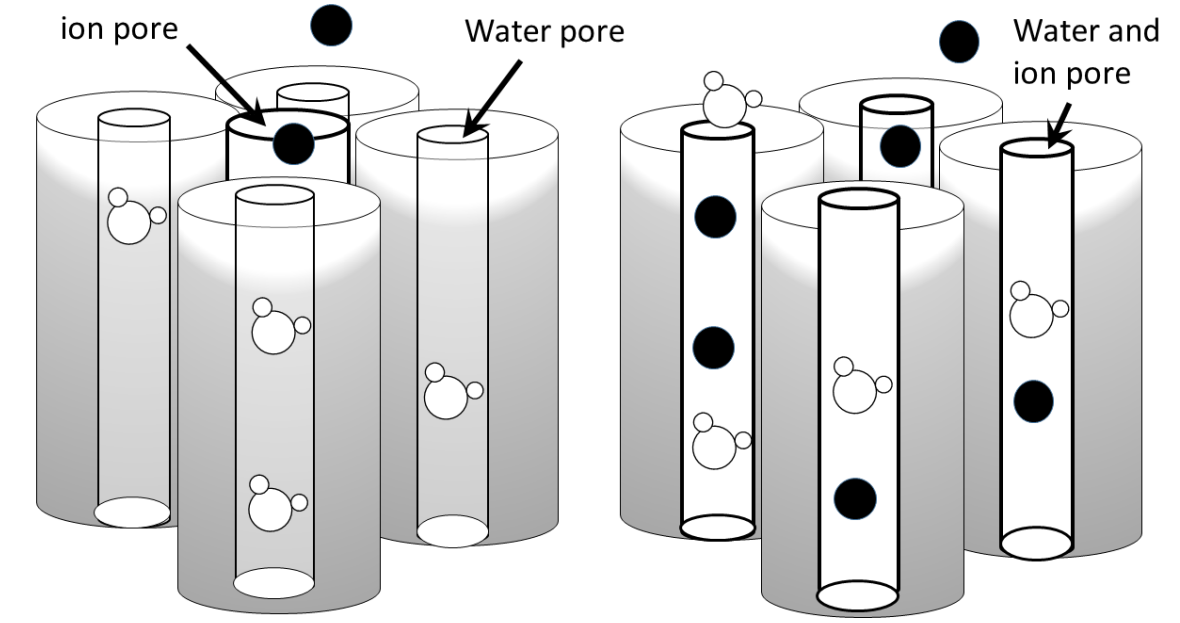
ion pore
Water pore
Water and
ion pore
AQP1, AtPIP2;1
BIB, AQP0, AQP 6

Figure 3

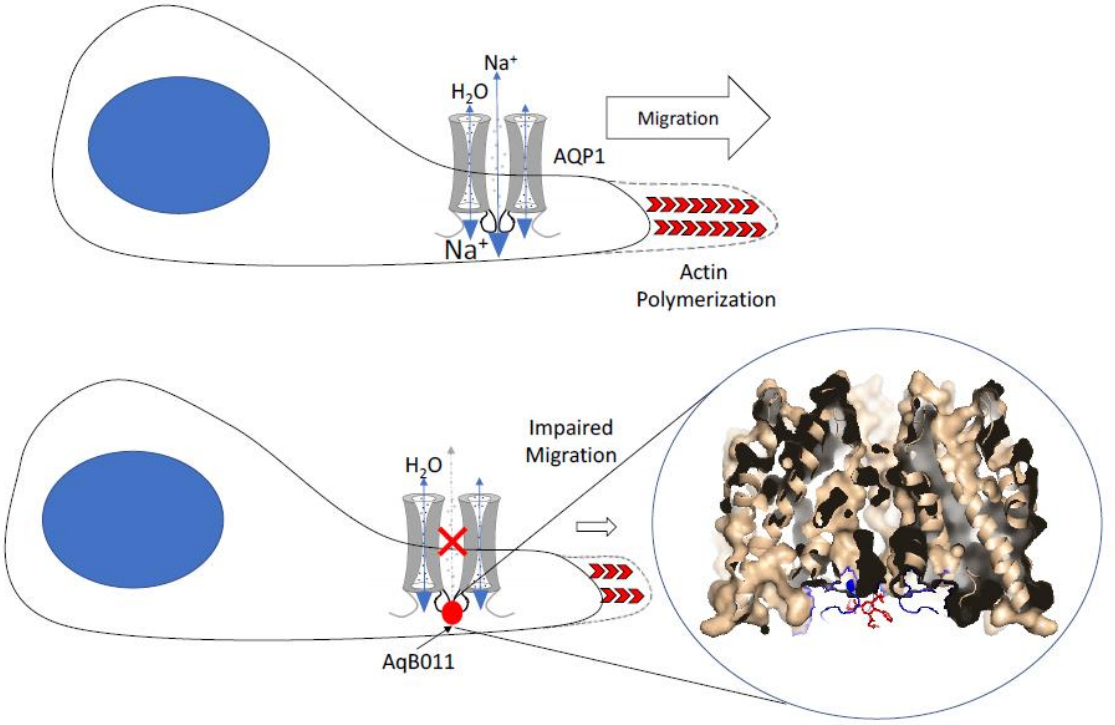
Na+
H2O
Migration
AQP1
Na+
Actin
Polymerization
Impaired
Migration
H2O
AqB011

Figure 4

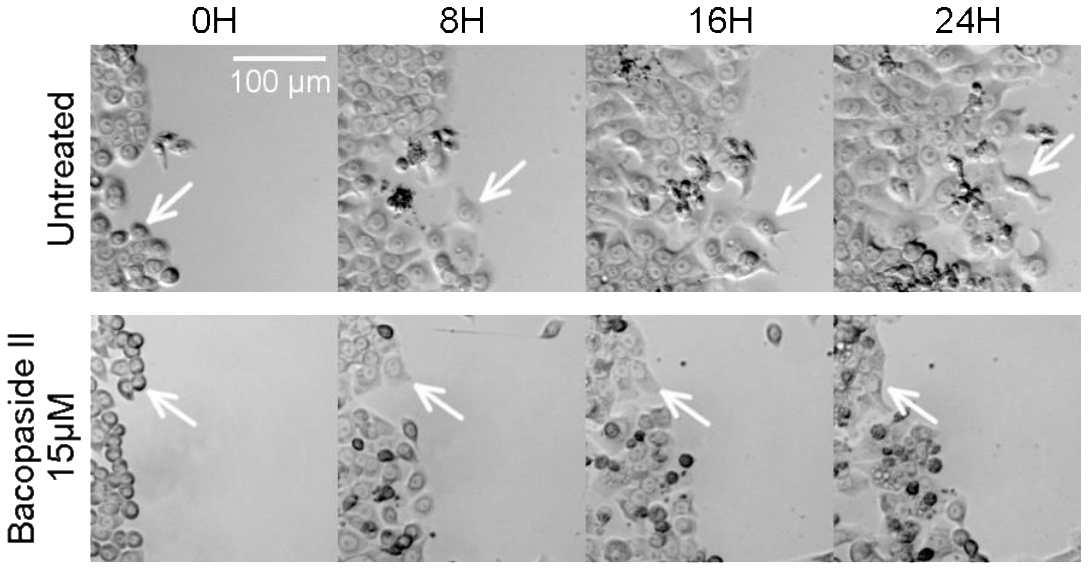

Figure 5


BIB GNLQAAISHSAALAAWERFGVEFILTFLVVLCYFVSTDPMKKFMGN-----SAASIGCAY
hAQP1 GNSLGRNDLADGVNSGQGLGIEIIGTLQLVLCVLATTDRRRRD----LGGSAPLAIGLSV
AtPIP2;7 TLGGGANTVADGYSKGTALGAEIIGTFVLVYTVFSATDPKRSARDSHIPVLAPLPIGFAV
AtPIP2;1 RYGGGANSLADGYSTGTGLAAEIIGTFVLVYTVFSATDPKRSARDSHVPVLAPLPIGFAV
AtPIP2;2 RYGGGANSLADGYNTGTGLAAEIIGTFVLVYTVFSATDPKRNARDSHVPVLAPLPIGFAV

Statement of Authorship

Title of Paper	Bumetanide derivatives AqB007 and AqB011 selectively block the aquaporin-1 ion channel conductance and slow cancer cell migration
Publication Status	☐ Published ☐ Accepted for Publication ☐ Submitted for Publication ☐ Unpublished and Unsubmitted w ork w ritten in manuscript style
Publication Details	Kourghi M, Pei JV, De Ieso ML, Flynn G, and Yool AJ (2016) Bumetanide derivatives AqB007 and AqB011 selectively block the aquaporin-1 ion channel conductance and slow cancer cell migration. Mol Pharmacol 89:133–140.

Principal Author

Name of Principal Author (Candidate)	Jinxin Pei and Mohamad Kourghi
Contribution to the Paper	Co-first authors, initiated and performed experiments, analysis on all samples, interpreted data, wrote the manuscript.
Overall percentage (%)	80%
Certification:	This paper reports on original research I conducted during the period of my Higher Degree by Research candidature and is not subject to any obligations or contractual agreements with a third party that would constrain its inclusion in this thesis. I am the primary author of this paper.
Signature	Date 23/5/17

Co-Author Contributions

By signing the Statement of Authorship, each author certifies that:

i. the candidate's stated contribution to the publication is accurate (as detailed above);

ii. permission is granted for the candidate in include the publication in the thesis; and

iii. the sum of all co-author contributions is equal to 100% less the candidate's stated contribution.

Name of Co-Author	Michael L. De Ieso
Contribution to the Paper	Performed the experiment and wrote the manuscript.
Signature	Date 23/5/17

Name of Co-Author	Gary Flynn
Contribution to the Paper	Developed the new research tool.
Signature	Date 5/26/2017

Please cut and paste additional co-author panels here as required.

Name of Co-Author	Andrea J. Yool		
Contribution to the Paper	Contributed to experimental design, and reviewing the manuscript.		
Agreed contribution percentage (%)	10%		
Signature		Date	23 May 2017

Chapter 2: Bumetanide Derivatives AqB007 and AqB011 Selectively Block the Aquaporin-1 Ion Channel Conductance and Slow Cancer Cell Migration[S]

Mohamad Kourghi, Jinxin V Pei, Michael L De Ieso, Gary Flynn, and Andrea J Yool

School of Medicine, University of Adelaide; Adelaide SA 5005 Australia (MK, JVP, MLDI, AJY)

Institute for Photonics and Advanced Sensing, University of Adelaide; Adelaide SA 5005 Australia (JVP, AJY)

Spacefill Enterprises LLC; Oro Valley, Arizona 85704 USA (GF)

Corresponding author: Prof Andrea Yool; Medical School South, level 4, Frome Rd, University of Adelaide, Adelaide SA 5005 Australia

andrea.yool@adelaide.edu.au ph: +61 8 8313 3359 fax: +61 8 8313 5384

ABBREVIATIONS: AqB, aquaporin ligand bumetanide derivative (in numbered series); AQP1, aquaporin-1; DMSO, dimethylsulfoxide; EtOAC, ethyl acetate; MW, molecular weight.

Abstract

Aquaporins (AQPs) in the major intrinsic family of proteins mediate fluxes of water and other small solutes across cell membranes. AQP1 is a water channel, and under permissive conditions, a nonselective cation channel gated by cGMP. In addition to mediating fluid transport, AQP1 expression facilitates rapid cell migration in cell types including colon cancers and glioblastoma. Work here defines new pharmacological derivatives of bumetanide that selectively inhibit the ion channel but not the water channel activity of AQP1. Human AQP1 was analyzed in the *Xenopus laevis* oocyte expression system by two-electrode voltage clamp and optical osmotic swelling assays. AqB011 was the most potent blocker of the AQP1 ion conductance (IC_{50} 14 μM) with no effect on water channel activity (at up to 200 μM). The order of potency for inhibition of the ionic conductance was AqB011> AqB007>> AqB006≥ AqB001. Migration of human colon cancer (HT29) cells was assessed with a wound-closure assay in presence of a mitotic inhibitor. AqB011 and AqB007 significantly reduced migration rates of AQP1-positive HT29 cells without affecting viability. The order of potency for AQP1 ion channel block matched the order for inhibition of cell migration, as well as *in silico* modeling of the predicted order of energetically favored binding. Docking models suggest that AqB011 and AqB007 interact with the intracellular loop D domain, a region involved in AQP channel gating. Inhibition of AQP1 ionic conductance could be a useful adjunct therapeutic approach for reducing metastasis in cancers that upregulate AQP1 expression.

Introduction

Osmotic water transport across biological membranes is facilitated via membrane proteins known as aquaporins (AQPs), found in all kingdoms of life (Reizer, Reizer et al. 1993, Park and Saier 1996, Campbell, Ball et al. 2008). To date, at least fifteen mammalian subfamilies have been identified, AQP0-AQP14 (Ishibashi 2009, Finn, Chauvigne et al. 2014) . Aquaporin is organised as a tetramer of subunits, each comprising six transmembrane domains and five loops (A to E), and carrying a monomeric pore that allows the movement of water or other small solutes (Jung, Bhat et al. 1994, Fu, Libson et al. 2000, Sui, Han et al. 2001).

There is increasing recognition that certain classes of aggressive cancers depend on upregulation of AQP1 for fast migration and metastasis (Monzani, Shtil et al. 2007). Though the precise mechanism for AQP1-enhanced motility remains unknown, both ion channels and water channels are essential in the cellular migration process (Schwab, Nechyporuk-Zloy et al. 2007). AQP1 expression has been linked to metastasis and invasiveness of colon cancer cells (Jiang 2009, Yoshida, Hojo et al. 2013). In mammary and melanoma cancer cells, AQP1 facilitates tumor cell migration in vitro and metastasis in vivo (Hu and Verkman 2006). Increased levels of AQP1 expression in astrocytoma correlate with clinical grade, serving as a diagnostic indicator of poor prognoses (El Hindy, Bankfalvi et al. 2013). AQP1-facilitated cell migration in glioma cannot be substituted by AQP4, indicating more than simple water channel function is involved in the migration-enhancing mechanism (McCoy and Sontheimer 2007).

A subset of aquaporins have been shown to have ion channel function, including AQP0, AQP1, AQP6, plant nodulin, and *Drosophila* Big Brain (Yool and Campbell 2012). In AQP1, multiple lines of evidence have shown the cGMP-dependent monovalent cation channel is located in the central pore at the four-fold axis of symmetry, and is pharmacologically distinct from the monomeric water pores (Anthony, Brooks et al. 2000, Saparov, Kozono et al. 2001, Boassa and Yool 2003, Yu, Yool et al. 2006, Zhang, Zitron et al. 2007). The AQP1 ion channel has a unitary conductance of 150 pS in physiological saline, slow activation and deactivation kinetics, and is permeable to Na^+, K^+, and Cs^+ but not divalent cations (Yool, Stamer et al. 1996, Anthony, Brooks et al. 2000). Loop D has been shown previously to be involved in cGMP-dependent gating of AQP1 ion channels (Yu, Yool et al. 2006). The low proportion of AQP1 water channels available to be gated as ion channels in reconstituted bilayers and heterologous expression systems has prompted uncertainty regarding the physiological relevance of the dual water and ion channel function in AQP1 (Saparov, Kozono et al. 2001, Tsunoda, Wiesner et al. 2004). Further work has indicated that the availability of AQP1 ion channels to be activated by cGMP depends in part on tyrosine phosphorylation at the carboxyl terminal domain (Campbell, Birdsell et al. 2012).

Our characterization here of selective non-toxic pharmacological blockers of the AQP1 ion channel opens the first opportunity to define the functional roles of the AQP1 ion conductance. Prior to 2009, available AQP1 blockers were limited by low potency, lack of specificity, or toxicity. Mercury potently blocks AQP1 water permeability by covalent modification of a cysteine residue in loop E (Preston, Jung

et al. 1993) but is highly toxic. Tetrethylammonium ion blocks the AQP1 water pore though not in all cell types (Brooks, Regan et al. 2000, Detmers, de Groot et al. 2006, Sogaard and Zeuthen 2008), and cadmium ion blocks the AQP1 ion channel (Boassa, Stamer et al. 2006); but both lack selectivity for aquaporins. Effective compounds discovered recently include the arylsulfonamides AqB013 which blocks AQP1 and AQP4 water channel permeability (Migliati, Meurice et al. 2009), and AqF026 which strongly potentiates AQP1 water channel activity (Yool, Morelle et al. 2013). Other arylsulfonamides have been proposed as blockers of AQP4 channels (Huber, Tsujita et al. 2009). A distinct class of agents acting on the external side of the membrane to block human AQP1 water flux has been identified as a source of candidate lead compounds for drug development (Seeliger, Zapater et al. 2013).

Work here characterizes a novel set of AqB compounds (*Aq:* aquaporin ligand; *B:* bumetanide derivative) that differentially block the AQP1 ion channel without affecting water permeability. The most potent of these, AqB011, is a promising tool for dissecting the role of the AQP1 ion channel, while sparing osmotic water permeability. Understanding functional roles and regulation of AQP1 is essential for determining the full range of physiological roles it might serve, and its possible value as a therapeutic target in cancer metastasis.

Materials and Methods

Oocyte preparation and injection

The use of animals in this study has been carried out in accord with the Guide for the Care and Use of Laboratory Animals, licensed under the South Australian Animal Welfare Act 1985, with protocols approved by University of Adelaide Animal Ethics Committee. Unfertilized oocytes were harvested from anesthetized *Xenopus laevis* frogs and defoliculated by incubation in Type 1A collagenase (2 mg/ml) with trypsin inhibitor (0.3 mg/ml) in OR-2 saline (82 mM NaCl, 2.5 mM KCl, 1 mM $MgCl_2$, 5 mM HEPES; pH 7.3) at 16-18°C for 2-3 hours. Human Aquaporin-1 cDNA was provided by Prof P Agre (Preston et al., 1992; GenBank accession number NM_198098). AQP1 subcloned into a *X. laevis* □-globin plasmid was linearized with BamHI and transcribed in vitro (T3 mMessage mMachine; Ambion Inc., Austin TX USA), and cRNA was resuspended in sterile water. Prepared oocytes were injected with 50 nl of water (non-AQP1-expressing control oocytes), or 50 nl of water containing 1 ng of AQP1 cRNA, and incubated for 2 or more days at 16°C in ND96 saline (96 mM NaCl, 2 mM KCl, 1 mM $MgCl_2$, 1.8 mM $CaCl_2$, 5 mM HEPES, pH 7.3) to allow protein expression. Successful expression was confirmed by osmotic swelling assays. Batches of AQP1-expressing oocytes which lacked robust cGMP-activated conductance responses were further incubated overnight in ND96 saline with the tyrosine phosphatase inhibitor bisperoxovanadium (100 μM; Santa Cruz Biotechnology, Dallas TX USA) as per published methods (Campbell, Birdsell et al. 2012). Chemicals were purchased from Sigma-Aldrich (St. Louis MO USA) unless otherwise specified.

AqB compounds: synthesis and preparation

The AqB compounds (custom-designed bumetanide derivatives) were synthesized by Dr G Flynn (Spacefill Enterprises LLC, Oro Valley AZ USA) as described in US-8,835,491-B2. To make AqB001, bumetanide was mixed with diazomethane (CH_2N_2) generated by reaction with Diazald® to create bumetanide methyl ester (MW 344.8; ClogP 2.10), which was dissolved in hot $CHCl_3$, diluted with hexanes, and allowed to cool to provide the purified methyl ester as white flakes, whose mass and NMR spectra were consistent with the desired product. Reaction of bumetanide with 1.2 equivalents of 1,1'-carbonyldiimidazole (CDI) in ethyl acetate (EtOAC) under argon with heating afforded an intermediate imidazolide, which upon cooling formed a white solid that could be isolated by filtration and stored under argon for later use. Alternatively, the imidazolide solution could be reacted in situ with 2 equivalents of an amine to form the corresponding amides. In a typical reaction, the reaction mixture would be partitioned between water and ethyl acetate (EtOAc), the organic layer washed with brine, the solution filtered and concentrated, and the residue crystalized to form EtOAc/hexanes. AqB-006 (MW 413.9; ClogP 1.04) was prepared using morpholine as the amine; AqB007 (MW 470.0; ClogP 0.79) resulted from 2-(4-methylpiperazine-1-yl) ethylamine; and AqB011 (MW 434.9; ClogP 1.80) was prepared using 2-(morpholine-1-yl)ethylamine. The structures of all compounds were confirmed by high resolution mass spectrometry and NMR analysis. Chemicals were purchased from Sigma-Aldrich (St. Louis MO USA) unless otherwise specified.

Powdered compounds were dissolved in dimethyl sulfoxide (DMSO) to create 1000x stock solutions for each desired final dosage. An equal dilution of DMSO (0.1%) alone in saline was used as the vehicle control.

Quantitative Swelling Assay

For double-swelling assays, each oocyte served as its own control. Swelling rates were assayed first without drug treatment (S1), then oocytes incubated for 2 h in isotonic saline with or without the AqB compounds were reassessed in a second swelling assay (S2). Swelling rates in 50% hypotonic saline (isotonic Na saline diluted with an equal volume of water) were quantified by relative increases in oocyte cross-sectional area imaged by videomicroscopy (charge-coupled device camera; Cohu, San Diego, CA) at 0.5 frames per second for 30s using NIH ImageJ software. Rates were measured as slopes of linear regression fits of relative volume as a function of time using Prism (GraphPad Software Inc., San Diego CA USA).

Electrophysiology

For two-electrode voltage clamp, capillary glass electrodes (1–3 MΩ) were filled with 1 M KCl. Recordings were done in standard Na^+ bath saline containing 100 mM NaCl, 2 mM KCl, 4.5 mM $MgCl_2$, and 5 mM HEPES, pH 7.3. cGMP was applied extracellularly at a final concentration of 10-20 μM using the membrane-permeable cGMP analog [Rp]-8-[para-chlorophenylthio]-cGMP. Ionic conductance was monitored for at least 20 min after cGMP addition to allow development of maximal plateau responses. Conductance was determined by voltage step protocols from +60

to -110mV from a holding potential of -40 mV. Recordings were made with a GeneClamp amplifier and pClamp 9.0 software (Molecular Devices, Sunnyvale CA USA).

Circular Wound Closure Assay

The cancer cell lines used in this study were HT29 human colorectal adenocarcinoma cells (Chen, Drabkowski et al. 1987) purchased from ATCC (HTB-38; American Type Culture Collection; Manassas VA USA) which strongly express endogenous AQP1; and SW480 human colorectal adenocarcinoma cells (CCL-228; from ATCC) which express AQP5 but show little AQP1 expression. mRNA levels were evaluated by quantitative PCR and protein levels by western blot (H Dorward et al., MS in review). Confluent cultures of HT29 and SW480 cells were used in migration assays to measure effects of AqB treatments on rates of wound closure. Cells were plated in flat-bottom 96-well plates at 1.25×10^5 cells/well in DMEM media with 10% fetal bovine serum, and incubated at 37°C and 5% CO_2 for 12-18 hours to allow monolayer formation. Circular wounds were created by aspirating a central circle of cells with a p10 pipette. Wells were washed 2-3 times with phosphate-buffered saline to remove cell debris. Culture media (DMEM with 2% bovine calf serum) containing either vehicle or drug treatments in the presence of a mitotic inhibitor 5-fluoro-2'-deoxyuridine (100 ng/ml) were administered into the wells. Cultures were imaged at 0 and 24 h, and analysed using ImageJ software to calculate percent wound closure by the change in area:

$((Area_0 – Area_{24})/Area_0) \times 100$

Cytotoxicity Assay

Cell viability was quantified using the AlamarBlue cell viability assay (Molecular Probes, Eugene OR USA). Cells were plated at 10^4 cells/well in 96-well plates, and fluorescence signal levels were measured with a FLUOstar Optima microplate reader after 24 h incubation with concentrations of AqB011 from 1 to 80 μM, to obtain quantitative measures of cell viability. Mercuric chloride (20 μM) was used as a positive control for cytotoxicity.

Molecular Modelling

In silico modeling was conducted with methods reported previously (Yool, Morelle et al. 2013). The crystal structure of human AQP1 was obtained from the Protein Data Bank (PDB ID: 1FQY). The tetrameric model (Supplemental Data) was generated in Pymol (Version 1.7.4 Schrödinger, LLC) using coordinates provided in the pdb file. Renderings of the AqB ligands were generated in Chemdraw (Version 13.0, PerkinElmer), then converted into pdb format using the on-line SMILES translation tool (National Cancer Institute, US Dept Health and Human Services). Both AQP1 and ligand coordinates were prepared for docking using MGLtools (Version 1.5.4, Scripps Institute, San Diego CA USA). The docking was carried using Autodock Vina (Trott and Olson 2010) with a docking grid covering the intracellular face of tetrameric pore.

Data Compilation and Statistics

Results compiled from replicate experiments are presented as box plots. The boxes represent 50% of the data, the error bars indicate the full range, and the horizontal

bars are the median values. n values are in italics above the x-axis. Statistical differences were analyzed with one-way ANOVA and post-hoc Bonferroni tests and reported as ** $p < 0.0001$, * $p < 0.05$, and not significant (NS; $p > 0.05$).

Results

AQP1 ion channel inhibition by novel bumetanide derivatives

A set of four related compounds with structural modifications at the carboxylic acid moiety of bumetanide were tested for effects on the cGMP-activated ionic conductance in AQP1-expressing oocytes. Two-electrode voltage clamp recordings of AQP1-expressing oocytes (**Figure 1**) illustrate inhibition of the ionic conductance by extracellular application of AqB007 (200 μM) and AqB011 (20 μM), but no appreciable block of the AQP1 ion channel with 200 μM AqB001 or AqB006. Initial recordings before cGMP application, and responses to the first application of cGMP recordings showed typical cGMP-dependent activation, as described previously (Anthony, Brooks et al. 2000). Oocytes were then transferred into saline with the indicated agents for 2 hours, during which time the ionic conductances uniformly recovered to initial levels (**Figure 2**). In response to the second application of cGMP, oocytes treated with vehicle (DMSO), AqB001 or AqB006 showed increases in conductance comparable to the first response. However, the cGMP-activated conductance responses were inhibited after treatment with AqB007 or AqB011.

Trend plots (**Fig 2A**) show that the ionic conductance in AQP1-expressing oocytes was initially low, and was activated by the first bath application of membrane permeable cGMP. The ionic conductance then recovered to basal level during a 2h incubation without cGMP, and was tested for reactivation by a second application of

cGMP after treatment with vehicle or AqB compounds. Recordings for oocytes incubated in saline without DMSO during the recovery period were comparable to those for the DMSO-treated group (not shown). Non-AQP1-expressing control oocytes showed no ionic conductance response to cGMP and no effect of the vehicle or drug treatments (**Fig 2B**).

Compiled data for the cGMP-activated ionic conductance values in AQP1-expressing oocytes are shown in the box plot (**Fig 3A**), and indicate the levels of block by 200 μM AqB007 and 20 μM AqB011 were statistically significant as compared with vehicle treated AQP1-expressing oocytes. Dose-response relationships (**Fig 3B**) yielded estimated IC_{50} values of 14 μM for AqB011 and 170 μM for AqB007.

AqB ion channel blockers have no effect on osmotic water permeability

Data for oocyte volumes standardized as a percentage of initial volume at time zero illustrate the mean swelling responses over 60 seconds after introduction of the oocytes into 50% hypotonic saline (**Fig 4A**). AQP1-expressing oocytes showed consistent osmotic swelling which was unaffected by treatment with vehicle (DMSO 0.1%) or AqB compounds at 200 μM each. Non-AQP1-expressing control oocytes showed little osmotic water permeability.

To analyze possible effects of the AqB compounds on water channel activity, a double-swelling assay was used (**Fig 4B**). After the first swelling (S1) in hypotonic saline, oocytes were incubated in isotonic saline with or without the AqB compounds (200 μM) for 2 h before assessing the second swelling response (S2). There were no significant differences between the first and second swelling rates in any of the

treatment groups, confirming that the AqB ion channel agents did not affect AQP1 osmotic water permeability.

Molecular modelling of candidate intracellular binding sites

Putative binding sites on the AQP1 ion pore for AqB011 and AqB007 in the intracellular loop D domain can be suggested based on structural modelling and docking analyses (**Figure 5**). In silico modeling suggested the sites for the most favorable energies of interaction for AqB007 and AqB011 were located at the intracellular face of the central pore (**Fig 5A**). Interestingly, the model predicted hydrogen bonding between the uniquely elongated moieties of the two effective AqB ligands and the initial pairs of arginine residues in the highly conserved loop D motifs from two adjacent subunits (**Fig 5B**); the same arginines (R159 and R160 in human AQP1) have been shown to be involved in AQP1 ion channel gating but not water channel activity in prior work (Yu, Yool et al. 2006). The more compact AqB006 docked weakly at a different position in the central vestibule (not shown). While in silico modeling does not define actual binding sites, it provides a testable hypothesis for future work, and offers intriguing support for the role of loop D in modulating AQP1 ion channel gating. The most favorable energy of interaction was calculated for AqB011 (at -9.2 kcal/mol). The next most favorable energy of interaction for AqB compounds with the AQP1 channel was for AqB007 (at -7.0 kcal/mol), followed by AqB006 (at -6.0 kcal/mol). This order of interaction strength for the AqB series matched their order of efficacy for inhibition of the AQP1 ion channel conductance (Figure 3).

Inhibition of AQP1 ion channel activity slows cancer cell migration

The effects of AqB006, AqB007 and AqB011 were tested in migration assays of human HT29 colon cancer cells (**Figure 6**) which natively express AQP1. Net migration rates were calculated from the percent closure of a circular wound area at 24 h (**Fig 6A**). Results showed that cancer cell migration was not impaired by AqB006, but was impaired significantly by AqB007 at 100 μM, and AqB011 at 50 μM and 100 μM, as compared with vehicle-treated control HT29 cells (**Fig 6B**). AqB011 was more effective than AqB007 in blocking migration, consistent with relative efficacies of the agents as blockers of the ion channel conductance. In contrast, AqB011 at 100 μM had no effect on the migration rate of SW480 colon cancer cells (**Fig. 6B**) which express AQP5, but not AQP1, suggesting that the inhibitory effect of AqB011 appears to be selective for AQP1.

AqB compounds show low cytotoxicity

There was no significant difference in viability between vehicle-treated and untreated cells, and no effect of treatment with AqB011 for HT29 cells (**Table 1**). Cell viability was assessed with alamarBlue assays. The persistence of the fluorescent signal at 24 h confirmed there was no appreciable cytotoxic effect of AqB011 treatment on HT29 cells at concentrations up to 80 μM. Mercuric chloride as a positive control caused significant cell death, measured as a decrease in fluorescence. AqB011 at doses used to block the AQP1 ionic conductance and cancer cell migration did not impact cell viability.

Discussion

The aim of this study was to search for selective small-molecule pharmacological agents capable of blocking the cGMP-activated cationic conductance in AQP1. Discovery of pharmacological modulators for AQP1 channels has been an important goal in the aquaporin field. AQP1 antagonist and agonist agents are expected to be useful for defining the complex roles of aquaporins in fundamental biological processes, as well as for characterizing AQP1 modulators as potential clinical agents in various conditions, such as cancer metastasis (Yool, Brown et al. 2009). AQP1 expression is upregulated in subtypes of aggressive cancer cells in which it facilitates cancer migration. Results here show that selective blockers of the AQP1 ion channel slow migration of human colon cancer cells in culture. Pharmacological inhibition of AQP1 is predicted to have a protective effect in reducing metastasis in cancer, but remains to be demonstrated in vivo.

Using bumetanide as a starting scaffold, we created an array of novel synthetic derivatives. Based on pilot data indicating a small inhibitory effect of AqB050 on the AQP1 ion channel at high doses (unpublished observations), we investigated a series of structurally related derivatives AqB006, AqB007, and AqB011, as well as a simple methylated version of bumetanide AqB001, to test for possible inhibitors of the AQP1 ionic conductance. Our findings demonstrated that AqB007 and AqB011 are effective inhibitors of the central ion pore of AQP1, with estimated IC_{50} values of 170 and 14 µM, respectively. Both AqB007 and AqB011 showed dose-dependent inhibition of the central ion pore, whereas the intrasubunit water pores were unaffected, enabling the first dissection of physiological roles of the distinct channel

functions. Measuring fluorescence signal intensity with the alumarBlue cell viability assay showed that AqB011 was not cytotoxic at doses that produced maximal ion channel inhibition.

The inhibition by AqB011 of AQP1 ionic conductance was consistent with molecular docking studies suggesting the site of interaction is at the intracellular face of the central pore. Results revealed that AqB011 is the most energetically favored compound followed by AqB007. The predicted interaction site of AqB011 and AqB007 with AQP1 is at the loop D domain. Differences in the structures and efficacies of AqB006, AqB007 and AqB011 indicate that the structure-activity relationship of ion channel inhibition is sensitive to specific chemical modifications at the carboxylic acid position of bumetanide. The length and structure of the modification appears to be critical, and appears based on in silico modeling to be the region that interacts with the AQP1 channel gating loop D domain. The absence of cytotoxic effects of AqB011 at doses sufficient to block the AQP1 ion channel activity indicates that the inhibition of migration is not due indirectly to cell death. The observation that AqB011 inhibited migration in AQP1-expressing HT29 colon cancer cells, but had no effect on the migration of AQP-5 expressing SW480 colon cancer cells provides support for the idea that AqB011 is selective for AQP1. The inhibition of migration seen with AqB011 is unlikely to result from off-target effects on general metabolic function, cytoskeletal organization, actin polymerization, or signaling pathways involved in cell motility, since SW480 cell migration remained unaffected by the presence of AqB011.

AQP1 is present in barrier epithelia involved in fluid movement in the body, including proximal tubule and choroid plexus (Agre, Preston et al. 1993). It is also expressed in peripheral microvasculature, dorsal root ganglion cells, eye ciliary epithelium and trabecular meshwork, heart ventricle, and other regions in which a direct role for osmotic water flux is less evident (Yool 2007). Additional roles suggested for AQP1 include angiogenesis (Nicchia, Stigliano et al. 2013); signal transduction (Oshio, Watanabe et al. 2006); increased mechanical compliance to changes in pressure (Baetz, Hoffman et al. 2009); axonal regeneration of spinal nerves (Zhang and Verkman 2015); recovery from injury (Hara-Chikuma and Verkman 2006); and exocytosis (Arnaoutova, Cawley et al. 2008). Relative contributions of the ion and the water channel functions in these diverse processes remain to be defined.

A possible role for the AQP1 ionic conductance (potentially in combination with water fluxes) in the control of cell volume associated with migration was supported by the results of the wound closure assays with AQP1-expressing HT29 cells. Cell migration was significantly impaired by AqB011 and AqB007, but not by AqB006. The greatest efficacy of migration block was seen with administration of AqB011. The comparable orders of efficacy for block of AQP1 ion channels in the oocyte expression system, and for block of cell migration in HT29 cultures, support the idea that the AqB011 effect on migration is mediated by block of the AQP1 ion channels directly. These data provide evidence that the ion channel activity of AQP1 has physiological relevance. Further work is needed to evaluate effects of blocking both water and ion channel activities of AQP1 together in migrating cells.

AqB011 is a new research tool for probing the physiological role of the AQP1 ion channel function in biological systems. This compound holds future promise as a possible adjunct clinical intervention in cancer metastasis. Exciting opportunities are likely to emerge from continuing discovery of pharmacological modulators for aquaporins for new treatments in cancers and other diseases.

Authorship Contributions

Participated in research design: Kourghi, Pei, De Ieso, Yool

Conducted experiments: Kourghi, Pei, De Ieso

Contributed new reagents or analytic tools: Flynn

Performed data analysis: Kourghi, Pei, De Ieso, Yool

Wrote or contributed to the writing of the manuscript: Kourghi, Pei, Flynn, Yool

References

Agre P, Preston GM, Smith BL, Jung JS, Raina S, Moon C, Guggino WB and Nielsen S (1993) Aquaporin CHIP: the archetypal molecular water channel. *Am J Physiol* **265**(4 Pt 2):F463-476.

Anthony TL, Brooks HL, Boassa D, Leonov S, Yanochko GM, Regan JW and Yool AJ (2000) Cloned human aquaporin-1 is a cyclic GMP-gated ion channel. *Mol Pharmacol* **57**(3):576-588.

Arnaoutova I, Cawley NX, Patel N, Kim T, Rathod T and Loh YP (2008) Aquaporin 1 is important for maintaining secretory granule biogenesis in endocrine cells. *Molecular endocrinology* **22**(8):1924-1934.

Baetz NW, Hoffman EA, Yool AJ and Stamer WD (2009) Role of aquaporin-1 in trabecular meshwork cell homeostasis during mechanical strain. *Experimental eye research* **89**(1):95-100.

Boassa D, Stamer WD and Yool AJ (2006) Ion channel function of aquaporin-1 natively expressed in choroid plexus. *J Neurosci* **26**(30):7811-7819.

Boassa D and Yool AJ (2003) Single amino acids in the carboxyl terminal domain of aquaporin-1 contribute to cGMP-dependent ion channel activation. *BMC Physiol* **3**:12.

Brooks HL, Regan JW and Yool AJ (2000) Inhibition of aquaporin-1 water permeability by tetraethylammonium: involvement of the loop E pore region. *Mol Pharmacol* **57**(5):1021-1026.

Campbell EM, Ball A, Hoppler S and Bowman AS (2008) Invertebrate aquaporins: a review. *J Comp Physiol B* **178**(8):935-955.

Campbell EM, Birdsell DN and Yool AJ (2012) The activity of human aquaporin 1 as a cGMP-gated cation channel is regulated by tyrosine phosphorylation in the carboxyl-terminal domain. *Mol Pharmacol* **81**(1):97-105.

Chen TR, Drabkowski D, Hay RJ, Macy M and Peterson W, Jr. (1987) WiDr is a derivative of another colon adenocarcinoma cell line, HT-29. *Cancer Genet Cytogenet* **27**(1):125-134.

Detmers FJ, de Groot BL, Muller EM, Hinton A, Konings IB, Sze M, Flitsch SL, Grubmuller H and Deen PM (2006) Quaternary ammonium compounds as water channel blockers. Specificity, potency, and site of action. *J Biol Chem* **281**(20):14207-14214.

El Hindy N, Bankfalvi A, Herring A, Adamzik M, Lambertz N, Zhu Y, Siffert W, Sure U and Sandalcioglu IE (2013) Correlation of aquaporin-1 water channel protein expression with tumor angiogenesis in human astrocytoma. *Anticancer research* **33**(2):609-613.

Finn RN, Chauvigne F, Hlidberg JB, Cutler CP and Cerda J (2014) The lineage-specific evolution of aquaporin gene clusters facilitated tetrapod terrestrial adaptation. *PLoS One* **9**(11):e113686.

Fu D, Libson A, Miercke LJ, Weitzman C, Nollert P, Krucinski J and Stroud RM (2000) Structure of a glycerol-conducting channel and the basis for its selectivity. *Science* **290**(5491):481-486.

Hara-Chikuma M and Verkman AS (2006) Aquaporin-1 facilitates epithelial cell migration in kidney proximal tubule. *Journal of the American Society of Nephrology : JASN* **17**(1):39-45.

Hu J and Verkman AS (2006) Increased migration and metastatic potential of tumor cells expressing aquaporin water channels. *FASEB journal : official publication of the Federation of American Societies for Experimental Biology* **20**(11):1892-1894.

Huber VJ, Tsujita M and Nakada T (2009) Identification of aquaporin 4 inhibitors using in vitro and in silico methods. *Bioorg Med Chem* **17**(1):411-417.

Ishibashi K (2009) New members of mammalian aquaporins: AQP10-AQP12. *Handb Exp Pharmacol*(190):251-262.

Jiang Y (2009) Aquaporin-1 activity of plasma membrane affects HT20 colon cancer cell migration. *IUBMB Life* **61**(10):1001-1009.

Jung JS, Bhat RV, Preston GM, Guggino WB, Baraban JM and Agre P (1994) Molecular characterization of an aquaporin cDNA from brain: candidate osmoreceptor and regulator of water balance. *Proceedings of the National Academy of Sciences of the United States of America* **91**(26):13052-13056.

McCoy E and Sontheimer H (2007) Expression and function of water channels (aquaporins) in migrating malignant astrocytes. *Glia* **55**(10):1034-1043.

Migliati E, Meurice N, DuBois P, Fang JS, Somasekharan S, Beckett E, Flynn G and Yool AJ (2009) Inhibition of aquaporin-1 and aquaporin-4 water permeability by a derivative of the loop diuretic bumetanide acting at an internal pore-occluding binding site. *Molecular pharmacology* **76**(1):105-112.

Monzani E, Shtil AA and La Porta CA (2007) The water channels, new druggable targets to combat cancer cell survival, invasiveness and metastasis. *Curr Drug Targets* **8**(10):1132-1137.

Nicchia GP, Stigliano C, Sparaneo A, Rossi A, Frigeri A and Svelto M (2013) Inhibition of aquaporin-1 dependent angiogenesis impairs tumour growth in a mouse model of melanoma. *J Mol Med (Berl)* **91**(5):613-623.

Oshio K, Watanabe H, Yan D, Verkman AS and Manley GT (2006) Impaired pain sensation in mice lacking Aquaporin-1 water channels. *Biochemical and biophysical research communications* **341**(4):1022-1028.

Park JH and Saier MH, Jr. (1996) Phylogenetic characterization of the MIP family of transmembrane channel proteins. *J Membr Biol* **153**(3):171-180.

Preston GM, Jung JS, Guggino WB and Agre P (1993) The mercury-sensitive residue at cysteine 189 in the CHIP28 water channel. *The Journal of biological chemistry* **268**(1):17-20.

Reizer J, Reizer A and Saier MH, Jr. (1993) The MIP family of integral membrane channel proteins: sequence comparisons, evolutionary relationships, reconstructed pathway of evolution, and proposed functional differentiation of the two repeated halves of the proteins. *Critical reviews in biochemistry and molecular biology* **28**(3):235-257.

Saparov SM, Kozono D, Rothe U, Agre P and Pohl P (2001) Water and ion permeation of aquaporin-1 in planar lipid bilayers. Major differences in structural determinants and stoichiometry. *J Biol Chem* **276**(34):31515-31520.

Schwab A, Nechyporuk-Zloy V, Fabian A and Stock C (2007) Cells move when ions and water flow. *Pflug Arch Eur J Phy* **453**(4):421-432.

Seeliger D, Zapater C, Krenc D, Haddoub R, Flitsch S, Beitz E, Cerda J and de Groot BL (2013) Discovery of novel human aquaporin-1 blockers. *ACS Chem Biol* **8**(1):249-256.

Sogaard R and Zeuthen T (2008) Test of blockers of AQP1 water permeability by a high-resolution method: no effects of tetraethylammonium ions or acetazolamide. *Pflugers Arch* **456**(2):285-292.

Sui H, Han B-G, Lee JK, Walian P and Jap BK (2001) Structural basis of water-specific transport through the AQP1 water channel. *Nature* **414**(6866):872-878.

Trott O and Olson AJ (2010) AutoDock Vina: improving the speed and accuracy of docking with a new scoring function, efficient optimization, and multithreading. *J Comput Chem* **31**(2):455-461.

Tsunoda SP, Wiesner B, Lorenz D, Rosenthal W and Pohl P (2004) Aquaporin-1, nothing but a water channel. *J Biol Chem* **279**(12):11364-11367.

Yool AJ (2007) Functional domains of aquaporin-1: keys to physiology, and targets for drug discovery. *Curr Pharm Des* **13**(31):3212-3221.

Yool AJ, Brown EA and Flynn GA (2009) Roles for novel pharmacological blockers of aquaporins in the treatment of brain oedema and cancer. *Clin Exp Pharmacol Physiol* **37**(4):403-409.

Yool AJ and Campbell EM (2012) Structure, function and translational relevance of aquaporin dual water and ion channels. *Mol Aspects Med* **33**(5):443-561.

Yool AJ, Morelle J, Cnops Y, Verbavatz JM, Campbell EM, Beckett EA, Booker GW, Flynn G and Devuyst O (2013) AqF026 is a pharmacologic agonist of the water channel aquaporin-1. *J Am Soc Nephrol* **24**(7):1045-1052.

Yool AJ, Stamer WD and Regan JW (1996) Forskolin stimulation of water and cation permeability in aquaporin-1 water channels. *Science* **273**(5279):1216-1218.

Yoshida T, Hojo S, Sekine S, Sawada S, Okumura T, Nagata T, Shimada Y and Tsukada K (2013) Expression of aquaporin-1 is a poor prognostic factor for stage II and III colon cancer. *Mol Clin Oncol* **1**(6):953-958.

Yu J, Yool AJ, Schulten K and Tajkhorshid E (2006) Mechanism of gating and ion conductivity of a possible tetrameric pore in aquaporin-1. *Structure* **14**(9):1411-1423.

Zhang H and Verkman AS (2015) Aquaporin-1 water permeability as a novel determinant of axonal regeneration in dorsal root ganglion neurons. *Exp Neurol* **265**:152-159.

Zhang W, Zitron E, Homme M, Kihm L, Morath C, Scherer D, Hegge S, Thomas D, Schmitt CP, Zeier M, Katus H, Karle C and Schwenger V (2007) Aquaporin-1 channel function is positively regulated by protein kinase C. *J Biol Chem* **282**(29):20933-20940.

Footnotes

MK and JVP are co-first authors.

This work was supported in part by the National Institutes of Health [Grant R01 GM059986]; and a 2015 pilot grant from The Institute for Photonics & Advanced Sensing, University of Adelaide.

Figure Legends

Figure 1. Chemical structures of selected bumetanide derivatives and electrophysiology traces showing representative effects of AqB001, AqB006, AqB007, and AqB011 on the ionic conductance responses activated by bath application of CPT-cGMP, before and after 2 h incubation in saline with and without the AqB compounds. See Methods for details.

Figure 2. Trend plots showing the ionic conductance responses for individual oocytes measured prior to cGMP (initial), after the first cGMP application, after 2 h incubation in saline without cGMP containing DMSO (vehicle) or AqB agents, and after the second application of cGMP. Reversible cGMP-dependent activation of an ionic conductance in AQP1-expressing oocytes (A) was not seen in non-AQP1 control oocytes (B). Inhibition was seen after treatment with AqB007, and AqB011, but not with vehicle, AqB001, or AqB006.

Figure 3. Dose-dependent block of the AQP1 ionic conductance. (A) Compiled box plot data showing statistically significant block of the cGMP-activated ionic conductance in AQP1-expressing oocytes by AqB007 and AqB011, but not with vehicle, AqB001, or AqB006. See Methods for details. (B) Dose response curves showing percent block of the activated ionic conductance in AQP1 expressing oocytes and estimated IC_{50} values. *n* values for dose-response data (in order of increasing concentration) for AqB007 were 8, 4, 2, 8; and for AqB011 were 8, 2, 2, 3, 6, 4, 3.

Figure 4. Lack of effect of AqB compounds on AQP1 osmotic water permeability measured by optical swelling assays. (A) Mean oocyte volume, standardized as a percentage of the initial volume for each oocyte, as a function of time after introduction into 50% hypotonic saline, with and without 2 h pre-treatment with AqB compounds at 200 μM, or vehicle (0.1% DMSO). (B) Compiled boxplot data showing the absence of any statistically significant differences between the first and second swelling rates, measured before (S1) and after (S2) 2 h incubations in saline alone or saline with 200 μM AqB compounds as indicated. See Methods for details.

Figure 5. In silico modeling of the energetically favored binding site for AqB011 in the center of the tetrameric channel of AQP1 (grey) at the intracellular side, bracketed by the gating loop D domains (green). The putative binding site suggests an interaction with two of the loop D domains from adjacent subunits. (A) is the full view of the tetramer, and (B) is a closer view slightly rotated to show proximity of the ligand to the conserved arginine residues in loop D.

Figure 6. Block of cell migration in AQP1-expressing HT29 but not SW480 cells treated with AqB011. (A) Illustrative diagram of the circular wound healing method, showing substantial closure of the wounded area in normal culture medium by 24 hours. (B) Compiled boxplot data from wound closure assays showing the dose-dependent inhibitory effects of AqB007 and AqB011, compared to DMSO and AqB006, on wound closure at 24 h in HT29 cell cultures. Migration of SW480 cells was not altered by AqB011.

Supplemental Data. Molecular modelling data in Protein Data Bank (pdb) format showing the compound AqB011 docked at the intracellular side of the tetrameric

human AQP1 channel (PDB ID: 1FQY), and interacting with loop D domains of subunits surrounding the central pore.

Table 1. HT29 cell levels of cytotoxicity after treatment with furfural, structurally related compounds, or $HgCl_2$ in the culture medium.

Agent [AqB011] (μM)	**Mean normalized cell viability (%) ± SEM** [§]	**n value**	
0 (untreated)	100.0 ± 0.70	8	---
0 (0.1% DMSO)	103.9 ± 0.91	8	NS
1	104.0 ± 1.06	4	NS
5	102.3 ± 2.26	4	NS
10	110.6 ± 2.12	4	NS
20	114.0 ± 0.84	4	NS
40	111.8 ± 1.33	4	NS
80	102.4 ± 2.95	4	NS
$HgCl_2$ (100 μM)	16.2 ± 0.20	3	**

[§] Percent viability was standardized as a percentage of the untreated mean value, measured as changes in alumarBlue fluorescence signal intensity. See Methods for details.

Figures

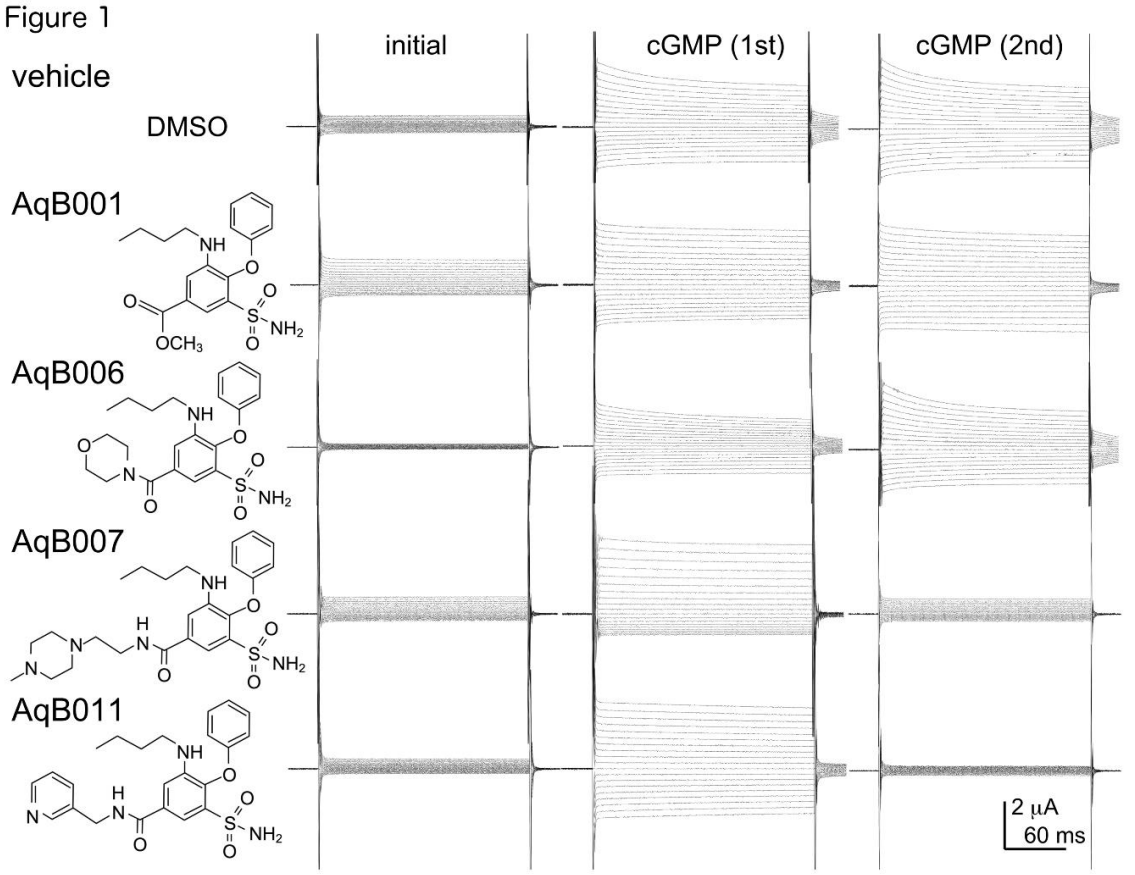
Figure 1
vehicle
DMSO
AqB001
AqB006
AqB007
AqB011
initial
cGMP (1st)
cGMP (2nd)
2 μA
60 ms

Figure 2

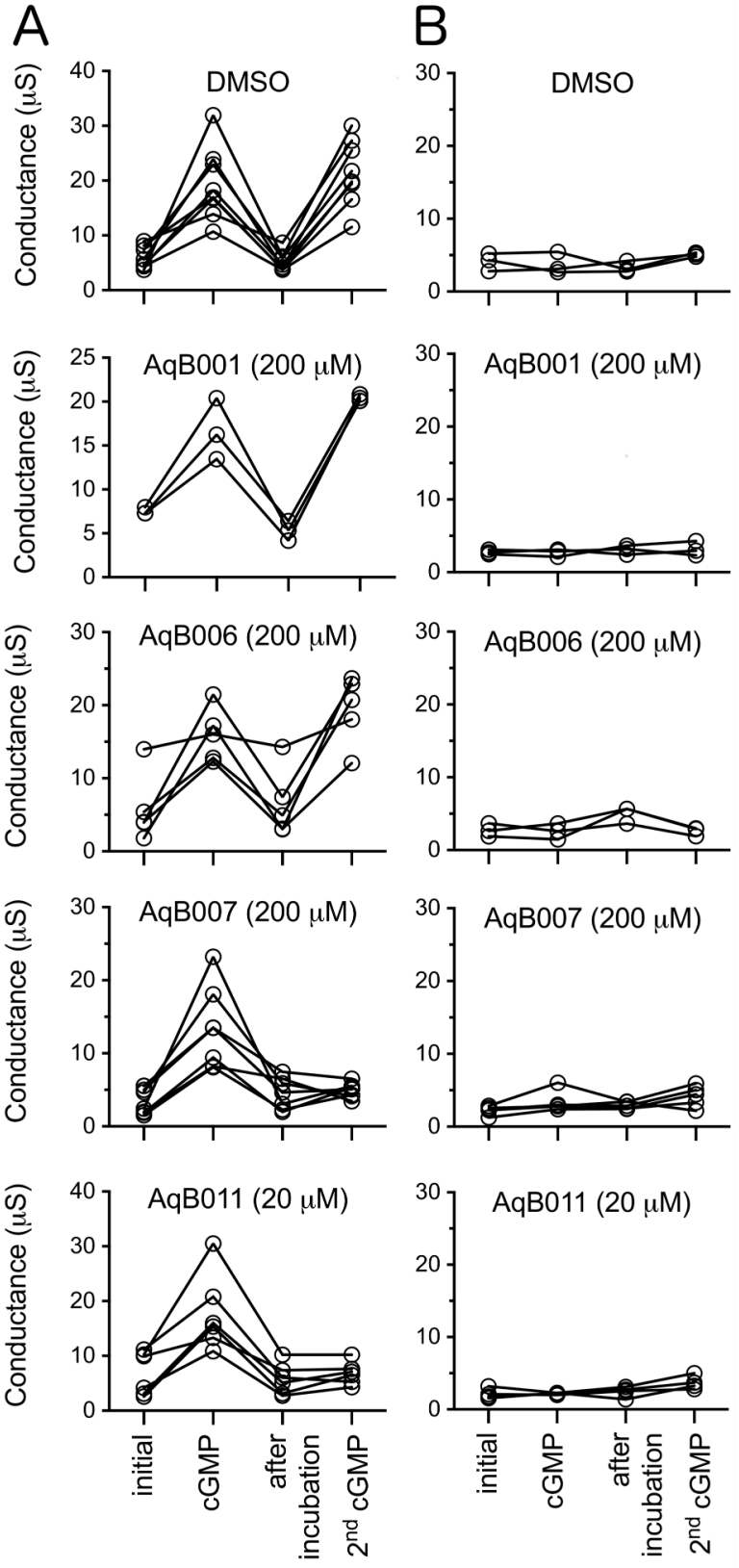
A
B
DMSO
DMSO
AqB001 (200 μM)
AqB001 (200 μM)
AqB006 (200 μM)
AqB006 (200 μM)
AqB007 (200 μM)
AqB007 (200 μM)
AqB011 (20 μM)
AqB011 (20 μM)
Conductance (μS)
initial
cGMP
after incubation
2nd cGMP

Figure 3

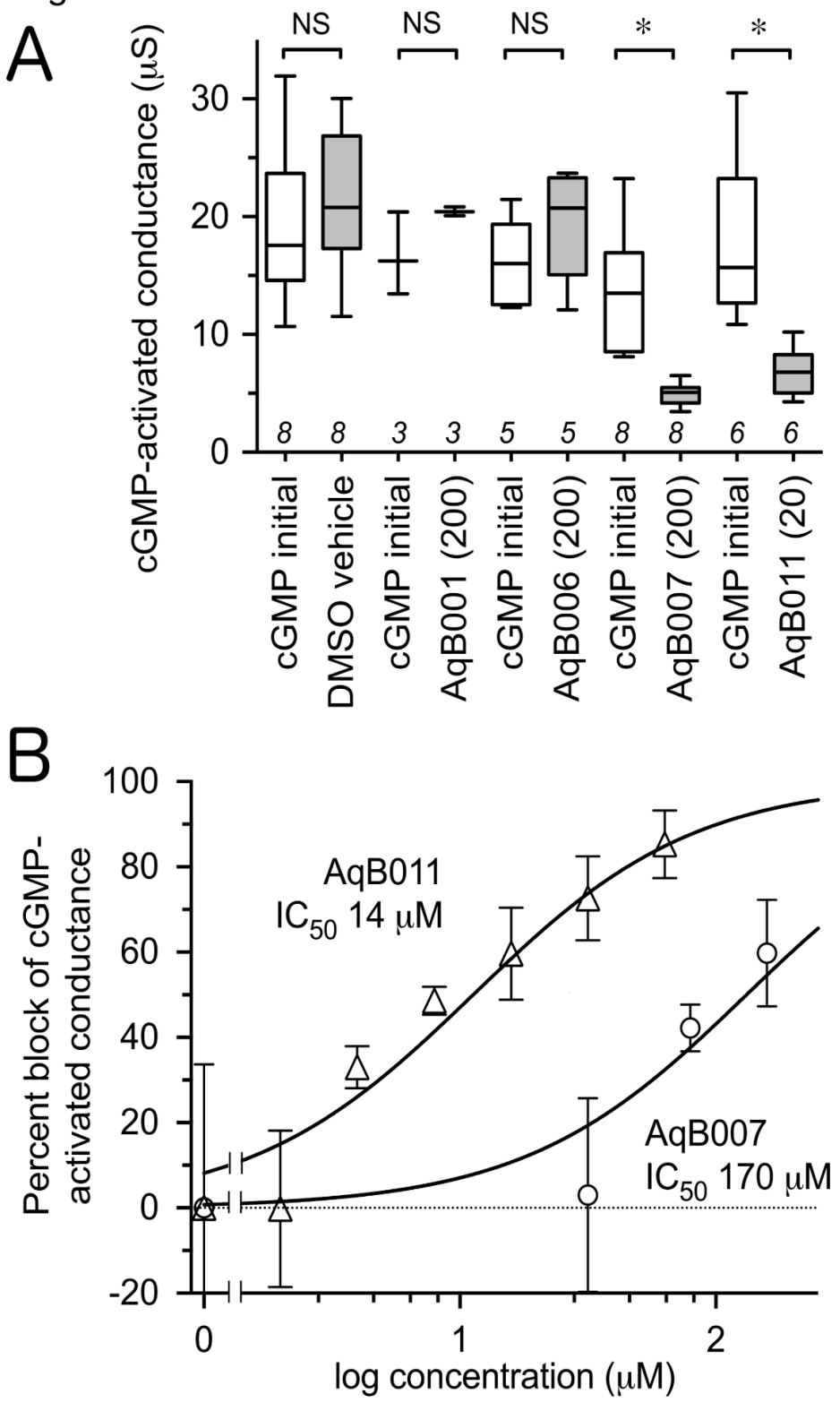
A
cGMP-activated conductance (μS)
NS
NS
NS
*
*
30
20
10
0
8
8
3
3
5
5
8
8
6
6
cGMP initial
DMSO vehicle
cGMP initial
AqB001 (200)
cGMP initial
AqB006 (200)
cGMP initial
AqB007 (200)
cGMP initial
AqB011 (20)
B
Percent block of cGMP-activated conductance
100
80
60
40
20
0
-20
AqB011
IC50 14 μM
AqB007
IC50 170 μM
0
1
2
log concentration (μM)

Figure 4

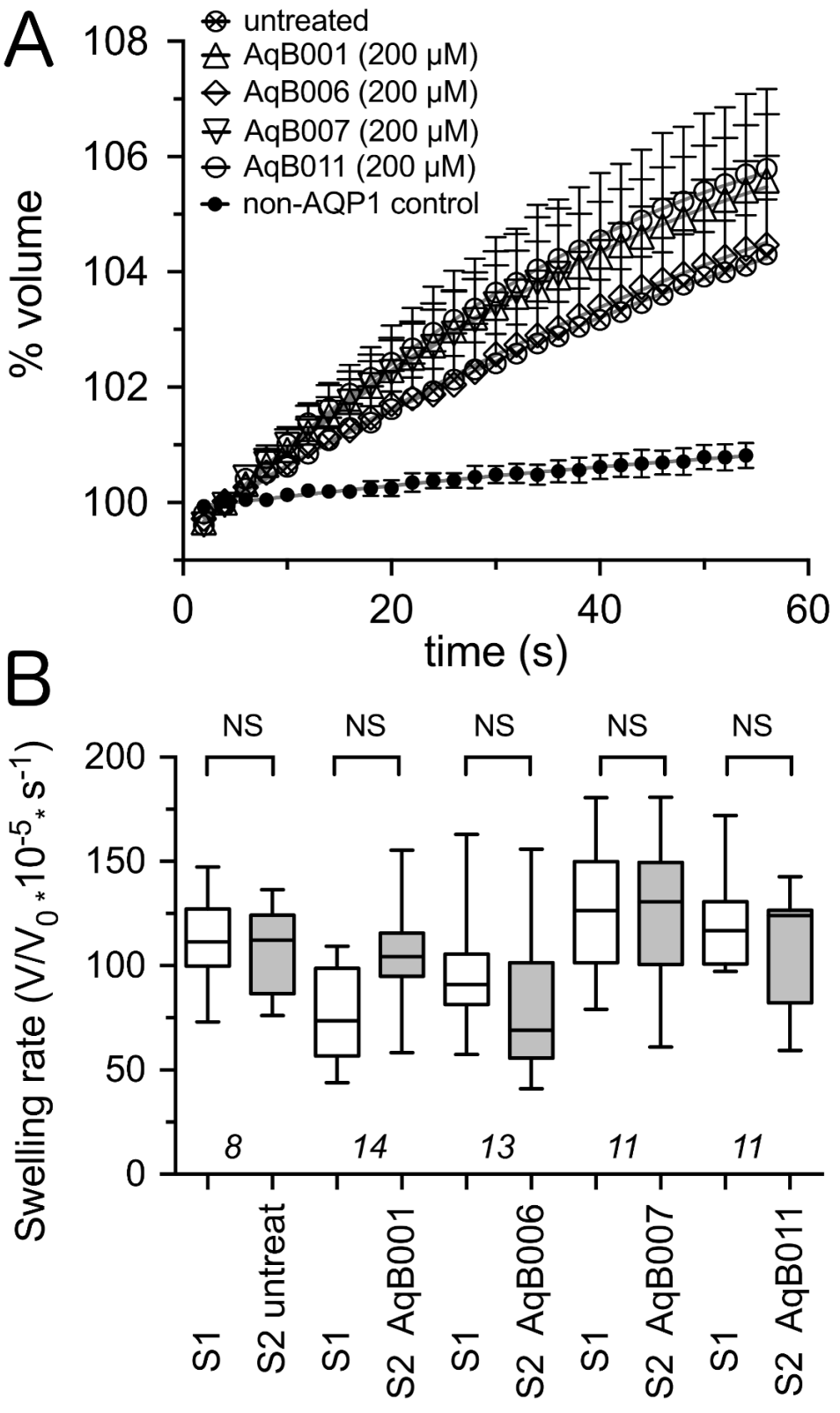
A
untreated
AqB001 (200 µM)
AqB006 (200 µM)
AqB007 (200 µM)
AqB011 (200 µM)
non-AQP1 control
% volume
108
106
104
102
100
0
20
40
60
time (s)
B
Swelling rate (V/V0*10-5* s-1)
NS
NS
NS
NS
NS
200
150
100
50
0
8
14
13
11
11
S1
S2 untreat
S1
S2 AqB001
S1
S2 AqB006
S1
S2 AqB007
S1
S2 AqB011

Figure 5

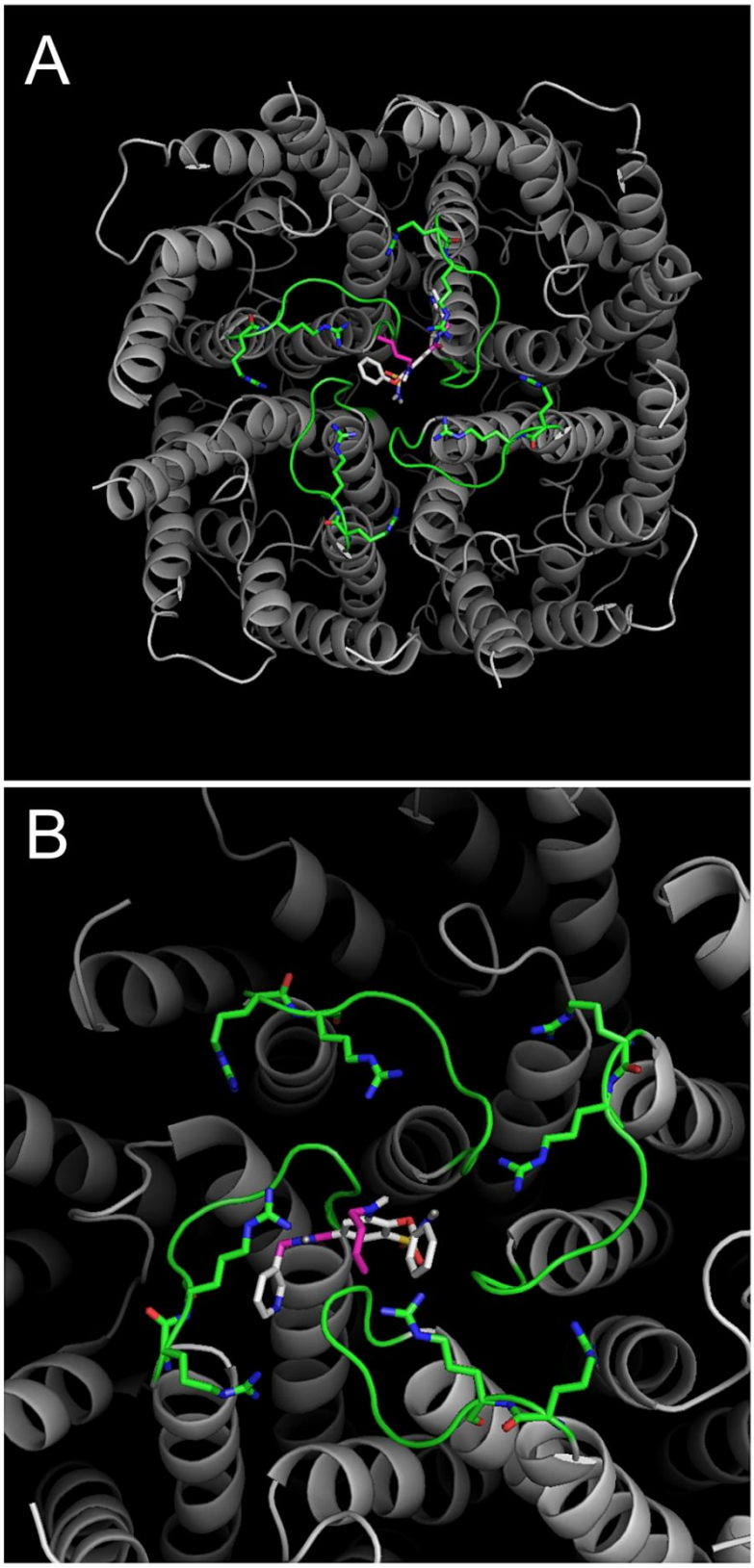

Figure 6

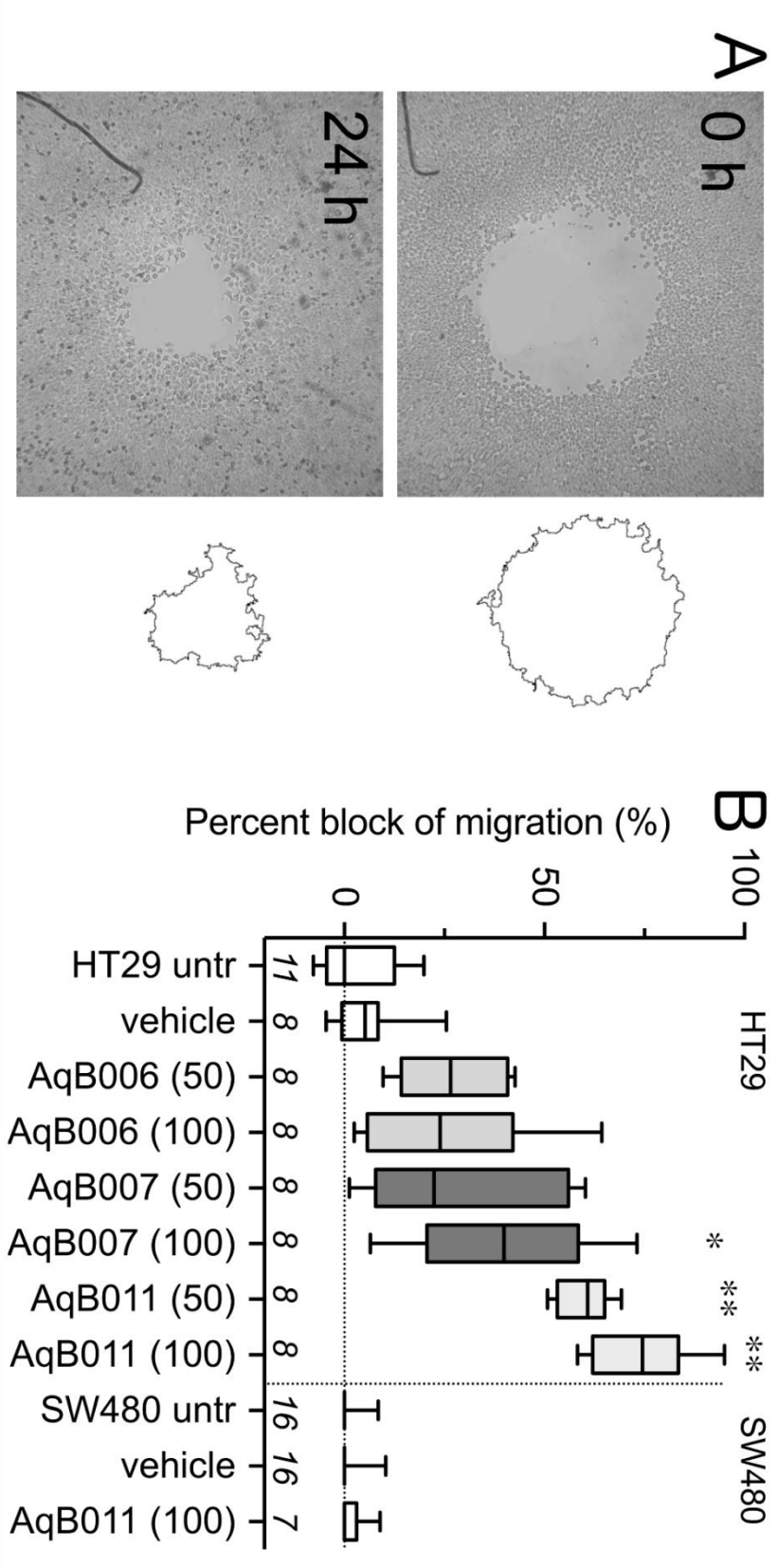
A
0 h
24 h
B
Percent block of migration (%)
0
50
100
HT29 untr
vehicle
AqB006 (50)
AqB006 (100)
AqB007 (50)
AqB007 (100)
AqB011 (50)
AqB011 (100)
SW480 untr
vehicle
AqB011 (100)
11
8
8
8
8
8
8
16
16
7
HT29
SW480
*
**
**

Appendix 1- Additional data provided in response to examiner's request on showing AQP1 and AQP5 are both expressed in HT29 colon cancer cell line

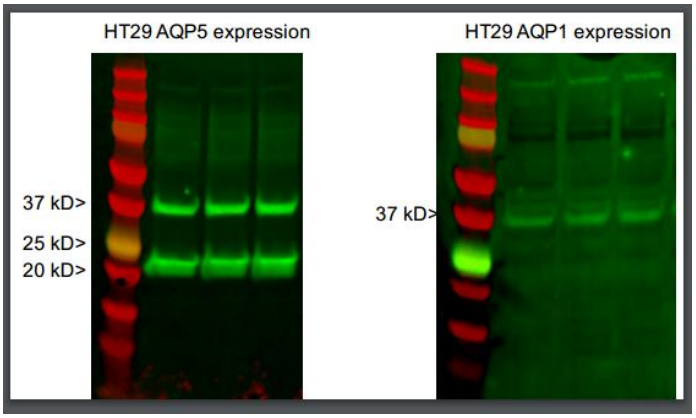

Appendix1: AQP1 and AQP5 protein expression level in HT29 colon cancer cell line. AQP1 protein expression was determined by western blot, with GAPDH used as a reference protein. Cultured cells were lysed with RIPA buffer for 10 minutes and centrifuged at 4°C for 15 minutes. Each sample was resolved by SDS-PAGE and transferred to polyvinylidene fluoride membranes. Membranes were blocked with Tris-buffered saline for 1 hour and incubated overnight at 4°C with rabbit anti-AQP1 and mouse anti-GAPDH antibodies. Membranes were then incubated with goat anti-rabbit IgG 800 infarred secondary antibody and donkey anti-mouse IgG 600 infrared antibody. Precision Plus Protein Dual Colour Standards protein ladder was used.

Statement of Authorship

Title of Paper	Chapter 3: Electrophysiology recordings confirm the interaction site of the inhibitor AqB011 on Loop D domain of AQP1 ion channel
Publication Status	☐ Published ☐ Accepted for Publication ☐ Submitted for Publication ☑ Unpublished and Unsubmitted w ork w ritten in manuscript style
Publication Details	

Principal Author

Name of Principal Author (Candidate)	Mohamad Kourghi
Contribution to the Paper	Contributed to electrophysiology and imaging experiments. Wrote the manuscript. Analysed and contributed to preparing figures 1, 2 and 3.
Overall percentage (%)	60%
Certification:	This paper reports on original research I conducted during the period of my Higher Degree by Research candidature and is not subject to any obligations or contractual agreements with a third party that would constrain its inclusion in this thesis. I am the primary author of this paper.
Signature	Date 6/09/2017

Co-Author Contributions

By signing the Statement of Authorship, each author certifies that:

i. the candidate's stated contribution to the publication is accurate (as detailed above);

ii. permission is granted for the candidate in include the publication in the thesis; and

iii. the sum of all co-author contributions is equal to 100% less the candidate's stated contribution.

Name of Co-Author	Saeed Nourmohammadi
Contribution to the Paper	Helped with electrophysiology experiments and writing the introduction.
Agree contribution (%)	20%
Signature	Date 6/9/2017

Name of Co-Author	Jinxin Pei		
Contribution to the Paper	Contributed in analysing data and preparing figure 3a.		
Agreed contribution percentage (%)	10%		
Signature		Date	6/9/17

Please cut and paste additional co-author panels here as required.

Name of Co-Author	Andrea J. Yool		
Contribution to the Paper	Contributed to experimental design, and reviewing the manuscript.		
Agreed contribution percentage (%)	10%		
Signature		Date	5/9/2017

Chapter 3: Electrophysiological confirmation of the site of interaction of the inhibitor AqB011 in the loop D domain of the human Aquaporin 1 ion channel

Mohamad Kourghi, Saeed Nourmohammadi, Jinxin V. Pei, and Andrea J. Yool

Abstract

Aquaporins are membrane integral proteins that assemble on the membrane and facilitate the transport of water and other small neutral molecules. Mammalian aquaporin 1 (AQP1) allows H_2O permeation and CO_2 transport. In addition AQP1 functions as a cation channel activated by cGMP. The cation channel of AQP1 was shown previously to be blocked by small molecule sulfonamide compounds, AqB007 (IC_{50} 170 μM) and AqB011 (IC_{50} 14 μM). The interaction site of the molecules with the channel was predicted by in silico docking modelling to be at loop D domain of the human AQP1 channel, in a proposed gating domain involving a pair of arginine residues at positions 159 and 160. Work here tested the hypothesis that AQP1 channels modified by mutation of the two predicted binding site arginine residues to alanines would have reduced sensitivity to block by AqB011. Human AQP1 channels with the double mutation (AQP1 R159A+R160A) and wild type AQP1 channels were expressed in *Xenopus laevis* oocytes and investigated by two-electrode voltage clamp, optical osmotic swelling assays and pharmacological analyses. The results revealed that the double mutation of R159 and R160 in the gating loop D domain caused a significant slowing of the rate of ion conductance activation as compared with wild type in response to application of membrane-permeable cGMP, and that the cGMP-dependent current in AQP1 R159A+R160A showed no significant

sensitivity to AqB011 at concentrations up to 50 μM, whereas the AQP1 wild type channel was blocked effectively by AqB011. These findings extend our understanding of the role of the loop D domain in ion channel activation in AQP1, and provide direct support for the location of the predicted site of interaction of AqB011 in the loop D domain of hAQP1.

Introduction

Aquaporins (AQPs) are classified as major intrinsic proteins (MIPs) (Reizer, Reizer et al. 1993). In mammals, classes of AQPs are differentially expressed in endothelial, epithelial and other cell types, and comprise key components of mechanisms for fluid homeostasis in single cells, barrier tissues and organs such as brain, kidneys, stomach, intestines and lungs which depend on facilitation of water transport across membranes (Benga, Popescu et al. 1986, Agre, Preston et al. 1993). Some classes of aquaporin channels have been found shown to transport molecules other than water across the cell membrane, including glycerol, ammonia, urea, protons, as well as CO_2 and O_2 gases (Uehlein, Lovisolo et al. 2003, Holm, Jahn et al. 2005, Hibuse, Maeda et al. 2006, Zhao, Bankir et al. 2006, Herrera and Garvin 2011, Uehlein, Sperling et al. 2012, Zwiazek, Xu et al. 2017).

Aquaporin ion channel function is not exclusive to AQP1. Recent work has shown that a plant aquaporin channel (AtPIP2;1) serves as a non-selective cation channel that is sensitive to Ca^{2+} and pH (Byrt, Zhao et al. 2016); the aquaporin-related Big Brain channel in Drosophila has been shown to carry a cationic conductance regulated by tyrosine kinase signalling (Yanochko and Yool 2002); and other members of the aquaporin family including lens MIP, AQP0, and AQP6 have been characterised as ion channels (Zampighi, Hall et al. 1985, Ehring and Hall 1988, Ehring, Zampighi et al. 1990, Yasui, Kwon et al. 1999).

What distinguishes AQP1 ion channels from other members of the family described thus far is its ability to conduct solutes through separate pathways with constitutive water transport mediated through the individual pores of the tetramer and ion

transport mediated by the central pore, which allows monovalent cations to pass through the channel after activation by intracellular cGMP. The AQP1 ion pore is highly permeable to K^+, Na^+, Cs^+, and Li^+; moderately permeable to TEA^+ and not appreciably permeable to divalent cations such as Ca^{2+} (Yool, Stamer et al. 1996).

Previous work identified two pharmacological blockers of AQP1 ion channel, AqB007 and AqB011, with AqB011 being the more potent blocker (Kourghi, Pei et al. 2016). Osmotic water fluxes were not altered, indicating the block was selective for the central pore region. Molecular dynamic simulations predicted that a pair of arginine residues located at positions 159 and 160 in the loop D domain of human AQP1 were involved in gating of the ion channel, and that mutation of the arginines impaired ion channel activation (Yool and Campbell 2012). Molecular docking studies independently converged on the same arginine residues as the candidate binding site for the AQP1 ion channel inhibitor AqB011 (Kourghi, Pei et al. 2016).

The purpose of this study was to test the proposed binding site of AqB011 compound by mutation of the candidate docking site. Arginine residues at positions 159 and 160 in the Loop D domain of human AQP1 were mutated to alanines. Human AQP1 wild-type and hAQP1 R159A+R160A mutant channels were expressed in *Xenopus laevis* oocytes and analysed by osmotic swelling assays, electrophysiology, and pharmacology. Results here show that the AQP1 R159A+R160A mutant channel could be activated by cGMP, although much more slowly than wild type, and the activated current though reduced in amplitude compared to wild type was insensitive

to the blocker AqB011. These results confirm the in silico predicted binding site of AqB011 on the loop D domain of hAQP1, and provide further support for the idea that the AQP1 central pore is the pathway for the gated cation current.

Materials and Methods

Site directed mutagenesis of AQP1

Site-directed mutations were generated in hAQP1, cloned in the *X. laevis* expression vector construct (pxBGev), using the QuikChange site-directed mutagenesis kit (Agilent Technologies, Forest Hills, VIC, Australia) with custom-synthesized primers as described previously (Yu, Yool et al. 2006). The correct sequence of the construct was confirmed by replicate DNA sequencing of the full-length cDNA constructs. Wild-type AQP1 and mutant R159A+R160A cDNAs were linearized using BamHI and transcribed with T3 RNA polymerase using the mMessage mMachine kit (Ambion, Austin, TX).

Oocyte preparation and injection

Unfertilized oocytes were harvested by partial ovariectomy from anesthetized *Xenopus laevis* frogs following Australian national guidelines and protocols approved by the University of Adelaide Animal Ethics Committee. Oocytes were defolliculated with collagenase (type 1A, 1 mg/ml; Sigma-Aldrich, St. Louis, MO) in the presence of trypsin inhibitor (0.05 mg/ml; Sigma-Aldrich, St. Louis, MO) for 1 to 1.5 hours in OR-2 saline (96 mM NaCl, 2 mM KCl, 5 mM $MgCl_2$, penicillin 100 units/ml, streptomycin 0.1 mg/ml, and 5 mM HEPES; pH7.6). Oocytes were then

washed 4 times with OR-2 saline at approximately 10 minute intervals before storage in isotonic Frog Ringers saline [96 mM NaCl, 2mM KCl, 5 mM $MgCl_2$, 0.6 mM $CaCl_2$, 5mM HEPES buffer, horse serum (5%; Sigma-Aldrich, St. Louis, MO), penicillin 100 units/ml streptomycin 0.1 mg/ml, and tetracycline 0.5mg/ml, pH 7.6]. Oocytes were injected with 50 nl of water (control oocytes), or 50 nl of water containing 1ng of AQP1 wild type cRNA, or 2ng of AQP1 R159A+R160A mutant cRNA. Oocytes were then transferred to sterile dishes containing Frog Ringers saline and incubated at 16 to 18 °C for 48 hours to allow time for protein expression. To confirm post hoc the successful expression of AQP1 channels in the oocyte membranes, after electrophysiological recordings the AQP1 wild type, mutant or control oocytes were placed in distilled water. AQP1-wt oocytes swelled and burst typically within 3-5 minutes, AQP1 R159A+R160A mutant oocytes showed membrane disruption due to swelling by approximately 8 minutes, whereas control oocytes remained generally unaffected in morphology for longer than 10 minutes in distilled water. Isotonic Na saline used for electrophysiology and osmotic swelling assays contained (in mM): NaCl 96 mM, KCl 2 mM, $MgCl_2$ 5 mM, $CaCl_2$ 0.6 mM, and HEPES 5 mM, pH 7.3, without antibiotics or serum.

Expression of human AQP1 channel on oocyte membrane

Swelling assays were performed in 50% hypotonic saline (isotonic Na saline diluted with equal volume of water). Prior to swelling assay the control (non-AQP expressing), AQP1-wt and AQP1 R159A+R160A oocytes were rinsed in isotonic

saline (without horse serum and antibiotics) for 10 minutes. Oocytes were then introduced to 50% hypotonic saline.

Rates of swelling were imaged using a grayscale camera device (Cohu, San Diego, CA) fixed on a dissecting microscope (Olympus SZ-PT; Olympus, Macquarie Park, Australia). Images were captured at 0.5 per second for 60 s. Swelling of the oocyte membrane were assessed with Image J software from National Institutes of Health (http://rsbweb.nih.gov/ij/). Swelling rates were measured as the slopes of the linear regression fits of relative volume as a function of time using Prism (GraphPad Software Inc.,San Diego, CA).

Electrophysiological recordings

Two-electrode voltage clamp recordings were performed at room temperature in standard isotonic Na^+ saline. Capillary glass pipettes (1–3 MΩ) were filled with 1 M KCl. Initial conductances were determined from current-voltage relationships measured prior to cGMP application. The membrane permeable compound 8-pCPT-cGMP (8-(4-chlorophenylthio)-guanosine-3′,5′-cyclic monophosphate) (Anthony, Brooks et al. 2000) was added as a bolus to the bath saline and diluted to the final concentration (10-20 μM) by trituration. Repeated steps to +40 mV at 6 s intervals were used to monitor activation of the ion current response. After recording the final conductance in cGMP, oocytes were transferred into isotonic Na saline with or without AqB011 for two hours which allowed recovery back to initial conductance levels, as described previously (Kourghi, Pei et al. 2016). Oocytes were then evaluated again with voltage clamp to determine the response to a second

application of bath CPT-cGMP, using the amplitude of reactivation to test for block by AqB011. From a holding potential of -40, voltage steps from +60 to -110mV were applied using a GeneClamp amplifier and Clampex 9.0 software (pClamp 9.0 Molecular Devices, Sunnyvale, CA, USA). Data were filtered at 2 kHz and stored to hard disk for analysis.

Results

Two-electrode voltage clamp recordings showed that the cGMP-activated ionic conductance of AQP1 wild type channels was inhibited by incubation in AqB011 (50 μM), but no appreciable block by AqB011 (50 μM) was observed for the AQP1 R159A+R160A mutant channels. Initial recordings were measure before the application of cGMP followed by increased ionic conductance in response to batch application of CPT-cGMP. The oocytes were then incubated in salines containing 50 μM AqB011 for 2 hours. During the incubation period the ionic conductance recovered to initial levels (Fig. 1A). In response to the second application of cGMP, oocytes treated with vehicle (DMSO) and AQP1 R159A+R160A mutants showed increases in conductance that were similar to the first response to cGMP. However, the ionic conductances in AQP1 wild type oocytes were not re-activated by application of second cGMP, indicating an inhibition of the ion current after AqB011 treatment. AQP1 R159A+R160A mutant channels were insensitive to the blocker.

Figure 1B illustrates the compiled box plot data for the ionic conductance values for AQP1-wt and AQP1 R159A+R160A mutants. Figure 1C shows the trend plots, in which the initial conductance in AQP1-wt and QP1 R159A+R160A expressing

oocytes were low. Followed by bath application of cGMP and achieving maximal activation response. Post incubation in 50 μM AqB011, and response to 2nd bath application of cGMP, in which the oocytes expressing wt AQP1 stayed blocked, and not reactivated, however there was no block in oocytes expressing AQP1 R159A+R160A mutants.

Figure 2A shows that the conductance responses differed in rates of activation after the bath application of CPT-cGMP. Oocytes expressing the AQP1 wild type channels activated more rapidly and reach a higher maximal current amplitude that did those expressing AQP1 R159A+R160A channels. cGMP activated currents were not observed in non-AQP1 expressing oocytes. The maximal activation in oocytes expressing AQP1 wild type was reached within 25 min, reaching a conductance averaging 20 μS. In contrast, approximately double that time was required to achieve maximal conductance in oocytes expressing AQP1 R159A+R160A mutants, to reach a conductance averaging 10μS.

The latency to the onset of activation was also considerably slower in the mutant construct (Fig 2B). The current in AQP1 wild type expressing oocytes began to rise above the initial baseline by 10 to 15 min after cGMP application; whereas in oocytes expressing R159A+R160A channels, the onset of a current response to cGMP was not observed until approximately 30 minutes. The long latency to activation observed here for the arginine double mutant construct is consistent with prior work which reported a lack of appreciable activation of the R159A+R160A mutant channels when assessed in a relatively short time frame needed for activation of AQP1 wild type channels (8 min after application of the nitric oxide donor, sodium

nitroprusside, which was used to stimulate endogenous oocyte cGMP production to activate AQP1 channels (Yu, Yool et al. 2006).

Fig 2C shows a scatter plot of times to half-maximal activation of the ion conductance in responses to cGMP. Significantly less time was required to activate the ionic conductance of the AQP1 wild type as compared to AQP1 R159A+R160A mutant channels.

Figure 3 shows osmotic water permeability data that confirmed successful expression of functional wild type and mutant AQP1 channels in oocyte plasma membrane. Based on relative osmotic water fluxes, the level of expression of the AQP1 R159A+R160A mutant channel appeared to be less than wild type, but both were significantly greater than non-AQP1 expressing control oocytes. A reduced efficacy of expression thus could explain approximately 10% of the reduced amplitude observed for the maximal ionic conductance response of the mutant as compared to wild type. However the overall conductance response in the arginine double mutant was half that of wild type, suggesting the ion conductance response was also impaired by reduced efficacy of ion channel gating. The mutation of AQP1 did not preclude the water channel activity that showed the channel was expressed, assembled and trafficked to the plasma membrane of oocytes.

Discussion

The aim of this study was to evaluate the candidate binding site for AqB011 in the loop D domain of AQP1, as postulated from previous in silico modelling. Previous work characterized the AqB011 compound as a novel inhibitor of the ion channel function of AQP1 (Kourghi, Pei et al. 2016) and showed that block of the AQP1 ion channel activity slowed migration of colon cancer cells (Kourghi, Pei et al. 2016) that rely on AQP1 expression for high motility. Molecular docking studies suggested that AqB011 showed the most favourable energy of interaction with a pair of positively charged arginine residues located on loop D domain of AQP1, a region that has been suggested to be involved in gating of the central pore of the AQP1 channel (Yu, Yool et al. 2006). To test this hypothesis, we used a mutant construct of the AQP1 channel in which the positively charged arginine residues in positions 159 and 160 of the human AQP1 amino acid sequence were replaced with alanine.

A concern that raised from introducing the double arginine mutations at positions 159 and 160 of AQP1 mRNA is the mutation could prevent the assembly and expression of AQP1. Prior work conducted by (Kitchen, Conner et al. 2016) and (Campbell, Birdsell et al. 2012) showed that the mutation does reduce the assembly and the level of expression of AQP1 channel on the phospholipid membrane. However the mutation does not completely prevent the expression of AQP1 channel on membrane (Campbell, Birdsell et al. 2012). The mutation impaired the ion channel function of AQP1 much more than the water permeability, showing that the loss of function could not be due solely to a loss of membrane expression.

Here we have confirmed prior work showing that the mutation did not prevent the channel from being expressed on the membrane of oocytes, and added new results showing that the AQP1R159A+R160A mutant, which was previously thought to be non-functional as an ion channel (Yu, Yool et al. 2006), can be activated by cGMP albeit at significantly slower rates, at a lower maximal amplitude, and a longer latency than for AQP wild type channels. Nonetheless the reduced ion channel function in the double arginine mutant was significantly different from controls and thus allowed evaluation of sensitivity to block by AqB011.

AqB011 had no effect on the activation of the ion conductance in the mutant channel in response to cGMP; however, the ion conductance in AQP wild type was significantly inhibited in agreement with prior work (Kourghi, Pei et al. 2016).

In sum, the results support the hypothesis of predicted interaction site of AqB011 on double Arginine residue on loop D domain of AQP1 ion channel. In addition our result provides a line of evidence to support the previous idea that the proposed central pore is the pathway for ion flux (Campbell, Birdsell et al. 2012).

References

Agre P, Preston GM, Smith BL, Jung JS, Raina S, Moon C, Guggino WB, Nielsen S (1993) Aquaporin CHIP: the archetypal molecular water channel. *Am J Physiol* **265:** F463-476

Benga G, Popescu O, Pop VI, Holmes RP (1986) p-(Chloromercuri) benzenesulfonate binding by membrane proteins and the inhibition of water transport in human erythrocytes. *Biochemistry* **25:** 1535-1538

Byrt CS, Zhao M, Kourghi M, Bose J, Henderson SW, Qiu J, Gilliham M, Schultz C, Schwarz M, Ramesh SA, Yool A, Tyerman S (2016) Non-selective cation channel activity of aquaporin AtPIP2;1 regulated by Ca^{2+} and pH. *Plant Cell Environ*

Campbell EM, Birdsell DN, Yool AJ (2012) The Activity of Human Aquaporin 1 as a cGMP-Gated Cation Channel Is Regulated by Tyrosine Phosphorylation in the Carboxyl-Terminal Domain. *Mol Pharmacol* **81:** 97-105

Ehring GR, Hall JE (1988) Single channel properties of lens MIP 28 reconstituted into planar lipid bilayers. *Proceedings of the Western Pharmacology Society* **31:** 251-253

Ehring GR, Zampighi G, Horwitz J, Bok D, Hall JE (1990) Properties of channels reconstituted from the major intrinsic protein of lens fiber membranes. *The Journal of general physiology* **96:** 631-664

Herrera M, Garvin JL (2011) Aquaporins as gas channels. *Pflugers Arch* **462:** 623-630

Hibuse T, Maeda N, Nagasawa A, Funahashi T (2006) Aquaporins and glycerol metabolism. *Biochimica et biophysica acta* **1758:** 1004-1011

Holm LM, Jahn TP, Moller AL, Schjoerring JK, Ferri D, Klaerke DA, Zeuthen T (2005) NH_3 and NH_4^+ permeability in aquaporin-expressing *Xenopus* oocytes. *Pflugers Arch* **450:** 415-428

Kourghi M, Pei JV, De Ieso ML, Flynn G, Yool AJ (2016) Bumetanide Derivatives AqB007 and AqB011 Selectively Block the Aquaporin-1 Ion Channel Conductance and Slow Cancer Cell Migration. *Mol Pharmacol* **89:** 133-140

Uehlein N, Lovisolo C, Siefritz F, Kaldenhoff R (2003) The tobacco aquaporin NtAQP1 is a membrane CO_2 pore with physiological functions. *Nature* **425:** 734-737

Uehlein N, Sperling H, Heckwolf M, Kaldenhoff R (2012) The *Arabidopsis* aquaporin PIP1;2 rules cellular CO_2 uptake. *Plant Cell Environ* **35:** 1077-1083

Yanochko GM, Yool AJ (2002) Regulated cationic channel function in *Xenopus* oocytes expressing *Drosophila big brain*. *The Journal of neuroscience : the official journal of the Society for Neuroscience* **22:** 2530-2540

Yasui M, Kwon TH, Knepper MA, Nielsen S, Agre P (1999) Aquaporin-6: An intracellular vesicle water channel protein in renal epithelia. *Proceedings of the National Academy of Sciences of the United States of America* **96:** 5808-5813

Yool AJ, Stamer WD, Regan JW (1996) Forskolin stimulation of water and cation permeability in aquaporin 1 water channels. *Science* **273:** 1216-1218

Zampighi GA, Hall JE, Kreman M (1985) Purified Lens Junctional Protein Forms Channels in Planar Lipid Films. *Proceedings of the National Academy of Sciences of the United States of America* **82:** 8468-8472

Zhao D, Bankir L, Qian LM, Yang DY, Yang BX (2006) Urea and urine concentrating ability in mice lacking AQP1 and AQP3. *Am J Physiol-Renal* **291:** F429-F438

Zwiazek JJ, Xu H, Tan X, Navarro-Rodenas A, Morte A (2017) Significance of oxygen transport through aquaporins. *Sci Rep* **7:** 40411

Figure legends

Figure1. The sensitivity of human AQP1 wild type ion channels to block by AqB011 is removed by mutation of loop D arginine residues (R159 and R160).

(A) Electrophysiology traces showing ion currents in AQP1 wild type and AQP1 R159A+R160A expressing oocytes in initial conditions, after the first cGMP activation, and after the second cGMP application following two hour incubation in saline with or without 50μM AqB011. (B) Compiled box plot data showing a statistically significant block of AQP1 wild type with 50 μM AqB011 as compared to vehicle control (DMSO), and absence of a blocking effect of AqB011 on AQP1 R159A+R160 channels. (C) Trend plots showing the ionic conductance of AQP1 wild type or AQP1 R159A+R160A for each oocyte measured before cGMP (initial), after cGMP, and after 2-hour incubation in saline without cGMP containing DMSO (vehicle) or 50μM AqB011. The ionic conductance in AQP1 activated by cGMP was not observed in control (non-AQP1 expressing) oocytes.

Figure 2. The time required to reach half maximal activation of the cGMP-activated current at +40 mV is significantly greater for AQP1 R159A+R160A expressing oocytes than for AQP1 wild type. (A) Development of the ionic conductance response was monitored after cGMP using brief repeated +40 mV steps (10 per minute). Traces only at every 40 minutes are displayed for clarity to illustrated differences in the relative rates of activation. (B) Scatter plot comparing the times to half-maximal activation of cGMP-activated currents in minutes (y axis) for AQP1 wild type and AQP1 R159A+R160A mutant expressing oocytes (x axis).

Figure 3. Schematic illustration of distinct pathways for water and ion transport through AQP1 wild type channels, expressed as tetramers in the phospholipid membrane bi-layer. Positively charged arginine residues located on the loop D domain of central pore serve as the predicted interaction site with AqB011.

Fig 4. Functional expression of AQP1 wild type and AQP1 R159A+R160 mutant channels in oocytes, confirmed by high osmotic water permeabilities as compared to non-AQP1 expressing controls. (A) AQP1 wild type (circles) and AQP1 R159A+R160 mutant (squares) show high osmotic water permeabilities assessed by quantitative swelling assays compared with nonAQP1-expressing control *X. laevis* oocytes (filled triangles). Relative volume changes as a function of time were measured from video-imaged cross-sectional areas. Data are mean ± S.D. for all oocytes in a representative experiment (n = 6 per group). (B) Compiled box plot data show osmotic water flux in oocytes expressing AQP1 wild type and AQP1 R159A+R160 mutant were significantly greater than non-AQP1 expressing controls.

Figures

Figure 1

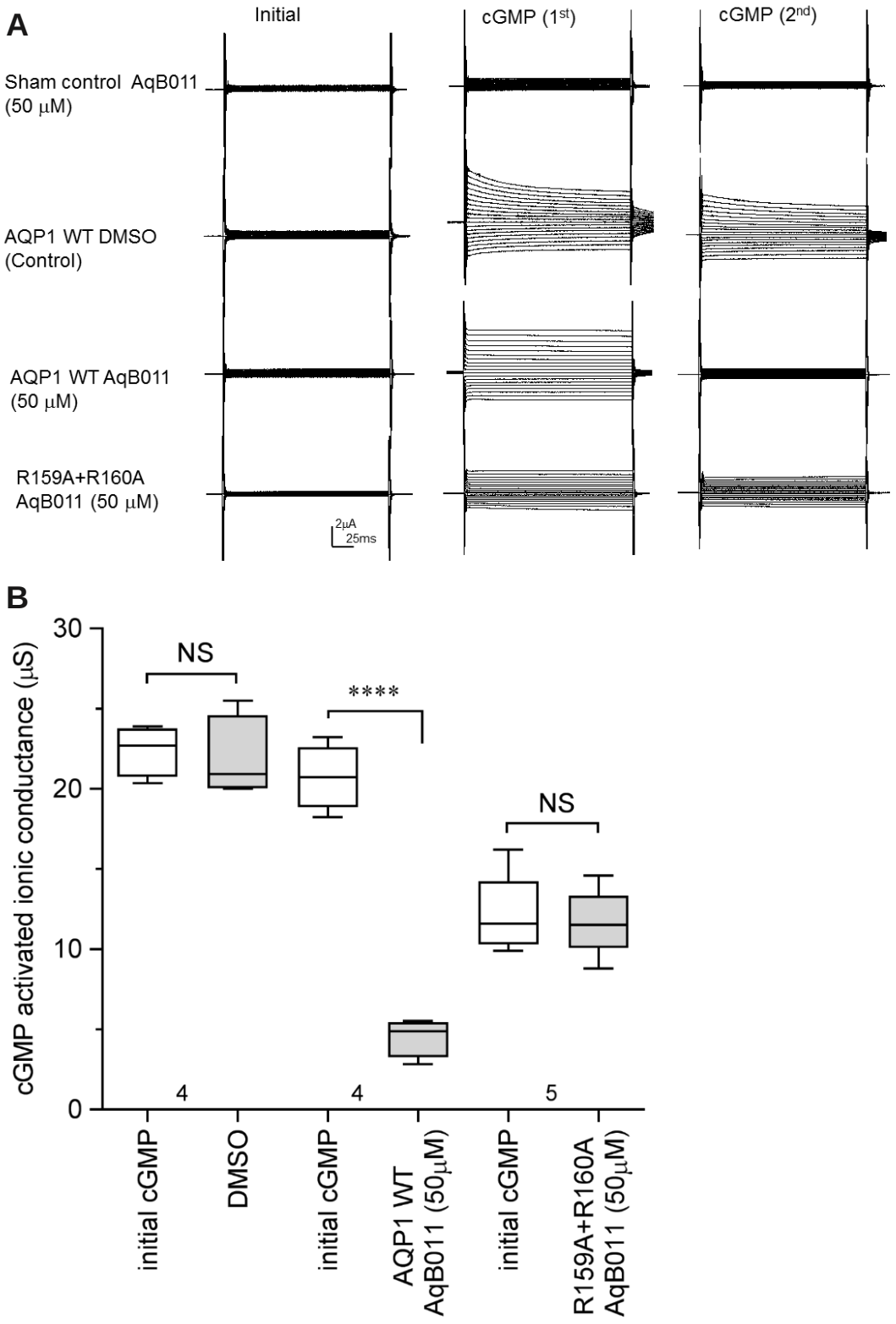

C

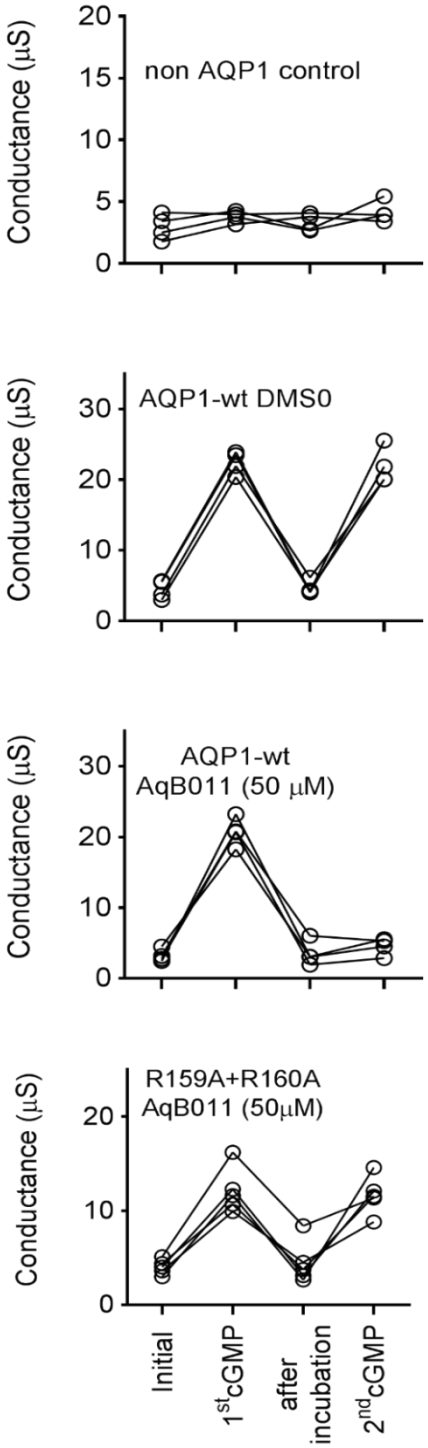
Conductance (μS)
non AQP1 control
AQP1-wt DMS0
AQP1-wt
AqB011 (50 μM)
R159A+R160A
AqB011 (50μM)
Initial
1st cGMP
after incubation
2nd cGMP

Figure 2

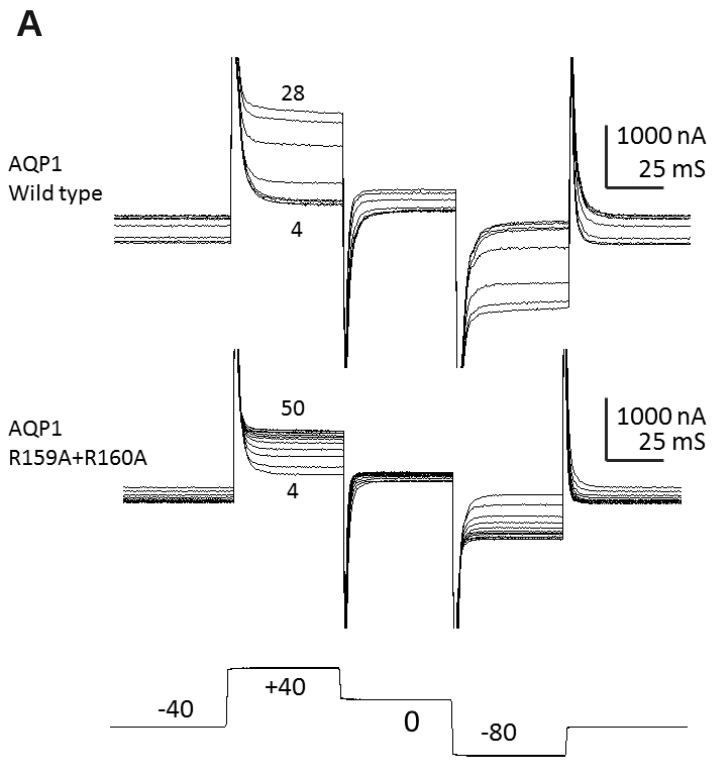

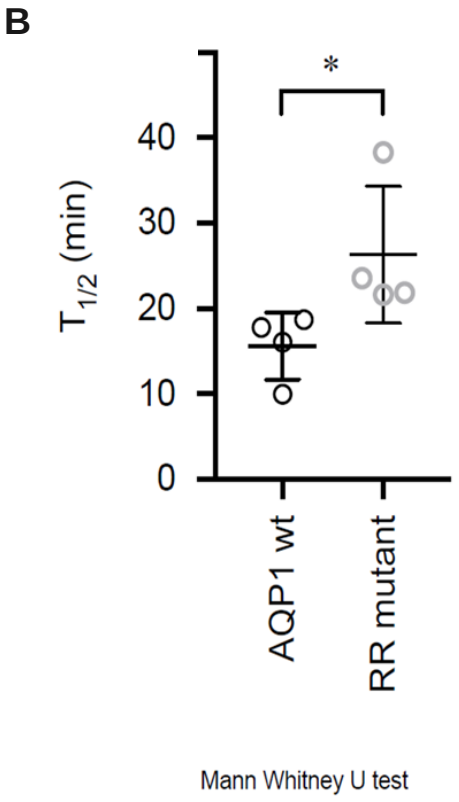

Mann Whitney U test

Figure 3

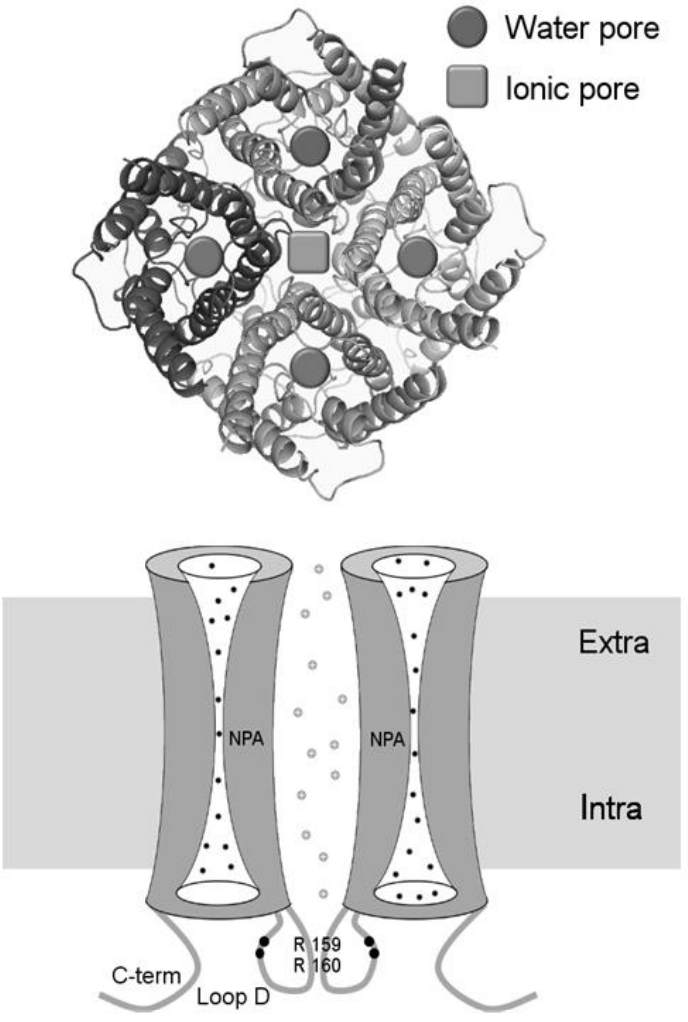
Water pore
Ionic pore
Extra
Intra
NPA
NPA
R 159
R 160
C-term
Loop D

Figure 4

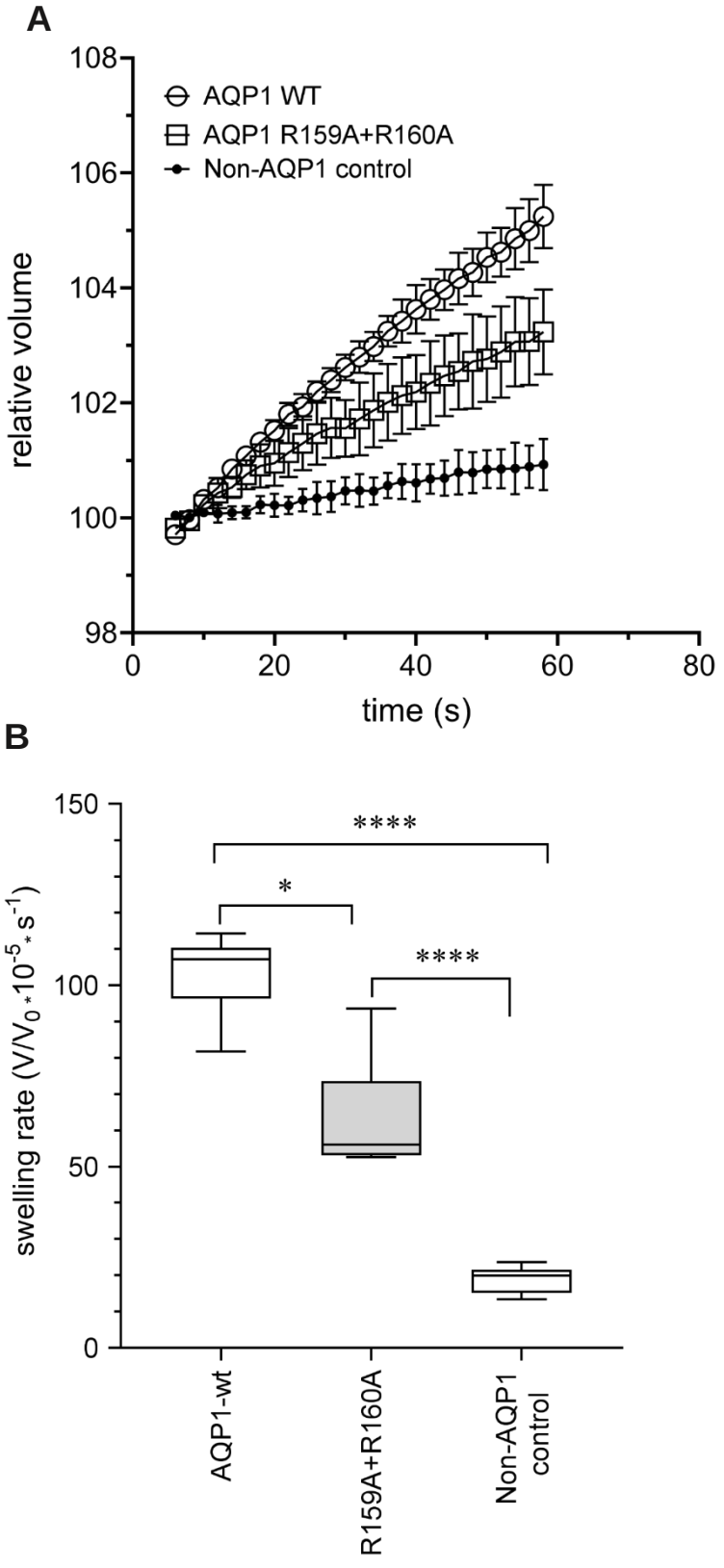
A
AQP1 WT
AQP1 R159A+R160A
Non-AQP1 control
relative volume
time (s)
B
swelling rate (V/V0*10-5*s-1)
****
*
****
AQP1-wt
R159A+R160A
Non-AQP1 control

Chapter4. Statement of Authorship

Statement of Authorship

Title of Paper	Differential Inhibition of Water and Ion Channel Activities of Mammalian Aquaporin-1 by Two Structurally Related Bacopaside Compounds Derived from the Medicinal Plant *Bacopa monnieri*
Publication Status	☑ Published ☐ Accepted for Publication ☐ Submitted for Publication ☐ Unpublished and Unsubmitted work written in manuscript style
Publication Details	Pal, J.V. et al. Differential Inhibition of Water and Ion Channel Activities of Mammalian Aquaporin-1 by Two Structurally Related Bacopaside Compounds Derived from the Medicinal Plant Bacopa monnieri. *Mol Pharmacol* 90, 498-507 (2016).

Principal Author

Name of Principal Author (Candidate)	Jinxin Pal
Contribution to the Paper	Initiated and performed experiments, analysis on all samples, interpreted data, wrote the manuscript.
Overall percentage (%)	70%
Certification:	This paper reports on original research I conducted during the period of my Higher Degree by Research candidature and is not subject to any obligations or contractual agreements with a third party that would constrain its inclusion in this thesis. I am the primary author of this paper.
Signature	Date 23/5/17

Co-Author Contributions

By signing the Statement of Authorship, each author certifies that:

i. the candidate's stated contribution to the publication is accurate (as detailed above);
ii. permission is granted for the candidate to include the publication in the thesis; and
iii. the sum of all co-author contributions is equal to 100% less the candidate's stated contribution.

Name of Co-Author	Mohamed Kourghi
Contribution to the Paper	Performed experiment and wrote the manuscript.
Signature	Date 22/05/2017

Name of Co-Author	Michael L. De Ieso
Contribution to the Paper	Performed experiment.
Signature	Date 23/5/17

Name of Co-Author	Ewan M. Campbell
Contribution to the Paper	Initiated the project.
Signature	Date 6/6/17.

Name of Co-Author	Hilary S. Dorward
Contribution to the Paper	Performed experiments.
Signature	Date 31/5/17

Name of Co-Author	Jennifer E. Hardingham
Contribution to the Paper	Initiated the project.
Signature	Date 1/6/17

Name of Co-Author	Andrea J. Yool
Contribution to the Paper	Initiated project, wrote the manuscript.
Signature	Date 23 May 2017

Published manuscript

Chapter 4: Differential inhibition of water and ion channel activities of mammalian Aquaporin-1 by two structurally related bacopaside compounds derived from the medicinal plant *Bacopa monnieri*.

Jinxin V Pei, Mohamad Kourghi, Michael L De Ieso, Ewan M Campbell, Hilary S Doward, Jennifer E. Hardingham and Andrea J Yool

School of Medicine, University of Adelaide; Adelaide SA 5005 Australia (JVP, MK, MLDI, JEH, AJY)

Institute for Photonics and Advanced Sensing, University of Adelaide; Adelaide SA 5005 Australia (JVP, AJY)

School of Biological Sciences, University of Aberdeen; Aberdeen AB242TZ Scotland (EMC)

Molecular Oncology Laboratory, Basil Hetzel Institute, The Queen Elizabeth Hospital, Woodville, SA, 5011 Australia. (HSD, JEH)

Corresponding author: Prof Andrea J Yool, Medical School South level 4, Frome Rd Adelaide SA 5005 AUSTRALIA

ph: +61 8 8313 3359

email: andrea.yool@adelaide.edu.au

fax: +61 8 8313 5384

ABBREVIATIONS: AQP, aquaporin; AqBxxx, numbered series of aquaporin modulators derived from bumetanide; AqFxxx, numbered series of aquaporin modulators derived from furosemide; FBS, fetal bovine serum; FUDR, 5-fluoro-2'-deoxyuridine; meWB, methanol extract of whole Bacopa; NCBI, National Center for Biotechnology Information; qRT-PCR, quantitative reverse-transcription polymerase chain reaction.

Abstract

Aquaporin-1 (AQP1) is a major intrinsic protein that facilitates flux of water and other small solutes across cell membranes. In addition to its function as a water channel in maintaining fluid homeostasis, AQP1 also acts as a non-selective cation channel gated by cGMP, a property shown previously to facilitate rapid cell migration in an AQP1-expressing colon cancer cell line. Here we report two new modulators of AQP1 channels, bacopaside I and bacopaside II, isolated from the medicinal plant *Bacopa monnieri*. Screening was conducted in the *Xenopus* oocyte expression system, using quantitative swelling and two-electrode voltage clamp techniques. Results showed bacopaside I blocked both the water (IC_{50} 117 μM) and ion channel activities of AQP1 but did not alter AQP4 activity, whereas bacopaside II selectively blocked the AQP1 water channel (IC_{50} 18 μM) without impairing the ionic conductance. These results fit with predictions from in silico molecular modelling. Both bacopasides were tested in migration assays using HT29 and SW480 colon cancer cell lines, with high and low levels of AQP1 expression respectively. Bacopaside I (IC_{50} 48 μM) and bacopaside II (IC_{50} 14 μM) impaired migration of HT29 cells, but had minimal effect on SW480 cell migration. Results here are the first to identify differential AQP1 modulators isolated from a medicinal plant. Bacopasides could serve as novel lead compounds for pharmaceutical development of selective aquaporin modulators.

Introduction

Aquaporin (AQP) water channels are in the family of major intrinsic proteins found from bacteria to humans (Agre, Preston et al. 1993, Reizer, Reizer et al. 1993, Calamita, Bishai et al. 1995), and are targets for the discovery of selective pharmacological modulators. Classes of aquaporins transport water and small uncharged molecules such as glycerol and urea through individual pores located in each subunit (Fu, Libson et al. 2000, Tajkhorshid, Nollert et al. 2002).

An expanding role for aquaporins as multifunctional channels is being recognized (Yool and Campbell 2012). In addition to facilitating water flux through intrasubunit pores, AQP1 also functions as a non-selective monovalent cation channel using the central pore at the four-fold axis of symmetry (Yool and Weinstein 2002, Yu, Yool et al. 2006, Campbell, Birdsell et al. 2012). The ion channel conductance is activated by interaction of cGMP in the intracellular Loop D domain, and modulated by the carboxyl terminal domain (Anthony, Brooks et al. 2000, Saparov, Kozono et al. 2001, Boassa and Yool 2003, Zhang, Zitron et al. 2007). cGMP appears to trigger opening of cytoplasmic hydrophobic barriers in the central pore, allowing hydration and cation permeation (Yu, Yool et al. 2006). Inhibition of the AQP1 ion channel has been shown to slow cell migration rates in a colon cancer cell line that expresses high levels of AQP1 (Kourghi, Pei et al. 2016).

Defining pharmacological modulators of aquaporins has been an area of keen interest (Papadopoulos and Verkman 2008, Devuyst and Yool 2010, Seeliger, Zapater et al. 2013). Early work identified blockers such as mercury (Preston, Jung et al. 1993), silver and gold (Niemietz and Tyerman 2002), acetazolamide (Gao, Wang et al. 2006), and

tetraethylammonium ion (Brooks, Regan et al. 2000, Yool, Brokl et al. 2002, Detmers, de Groot et al. 2006), but these remained limited in usefulness because of toxicity, lack of specificity, or variable efficacy across experimental systems (Yang, Kim et al. 2006, Yool 2007). More recently, small molecule pharmacological agents with therapeutic potential have been identified. Complexes of gold-based compounds have promise for the selective block of specific classes of aquaporins; functionalized bipyrene and terpyridines coordinating Au(III) were shown to block aquaglyceroporin AQP3 with little effect on AQP1 (Martins, Ciancetta et al. 2013). Intracellular arylsulfonamide modulators of AQP1 include the bumetanide derivative, AqB013, which blocks AQP1 and AQP4 water permeability (Migliati, Meurice et al. 2009); AqB011 which blocks the AQP1 cation channel (Kourghi, Pei et al. 2016); and the furosemide derivative AqF026 which potentiates water channel activity of AQP1 (Yool, Morelle et al. 2013). Other arylsulfonamide agents have been proposed as blockers of AQP4 (Huber, Tsujita et al. 2007, Huber, Tsujita et al. 2009). , Growing evidence is demonstrating that specific arylsulfonamides act as AQP modulators in vitro and in vivo (Pei, Burton et al. 2016). Diverse small molecules acting at the extracellular side present a valuable array of novel inhibitors of AQP1 (Seeliger, Zapater et al. 2013), indicating that other compounds in addition to coordinated metal ligands and arylsulfonamides are of interest for the development of AQP modulators. Lack of effects for a broad panel of AQP modulators tested in one study might reflect problems with synthesis or solubilization of the agents, or could indicate that the type of bioassay used influences apparent drug efficacy (Esteva-Font, Jin et al. 2016).

The present study was aimed at broadening the panel of AQP modulatory agents by evaluating natural medicinal plants as sources of active compounds. Quantitative swelling assays of mammalian AQP1 and AQP4 channels in the *Xenopus* expression system were used for screening extracts from a variety of traditional medicinal herbs, and identified *Bacopa monnieri* as one of several promising sources. Work here tested the hypothesis that chemical constituents of *B. monnieri* could be identified and characterized as pharmacological agents that modulate mammalian AQP1 by interacting at domains associated with pore functions.

Data here show that bacopaside I blocks both the water and ion channel activities of AQP1 but does not alter AQP4 activity, and bacopaside II selectively blocks the AQP1 water channel without impairing the ionic conductance. Results fit well with in silico docking for predicted energies of interaction at a pore-occluding intracellular site. Bacopasides I and II showed the same order of efficacy in blocking migration of AQP1-expressing HT29 colon cancer cells, with minimal effects on SW480 cells that express AQP1 at low levels. Results here are the first to identify AQP1 channels as one of the candidate targets of action of the Ayurvedic medicinal plant, water hyssop, and to define new lead compounds for the development of AQP modulators.

Materials and Methods

Bacopa methanol extraction and fractionation

Bacopa monnieri stems and leaves were obtained with permission from The Botanic Gardens of Adelaide (Adelaide, South Australia). Chopped bacopa plant material (100 g) was dried, then refluxed in 500ml of methanol for 2 hours at room temperature. The

suspension was filtered using Whatman No. 1 paper to obtain a methanol extract of whole bacopa (meWB). Half of the meWB extract was aliquoted into microfuge tubes, dried under vacuum (SpeedVac) into a solid brown paste, and reconstituted in saline for oocyte swelling assays. The other half of the meWB was fractionated using small-scale reverse phase C18 silica column (Alltech Prevail C18, Grace; Deerfield, IL). The mobile phases used for fractionation were a series of six water-methanol mixtures with H_2O:CH_3OH ratios ranging from 5:0 to 0:5. The fractions were dried in under vacuum and reconstituted in saline for oocyte swelling assays. Fractions containing AQP1 blocking activity were analyzed with mass spectrometry by Flinders Analytical (Flinders University, South Australia). Bacopaside I was identified by precise molecular weight as a major component in the active fractions, and bacopasides I and II were purchased from a commercial source (Chromadex; Irvine CA USA), solubilized in methanol to yield 100x stock solutions, and stored at -20°C. Experimental solutions were prepared by mixing the bacopaside stocks (1 part in 100) with isotonic saline or culture medium to yield final concentrations of 10 to 200 μM. Vehicle control salines were made using the same volume of methanol alone in isotonic saline or culture medium.

Oocyte preparation and cRNA injection

Unfertilized oocytes were isolated from *Xenopus laevis* frogs in accord with University Animal Ethics Committee-approved protocols, defolliculated by treatment with collagenase (type 1A, 2 mg/ml; Sigma, St. Louis, MO) and trypsin inhibitor (0.67 mg/ml; Sigma, St. Louis, MO) in OR-2 saline (82 mM NaCl, 2.5 mM KCl, 1 mM $MgCl_2$, and 5 mM HEPES; pH 7.6) at 16°C for 1.5 hours, washed in OR-2 saline, and then

incubated in isotonic oocyte saline [96 mM NaCl, 2 mM KCl, 0.6 mM $CaCl_2$, 5 mM $MgCl_2$, and 5 mM HEPES supplemented with 10% horse serum (Sigma, St. Louis, MO), 100 U/ml penicillin, 100 μg/ml streptomycin and 50 μg/ml tetracycline, pH 7.6] at 16°C. Oocytes were injected with 1-4 ng of AQP1, AQP4 or AQP1 R159A+R160A cRNA in 50 nl sterile water and incubated for 2 to 3 days at 16-18°C to allow protein expression. Oocytes not injected with cRNA served as non-AQP-expressing control cells.

Human AQP1 (National Center for Biotechnology Information NCBI GenBank: BC022486.1) and rat AQP4 (AF144082.1) cDNAs from P. Agre (The Johns Hopkins University, Baltimore, MD) were subcloned into a modified Xenopus β-globin expression plasmid. The double mutant construct human AQP1 R159A+R160A cDNA was generated by site-direct mutation (QuikChange; Stratagene, La Jolla, CA) and sequenced to confirm no errors were introduced (Yu, Yool et al. 2006). cDNAs were linearized with BamHI and transcribed using T3 polymerase (T3 mMessage mMachine; Ambion Inc., Austin, TX). cRNAs were resuspended in sterile water and stored at -80°C.

Quantitative oocyte swelling assays

Immediately prior to swelling assays, control and AQP-expressing oocytes were preincubated in isotonic saline (serum- and antibiotic-free) with or without meWB or bacopaside compounds or with methanol vehicle at 16-18°C, for incubation periods as indicated. Osmotic water permeability was determined as the linear rate of change in volume as a function of time, immediately after introduction into 50% hypotonic saline

(isotonic saline diluted with equal volume of water). Oocytes were imaged using a computer controlled charge-coupled-device grayscale camera (Cohu, San Diego, CA) mounted on a dissecting microscope (Olympus SZ-PT; NSW Australia). Images were taken at 0.5 frames per second for 60 seconds; cross-sectional areas were quantified using ImageJ software (Research Services Branch; National Institutes of Health, MD USA). Swelling rates were calculated as the slopes of linear regression fits of volume as a function of time in hypotonic saline. Data were analyzed and compiled for multiple batches of oocytes for statistical analyses and to generate dose-response curves, which were fit by sigmoidal non-linear variable-slope dose-response regression functions using Prism (GraphPad Software Inc., San Diego, CA USA).

Molecular docking

In silico modeling was done with methods reported previously (Yool et al., 2013). The protein crystal structures for human AQP1 (PDB ID. 1FQY) and human AQP4 (PDB ID. 3GDB) were obtained from the protein data bank (NCBI Structure). Bacopaside I and II structures were obtained from PubChem (NCBI) and converted into a software-compatible 3D structures in .pdb format using the Online SMILES Translator and Structure File Generator (National Cancer Institute, US Dept Health and Human Services). Ligand and receptor coordinates were prepared for docking using Autodock (Version 4.2, Scripps Research Institute, La Jolla, CA USA). Autodock Vina (Trott and Olson 2010) was used to run the flexible ligand docking simulations with two docking grids covering both intracellular and extracellular faces of the monomeric pores. 3D docking result files and docking energy values were exported from Autodock, and

results were viewed using PyMol software (Version 1.8, Schrödinger, LLC). Data for AQP1 and AQP4 docking results in .pse format are provided as Supplemental Files 1 and 2.

Electrophysiology

For two-electrode voltage clamp, capillary glass electrodes (1–3 MΩ) were filled with 1 M KCl. Recordings were done in standard isotonic Na^+ bath saline containing 100 mM NaCl, 2 mM KCl, 4.5 mM $MgCl_2$, and 5 mM HEPES, pH 7.3. cGMP was applied extracellularly at a final concentration of 10-20 μM using the membrane-permeable cGMP analog [Rp]-8-[para-chlorophenylthio]-cGMP (Sigma Chemical, Castle Hill NSW Australia). Ionic conductance was monitored for at least 20 min after cGMP addition to allow development of maximal plateau responses. Conductance was determined by linear fit of the current amplitude as a function of voltage, with a step protocol from +60 to -110mV and holding potential of -40 mV. After the first activation by cGMP, oocytes were incubated in isotonic saline with or without bacopaside I or bacopaside II for two hours to allow recovery. After incubation, a second application of cGMP was used to test for reactivation, to determine if any block of the ionic conductance was evident. Using the same protocol, AQP1-expressing oocytes were demonstrated previously to show cGMP-dependent activation, complete recovery during a 2 h incubation in saline alone, and full reactivation of the ionic conductance response to a second application of cGMP, whereas non-AQP1-expressing control oocytes showed a low ionic conductance and no significant response to drug treatments throughout the same

protocol (Kourghi, Pei et al. 2016). Recordings were made with a GeneClamp amplifier and pClamp 9.0 software (Molecular Devices, Sunnyvale CA USA).

Cancer cell culture and migration assays

HT29 and SW480 colon cancer cell lines (from American Type Culture Collection ATCC, Manassas, VA USA) were cultured in complete medium composed of Dulbecco's Modified Eagles Medium (DMEM) supplemented with 1 x glutaMAX™ (Life Technologies Mulgrave, VIC, Australia), penicillin and streptomycin (100 U/ml each) and 10% fetal bovine serum (FBS). Cultures were maintained in 5% CO_2 at 37°C. Cells were seeded in a flat-bottom 96-well plates at 1.25 x 10^6 cells/ml to produce a confluent monolayer. For 12 to 18 hours prior to wounding, cells were serum-starved in 2% FBS, in the presence of 400 nM of the mitotic inhibitor 5-fluoro-2'-deoxyuridine, FUDR (Parsels, Parsels et al. 2004). For wounding, a sterile p10 pipette tip was attached to the end of a vacuum tube, and a circular wound was created by brief perpendicular contact of the tip with base of the well. Each well was then washed three times with phosphate buffered saline (PBS) to remove detached cell debris. Cultures were maintained during the wound closure assay in 2% FBS medium with FUDR. Wound images were imaged at 10x magnification with a Canon 6D camera mounted on a Olympus inverted microscope. Image dimensions and pixel density were standardized across each image series using XnConvert software. Linear outlines and areas of the wound were generated using ImageJ software (National Institutes of Health). Wound closure data as a function of time were calculated as a percentage of the initial wound areas for the same wells.

Quantitative RT-PCR

Cells at 70-80% confluence were harvested and RNA extracted using the PureLink™ RNA Mini kit (Life Technologies). RNA was quantified using the NanoDrop 2000 spectrophotometer (Thermo Scientific, Waltham, MA, USA) and the integrity (RIN score) assessed using the 2100 Bioanalyzer (Agilent Technologies, Santa Clara, CA, USA). RNA (500 ng) was reverse transcribed using the iScript™ cDNA synthesis kit (Bio-rad, Carlsbad, CA, USA). qPCR of AQP1 and the reference gene phosphomannose mutase 1 (PMM1) was performed using multiplex Taqman expression assays (Life Technologies) and SsoFast™ probes supermix (Bio-rad) in triplicate in the Rotorgene 6000 (Qiagen).

Western blot

Cultured cells were lysed with RIPA buffer containing 1% β-mercaptoethanol, 1% HALT protease inhibitor 100X solution, 150 U Benzonase (all from Sigma, St Louis, MO, USA) on ice for 10 minutes, homogenized by passing through a 21 gauge syringe and centrifuged 14,000 x g for 15 minutes at 4◦C to pellet the cell debris. Protein was quantified (EZQ® assay, Life Technologies). Each sample (50 µg) was resolved by SDS-PAGE on a 12% Mini-PROTEAN® TGX Stain-Free™ Gels (Bio Rad) and transferred to PVDF membranes using the Trans-Blot® Turbo™ Transfer Pack and System (Bio Rad). Membranes were blocked with TBST containing 5% skim milk for 1hour and incubated overnight at 4◦C with anti- AQP1 (H-55) (1/500; Santa Cruz, USA). Following three washes in TBST, membranes were incubated with goat anti-

rabbit IgG HRP secondary antibody (1/ 2000) and Streptactin-HRP Conjugate (1/10000) (both Bio-Rad) at room temperature for 1h, and washed. Chemiluminescence using Clarity™ Western ECL Blotting Substrate (Bio-Rad) was used for detection and blots imaged using the ChemiDoc™ Touch Imaging System (Bio-Rad). Image Lab™ Software was used to validate western blotting data via total protein normalization (Bio-Rad).

Immunocytochemistry

HT29 and SW480 cells grown on coverslips to 50% confluence were fixed with 4% paraformaldehyde and permeabilized with 0.5% Triton X-100. Image-iT® FX Signal Enhancer (Life Technologies) was used as per manufacturer's instructions. AQP1 was labelled with a 1/400 dilution of rabbit polyclonal anti-human AQP1 (Abcam®, Cambridge, UK), visualized with a secondary antibody at 1/200 dilution (goat anti rabbit IgG H&L Alexa Fluor® 568; Life Technologies). Cells were counterstained with NucBlue® Fixed Cell Ready ProbesTM Reagent (Life Technologies). Coverslips were mounted in ProLong® Gold antifade reagent (Life Technologies) and imaged with a Zeiss LSM 700 microscope (Carl Zeiss, Jena, Germany).

Live cell imaging

Cells were seeded on an 8-well uncoated Ibidi µ-Slide (Ibidi, Munich Germany) at a density of 1.0 x 10^6 cells/ml. For 12 to 18 hours prior to wounding, cells were serum-starved in medium with 2% FBS in the presence of FUDR (400 nM). Five circular wounds were created in each well using techniques described for the migration assays (above). The slide was mounted on a Nikon Ti E Live Cell Microscope (Nikon, Tokyo

Japan) in an enclosed chamber kept at 37 °C with 5% CO_2. Images were taken at 5 min intervals for 24 hours, using Nikon NIS-Elements software (Nikon, Japan). AVI files were exported from NIS-Elements and converted into TIFF files using ImageJ (NIH). Converted files were analyzed using Fiji software (Schindelin, Arganda-Carreras et al. 2012) with the Manual Tracking plug-in.

Cytotoxicity assay

HT29 cell viability was quantified using the AlamarBlue assay (Molecular Probes, Eugene, OR USA). Cells were plated at 10^4 cells/well in 96-well plates, and fluorescence signal levels were measured with a FLUOstar Optima microplate reader after 24 h incubation with concentrations of bacopaside I from 0 to 100 μM or bacopaside II from 0 to 30 μM, to obtain quantitative measures of cell viability. Mercuric chloride (100 μM) was used as a positive control for cytotoxicity.

Results

Extracted compounds from Bacopa monnieri inhibited AQP1 water channel activity.

Methanol-extracted whole Bacopa (meWB) reconstituted in isotonic saline inhibited the water permeability of AQP1-expressing oocytes (Fig 1A). After 2 hours preincubation in 1 mg/ml meWB, swelling rates of AQP1-expressing oocytes were significantly reduced ($p<0.001$) as compared with untreated AQP1-expressing oocytes. Fractionated samples of meWB reconstituted at 0.1 mg/ml each were tested for biological activity using oocyte swelling assays (Fig 1B) after 2 hours preincubation. AQP1-mediated swelling was significantly decreased by fractions 3 and 4; other fractions had no effect. Combined fractions 3 and 4 were analyzed by mass spectrometry and revealed the presence of a major compound identified by precise molecular weight as bacopaside I. Commercially purchased bacopasides I and II were found to block osmotic water permeability in AQP1-expressing oocytes (Fig 1C) and showed a dose-dependent effect (Fig 1D). The inhibition of AQP1-mediated osmotic water fluxes showed IC_{50} values of approximately 18 μM for bacopaside II, and approximately 117 μM for bacopaside I.

Inhibition bacopasides I and II was time-dependent and reversible.

AQP4-expressing oocytes showed no block of water channel activity after 2 h preincubation in isotonic saline containing bacopaside I at 178 μM (Fig 2A). The blocking effect of bacopaside was specific for AQP1. The inhibitory effect of bacopasides I and II on AQP1 water channel activity took time to develop, with near

maximum block achieved by approximately 2 h (Fig 2B). The magnitude of inhibition of AQP water flux increased as a function of the duration of preincubation in 178 μM bacopaside I or 35 μM bacopaside II. For bacopaside I, half-maximal block was reached after approximately 50 min, and maximum block after 120 min of preincubation. For bacopaside II, half-maximal block was reached after approximately 30 min, and maximum block after 80 min of preincubation. Longer times provided no appreciable further enhancement of the magnitude of inhibition. Comparably slow time-dependent onset of block has been noted previously for other AQP1 ligands such as AqB013, AqB011 and AqF026, which are thought to bind at the intracellular side of the channel (Migliati, Meurice et al. 2009, Yool, Morelle et al. 2013, Kourghi, Pei et al. 2016), and require time to travel across the plasma membrane to the cytoplasmic side. The blocking effects of bacopasides I and II on AQP1 water channel activity were reversible (Fig 2C). AQP1 channels were preincubated 2 hours with 178 μM bacopaside I or 35 μM bacopaside II, followed by washout of the drug with isotonic saline. The osmotic water permeability showed approximately 25% recovery by 120 min after the washout of bacopaside I, and half-maximal recovery by 160 min. For bacopaside II, water permeability showed 25% recovery by 150 min after washout of the blocker, and half-maximal recovery by 200 min.

The ion channel conductance of AQP1 was inhibited by bacopaside I but not by bacopaside II.

Two-electrode voltage clamp recordings from AQP1-expressing oocytes demonstrated the cGMP-dependent activation of the ionic conductance (Fig 3A) as described

previously (Anthony, Brooks et al. 2000), which was reversible by 2 h incubation in saline without membrane-permeable cGMP (Kourghi, Pei et al. 2016). Re-activation of the ionic response by a second dose of cGMP was partly blocked in AQP1-expressing oocytes after 2 h incubation in 50 μM bacopaside I, and strongly blocked at 100 μM bacopaside I. In contrast, the reactivation of the ion conductance was unimpaired after incubation with 10 μM or 20 μM bacopaside II (Fig 3B).

Identification of candidate intracellular binding sites.

Protein crystal structures of AQP1 and AQP4, and three-dimensional structural renditions of bacopaside I and bacopaside II were prepared and run on interaction simulations using Autodock Vina software to identify predicted binding sites. An array of candidate docking sites for bacopasides I and II on AQP1 and -4 channels were considered with in silico computational docking analyses. Of a total of 8 possible positions evaluated for bacopaside I, the dominant energetically-favored configurations for intracellular binding yielded values of -9.2 Kcal/mol for AQP1, and -8.0 Kcal/mol for AQP4. Similarly out of all possible positions evaluated, the energetically-favored configurations for bacopaside II yielded values of -9.3 Kcal/mol for AQP1, and -7.8 Kcal/mol for AQP4.

In the poses reflecting the most favored docking positions, the intracellular face of the water pore was effectively occluded by bacopasides I and II in AQP1, but not in AQP4 channels (Fig 4A,B,C,D). For AQP1, the bacopasides appeared to nest well into the internal vestibule of the intrasubunit water pore. For AQP4 the optimal interaction was seen for bacopaside sitting in a groove between transmembrane domains 4 and 5, a

position where subunits interface near the central pore that might not be accessible in the assembled tetrameric channel.

Closer inspection of specific amino acid residues in the predicted AQP1 docking site (using Chimera visualization software) suggested that the poly-arginine motif in the Loop D domain could enable hydrogen bond formation with the sulfonyl moiety on the glucopyranosyl sugar of bacopaside I (Fig 4E) at residues corresponding to R159 and R160 in human AQP1. These arginines are part of a highly conserved amino acid pattern seen in AQP1 channels from diverse species, and required for cGMP gating of the AQP1 ionic conductance (Yu, Yool et al. 2006). The site-directed double mutation of arginines R159 and R160 to alanines did not prevent normal expression of AQP1-mediated osmotic water permeability, indicating that the AQP1 mutant constructs were expressed and targeted to the oocyte plasma membrane as described previously (Yu, Yool et al. 2006); however, the efficacy of bacopaside I in inhibiting osmotic water permeability was abolished in the mutant construct at doses up to 100 μM (Figure 1D, supporting the suggested role of the loop D arginine residues in stabilizing the docking of the bacopaside I ligand.

Bacopaside II was more effective than bacopaside I in blocking migration of AQP1-expressing colon cancer cells. HT29 cells have a higher endogenous level of AQP1 expression as compared with SW480 cells, as demonstrated by quantitative RT-PCR (Fig. 5A), western blot (Fig. 5B), and immunocytochemistry (Fig 5C) analyses. Wound closure assays showed robust migration of HT29 cells in medium with vehicle (Fig 6A), resulting in little open area remaining at 24 h. In contrast, treatment with

bacopaside II (Fig. 6B) substantially reduced the amount of wound closure.Dose-dependent block of cell migration measured by wound closure (Fig 6C) was observed for both bacopaside I and bacopaside II on HT29 cells. The calculated IC_{50} value for bacopaside I was approximately 48 μM and for bacopaside II was 14 μM in HT29 cells. There was a small reduction of migration observed for SW480 cells treated with bacopaside II (Fig 6C), which was consistent with the relatively low expression of AQP1 channels in this cell line.

Time-lapse imaging demonstrated bacopasides I and II differentially decreased the rate of migration of AQP1-expressing HT29 colon cancer cells. Cultured HT29 cancer cells showed different rates of migration into the open wound areas in in vehicle bacopaside I and bacopaside II treatment conditions (Fig 7A,B,C). Time lapse images showed the rates of cell migration were significantly impeded in 50 μM bacopaside I and in 15 μM bacopaside II (Fig 7B,C) as compared with vehicle-treated HT29 cells (Fig 7A). No appreciable difference in cell viability was observed in any of the treatment groups during the 24 time course of the experiment.

In the vehicle-treated group, trajectory plots of individual cells sampled at 50 min intervals over 24 h (Fig 7D) showed generally directional movements of HT29 cells into the open wound spaces. In bacopaside I treatment group, the HT29 cells lacked directional migration and moved short distances between successive frames. In the bacopaside II treated group, the impairment of movement was evident but less severe. The collective trend of trajectories of the vehicle-treated group appeared to be linear and extended, whereas that in the bacopaside I treated group was recursive and

compressed; the bacopaside II group showed an intermediate level of restriction of movement.

The net displacement (distance travelled) per time interval was greater in the vehicle treated than the bacopasides I or II treated groups. Frequency histograms showing the number of events observed were compiled as binned values of distances travelled per 50 min interval (Fig 7E), and showed that more cells travelled longer distances in the vehicle treated group as compared with the bacopasides I and II treated groups. Distances moved per 50 min interval were well fit by Gaussian distributions. The decreased mean distances moved in both bacopaside I and II treated groups were seen as a left shift in the peaks of the frequency histograms. Compiled data in a summary histogram (Fig 7F) confirmed the significant decrease in mean total distance travelled by cells during the 24 hours of tracking in bacopaside I or II as compared with vehicle treated cells. Analysis of cytotoxicity by AlamarBlue assay showed that bacopaside I had no significant effect on cell viability at 50 or 75 μM, and bacopaside II had no effect on viability at 15 or 20 μM (Table 1). Concentrations of bacopasides that significantly blocked AQP1 water channel activity and HT29 cell migration were not appreciably cytotoxic.

Discussion

Results here demonstrated that two structurally similar compounds, bacopaside I and bacopaside II derived from a medicinal herb, act differentially as pharmacological inhibitors of mammalian aquaporin channels. In silico modeling predicted that bacopasides I and II have favorable energies of interaction at the intracellular vestibule of AQP1, occluding the intrasubunit water pore. Modeling results were consistent with observed effects of these agents as AQP1 inhibitors. Predicted energies of interaction for docking on AQP1 were higher for bacopaside II than bacopaside I, fitting the observed order of efficacy in blocking AQP1-mediated swelling of oocytes and the same order of efficacy in blocking migration of AQP1-expressing HT29 colon cancer cells, with minimal effects on SW480 cells that express little AQP1. The docking of bacopasides I and II to occlude the water pore appeared principally to involve the trisaccharide rings, which projected down into the AQP1 intrasubunit pore. Future work exploring polysaccharides and related osmolytes as endogenous modulators of AQP channels could be of interest. The lack of a favorable docking interaction of bacopaside with the AQP4 water pore was consistent with the insensitivity of AQP-4 expressing oocytes to bacopaside I in osmotic swelling assays. Based on the docking model, candidate residues that could contribute to the proposed binding of bacopaside sugar rings in the hAQP1 intracellular water pore appear to include amino acids serine 71 in the loop B region, and tyrosine 97 in the adjacent membrane spanning domains, but remain to be defined.

Inhibition of AQP1 water channel activity by bacopasides I and II showed a slow onset that was consistent with prerequisite transit of the agent across the plasma membrane

to access the intracellular side. The latency period (approximately 2 h) was comparable to that described for other aquaporin modulators AqB013 and AqF026, also thought to act at the cytoplasmic side (Migliati, Meurice et al. 2009, Yool, Morelle et al. 2013).

Accumulating evidence suggests pharmacological agents can be defined with subtype selectivity for AQP classes. Prior work showed that external application of AqF026 potentiated water permeability in AQP1 (EC_{50} 3.3 μM), but a 15-fold higher concentration was required to potentiate AQP4 (Yool, Morelle et al. 2013). Metal complexes acted as blockers of glycerol permeability in AQP3 (at an external site predicted to involve cysteine (C40) and arginine (R218) residues), with comparatively small effects on AQP1 water permeability (Martins, Ciancetta et al. 2013). Results here for bacopaside I showed block of osmotic water permeability for AQP1 but not AQP4 channels. This difference in bacopaside sensitivity between related aquaporins suggests that the inhibitory effects seen for AQP1 are exerted directly on the heterologously expressed channel, and not due to side effects on endogenous oocyte channels or transporters.

The reversibility of block indicated that functional properties and expression of the channels in plasma membrane were not impaired. Data here cannot rule out possible actions of bacopasides on other molecules not yet assessed; however, the lack of effect of bacopaside treatment on migration in a cancer cell line SW480 with low AQP1 expression suggests the mechanism of action is reasonably selective, and does not appreciably impact diverse signalling and transport processes needed for basic maintenance and non-AQP1 dependent motility. Cytotoxicity assays showed that the

viability of AQP1-expressing HT29 cancer cells was not affected by bacopasides I and II at doses that significantly blocked ion flux and cell migration.

Bacopasides I and II are triterpene glycosides, composed of a hydrophobic pentacyclic terpene backbone (estimated logP value approximately 9; enabling membrane permeability), and three linked polar sugar groups (arabinofuranosyl—glucopyranosyl—arabinopyranose in bacopaside I; and arabinofuranosyl—sulfonyl-glucopyranosyl—glucopyranose in bacopaside II) that appear from in silico modeling to lodge via H-bonds into the water pore entrance of AQP1, with the exception of the sulfonyl group which appears to require an interface with positively charged residues (arginines in the adjacent AQP1 Loop D domain). Mutation of the key Loop D arginines to alanines appeared to cause destabilization of the overall binding of the bacopaside I compound on AQP1, seen as a decreased efficacy of water pore block and increased IC_{50} value in the R159A+R160A mutant.

The ability of modulators to differentially block the ionic conductance is an important consideration in processes such as rapid cell migration which appear to require AQP1 cation channel function (Kourghi, Pei et al. 2016). Interaction of the sulfonyl group with Loop D arginines was consistent with the observed block of the cGMP-activated ionic conductance by bacopaside I not II. Bacopaside I showed a lower IC_{50} value for inhibiting HT29 cancer cell migration (~48 μM) than for inhibiting the AQP1 ionic conductance alone (~117 μM), and the cell migration trajectories in bacopaside I-treated group were more compressed than those in the bacopaside II-treated group, suggesting that simultaneous block of both water and ion channel activities of AQP1

might be more effective in blocking AQP1-dependent cell migration than impairing either function alone.

Although the overall amino acid sequence similarity between AQP1 and AQP4 channels is high (>40% identity and 60% homology), AQP4-mediated osmotic swelling was not sensitive to block by bacopaside I. The docking model suggested the bulky terpene might sterically hinder docking near the AQP4 water pore. As well, the Loop D domain of AQP4 lacks the key arginines 159 and 160 suggested here to be important for the sulfonyl group coordination, showing instead serine and lysine in the equivalent positions, which might be less effective as putative coordination sites.

The identification of bacopasides as novel AQP modulators expands the database of pharmacophore properties of AQP ligands. Bacopasides I and II themselves might not be ideal as drug candidates, exceeding limits of Lipinski's Rule of Five for molecular weight, hydrophobicity, and numbers of hydrogen bond donors and acceptors—although natural products often show biological activity as exceptions to the rule (Ganesan 2008). Bacopasides administered in vivo are likely to act as metabolic derivatives as well as intact compounds. More work is needed to define in vivo metabolites of bacopasides and characterize their effects on aquaporins. Nonetheless, bacopasides could serve as lead compounds for the design of small-molecule blockers of aquaporins. Results here suggest the trisaccharide moiety is a key component. An intriguing idea would be to design compact membrane-permeable trisaccharides for blocking water flux; while addition of key sulfonyl or other groups could inhibit parallel AQP functions. Endogenous polysaccharide osmolytes in cells might function as

natural modulators of aquaporin channels, a concept that has not to our knowledge been considered previously.

Bacopa monnieri extract (also known as brahmi) has been used in Ayurvedic remedies since ancient times to improve memory and treat anxiety and depression (Russo and Borrelli 2005). Brahmi has been suggested to have beneficial effects on psychological state, cognitive performance, and memory in human subjects and animal models; neuroprotective effects after ischemic brain injury; and anti-inflammatory actions in processes linked to neurodegenerative disorders (Singh and Dhawan 1982, Sairam, Dorababu et al. 2002, Rehni, Pantlya et al. 2007, Zhou, Shen et al. 2007, Saraf, Prabhakar et al. 2010, Aguiar and Borowski 2013, Downey, Kean et al. 2013, Liu, Yue et al. 2013, Kongkeaw, Dilokthornsakul et al. 2014, Williams, Munch et al. 2014). A meta-analysis of human clinical studies (generally with *B. monnieri* administered 250-450 mg/day for up to several months) improved mental response time and attention, and had potential benefits on memory (Kongkeaw, Dilokthornsakul et al. 2014). No serious adverse events were noted; minor side effects included diarrhea and dry mouth.

Beneficial outcomes ascribed to brahmi could in part involve block of AQP1 channels. AQP1 is expressed abundantly in brain choroid plexus where cerebral spinal fluid is produced (Boassa and Yool 2005, Johansson, Dziegielewska et al. 2005), and in proximal kidney to facilitate water reabsorption (Nielsen and Agre 1995). AQP1 is found in peripheral vasculature endothelia, red blood cells, and other cell types (Nielsen, Smith et al. 1993). Block of AQP1 could contribute to the anti-inflammatory benefits of brahmi treatment. Macrophages express AQP1 channels, which are

required for IL-1β release and neutrophilic inflammation responses (Rabolli, Wallemme et al. 2014). An alcoholic extract of *B. monnieri* decreased TNF-alpha production in mouse macrophages preincubated for 1 h, with an IC_{50} near 1 mg/ml (Williams, Munch et al. 2014).

Pharmacological inhibitors of AQP1 channels could be useful for intervention in many conditions, including slowing metastasis in AQP1-positive cancer subtypes. In a subset of aggressive cancers, AQP1 expression is upregulated (Saadoun, Papadopoulos et al. 2002, Moon, Soria et al. 2003, Yool, Brown et al. 2009, El Hindy, Bankfalvi et al. 2013). AQP1 channels located at lamellipodial edges have been implicated in enhancing migration and metastasis (Hu and Verkman 2006, McCoy and Sontheimer 2007). Block of the AQP1 ion channel has been shown to slow migration in AQP1-expressing HT29 colon cancer cells (Kourghi, Pei et al. 2016).

A comprehensive portfolio of effective and selective aquaporin modulators is needed for clinical and basic research. Further exploration of AQP modulators in traditional herbal medicines is merited (Pei, Burton et al. 2016). New ligand modulators of aquaporin channel activity could be present in the armamentarium of traditional herbal medicines, but remain to be discovered.

Acknowledgments

Thanks to John Sandham and The Botanic Gardens of Adelaide for identified samples of the water hyssop *Bacopa monnieri*; and to Dr Agatha Labrinidis and the Adelaide Microscopy core facility for access to equipment, support and training in live cell imaging.

Footnote

This work was supported by funding from the University of Adelaide Institute for Photonics and Advanced Sensing 2015 Pilot Grant program, and Australian Research Council Discovery Project grant DP160104641.

Authorship contributions

Participated in the research design: Pei, Campbell, Yool, Hardingham

Conducted experiments: Pei, Kourghi, De Ieso, Campbell, Doward

Performed data analysis: Pei, Kourghi, De Ieso, Yool

Wrote or contributed to writing of the manuscript: Pei, Kourghi, De Ieso, Yool

References

Agre P, Preston GM, Smith BL, Jung JS, Raina S, Moon C, Guggino WB and Nielsen S (1993) Aquaporin CHIP: the archetypal molecular water channel. *The American journal of physiology* **265**(4 Pt 2):F463-476.

Aguiar S and Borowski T (2013) Neuropharmacological review of the nootropic herb Bacopa monnieri. *Rejuvenation Res* **16**(4):313-326.

Anthony TL, Brooks HL, Boassa D, Leonov S, Yanochko GM, Regan JW and Yool AJ (2000) Cloned human aquaporin-1 is a cyclic GMP-gated ion channel. *Mol Pharmacol* **57**(3):576-588.

Boassa D and Yool AJ (2003) Single amino acids in the carboxyl terminal domain of aquaporin-1 contribute to cGMP-dependent ion channel activation. *BMC Physiol* **3**:12.

Boassa D and Yool AJ (2005) Physiological roles of aquaporins in the choroid plexus. *Curr Top Dev Biol* **67**:181-206.

Brooks HL, Regan JW and Yool AJ (2000) Inhibition of aquaporin-1 water permeability by tetraethylammonium: involvement of the loop E pore region. *Molecular pharmacology* **57**(5):1021-1026.

Calamita G, Bishai WR, Preston GM, Guggino WB and Agre P (1995) Molecular cloning and characterization of AqpZ, a water channel from Escherichia coli. *The Journal of biological chemistry* **270**(49):29063-29066.

Campbell EM, Birdsell DN and Yool AJ (2012) The activity of human aquaporin 1 as a cGMP-gated cation channel is regulated by tyrosine phosphorylation in the carboxyl-terminal domain. *Mol Pharmacol* **81**(1):97-105.

Detmers FJ, de Groot BL, Muller EM, Hinton A, Konings IB, Sze M, Flitsch SL, Grubmuller H and Deen PM (2006) Quaternary ammonium compounds as water channel blockers. Specificity, potency, and site of action. *J Biol Chem* **281**(20):14207-14214.

Devuyst O and Yool AJ (2010) Aquaporin-1: new developments and perspectives for peritoneal dialysis. *Perit Dial Int* **30**(2):135-141.

Downey LA, Kean J, Nemeh F, Lau A, Poll A, Gregory R, Murray M, Rourke J, Patak B, Pase MP, Zangara A, Lomas J, Scholey A and Stough C (2013) An Acute, Double-Blind, Placebo-Controlled Crossover Study of 320 mg and 640 mg Doses of a Special Extract of Bacopa monnieri (CDRI 08) on Sustained Cognitive Performance. *Phytother Res* **27**:1407-1413.

El Hindy N, Bankfalvi A, Herring A, Adamzik M, Lambertz N, Zhu Y, Siffert W, Sure U and Sandalcioglu IE (2013) Correlation of aquaporin-1 water channel protein expression with tumor angiogenesis in human astrocytoma. *Anticancer research* **33**(2):609-613.

Esteva-Font C, Jin BJ, Lee S, Phuan PW, Anderson MO and Verkman AS (2016) Experimental Evaluation of Proposed Small-Molecule Inhibitors of Water Channel Aquaporin-1. *Mol Pharmacol* **89**(6):686-693.

Fu D, Libson A, Miercke LJ, Weitzman C, Nollert P, Krucinski J and Stroud RM (2000) Structure of a glycerol-conducting channel and the basis for its selectivity. *Science* **290**(5491):481-486.

Ganesan A (2008) The impact of natural products upon modern drug discovery. *Curr Opin Chem Biol* **12**(3):306-317.

Gao J, Wang X, Chang Y, Zhang J, Song Q, Yu H and Li X (2006) Acetazolamide inhibits osmotic water permeability by interaction with aquaporin-1. *Analytical biochemistry* **350**(2):165-170.

Hu J and Verkman AS (2006) Increased migration and metastatic potential of tumor cells expressing aquaporin water channels. *FASEB journal : official publication of the Federation of American Societies for Experimental Biology* **20**(11):1892-1894.

Huber VJ, Tsujita M, Kwee IL and Nakada T (2009) Inhibition of aquaporin 4 by antiepileptic drugs. *Bioorg Med Chem* **17**(1):418-424.

Huber VJ, Tsujita M, Yamazaki M, Sakimura K and Nakada T (2007) Identification of arylsulfonamides as Aquaporin 4 inhibitors. *Bioorg Med Chem Lett* **17**(5):1270-1273.

Johansson PA, Dziegielewska KM, Ek CJ, Habgood MD, Mollgard K, Potter A, Schuliga M and Saunders NR (2005) Aquaporin-1 in the choroid plexuses of developing mammalian brain. *Cell Tissue Res* **322**(3):353-364.

Kongkeaw C, Dilokthornsakul P, Thanarangsarit P, Limpeanchob N and Norman Scholfield C (2014) Meta-analysis of randomized controlled trials on cognitive effects of Bacopa monnieri extract. *J Ethnopharmacol* **151**(1):528-535.

Kourghi M, Pei JV, De Ieso ML, Flynn G and Yool AJ (2016) Bumetanide Derivatives AqB007 and AqB011 Selectively Block the Aquaporin-1 Ion Channel Conductance and Slow Cancer Cell Migration. *Mol Pharmacol* **89**(1):133-140.

Liu X, Yue R, Zhang J, Shan L, Wang R and Zhang W (2013) Neuroprotective effects of bacopaside I in ischemic brain injury. *Restorative neurology and neuroscience* **31**(2):109-123.

Martins AP, Ciancetta A, de Almeida A, Marrone A, Re N, Soveral G and Casini A (2013) Aquaporin inhibition by gold(III) compounds: new insights. *ChemMedChem* **8**(7):1086-1092.

McCoy E and Sontheimer H (2007) Expression and function of water channels (aquaporins) in migrating malignant astrocytes. *Glia* **55**(10):1034-1043.

Migliati E, Meurice N, DuBois P, Fang JS, Somasekharan S, Beckett E, Flynn G and Yool AJ (2009) Inhibition of aquaporin-1 and aquaporin-4 water permeability by a derivative of the loop diuretic bumetanide acting at an internal pore-occluding binding site. *Mol Pharmacol* **76**(1):105-112.

Moon C, Soria JC, Jang SJ, Lee J, Obaidul Hoque M, Sibony M, Trink B, Chang YS, Sidransky D and Mao L (2003) Involvement of aquaporins in colorectal carcinogenesis. *Oncogene* **22**(43):6699-6703.

Nielsen S and Agre P (1995) The aquaporin family of water channels in kidney. *Kidney Int* **48**(4):1057-1068.

Nielsen S, Smith BL, Christensen EI and Agre P (1993) Distribution of the aquaporin CHIP in secretory and resorptive epithelia and capillary endothelia. *Proc Natl Acad Sci U S A* **90**(15):7275-7279.

Niemietz CM and Tyerman SD (2002) New potent inhibitors of aquaporins: silver and gold compounds inhibit aquaporins of plant and human origin. *FEBS letters* **531**(3):443-447.

Papadopoulos MC and Verkman AS (2008) Potential utility of aquaporin modulators for therapy of brain disorders. *Prog Brain Res* **170**:589-601.

Parsels LA, Parsels JD, Tai DC, Coughlin DJ and Maybaum J (2004) 5-fluoro-2'-deoxyuridine-induced cdc25A accumulation correlates with premature mitotic entry and clonogenic death in human colon cancer cells. *Cancer Res* **64**(18):6588-6594.

Pei JV, Burton JL, Kourghi M, De Ieso ML and Yool AJ (2016) Drug discovery and therapeutic targets for pharmacological modulators of aquaporin channels., in *Aquaporins in Health and Disease: New Molecular Targets For Drug Discovery* (Soveral G, Casinin A and Nielsen S eds) pp 275-297., CRC Press, Oxfordshire, UK.

Preston GM, Jung JS, Guggino WB and Agre P (1993) The mercury-sensitive residue at cysteine 189 in the CHIP28 water channel. *The Journal of biological chemistry* **268**(1):17-20.

Rabolli V, Wallemme L, Lo Re S, Uwambayinema F, Palmai-Pallag M, Thomassen L, Tyteca D, Octave JN, Marbaix E, Lison D, Devuyst O and Huaux F (2014) Critical role of aquaporins in interleukin 1beta (IL-1beta)-induced inflammation. *J Biol Chem* **289**(20):13937-13947.

Rehni AK, Pantlya HS, Shri R and Singh M (2007) Effect of chlorophyll and aqueous extracts of Bacopa monniera and Valeriana wallichii on ischaemia and reperfusion-induced cerebral injury in mice. *Indian journal of experimental biology* **45**(9):764-769.

Reizer J, Reizer A and Saier MH, Jr. (1993) The MIP family of integral membrane channel proteins: sequence comparisons, evolutionary relationships, reconstructed pathway of evolution, and proposed functional differentiation of the two repeated halves of the proteins. *Critical reviews in biochemistry and molecular biology* **28**(3):235-257.

Russo A and Borrelli F (2005) Bacopa monniera, a reputed nootropic plant: an overview. *Phytomedicine : international journal of phytotherapy and phytopharmacology* **12**(4):305-317.

Saadoun S, Papadopoulos MC, Davies DC, Bell BA and Krishna S (2002) Increased aquaporin 1 water channel expression in human brain tumours. *British journal of cancer* **87**(6):621-623.

Sairam K, Dorababu M, Goel RK and Bhattacharya SK (2002) Antidepressant activity of standardized extract of Bacopa monniera in experimental models of depression in rats. *Phytomedicine : international journal of phytotherapy and phytopharmacology* **9**(3):207-211.

Saparov SM, Kozono D, Rothe U, Agre P and Pohl P (2001) Water and ion permeation of aquaporin-1 in planar lipid bilayers. Major differences in structural determinants and stoichiometry. *J Biol Chem* **276**(34):31515-31520.

Saraf MK, Prabhakar S and Anand A (2010) Neuroprotective effect of Bacopa monniera on ischemia induced brain injury. *Pharmacology, biochemistry, and behavior* **97**(2):192-197.

Schindelin J, Arganda-Carreras I, Frise E, Kaynig V, Longair M, Pietzsch T, Preibisch S, Rueden C, Saalfeld S, Schmid B, Tinevez JY, White DJ, Hartenstein V,

Eliceiri K, Tomancak P and Cardona A (2012) Fiji: an open-source platform for biological-image analysis. *Nat Methods* **9**(7):676-682.

Seeliger D, Zapater C, Krenc D, Haddoub R, Flitsch S, Beitz E, Cerda J and de Groot BL (2013) Discovery of novel human aquaporin-1 blockers. *ACS Chem Biol* **8**(1):249-256.

Singh HK and Dhawan BN (1982) Effect of Bacopa monniera Linn. (brahmi) extract on avoidance responses in rat. *Journal of ethnopharmacology* **5**(2):205-214.

Tajkhorshid E, Nollert P, Jensen MO, Miercke LJ, O'Connell J, Stroud RM and Schulten K (2002) Control of the selectivity of the aquaporin water channel family by global orientational tuning. *Science* **296**(5567):525-530.

Trott O and Olson AJ (2010) AutoDock Vina: improving the speed and accuracy of docking with a new scoring function, efficient optimization, and multithreading. *Journal of computational chemistry* **31**(2):455-461.

Williams R, Munch G, Gyengesi E and Bennett L (2014) Bacopa monnieri (L.) exerts anti-inflammatory effects on cells of the innate immune system in vitro. *Food Funct* **5**(3):517-520.

Yang B, Kim JK and Verkman AS (2006) Comparative efficacy of HgCl2 with candidate aquaporin-1 inhibitors DMSO, gold, TEA^+ and acetazolamide. *FEBS Lett* **580**(28-29):6679-6684.

Yool AJ (2007) Functional domains of aquaporin-1: keys to physiology, and targets for drug discovery. *Curr Pharm Des* **13**(31):3212-3221.

Yool AJ, Brokl OH, Pannabecker TL, Dantzler WH and Stamer WD (2002) Tetraethylammonium block of water flux in Aquaporin-1 channels expressed in

kidney thin limbs of Henle's loop and a kidney-derived cell line. *BMC physiology* **2**:4.

Yool AJ, Brown EA and Flynn GA (2009) Roles for novel pharmacological blockers of aquaporins in the treatment of brain oedema and cancer. *Clin Exp Pharmacol Physiol* **37**(4):403-409.

Yool AJ and Campbell EM (2012) Structure, function and translational relevance of aquaporin dual water and ion channels. *Mol Aspects Med* **33**(5):443-561.

Yool AJ, Morelle J, Cnops Y, Verbavatz JM, Campbell EM, Beckett EA, Booker GW, Flynn G and Devuyst O (2013) AqF026 is a pharmacologic agonist of the water channel aquaporin-1. *Journal of the American Society of Nephrology : JASN* **24**(7):1045-1052.

Yool AJ and Weinstein AM (2002) New roles for old holes: Ion channel function in aquaporin-1. *News Physiological Sciences* **17**:68-72.

Yu J, Yool AJ, Schulten K and Tajkhorshid E (2006) Mechanism of gating and ion conductivity of a possible tetrameric pore in aquaporin-1. *Structure* **14**(9):1411-1423.

Zhang W, Zitron E, Homme M, Kihm L, Morath C, Scherer D, Hegge S, Thomas D, Schmitt CP, Zeier M, Katus H, Karle C and Schwenger V (2007) Aquaporin-1 channel function is positively regulated by protein kinase C. *J Biol Chem* **282**(29):20933-20940.

Zhou Y, Shen YH, Zhang C, Su J, Liu RH and Zhang WD (2007) Triterpene saponins from Bacopa monnieri and their antidepressant effects in two mice models. *Journal of natural products* **70**(4):652-655.

Table 1. Analysis of cytotoxicity in HT29 colon cancer cells at 24 h treatment, using an AlumarBlue fluorescence assay.

Concentration (μM)	**Mean normalized cell viability (%), mean ± SEM** [§]	**n value**	**signif**
bacopaside I			
0	108 ± 4.8	17	NS
0 (vehicle)	100 ± 3.1	17	---
50	97 ± 2.1	8	NS
75	79 ± 4.2	8	NS
100	59 ± 3.2	8	*
bacopaside II			
0	113 ± 6.2	16	NS
0 (vehicle)	100 ± 5.7	16	---
15	104 ± 18	8	NS
20	123 ± 17	8	NS
30	47 ± 5.7	8	*
$HgCl_2$			
100	16.1 ± 4.6	6	*

§ Percent viability was standardized as a percentage of the vehicle-treated mean value, measured as changes in AlumarBlue fluorescence signal intensity. See Methods for details. * Statistically significant differences ($p<0.05$), compared with vehicle-treated, were analyzed by ANOVA with post-hoc Dunnett's multiple comparison test (GraphPad Prism). NS is not significant.

Figure Legends

Figure 1. Block of osmotic water permeability in AQP1-expressing oocytes by water hyssop (*Bacopa monnieri*) extract, and constituent compounds bacopaside I and bacopaside II. **A.** Mean swelling responses of AQP1-expressing oocytes in 50% hypotonic saline, standardized to the initial volume V_0, were blocked by 2 h preincubation in reconstituted extract of water hyssop (at 1 mg/ml). Control non-AQP1 oocytes showed little change in volume. Data are mean values for all oocytes assessed from a single batch of oocytes; error bars are SEM; n values are 6 per treatment group. **B.** Column elution of methanol-extracted Bacopa identified two active fractions which caused block of AQP1 osmotic water permeability at 0.1 mg/ml each (which were further analyzed by mass spectroscopy to identify candidate compounds). Data are mean ± SEM, n values in italics are above the x-axis. **C.** Candidate compounds bacopaside I and bacopaside II at 50 µM differentially blocked osmotic water permeability in AQP1-expressing oocytes, causing a decrease in the rate of swelling as compared with untreated AQP1-expressing oocytes. Data are mean ± SEM; n values are 8 (AQP1 untreated), 5 (bacopaside I), 7 (bacopaside II), and 8 (non-AQP1 control). **D.** Dose-dependent block of AQP1-mediated osmotic swelling by bacopasides I and II, with estimated IC_{50} values of 117 µM and 18 µM, respectively. No sensitivity to bacopaside I was seen for the AQP1 R159,160A double mutant at doses up to 100 µM. **E.** Chemical structures of bacopasides I and II.

Figure 2. Subtype selectivity and temporal properties of block onset and recovery with bacopaside I in AQP1-but not AQP4-expressing oocytes. **A.** Mean swelling responses of AQP4-expressing oocytes in 50% hypotonic saline were not affected after 2 h preincubation in 178 µM bacopaside I. Data are mean ± SEM; n values are 8 (AQP4 alone), 8 (AQP4 with bacopaside I), and 6 (non-AQP4 control). **B.** Time-dependent establishment of block of AQP1-mediated osmotic water permeability required preincubation of oocytes in 178 µM bacopaside I or 35 µM bacopaside II, with approximately 2 h needed to achieve maximal inhibition. n values are 12 to 14 oocytes per time point; each oocyte was used for a single measurement. **C.** Time-dependent recovery from block in AQP1-expressing oocytes preincubated 2 h in 178 µM bacopaside I or 35 µM bacopaside II, and assessed at different intervals after transfer back into standard isotonic saline at time 0 ('washout'). n values are 10 to 13 oocytes per time point; each oocyte was used for a single measurement.

Figure 3. Block of the cGMP-dependent ionic conductance of AQP1-expressing oocytes by bacopaside I, but not bacopaside II. **A.** Representative sets of traces recorded by two-electrode voltage clamp of AQP1-expressing oocytes showing the initial conductance; the response induced by the first application of membrane-permeable cGMP; the recovery of the response to near initial levels after 2 h incubation in isotonic saline containing bacopaside I (50 or 100 µM) or bacopaside II (10 or 20 µM); and the final response to a second application of cGMP. **B.** Trend plots showing the amplitude of the ionic currents, before and after the first activation

by GMP, the recovery after incubation, and the response reactivated by a second cGMP application. Consistent recovery was seen after 10 or 20 μM bacopaside II, but not after incubation with 50 or 100 μM bacopaside I indicating establishment of ion channel block. n values are between 3 to 6 for each treatment. (The levels of block by 50 or 100 μM bacopaside I were statistically significant ($p<0.05$) as compared with vehicle treated AQP1 expressing oocytes).

Figure 4. In silico docking models illustrating predictions for the most favorable sites of interaction of bacopaside I and bacopaside II on AQP1 and AQP4 subunit proteins. AQP subunit models were assembled from crystal structural data for human AQP1 (PDB ID. 1FQY) and human AQP4 (PDB ID. 3GDB); see Methods for details. Subunit views are from the cytoplasmic side with the water pore in the center. The intracellular domain for Loop D, adjacent to the channel tetrameric axis of symmetry, is highlighted in dark gold. **A.** Bacopaside I is predicted by in silico docking to occlude the cytoplasmic side of the intrasubunit water pore in AQP1. **B.** Favorable interactions at the AQP4 water pore are not evident for bacopaside I; this ligand appears to interact poorly with AQP4, and the best fit is seen near membrane-spanning domains distant from the pore (inset). **C.** Bacopaside II is predicted to have the most favorable energy of interaction at a position occluding the cytoplasmic side of the AQP1 water pore. **D.** Predicted binding of bacopaside II with AQP4 is distant from the water pore (inset), in a position similar to that seen for bacopaside I. **E.** Enlarged view of the predicted interaction of the sugar-linked sulfur group of bacopaside I with the conserved Loop D arginine residues in AQP1. **F.** Enlarged

view of the predicted binding of the trisaccharide moiety of bacopaside II deep into the cytoplasmic vestibule of the AQP1 water pore.

Figure 5. HT29 cells have higher level of AQP1 expression than SW480 cells. **A**. The AQP1 RNA level was higher in HT29 cell line as compared to SW480 cellas demonstrated using quantitative RT-PCR. **B**. The AQP1 protein level was higher in HT29 than SW480 cells as demonstrated by western blot. **C**. The AQP1 positive signal (green) was stronger in HT29 than in SW480 cells. Cell nucleii were counterstained (blue). See Methods for details.

Figure 6. Dose-dependent inhibition of migration by bacopasides I and II in AQP1-expressing HT29 cells, but not in SW480 cells with low AQP1 expression. Cell migration was assessed in the presence of a mitotic inhibitor by rates of closure of circular wounds created by aspiration with a pipette tip in confluent cultures (see Methods for details). **A, B**. Cell migration was assessed in vehicle (A) or with 15 µM bacopaside II (B), added immediately after wounding. Images are shown for confluent HT29 cultures after initial wounding at time 0 (upper panels) and at 24 h (lower panels). **C.** Dose-dependent block of HT29 cell migration was seen with bacopasides I and II, with IC_{50} values estimated at 48 and 14 µM respectively. Partial block of SW480 migration at the highest doses tested did not exceed 20%. Doses beyond the ranges shown were not considered valid due to the onset of concomitant cytotoxicity.

Figure 7. Live-cell imaging of the inhibitory effect of bacopaside I and II on migration of HT29 cells. Single cells at the boundaries of circular wounds were tracked with time-lapse images taken at 25 minute intervals for 10 hours at 37°C. **A, B, C.** Panels of six images each from time-lapse series for clarity shown at 50 minute intervals. (A) HT29 cells with vehicle treatment (upper set); **(B)** HT29 cells treated with 50 mM bacopaside I; and **(C)** HT29 cells treated with 15 mM bacopaside II. **D.** Trajectory plots of 10 individual cells per treatment group, monitored by cell nucleus position as a function of time. Data were converted to absolute values and referenced to the starting position at time 0. Plots illustrate the cumulative total movement of 10 single cells over a duration of 600 min, with vehicle, bacopaside I or with bacopaside II. **E.** Frequency histograms of the distances moved by individual cells per 50 minute interval over 600 min of imaging, sampled for 10 cells per treatment group. Histograms were fit with Gaussian distribution functions (R^2 values >0.94); best-fit values for the mean distances moved per cell per 50 min interval were 10.1 ± 0.5 for untreated, 4.7 ± 0.2 for bacopaside I treated and 7.8 ± 0.2 for bacopaside II treated (mean ± SEM). **F.** Summary histogram showing the total distance travelled by single cells in 600 min, showing significant inhibition of cell motility by both bacopaside I and II compared to vehicle treated cells (ANOVA test; $p < 0.05$). Data are mean ± SEM; n values are 10 cells per treatment group. Distances shown are in pixels; the conversion is 7.45 pixels per 1mm.

Figure 1

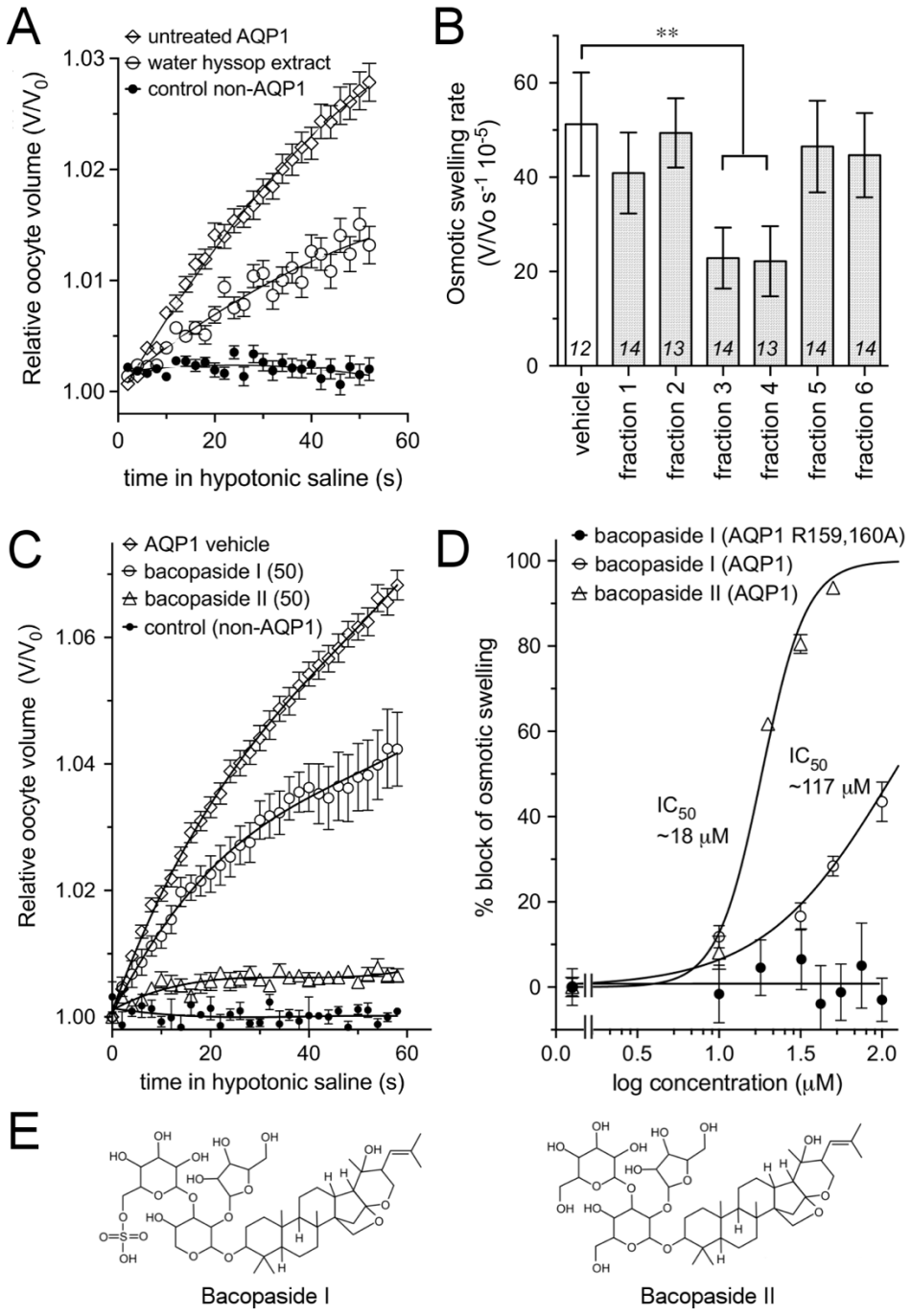
A
untreated AQP1
water hyssop extract
control non-AQP1
Relative oocyte volume (V/V0)
time in hypotonic saline (s)
B
**
Osmotic swelling rate (V/Vo s-1 10-5)
12
14
13
14
13
14
14
vehicle
fraction 1
fraction 2
fraction 3
fraction 4
fraction 5
fraction 6
C
AQP1 vehicle
bacopaside I (50)
bacopaside II (50)
control (non-AQP1)
Relative oocyte volume (V/V0)
time in hypotonic saline (s)
D
bacopaside I (AQP1 R159,160A)
bacopaside I (AQP1)
bacopaside II (AQP1)
% block of osmotic swelling
IC50 ~18 μM
IC50 ~117 μM
log concentration (μM)
E
Bacopaside I
Bacopaside II

Figure 2

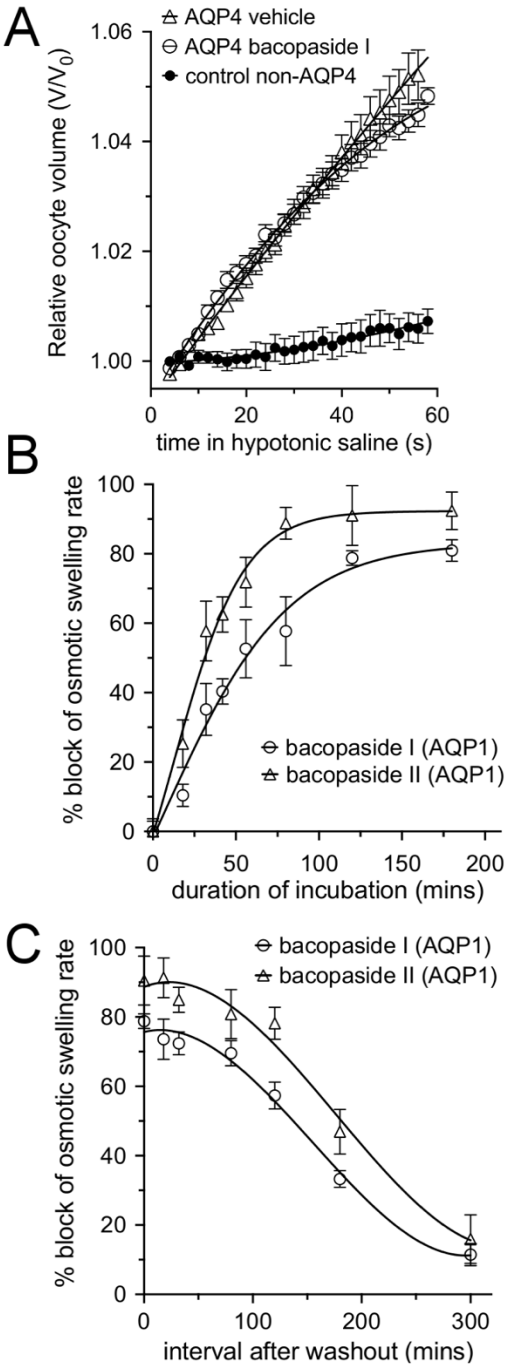
A
AQP4 vehicle
AQP4 bacopaside I
control non-AQP4
Relative oocyte volume (V/V0)
1.06
1.04
1.02
1.00
0
20
40
60
time in hypotonic saline (s)
B
% block of osmotic swelling rate
100
80
60
40
20
0
bacopaside I (AQP1)
bacopaside II (AQP1)
0
50
100
150
200
duration of incubation (mins)
C
% block of osmotic swelling rate
bacopaside I (AQP1)
bacopaside II (AQP1)
100
80
60
40
20
0
0
100
200
300
interval after washout (mins)

Figure 3

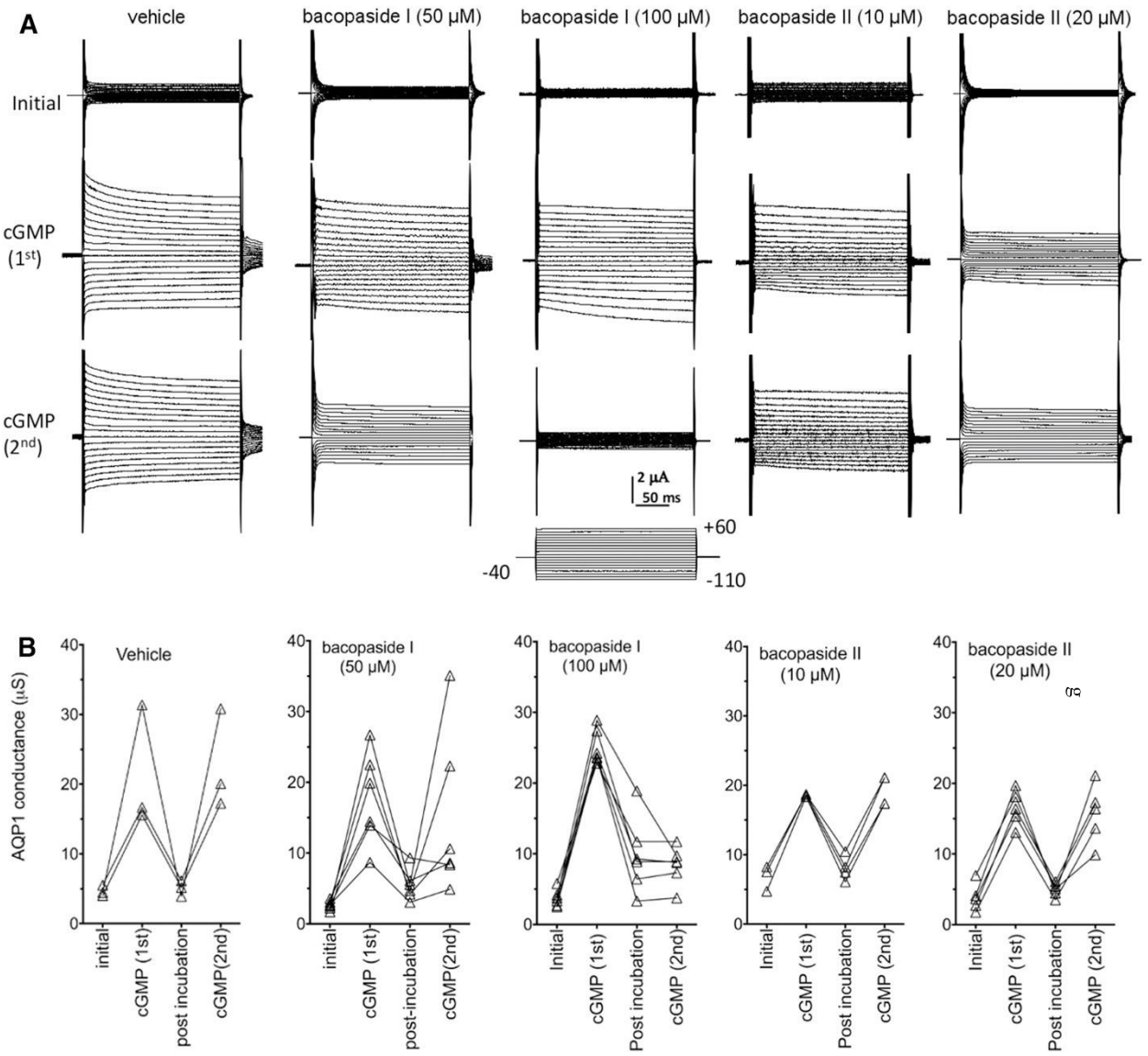
A
vehicle
bacopaside I (50 µM)
bacopaside I (100 µM)
bacopaside II (10 µM)
bacopaside II (20 µM)
Initial
cGMP (1st)
cGMP (2nd)
2 µA
50 ms
+60
-40
-110
B
AQP1 conductance (µS)
Vehicle
bacopaside I (50 µM)
bacopaside I (100 µM)
bacopaside II (10 µM)
bacopaside II (20 µM)
initial
cGMP (1st)
post incubation
cGMP(2nd)
post-incubation
Initial
Post incubation
cGMP (2nd)

Figure 4

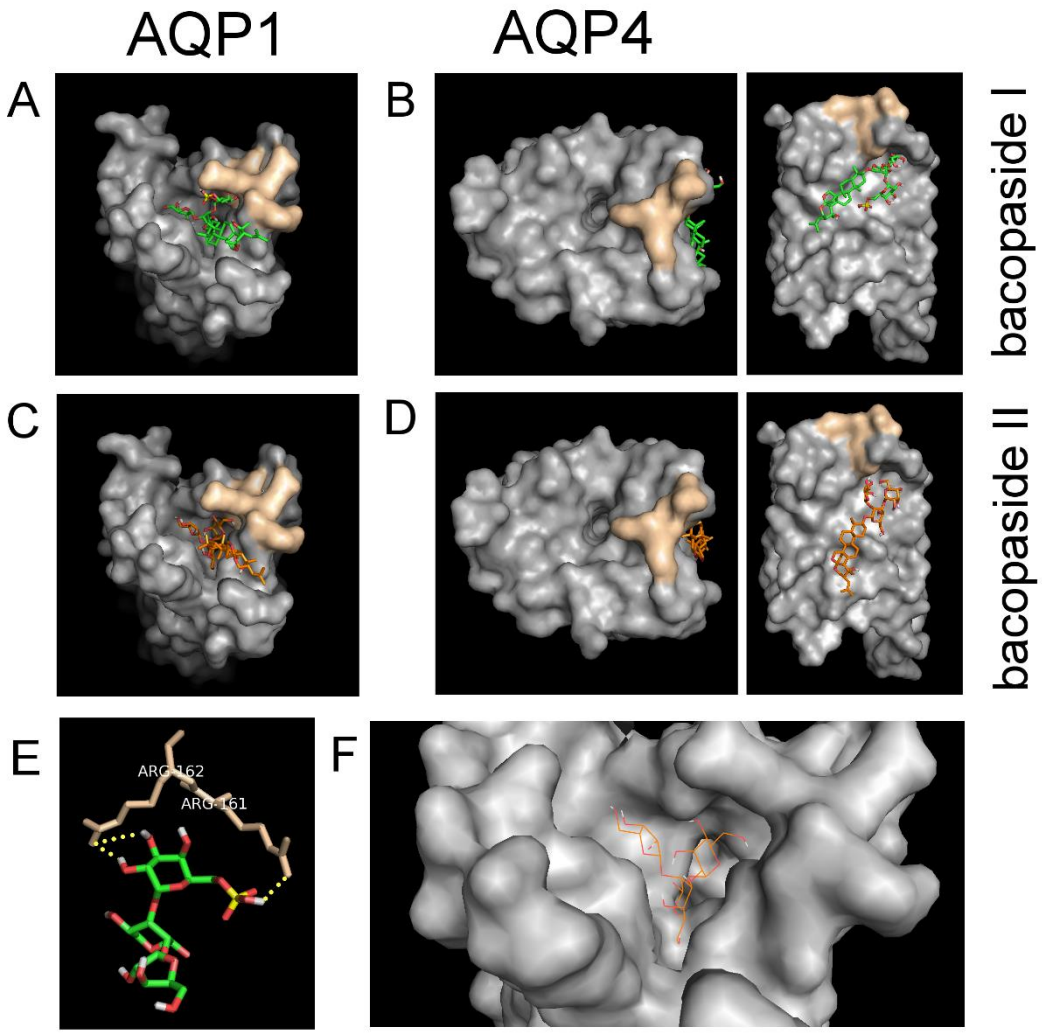

Figure 5

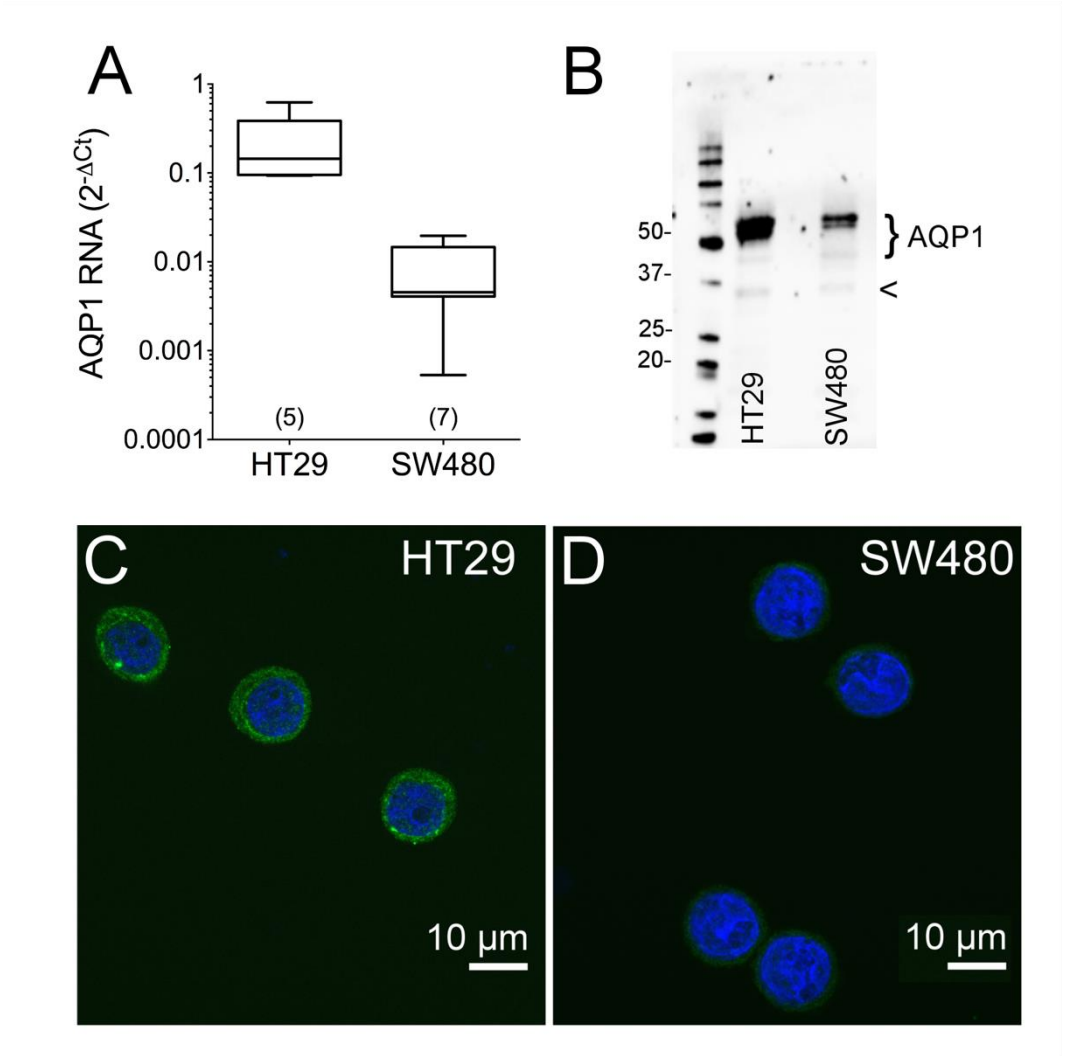
A
AQP1 RNA ($2^{-\Delta Ct}$)
1
0.1
0.01
0.001
0.0001
(5)
(7)
HT29
SW480
B
50-
37-
25-
20-
AQP1
HT29
SW480
C
HT29
10 µm
D
SW480
10 µm

Figure 6

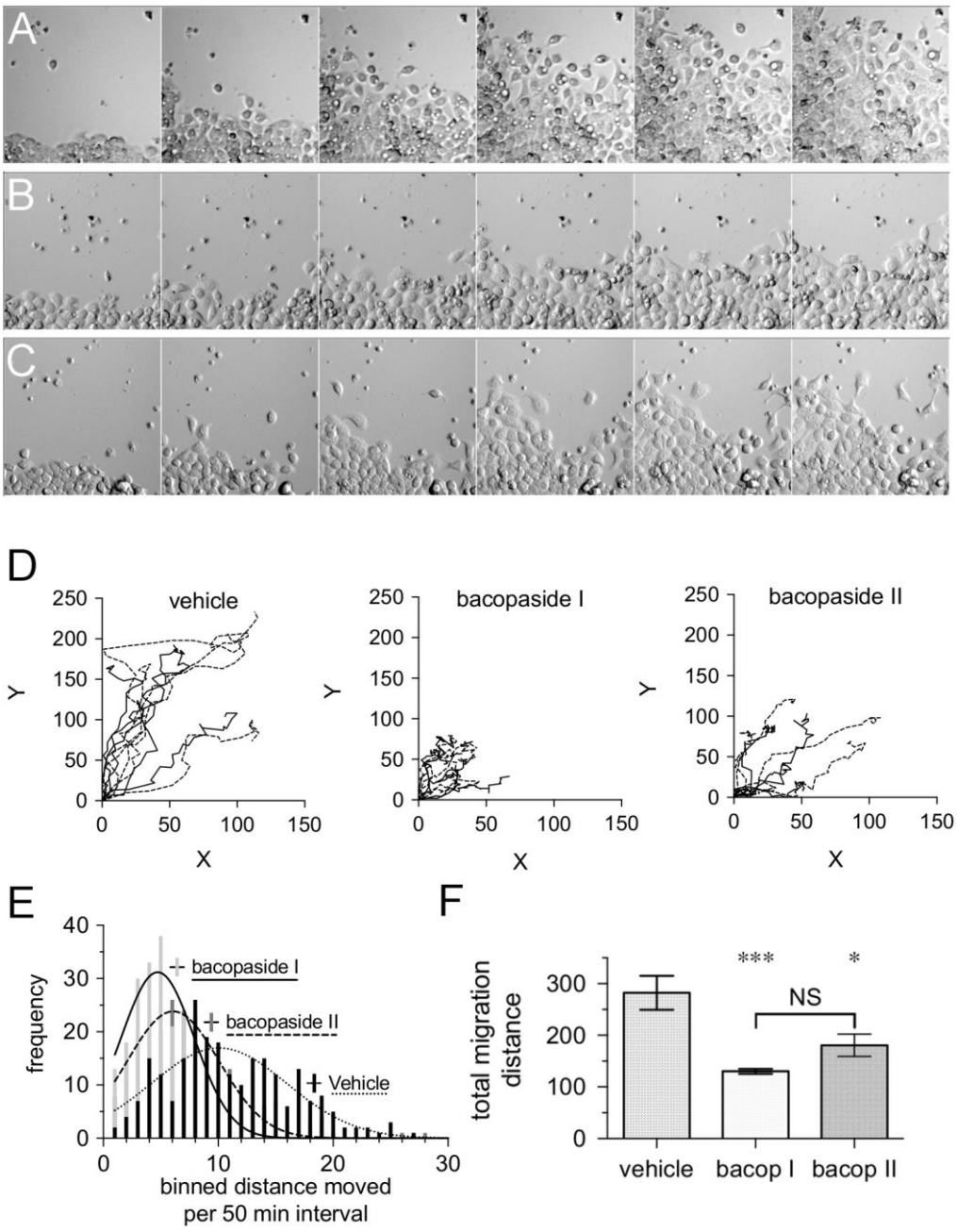
A
B
C
D
vehicle
bacopaside I
bacopaside II
Y
X
250
200
150
100
50
0
0
50
100
150
E
frequency
bacopaside I
bacopaside II
Vehicle
40
30
20
10
0
10
20
30
binned distance moved
per 50 min interval
F
total migration
distance
***
*
NS
300
200
100
0
vehicle
bacop I
bacop II

Statement of Authorship

Title of Paper	Chapter 5: A therapeutic agent used for treatment of sickle cell anaemia, 5-hydroxymethyl-2-furfural, is a blocker of the AQP1 ion conductance
Publication Status	☐ Published ☐ Accepted for Publication ☐ Submitted for Publication ☑ Unpublished and Unsubmitted work written in manuscript style
Publication Details	

Principal Author

Name of Principal Author (Candidate)	Mohamad Kourghi
Contribution to the Paper	Contributed to electrophysiology and imaging experiments. Wrote the manuscript. Analysed and contributed to preparing figures 1, 2 and 3.
Overall percentage (%)	80%
Certification:	This paper reports on original research I conducted during the period of my Higher Degree by Research candidature and is not subject to any obligations or contractual agreements with a third party that would constrain its inclusion in this thesis. I am the primary author of this paper.
Signature	Date 6/09/2017

Co-Author Contributions

By signing the Statement of Authorship, each author certifies that:

i. the candidate's stated contribution to the publication is accurate (as detailed above);

ii. permission is granted for the candidate in include the publication in the thesis; and

iii. the sum of all co-author contributions is equal to 100% less the candidate's stated contribution.

Name of Co-Author	Saeed Nourmohammadi
Contribution to the Paper	Helped with data analysis and writing the introduction.
Agree contribution (%)	10%
Signature	Date 6/9/2017

Please cut and paste additional co-author panels here as required.

Name of Co-Author	Andrea J. Yool		
Contribution to the Paper	Contributed to experimental design, and reviewing, editting the manuscript.		
Agreed contribution percentage (%)	10%		
Signature		Date	5/9/2012

Chapter 5: A therapeutic agent used for treatment of sickle cell anaemia, 5-hydroxymethyl-2-furfural, is a blocker of the Aquaporin 1 ion conductance

Mohamad Kourghi, Saeed Nourmohammadi, Andrea Yool

Abstract

Sickle cell disease (SCD) is a set of disorders caused by inherited mutations in the oxygen-carrying molecule haemoglobin (Hb) in red blood cells (RBCs). The pathological shape change ('sickling') of RBCs under hypoxic conditions is associated with activation of a cationic leak current (the P_{sickle} current), which is known to be involved in cellular dehydration leading to Hb polymerisation, and blocked by application of 1 mM 5-hydroxylmethyl-2-furfural (5HMF). The RBC sickling phenomenon has been linked previously to K^+ channels and transporters, but the molecular basis of the non-selective cation leak current has remained a mystery. Human aquaporin-1 (AQP1) channels, expressed in membranes of many cells including RBCs, have previously been shown to function as non-selective cation channels gated by cGMP. Work here is the first to test the hypothesis that AQP1 ion channels are involved in mediating the P_{sickle} current. Human AQP1 channels expressed in Xenopus oocytes were analysed for sensitivity to 5HMF and four structurally related compounds, with ion conductance measured by two-electrode voltage clamp and osmotic water permeability by optical swelling assays. The known AQP1 ion channel blocker AqB011 served as a positive control. None of the furfural-related agents affected AQP1 water channel activity at concentrations up to 5 mM. Of

the furfural-related compounds, 5HMF was the most potent blocker of the AQP1 ion conductance (IC_{50} of 432 μM) The order of potency for inhibition of the ionic conductance was 5HMF> 5-Nitro-2-Furoic acid (IC_{50} ~1.2 mM) > 5-Acetoxymethyl-2-Furaldehyde (IC_{50} 3.2 mM), and no block of ionic conductance was observed with Methyl 5-nitro-2-furoate. The dose-dependent block of AQP1 ion conductance by 5HMF fit with the doses known to be needed for therapeutic effects in RBCs from SCD patients, suggesting AQP1 is a logical candidate for the P_{sickle} molecular mechanism. Blocking the AQP1 cationic conductance with furfural agents would be predicted to slow dehydration and RBC sickling, consistent with the observed protective effects against sickling seen in vivo.

Introduction

Sickle cell disease SCD arises when a person inherits two copies of the abnormal haemoglobin gene (HbS), one from each parent. The predominant class of mutation results in glutamic acid being replaced by valine at the position 6 of Beta Hb chain. The loss of negatively charged residues is thought to promote polymerisation of HbS to form long rigid polymers that distort RBC shape and cause the sickling (Perutz and Mitchison 1950, Higgs 1986). Clinical complications fall into two categories: (i) a chronic anaemia from reduced circulating RBC numbers, and (ii) acute ischaemia due to the occlusion of capillaries and small vessels by sickled cells which block the microvasculature. A broad range of clinical symptoms depends on the organ(s) involved, and the severity differs between individuals (Steinberg 1999, Nagel 2001). As there are no cure for SCD (Steinberg 1999, Rees, Williams et al. 2010),

investigations have looked for other approaches as effective therapies. Other methods include the development of compounds which directly interpolate with HbS molecules and thereby reduce polymerization upon deoxygenation. Naturally occurring 5-hydroxymethyl-2-furfural (5HMF) form Schiff bases with HbS, allosterically increasing its oxygen affinity, and reducing polymerization and RBC sickling (Zaugg, Walder et al. 1977, Abdulmalik, Safo et al. 2005). 5HMF also knows as Aes-103 is currently in phase II clinical trials in SCD patients in the USA and UK (National Institutes of Health, 2013). 5HMF is likely to be acting at more than one level. Other work has shown that 5HMF also has a beneficial effect by increasing the expression of mRNA gene encoding $Hgb\beta_{mi,}$ and also attenuated colitis in WT and $Hgb\beta_{ma}KO$ mice (Gorczynski, Alexander et al. 2017). Moreover 5HMF has shown to reduce anti-oxidant glutathione (GSSH) levels thereby causing a decrease in inflammatory cytokine production and also protect from colitis (Janzowski, Glaab et al. 2000, Gorczynski, Alexander et al. 2017). Less well understood but potentially important is the ability of 5HMF to block the P_{sickle} current associated with the RBC dehydration that appears to facilitate the sickling shape change in affected RBCs (Hannemann, Cytlak et al. 2014).

There are numerous cation pathways that are associated with the SCD (Joiner 1993, Gibson and Ellory 2002, Lew and Bookchin 2005) . These include the K^+–Cl^- cotransporter (or KCC) and the Ca^{2+}-activated K^+ channel (or Gardos channel), plus a third pathway that is less well understood known as 'P_{sickle}'. The mechanism of P_{sickle} pathways is yet to be identified, however it is likely to be a cation conductance that is activated due to RBC change of shape, HbS polymerization and

deoxygenation (Joiner, Dew et al. 1988, Joiner 1993, Ma, Rees et al. 2012). P_{sickle} activation results in Ca^{2+} entry, and Mg^{2+} exit (Ortiz, Lew et al. 1990, Willcocks, Mulquiney et al. 2002). As a consequence the loss of cellular cations leads to dehydration and increased concentration of HbS, therefore increased HbS polymerisation and cell sickling (Brugnara 1993).

Discovered in the late 1980s (Agre, Saboori et al. 1987), Aquaporin-1 (AQP1) is a member of the family of intrinsic membrane proteins expressed in plasma membranes of many tissues. AQP1, expressed in organs including kidney, vascular system, heart and brain (Venero, Vizuete et al. 2001, Badaut, Lasbennes et al. 2002, Papadopoulos, Krishna et al. 2002, Speake, Freeman et al. 2003), as well as in the plasma membrane of red blood cells (Ma, Yang et al. 1998, Maeda, Hibuse et al. 2009).

A number of classes of AQPs have been shown to function as ion channels, including AQP0, AQP1, AQP6, *Drosophila* Big Brain, and plant nodulin and PIP2;1 (Campbell, Birdsell et al. 2012, Byrt, Zhao et al. 2016). To date, 15 classes of AQPs have been identified in mammals: AQP0-AQP14 (Ishibashi 2009, Finn, Chauvigne et al. 2014). AQP1 is regulated by cGMP activation at the loop D domain (Yu, Yool et al. 2006) and functions as a non-selective monovalent cation channel at the central pore, distinct from the monomeric water pores (Anthony, Brooks et al. 2000, Saparov, Kozono et al. 2001, Boassa and Yool 2002, Zhang, Zitron et al. 2007). The AQP1 ion channel is permeable to Na^+, K^+, and Cs^+ cations with a unitary conductance of 150 picosiemens in physiological saline, and shows slow activation and deactivation

kinetics (Yool, Stamer et al. 1996, Anthony, Brooks et al. 2000) with efficacy of gating dependent on tyrosine phosphorylation at the carboxyl terminal domain (Campbell, Birdsell et al. 2012).

The possible role of AQP1 ion channels in the P_{sickle} conductance of red blood cells has not previously been considered. Work here tested the hypothesis that the therapeutic agent furfural acts as a pharmacological inhibitor of the AQP1 cation permeability. This work is the first to suggest AQP1 could be a key component of the molecular mechanisms of the P_{sickle} current. Future work will be needed to compare the effects of AQP1 ion channel blockers on sickle cell and normal RBCs, to determine if AQP1 ion channel inhibition slows the solute loss and dehydration that accompany HbS polymerisation and RBC sickling. Potential therapeutic agents targeted to AQP1 ion channels could be of interest for expanding the range of clinical options available for treating sickle cell disease.

Materials and Methods

Oocyte preparation and injection

Unfertilized oocytes were harvested from *Xenopus laevis* frogs and were defoliculated by incubation in collagenase (type 1A, 1 mg/ml; Sigma-Aldrich, St. Louis, MO) and trypsin inhibitor (0.05 mg/ml; Sigma-Aldrich, St. Louis, MO) in OR-2 saline (96 mM NaCl, 2 mM KCl, 5 mM $MgCl_2$, penicillin 100units/ml streptomycin 0.1 mg/ml, and 5 mM HEPES pH7.6) for 1 to 1.5 hours. Oocytes were stored in Frog Ringer saline consisting of 96 mM NaCl, 2mM KCl, 5 mM $MgCl_2$, 0.6 mM $CaCl_2$, 5mM

HEPES buffer, horse serum (5%; Sigma-Aldrich, St. Louis, MO), penicillin 100 units/ml streptomycin 0.1 mg/ml, and tetracycline 0.5mg/ml, pH 7.6. Oocytes were injected slowly (over 5-10s) with 5o nl of water (control oocytes), or 50 nl of water containingng 1ng of AQP1 cRNA. Oocytes were then incubated for a minimum of 48 hours at 16°C in Frog Ringer saline (96 mM NaCl, 2 mM KCl, 1 mM $MgCl_2$, 1.8 mM $CaCl_2$, and 5 mM HEPES, pH 7.3) to allow sufficient time for translation and the expression of the channel on cell membrane before electrophysiology. Successful expression was confirmed by swelling tests, in which AQP1 expressing and control oocytes (sham injected) were placed in distilled water. AQP1 expressing oocytes swelled and burst within few minutes whereas control oocytes remained intact for up to 10 minutes in distilled water.

Osmotic Swelling Assay

For double-swelling assays, each oocyte served as its own control. Swelling rates were assayed first without drug treatment (S1), and then oocytes incubated for 2 hours in isotonic saline with or without the 5HMF or related compounds were reassessed in a second swelling assay (S2). Swelling rates in 50% hypotonic saline (isotonic Na saline diluted with an equal volume of water) were quantified by relative increases in the oocyte cross-sectional area imaged by videomicroscopy (charge-coupled device camera; Cohu, San Diego, CA) at 0.5 frames per second for 30 seconds using National Institutes of Health ImageJ software (Bethesda, MD). Rates were measured as the slopes of the linear regression fits of relative volume as a function of time using Prism (GraphPad Software Inc.,San Diego, CA).

Electrophysiology

For two-electrode voltage clamp, capillary glass electrodes (1–3 MΩ) were filled with 1 M KCl. Unless specified, all recordings were done in standard divalent free Na^+ bath saline containing 100 mM NaCl, 2 mM KCl, 4.5 mM $MgCl_2$, and 5 mM HEPES, pH 7.3. Two electrode recording pipettes were used conventionally to control voltage and deliver current. Ionic conductance was monitored throughout by voltage step protocols from a holding potential of -40, with voltage steps from +60 to -110mV used to calculate the conductance. Recordings were made using a GeneClamp amplifier and Clampex 9.0 software (pClamp 9.0 Molecular Devices, Sunnyvale, CA, USA). Data were filtered at 2 kHz, digitized at 2 kHz, and stored to hard disk for analysis.

Data Compilation and Statistics

Results compiled from replicate experiments are presented as box plots or scatter plots to show the full range of data points. The box represents 50% of the data, the error bars indicate the full range, and the horizontal bar is the median value. Statistical differences were analyzed using one-way ANOVA with Bonferroni post-hoc test and reported as $P<0.0001$ (***), $p< 0.0020$ (**), $p<0.05$ (*) and not significant (NS; $P>0.05$).

Results

Inhibition of AQP1 ionic conductance by 5HMF and related compounds. 5HMF and 3 structurally similar compounds (5-Nitro-2-Furoic acid, 5-Acetoxymethyl-2-Furaldehyde, Methyl 5-nitro-2-furoate) were tested for effects on AQP1 ionic conductance expressed in oocytes. Two-electrode voltage clamp recordings shows that the cGMP activated ionic conductance of AQP1 is inhibited by incubation in 5HMF (1mM), 5-Nitro-2-Furoic acid (3mM), and 5-Acetoxymethyl-2-Furaldehyde (5mM), but no appreciable block of Methyl 5-nitro-2-furoate (5mM) on the AQP1 ion channel.

Initial recordings were measured before the bath application of CPT-cGMP, followed by bath application of CPT-cGMP which triggered an activation of ionic conductance in AQP1 expressing oocytes.

The Oocytes were then incubated in salines with the indicated agents for 1 hour. During the incubation period the ionic conductance recovered to initial levels (Fig. 1). In response to the second application of CPT-cGMP, oocytes treated with vehicle (DMSO) and 5mM Methyl 5-nitro-2-furoate showed an increase in conductance that were similar to the first response. This observation shows that Methyl 5-nitro-2-furoate is not a blocker of the AQP1 ion channel. However the AQP 1 ionic conductance responses did not reactivate in response to second cGMP application post 1 hour incubation in 1mM 5HMF, 3mM 5-Nitro-2-Furoic acid, and 5mM 5-Acetoxymethyl-2-Furaldehyde indicating an inhibition of ionic conductance. Trend plots (Fig 2) show that the initial conductance in AQP1-expressing oocytes were low. The conductance responses were increased after the application of membrane permeable CPT-CGMP.

The oocytes were then transferred into salines containing the mentioned agents to test for any blocking effect. After the incubation period the current was measured again prior to second cGMP application during which the conductance had recovered to initial levels. After the application of second cGMP the ionic current remained blocked by 5HMF, 5-Nitro-2-Furoic acid and 5-Acetoxymethyl-2-Furaldehyde, however it was reactivated by DMSO and Methyl 5-nitro-2-furoate indicating no block. Non AQP1 expressing control oocytes did not show any ionic conductance in response to cGMP and to vehicle and any of the drug treatments.

Figure 3 shows the compiled box plot data for the AQP1 ionic conductance values, indicating the amount of block by 1mM 5HMF, 3 mM 5-Nitro-2-Furoic acid and 5mM Methyl 5-nitro-2-furoate were statistically significant as compared with initial responses to cGMP before treatment. Dose response relationships reveal that the IC50 value for 5HMF is 432 μM, 1.193 mM for 5-Nitro-2-Furoic acid, and approximately 3.2 mM for 5-Acetoxymethyl-2-Furaldehyde (Fig 3B).

Figure 4 shows the maximum block of AQP1 cationic conductance was achieved at 1 hr incubation. The oocytes were tested in 15 minutes, 30 minutes and 1 hour time sets in 1 mM 5HMF. At 1 hr incubation maximum block of 80% of AQP1 cationic conductance was observed, 40% block at half hour and 20% block at 15 minutes.

5HMF and the 3 related compounds have no effect on the water permeability of AQP1 measure by osmotic swelling assay (Fig 5). AQP1 expressing oocytes were transferred into 50% hypotonic saline over 60 seconds to measure the first swelling assay (S1).

Then the oocytes were transferred into saline containing the compounds at 5mM over 1 hour to test for block on osmotic water permeability followed by second swelling (S2). There were no significant differences between the first and second swelling rates in any of the treatment groups, indicating that the 5HMF and the 3 structurally related compounds have no effect on AQP1 osmotic water permeability.

Discussion

Sickle cell anemia is a hereditary disease caused by change in structure and function of HbS. Hemolytic and vaso-occlusive crises are the main symptoms of sickle cell anaemia (Cagici, Asma et al. 2016). Hypoxic conditions may result in intracellular HbS polymerization, which changes the cell morphology and flexibility. This sickling of RBCs results in occlusion of the capillaries and subsequent vaso-occlusive crises. Vaso-occlusive crises are experienced as severe pain attacks. Cellular loss of K^+, Cl^- and water leads to dehydration and increased concentration of HbS in patients with SCD (Joiner 1993, Gibson and Ellory 2002, Lew and Bookchin 2005). This increase in HbS leads to change in kinetics of HbS by delaying the time upon deoxygenation and increased HbS polymerisation and sickling. Therefore considerable amount of interest is dedicated to sickle cell dehydration (Brugnara 1993). AQP1 water channel is the second member of the family of intrinsic membrane proteins expressed in endothelial and epithelial membrane of many tissue including on membrane of RBCs (Ma, Yang et al. 1998, Agre 2004, Maeda, Hibuse et al. 2009). In addition to maintaining water homeostasis AQP1 also functions as a non-selective cation channel activated by cGMP (Anthony, Brooks et al. 2000, Boassa and Yool 2002). Previously it is shown

that 5HMF allosterically interacts with HbS and decreases polymerisation and sicking. Should 5HMF block the cationic conductance of AQP1 it is possible that it has dual function of also retaining cellular cation loss thus enhancing the hydration state of RBC. Therefore in this study we investigated if 5HMF and 3 selected structurally related compounds were capable of blocking the cGMP-activated cationic conductance in AQP1. The results showed that 5HMFsignificantly blocked the cationic conductance of AQP1 with IC50 of 432 μM. The order of potency of block is 5HMF> 5-Nitro-2-Furoic acid > 5-Acetoxymethyl-2-Furaldehyde > Methyl 5-nitro-2-furoate. Osmotic swelling assay results showed that the compounds had no effect in water permeability of AQP1 indicating that they are specific blockers for ion channel, not the water channel.

References

Agre P (2004) Nobel Lecture. Aquaporin water channels. *Bioscience reports* **24:** 127-163

Agre P, Saboori AM, Asimos A, Smith BL (1987) Purification and partial characterization of the Mr 30,000 integral membrane protein associated with the erythrocyte Rh(D) antigen. *The Journal of biological chemistry* **262:** 17497-17503

Anthony TL, Brooks HL, Boassa D, Leonov S, Yanochko GM, Regan JW, Yool AJ (2000) Cloned human aquaporin-1 is a cyclic GMP-gated ion channel. *Mol Pharmacol* **57:** 576-588

Badaut J, Lasbennes F, Magistretti PJ, Regli L (2002) Aquaporins in brain: distribution, physiology, and pathophysiology. *J Cereb Blood Flow Metab* **22:** 367-378

Boassa D, Yool AJ (2002) Contribution of single amino acids in the carboxyl terminal domain of Aquaporin-1 channels to cGMP-dependent activation. *Biophys J* **82:** 275a-275a

Brugnara C (1993) Membrane transport of Na and K and cell dehydration in sickle erythrocytes. *Experientia* **49:** 100-109

Byrt CS, Zhao M, Kourghi M, Bose J, Henderson SW, Qiu J, Gilliham M, Schultz C, Schwarz M, Ramesh SA, Yool A, Tyerman S (2016) Non-selective cation channel activity of aquaporin AtPIP2;1 regulated by Ca^{2+} and pH. *Plant Cell Environ*

Cagici CA, Asma S, Sener M (2016) Septorhinoplasty in sickle cell anemia: a case report. *Braz J Otorhinolaryngol*

Campbell EM, Birdsell DN, Yool AJ (2012) The Activity of Human Aquaporin 1 as a cGMP-Gated Cation Channel Is Regulated by Tyrosine Phosphorylation in the Carboxyl-Terminal Domain. *Mol Pharmacol* **81:** 97-105

Finn RN, Chauvigne F, Hlidberg JB, Cutler CP, Cerda J (2014) The lineage-specific evolution of aquaporin gene clusters facilitated tetrapod terrestrial adaptation. *PloS one* **9:** e113686

Gibson JS, Ellory JC (2002) Membrane transport in sickle cell disease. *Blood Cells Mol Dis* **28:** 303-314

Higgs DR (1986) Hemoglobin - Molecular, Genetic and Clinical Aspects - Bunn,Hf, Forget,Bg. *Nature* **323:** 679-679

Ishibashi K (2009) New members of mammalian aquaporins: AQP10-AQP12. *Handbook of experimental pharmacology***:** 251-262

Joiner CH (1993) Cation transport and volume regulation in sickle red blood cells. *Am J Physiol* **264:** C251-270

Joiner CH, Dew A, Ge DL (1988) Deoxygenation-induced cation fluxes in sickle cells: relationship between net potassium efflux and net sodium influx. *Blood Cells* **13:** 339-358

Kishore BK, Krane CM, Di Iulio D, Menon AG, Cacini W (2000) Expression of renal aquaporins 1, 2, and 3 in a rat model of cisplatin-induced polyuria. *Kidney Int* **58:** 701-711

Lew VL, Bookchin RM (2005) Ion transport pathology in the mechanism of sickle cell dehydration. *Physiol Rev* **85:** 179-200

Ma T, Yang B, Gillespie A, Carlson EJ, Epstein CJ, Verkman AS (1998) Severely impaired urinary concentrating ability in transgenic mice lacking aquaporin-1 water channels. *The Journal of biological chemistry* **273:** 4296-4299

Ma YL, Rees DC, Gibson JS, Ellory JC (2012) The conductance of red blood cells from sickle cell patients: ion selectivity and inhibitors. *J Physiol* **590:** 2095-2105

Maeda N, Hibuse T, Funahashi T (2009) Role of aquaporin-7 and aquaporin-9 in glycerol metabolism; involvement in obesity. *Handbook of experimental pharmacology***:** 233-249

Nagel RL (2001) The challenge of painful crisis in sickle cell disease. *JAMA* **286:** 2152-2153

Ortiz OE, Lew VL, Bookchin RM (1990) Deoxygenation permeabilizes sickle cell anaemia red cells to magnesium and reverses its gradient in the dense cells. *J Physiol* **427:** 211-226

Papadopoulos MC, Krishna S, Verkman AS (2002) Aquaporin water channels and brain edema. *Mt Sinai J Med* **69:** 242-248

Perutz MF, Mitchison JM (1950) State of haemoglobin in sickle-cell anaemia. *Nature* **166:** 677-679

Saparov SM, Kozono D, Rothe U, Agre P, Pohl P (2001) Water and ion permeation of aquaporin-1 in planar lipid bilayers. Major differences in structural determinants and stoichiometry. *The Journal of biological chemistry* **276:** 31515-31520

Speake T, Freeman LJ, Brown PD (2003) Expression of aquaporin 1 and aquaporin 4 water channels in rat choroid plexus. *Biochimica et biophysica acta* **1609:** 80-86

Steinberg MH (1999) Management of sickle cell disease. *N Engl J Med* **340:** 1021-1030

Venero JL, Vizuete ML, Machado A, Cano J (2001) Aquaporins in the central nervous system. *Prog Neurobiol* **63:** 321-336

Willcocks JP, Mulquiney PJ, Ellory JC, Veech RL, Radda GK, Clarke K (2002) Simultaneous determination of low free Mg^{2+} and pH in human sickle cells using 31P NMR spectroscopy. *The Journal of biological chemistry* **277:** 49911-49920

Yool AJ, Stamer WD, Regan JW (1996) Forskolin stimulation of water and cation permeability in aquaporin 1 water channels. *Science* **273:** 1216-1218

Yu J, Yool AJ, Schulten K, Tajkhorshid E (2006) Mechanism of gating and ion conductivity of a possible tetrameric pore in aquaporin-1. *Structure* **14:** 1411-1423

Zhang W, Zitron E, Homme M, Kihm L, Morath C, Scherer D, Hegge S, Thomas D, Schmitt CP, Zeier M, Katus H, Karle C, Schwenger V (2007) Aquaporin-1 channel function is positively regulated by protein kinase C. *The Journal of biological chemistry* **282:** 20933-20940

Figure legends

Figure 1: Electrophysiology IV traces showing the representative effects of 5HMF, 5-Nitro-2-Furoic acid, 5-Acetoxymethyl-2-Furaldehyde and Methyl 5-nitro-2-furoate on the ionic conductance of AQP1 after 2-hour incubation in saline with and without the compounds. The predicted energy of interaction is presented on the right for each compound. (B) Table of the name and structure of each compound tested for blocking effect on AQP1 central ion pore.

Figure 2: Trend plots illustrating the AQP1 ionic conductance for each oocyte measured before cGMP (initial), after cGMP, after 2-hour incubation in saline without cGMP containing DMSO (vehicle) or 5HMF and related compounds and after the application of the second cGMP. The ionic conductance in AQP1 activated by cGMP (A) is not observed in control (non-AQP1 expressing) oocytes (B). The current was blocked with 5HMF, 5-Nitro-2-Furoic acid and 5-Acetoxymethyl-2-furaldehyde but not with vehicle or Methyl 5-nitro-2-furoate.

Figure 3: Dose dependent block of cGMP activated AQP1 ionic conductance. (A) Compiled box plot data showing a statistically significant block with 5HMF, acid and 5-Acetoxymethyl-2-furaldehyde but not with vehicle or methyl 5-nitro-2-furoate on the cGMP activated ionic conductance of AQP1. Data are mean ± SEM, n values are shown above the x-axis. See Materials and Methods for details. (B) Dose-response

curves of percent block and estimated IC50 values of the activated ionic conductance in AQP1-expressing oocytes.

Figure 4: Time recovery of block of AQP1 ionic conductance from 1mM 5HMF at different time points. At 1 hour incubation in 1mM 5HMF 75-80% block is observed in AQP1 ionic current. At 30 minutes 35 to 40% block is observed and at 15 minutes incubation in 1mM 5HMF 20% block in AQP1 ionic conductance is observed. Data are mean ± SEM; n values are displayed above the x-axis.

Figure 5: The 5HMF and related compounds do not affect the osmotic water permeability of AQP1 measured by optical swelling assays. (A) Mean of swelling responses of AQP1 untreated, and AQP1 incubated in 5mM 5HMF, 5mM 5-methoxy-2-furoic acid, 5mM 5-Acetoxymethyl-2-furaldehyde, Methyl 5-nitro-2-furoate in 50% hypotonic saline. Non-AQP expressing oocytes showed little change in volume. Data are mean values for all oocytes assessed from different batches of oocytes; error bars are S.E.M.; n values are 6 per treatment group. (B) Compiled box plot data showing lack of any statistically significant differences between the swelling rates measured before (S1) and after (S2) 2-hour incubations in saline alone or saline containing 5mM 5HMF and compounds as indicated. See Materials and Methods for details.

Figures

Figure 1

A

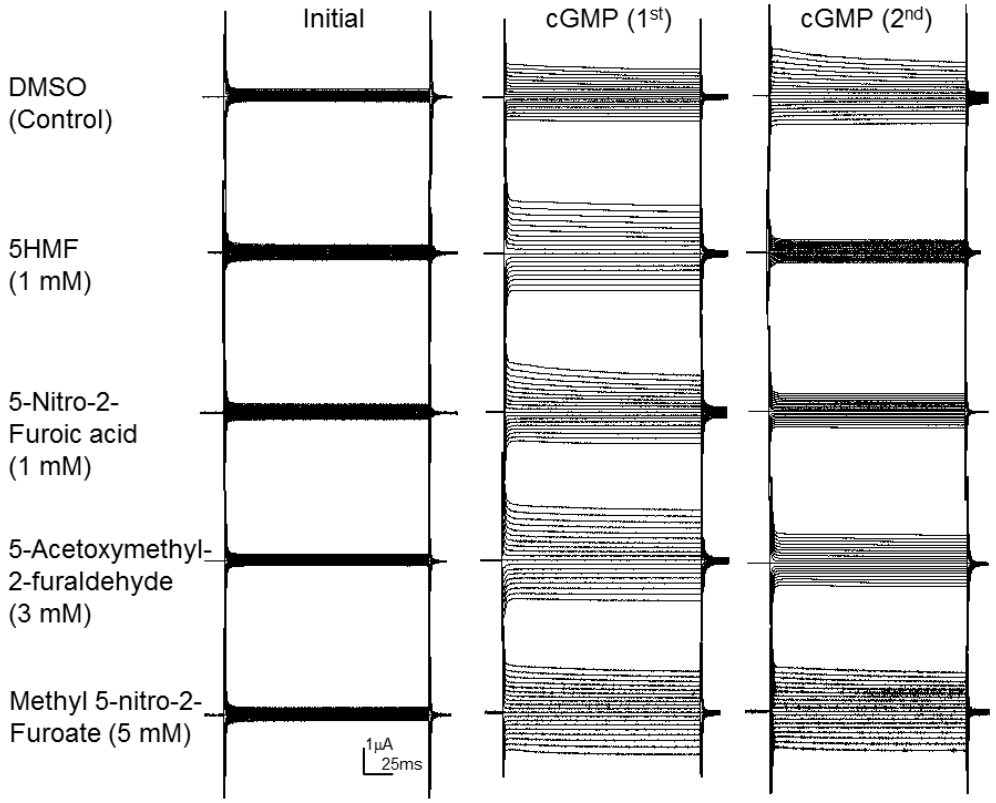

Predicted energy of interaction
-4.9
-4.3
-4.0
-3.9

B

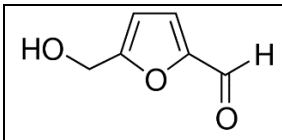	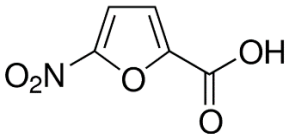	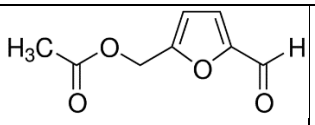	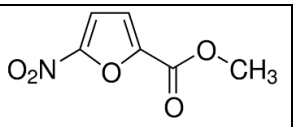
5-(Hydroxymethyl) furfural (5HMF)	5-Nitro-2-furoic acid	5-Acetoxymethyl-2-furaldehyde	Methyl 5-nitro-2-furoate

Figure 2

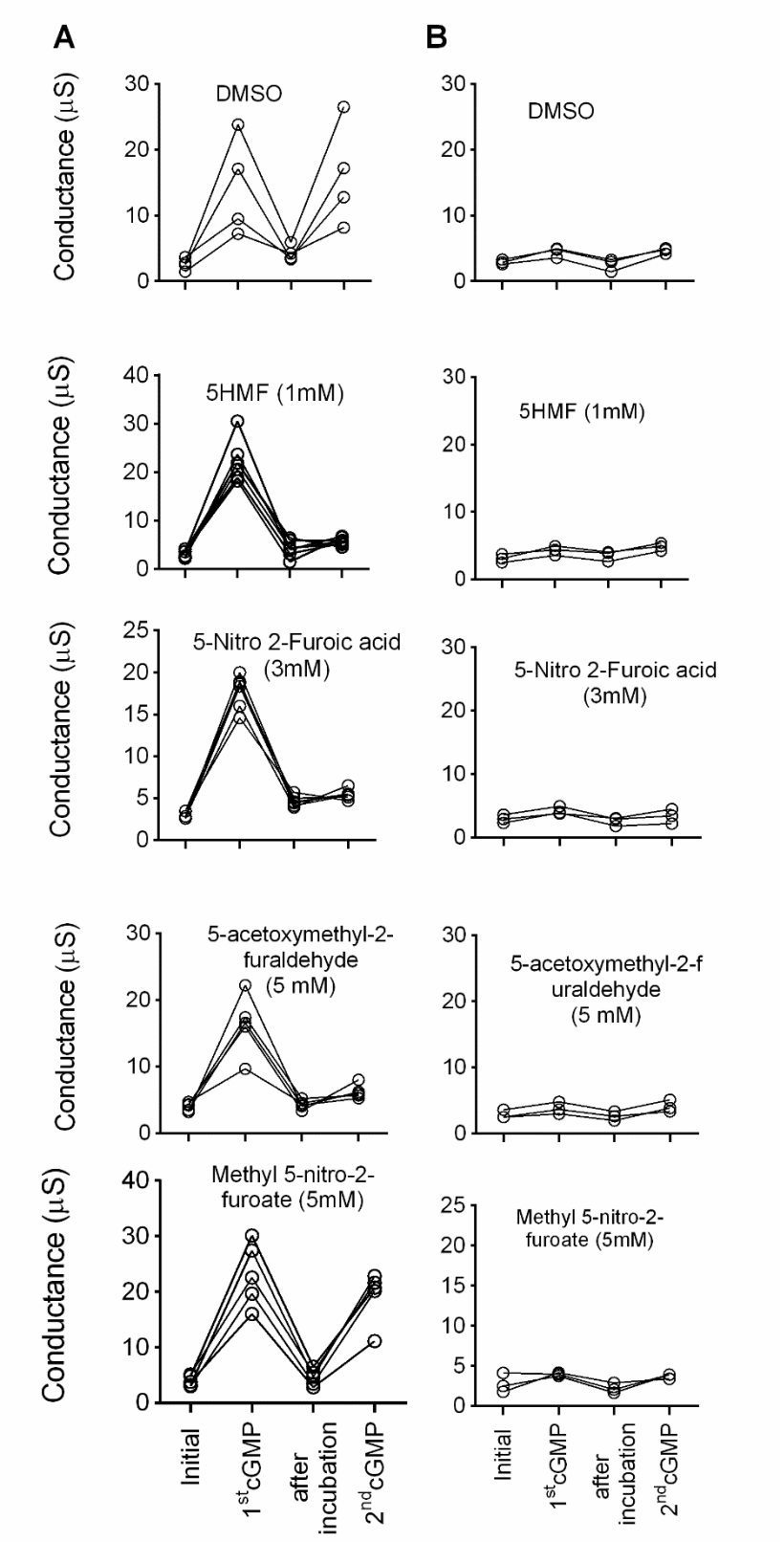
A
B
Conductance (μS)
DMSO
5HMF (1mM)
5-Nitro 2-Furoic acid (3mM)
5-acetoxymethyl-2-furaldehyde (5 mM)
Methyl 5-nitro-2-furoate (5mM)
Initial
1st cGMP
after incubation
2nd cGMP

Figure 3

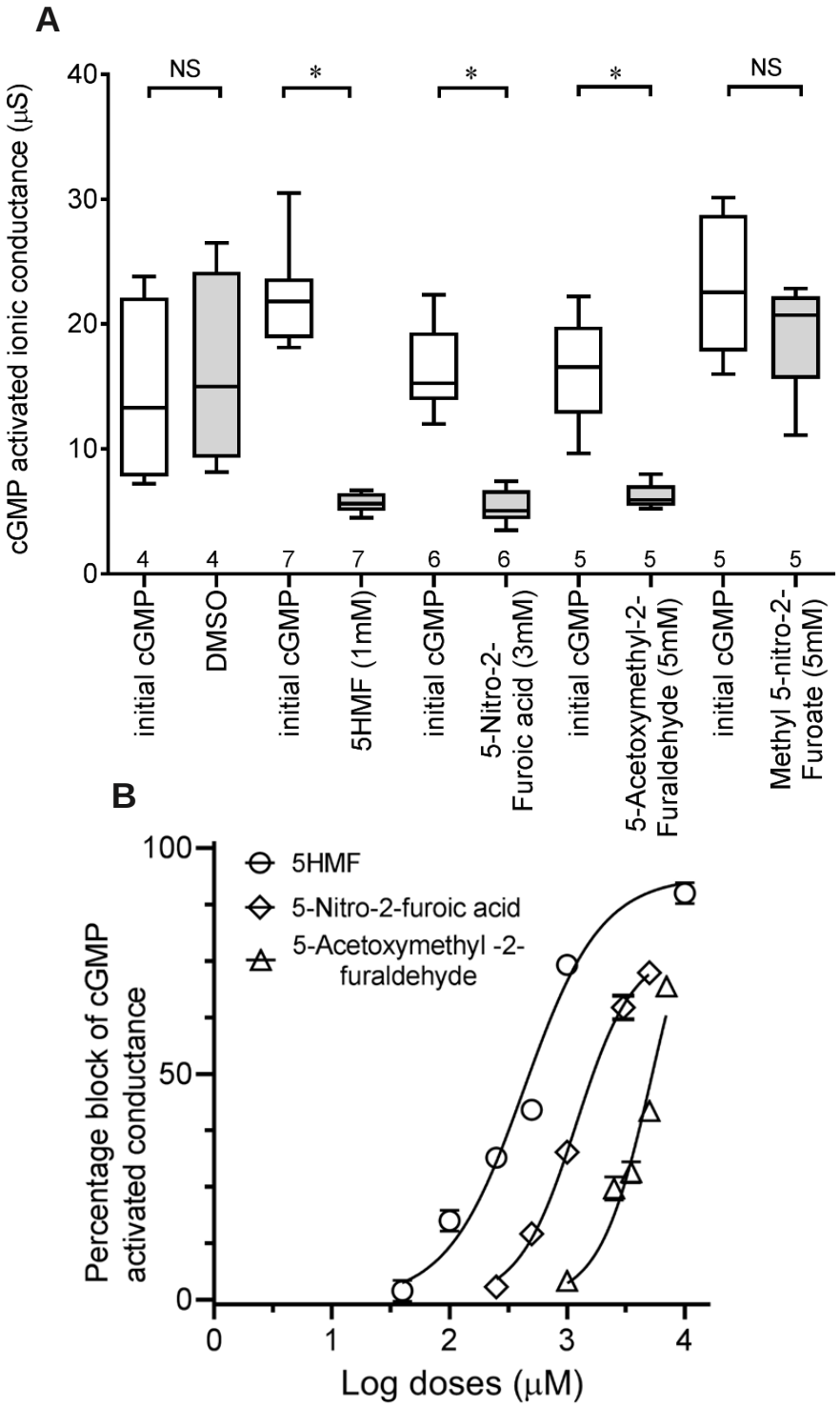

	5HMF	5-Nitro-2-furoic acid	5-Acetoxymethyl-2-furaldehyde
IC50	432 μM	1.193 mM	3.296 mM

Figure 4

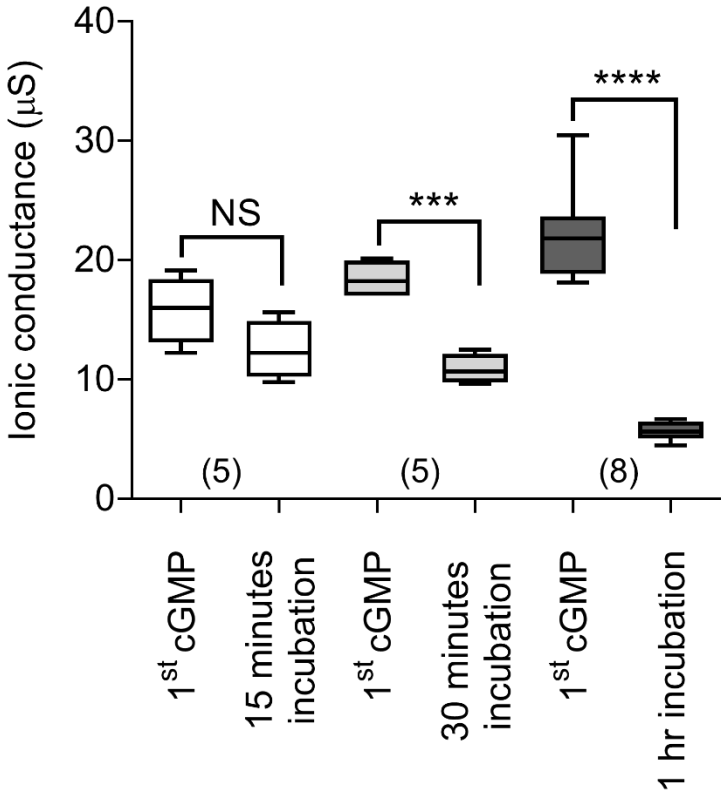
Ionic conductance (μS)
40
30
20
10
0
NS
***
****
(5)
(5)
(8)
1st cGMP
15 minutes incubation
1st cGMP
30 minutes incubation
1st cGMP
1 hr incubation

Figure 5

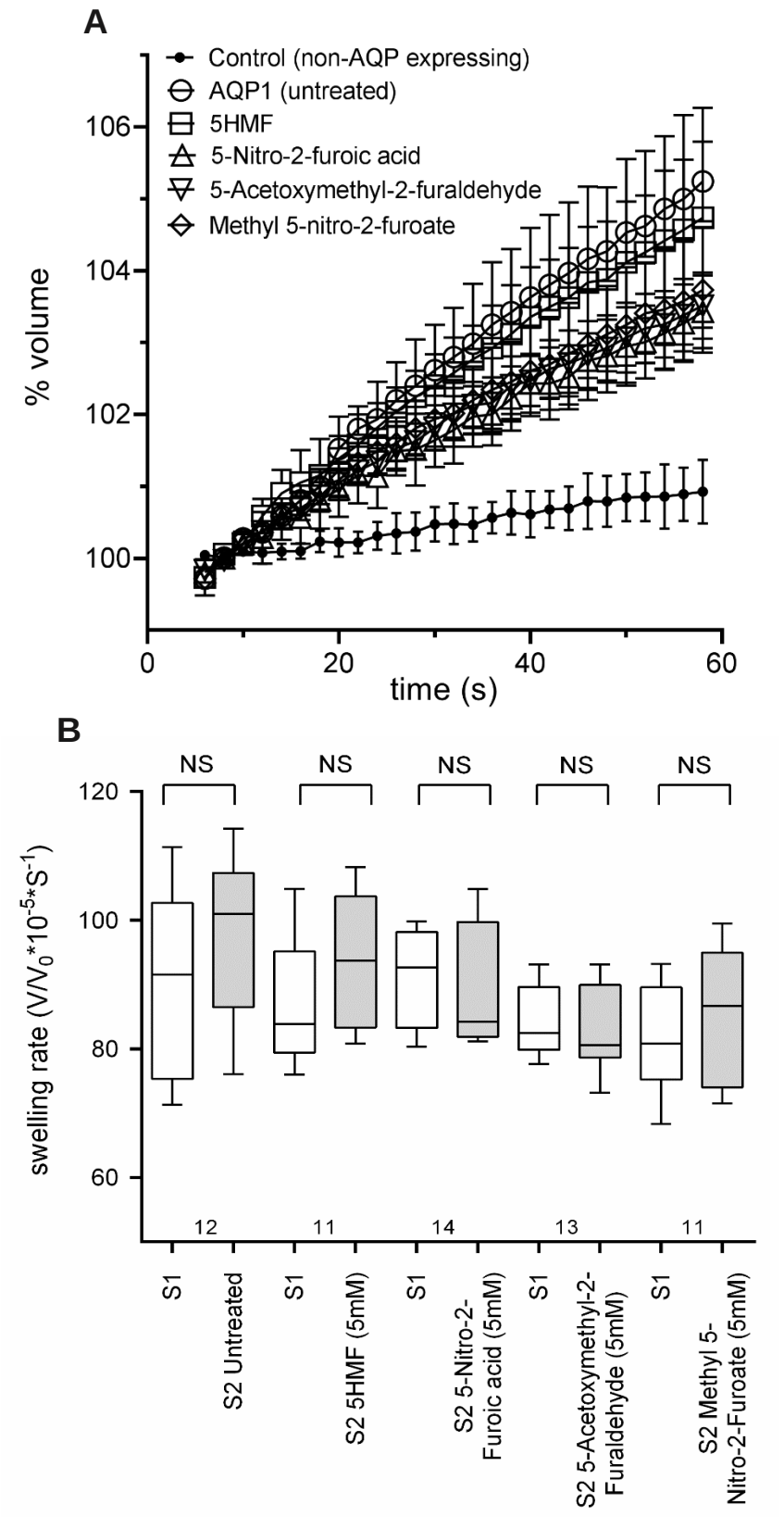
A
Control (non-AQP expressing)
AQP1 (untreated)
5HMF
5-Nitro-2-furoic acid
5-Acetoxymethyl-2-furaldehyde
Methyl 5-nitro-2-furoate
% volume
106
104
102
100
0
20
40
60
time (s)
B
NS
NS
NS
NS
NS
swelling rate (V/V0*10-5*S-1)
120
100
80
60
12
11
14
13
11
S1
S2 Untreated
S1
S2 5HMF (5mM)
S1
S2 5-Nitro-2-Furoic acid (5mM)
S1
S2 5-Acetoxymethyl-2-Furaldehyde (5mM)
S1
S2 Methyl 5-Nitro-2-Furoate (5mM)

Chapter 6. Statement of authorship

Statement of Authorship

Title of Paper	Non-selective cation channel activity of aquaporin AtPIP2;1 regulated by Ca2+ and pH.
Publication Status	☑ Published ☐ Accepted for Publication ☐ Submitted for Publication ☐ Unpublished and Unsubmitted work written in manuscript style
Publication Details	Byrt, C. S., M. Zhao, M. Kourghi, J. Bose, S. W. Henderson, J. Qiu, M. Gilliham, C. Schultz, M. Schwarz, S. A. Ramesh, A. Yool and S. Tyerman (2016). "Non-selective cation channel activity of aquaporin AtPIP2;1 regulated by Ca2+ and pH." Plant Cell Environ.

Principal Author

Name of Principal Author	Caitlin Byrt		
Contribution to the Paper	Drafted paper, coordinated, performed and designed experiments.		
Overall percentage (%)	33%		
Signature		Date	27/7/2017

Co-Author Contributions

By signing the Statement of Authorship, each author certifies that:

i. the candidate's stated contribution to the publication is accurate (as detailed above);

ii. permission is granted for the candidate in include the publication in the thesis; and

iii. the sum of all co-author contributions is equal to 100% less the candidate's stated contribution.

Name of Co-Author (Candidate)	Mohamad Kourghi		
Contribution to the Paper	Contributed to electrophysiology experiments and writing the manuscript. Helped in data collection and analysis of figure 10.		
Certification:	This paper reports on original research I conducted during the period of my Higher Degree by Research candidature and is not subject to any obligations or contractual agreements with a third party that would constrain its inclusion in this thesis. I am the primary author of this paper.		
Agree contribution (%)	33%		
Signature		Date	15/08/17

Name of Co-Author	Manchun Zhao
Contribution to the Paper	Performed experiments, designed experiments, helped write paper.
Signature	Date 5/9/2017

Please cut and paste additional co-author panels here as required.

Name of Co-Author	Jayakuma Bose
Contribution to the Paper	Performed experiments and helped write paper
Signature	Date 01/08/2017

Name of Co-Author	Sam Henderson
Contribution to the Paper	Performed experiments and helped write paper.
Signature	Date 28/7/17

Name of Co-Author	Jiane Qui
Contribution to the Paper	Performed experiments and helped write paper
Signature	Date 31/07/2017

Name of Co-Author	Matthew Gilliham
Contribution to the Paper	Contributed to writing paper and design of experiments
Signature	Date 01/08/2017

Name of Co-Author	Carolyn Schultz
Contribution to the Paper	Helped design experiments
Signature	Date 5/9/2017

Published Manuscript

Chapter 6: Non-selective cation channel activity of aquaporin AtPIP2;1 regulated by Ca^{2+} and pH

Caitlin S. Byrt, Manchun Zhao, Mohamad Kourghi, Jayakumar Bose, Sam W. Henderson, Jiaen Qiu, Matthew Gilliham, Carolyn Schultz, Manuel Schwarz, Sunita A. Ramesh, Andrea Yool & Steve Tyerman

Australian Research Council Centre of Excellence in Plant Energy Biology, Waite Research Institute and School of Agriculture, Food and Wine, The University of Adelaide, Glen Osmond, South Australia 5064, Australia (CSB, MZ, JB, SWH, JQ, MG, CS, MS, SAR, ST)

Discipline of Physiology, School of Medicine, University of Adelaide, South Australia 5005, Australia and [3]Waite Research Institute and School of Agriculture, Food and Wine,The University of Adelaide, Glen Osmond, South Australia 5064, Australia (MK, AJY)

Key-words: ion transport; PIP; plasma membrane; root; water transport.

Corresponding Author:

Professor Stephen Tyerman

University of Adelaide

Plant Research Centre: School of Agriculture, Food and Wine

Tel: +61 8 3136663

Fax: 8313 0431

e-mail: steve.tyerman@adelaide.edu.au

ABSTRACT

The aquaporin AtPIP2;1 is an abundant plasma membrane intrinsic protein in Arabidopsis thaliana that is implicated in stomatal closure, and is highly expressed in plasma membranes of root epidermal cells. When expressed in Xenopus *laevis* oocytes, AtPIP2;1 increased water permeability and induced a non-selective cation conductance mainly associated with Na^+. A mutation in the water pore, G103W, prevented both the ionic conductance and water permeability of PIP2;1. Coexpression of AtPIP2;1 with AtPIP1;2 increased water permeability but abolished the ionic conductance. AtPIP2;2 (93% identical to AtPIP2;1) similarly increased water permeability but not ionic conductance. The ionic conductance was inhibited by the application of extracellular Ca^{2+} and Cd^{2+}, with Ca^{2+} giving a biphasic dose–response with a prominent IC_{50} of 0.32mм comparable with a previous report of Ca^{2+} sensitivity of a non-selective cation channel (NSCC) in Arabidopsis root protoplasts. Low external pH also inhibited ionic conductance (IC_{50} pH6.8). Xenopus oocytes and Saccharomyces cerevisiae expressing AtPIP2;1 accumulated more Na^+ than controls. Establishing whether AtPIP2;1 has dual ion and water permeability in planta will be important in understanding the roles of this aquaporin and if AtPIP2;1 is a candidate for a previously reported NSCC responsible for Ca^{2+} and pH sensitive Na^+ entry into roots.

INTRODUCTION

Plant aquaporins are membrane proteins that transport water and a range of neutral solutes. Some aquaporins transport only water and others transport gases (carbon dioxide and ammonia), metalloids (boron, silicon and arsenic) or reactive oxygen species (hydrogen peroxide) (Uehlein et al. 2003; Loqué et al. 2005; Ma et al. 2006; Takano et al. 2006; Dynowski et al. 2008; Kamiya et al. 2009). A subset of animal aquaporins transport water and ions (Yool & Campbell 2012), but there is limited evidence of transport of ions by plant aquaporins (Weaver et al. 1994; Rivers et al. 1997; Holm et al. 2005). If a subset of aquaporins co-transports water and ions in planta, then there may be novel roles for aquaporins in plant nutrient transport and osmotic adjustment. Root water uptake and stress-induced inhibition of root hydraulic conductivity are mediated by plasma membrane intrinsic proteins (PIPs) (Tournaire-Roux et al. 2003). One of the most highly expressed aquaporins in Arabidopsis roots is AtPIP2;1 (Alexandersson et al. 2005). AtPIP2;1 is a plasma membrane intrinsic protein that facilitates the transport of water across the plasma membrane. The function of AtPIP2;1 is important for maintaining whole plant water status, and the water channel activity is inhibited by divalent cations (Verdoucq et al. 2008). For example, when AtPIP2;1 is mislocalized in the endoplasmic reticulum instead of the plasma membrane, a 36–45% reduction in root hydraulic conductivity is observed (Sorieul et al. 2011). In Arabidopsis, root plasma membrane vesicles show water channel activity that is inhibited by Ca^{2+} with an IC_{50} of 75μM (Gerbeau et al. 2002), and similarly in AtPIP2;1-expressing proteoliposomes water channel activity is inhibited by Ca^{2+}, with an IC_{50} of 42μM (+/25μM) (Verdoucq et al. 2008). A range of

divalent cations inhibited the osmotic water permeability of AtPIP2;1 expressing proteoliposomes, particularly Ca^{2+}, Cd^{2+} and Mn^{2+}, and the permeability to water was blocked by H^{+}, with a half inhibition at pH7.15 (Verdoucq et al. 2008). AtPIP2;1 is also important for light-dependent changes in leaf water transport, where hydraulic conductivity in the rosette under darkness is influenced by PIP2;1 phosphorylation at Ser-280 and Ser-283 (Prado et al. 2013). When Arabidopsis roots are exposed to salt the abundance and phosphorylation status of PIP2;1 changes. NaCl treatment increases the trafficking of AtPIP2 isoforms between the plasma membrane and intracellular compartments, reducing the abundance of PIP2 proteins on the plasma membrane and the hydraulic conductivity of salt-stressed root cells (Boursiac et al. 2005; Sutka et al. 2011). A rapid (half-time, 45min) decrease (70%) in root hydraulic conductivity was observed after exposure to 100мм NaCl (Boursiac et al. 2005). In standard conditions, Arabidopsis roots contain poly-phosphorylated, singly phosphorylated and dephosphorylated forms of AtPIP2;1 in a relative abundance ratio of 1:1:2 (Prak et al. 2008). NaCl acts on AtPIP2;1 with unphosphorylated Ser^{283} to favour intracellular accumulation. NaCl treatment resulted in a 30% decrease in the level of Ser^{283} phosphorylation and an increase in the relative abundance of singly and unphosphorylated forms (Prak et al. 2008). The physiological importance of salt induced cycling of AtPIP2;1 in standard conditions, or under environmental stresses is not yet clear (Verdoucq et al. 2014). If Na^{+} permeated AtPIP2;1 in planta, then internalization of AtPIP2;1 from the root epidermal plasma membrane in response to salt stress could be a mechanism to avoid Na^{+} accumulation. Given that a non-selective cation channel in the plasma membrane of protoplasts isolated from

Arabidopsis roots was inhibited by Ca^{2+} and low pH (Demidchik & Tester 2002), and that both Ca^{2+} and low pH have been reported to inhibit water channel activity of AtPIP2;1 (Verdoucq et al. 2008; Tournaire-Roux et al. 2003) we investigated if AtPIP2;1 could confer a cation conductance when expressed in heterologous systems and if this was sensitive to Ca^{2+} and external pH. Here, we report that in heterologous systems AtPIP2;1 induces a Na^{+} conductance that is inhibited by external Ca^{2+} and low external pH.

MATERIALS AND METHODS Chemicals

All chemicals were supplied by Sigma (St Louis, MO, USA) except where stated otherwise.

Cloning, preparation of constructs and cRNA

Complementary DNA made from RNA extracted from Arabidopsis thaliana (Col-0) was used to amplify fragments coding for the plasma membrane intrinsic proteins (PIPs) of interest. The primers used for amplification of AtPIP2;1 (At3g53420), AtPIP1;2 (At2g45960), AtPIP1;4 (At4g00430), AtPIP1;5 (At4g23400), AtPIP2;2 (At2g37170), AtPIP2;6 (At2g39010) and generating the G103W AtPIP2;1 mutant by site-directed mutagenesis are reported in Table S1.Previous research indicated that the AtPIP2;1 G103W mutation blocks the water pore (Shelden et al. 2009). Standard PCR conditions were used (98°C for 30s, 25 cycles of 98°C for 10s, 55°C for 30s, 72°C for 30s; final extension 72°C for 10min for AtPIP2;1) with Phusion High-Fidelity DNA Polymerase. The amplified products were cloned into pENTR TOPO® vector using a pENTR Directional TOPO® Cloning Kit (Invitrogen, Carlsbad, CA, USA), transformed into chemically competent Escherichia coli One shot® TOPO10 cells (Invitrogen). AtPIP2;1

cDNA was then recombined by Gateway LR recombination reactions using LR Clonase™ into pGEMHE-DEST (Gateway enabled) following Preuss et al. (2011), and the pYES3-DEST expression vector, transformed into E. coli and confirmed by sequencing. pYES3-DEST (Shelden et al. 2009) is a modified version of pYES2 (Invitrogen) converted to a Gateway enabled vector using the Gateway Vector Conversion System (Invitrogen). It has the GAL1 promoter for galactose inducible expression and the URA3 gene for uracil selection. Plasmid DNA was extracted using a Sigma Genelute Plasmid Purification Kit. One microgram quantities of pGEMHEDEST plasmid DNA containing the genes of interest were linearized, in preparation for cRNA synthesis, with the restriction enzyme Nhe I or Sph I (New England BioLabs Inc., Beverly, MA, USA).

A DNA fragment encoding the AtPIP2.1-mCherry fusion protein was PCR amplified from the binary vector PM-RK (Nelson et al. 2007) using Phusion high-fidelity polymerase. The reaction consisted of 5ng plasmid template, 0.2 units of Phusion polymerase and 500nM forward (5′-ATGGCAAAGGATGTGGAAG-3′) and reverse (5′-TTAAGATCTGTACAGCTCGTCC-3′) primers. The PCR fragment was A-tailed with Taq polymerase (NewEngland BiolabsInc.), subcloned into pCR8/GW/TOPO (LifeTechnologies, Rockville, MD, USA) and recombined into the Xenopus *laevis* expression vector pGEMHE-DEST (Shelden et al. 2009) using LR Clonase II enzyme (Life Technologies). The pGEMHE expression vector harbouring AtPIP2;1-mCherry was linearized with NheI restriction endonuclease, purified by phenol/chloroform extraction and used as a template for in vitro capped RNA (cRNA) synthesis. cRNA was synthesized using the mMESSAGE mMACHINE T7 kit (Ambion, Austin, TX, USA)

following manufacturer's instructions. The cRNA was purified by phenol/chloroform extraction and was ethanol precipitated and resuspended in nuclease-free water.

Preparation of Xenopus *laevis* oocytes

Unfertilized oocytes were harvested from X.*laevis* frogs and defoliculated by incubation in collagenase (type 1A, 2mgmL^{1}) and trypsin inhibitor (1mgmL^{1}) in 96mM NaCl, 2mM KCl, 5mM $MgCl_2$ and 5mM HEPES, pH7.6 for 1 to 1.5h. The majority of the experiments were conducted in a laboratory in the Plant Research Centre at the Waite Campus, with the exception experiments investigating the influence of varying Ca^{2+} concentrations and solutions with Cd^{2+} on AtPIP2;1 ionic conductance, which were conducted in the Medical School South Building, North Terrace Campus, and the respective differences in protocols are as indicated. At Waite, oocytes were stored at 18°C in Ringer's solution: 96mM NaCl, 2mM KCl, 5mM $MgCl_2$, 0.6 mM $CaCl_2$, 5mM Hepes, 5% (v/v) horse serum and antibiotics (0.05mgmL^{1} tetracycline, 100 units/mL penicillin/0.1mgmL^{1} streptomycin); replaced daily. Oocytes were injected with 46nL of RNAse-free water using a micro-injector (Nanoinject II, automaticnanolitre injector, Drummond Scientific) with varied concentrations of cRNA (1–25ng). Water-injected oocytes as controls were included in all experiments. The oocytes were incubated in Ringer's solution as defined above prior to experimentation. In the Medical School South Building, oocytes were injected with 50nL of RNAse-free water containing 0 or 12ng of AtPIP2;1 cRNA and ooyctes were incubated in 62mM NaCl, 36mM KCl, 5mM $MgCl_2$, 0.6mM $CaCl_2$, 5mM HEPES buffer, 5% horse serum, 100 units/mL penicillin, 0.1mgmL^{1} streptomycin, 0.5mgmL^{1} tetracycline, pH7.6 for 1 to 1.5days prior to experiments. AtPIP2;1 expression was confirmed in a subset of oocytes from each

injected batch by swelling tests where AtPIP2;1-cRNA and water injected oocytes were placed in distilled water; AtPIP2;1 expressing oocytes swelled and burst within a few minutes whereas water injected oocytes remained intact for up to 10min.

Localization of AtPIP2;1 in Xenopus *laevis* oocytes

Oocytes were injected with 11ng of AtPIP2;1-mCherry cRNA, or with nuclease-free water, in a total volume of 46nL. Oocytes were incubated post-injection in Ringer's solution. Oocytes were imaged 2days post-injection on chambered glass slides using a Zeiss LSM 5 Pascal laser scanning confocal microscope equipped with a Plan-Neofluar 10×/0.3 objective lens. The mCherry fluorophore was excited using a 543nm HeNe laser. The emission spectrum was collected though a 560nm long pass filter. Raw data was processed using Zeiss AIM software (Carl Zeiss, Oberkochen, Germany).

Water permeability

Twenty-four hours after injection with cRNA or nuclease-free water, oocytes were transferred to 5mL hypo-osmotic solution, Ringers' solution diluted fivefold with sterile water. The osmolality of each solution was determined using a Fiske® 210 Micro-Sample freezing-point osmometer (Advanced Instruments, Inc., USA). Oocytes were viewed with a Nikon SMZ800 light microscope (Nikon, Japan) with the 1.5× objective lens WD45. The changes in volume were captured with a Vicam colour camera (Pacific Communications, Australia) at 2× magnification and recorded with IC CAPTURE 2.0 software (The Imagine Source, USA) as AVI format video files. Images

were acquired every 3s for 1.5min for each oocyte. Image J software (National Institute of Health, USA) was used to calculate the change in total area of the oocytes captured in the AVI video file. Osmotic permeability (P_{os}) was calculated from the increase in volume with time (n=5–10) using the following equation $P_{os} = V_o(d(V/V_o)/dt)/S \times V_w (Osm_{in} Osm_{out})$, where V_o is the initial oocyte volume (mm^3); $d(V/V_o)/dt$ is the rate of initial relative cell volume change ($mm^3\ s^1$); S is the initial surface area (mm^3); V_w is the partial molar volume of water $18cm^3\ mol^1$; $Osm_{in} Osm_{out}$ is the change in osmolality.

Electrophysiology

Two-electrode voltage clamp (TEVC) was performed on X. *laevis* oocytes between 24 and 48h post injection with water, with or without cRNA following Preuss et al. (2011). Borosilicate glass pipettes (Harvard Apparatus, GC150F-10, 1.5mm O.D.×0.86mm I.D.) for voltage and current injecting electrodes were pulled to give between 0.5 and 1MΩ resistance in ND96 solution (see below) with a filling solution of 3M KCl. A bath clamp system was used to minimize the effect of series resistance in the bath solution. The bath current and voltage sensing electrodes consisted of a silver–silver chloride electrode connected to the bath by 2% agar/3M KCl bridges. The bath solution was continuously perfused during the experiments. Each oocyte was carefully stabbed with the voltage and current electrodes and membrane voltage allowed to stabilize. TEVC experiments were conducted on oocytes with membrane potentials, when in ND96 between 25 and 50mV, and hyperpolarized oocytes with lower membrane potentials were avoided. Voltage clamp experiments were performed with an Oocyte Clamp OC-725C (Warner Instruments, Hamden, CT, USA) with a Digidata 1440A

data acquisition system interface (Axon Instruments, Foster City, CA, USA) at room temperature (20–22°C). The voltage clamp protocol was set upas follows: 40mVfor 0.5s;then, the membrane potential was decreased in 20mV steps from 40 through to 100 or 110mV; each voltage was held for 2s, followed by 40mV for 0.5s. Recordings were made using a GeneClamp amplifier and CLAMPEX 9.0 software (pClamp 9.0 Molecular Devices, CA, USA). TEVC was initially performed in ND96 solution consisting of 96mм NaCl, 2mм KCl, 1mм $MgCl_2$, 1.8mм $CaCl_2$, 5mм HEPES pH7.5 with TRIS base. Solutions with lower NaCl had otherwise the same composition as ND96 and were made isotonic with ND96 using mannitol. A series of solutions with constant Na^+ concentration of 50mм and varied Cl concentration were made using MES (2-(Nmorpholino) ethanesulfonic acid) as a substitute anion. Ethylene glycol-bis (β-aminoethyl ether)-N,N,N′,N′-tetraacetic acid (EGTA)-buffered divalent free saline (96mм NaCl, 2mм KCl, 5mм HEPES, 10mм EGTA, pH7.6) and divalent free salines containing varying EGTA-buffered calcium concentrations were used in experiments with defined and lower Ca^{2+} or Cd^{2+}. The required total concentration of Ca^{2+} needed to achieve the desired free Ca^{2+} concentration in 10mм EGTA was calculated using http://maxchelator.stanford.edu/ CaEGTA-NIST.htm.

Ion-selective microelectrode flux measurements

The water and cRNA injected oocytes were incubated for 48h in Ringer's solution; then, the oocytes were transferred to basal salt medium (BSM; 5mм NaCl, 2mм KCl, 50 μм $CaCl_2$, 5mм HEPES) with the osmolality (adjusted with D-mannitol) of 231mosmolkg^1; the net Na^+ flux was measured noninvasively using ion-selective microelectrodes (the MIFE^{TM} technique; University of Tasmania, Hobart, Australia), as described previously

(Newman 2001). Microelectrode fabrication, conditioning and calibration followed Jayakannan et al. (2011), Bose etal. (2013) and Shabalaetal. (2013).During measurements, the ion-selective electrodes were positioned using a 3D-micromanipulator (MMT-5, Narishige, Tokyo, Japan), 100µm from the oocyte surface. A computer-controlled stepper motor moved the electrode between two positions (100 and 200µm, respectively) from the oocyte surface in 6s cycles. The CHART software (Newman 2001) recorded the potential difference between the two positions and converted them into electrochemical potential differences using the calibrated Nernst slope of the electrode. Net ion fluxes were calculated using the MIFEFLUX software for spherical geometry (Newman 2001).

Yeast growth assay and ion content

The pYES3-DEST-AtPIP2;1 vector and pYES3-DEST empty vector were transformed into Saccharomyces cerevisiae strain INVSc2 (Invitrogen) using the LiAc method, and selected on synthetic defined medium without uracil supplemented with 2% (w/v) D-glucose. Twenty-millilitre liquid cultures (5.7% (w/v) Yeast Nitrogen Base without amino acids, phosphates or NaCl, MP Biomedicals; 95mgL^{1} L-Histidine-HCL, 1% (w/v) KH_2PO_4, pH5.5 with TRIS and either no NaCl, 0.1м NaCl or 0.5м NaCl as specified and 2% (w/v) D-galactose) in 50mL conical flasks were inoculated with 50µL of transformed yeast from 1mL starter cultures with 2% (w/v) D-glucose at an OD_{600} of 0.5. Cultures were grown at 28°C for 24h at 200rpm. Cells were extracted by centrifugation (1500g, 3 min) and washed twice with solution of an equal osmolality (1.1м sorbitol, 20мм $MgCl_2$). Cell pellet weight was measured. Pellets were frozen at 20°C for 24h, then resuspended in 2mL of MilliQ water and boiled for 30min to lyse

cells. Samples were diluted 1:10, and the Na^+ and K^+ contents of cells grown in liquid culture were measured by flame photometry (model 420 Flame Photometer, Sherwood, Cambridge, UK).

Statistics

All graphs and statistics were performed in Graphpad Prism 6. All data shown are mean±SEM. Different letters indicate significance ($P<0.05$) between values as determined by analysis of variance with post hoc tests as detailed in the figure legends or text.

RESULTS Water permeation through AtPIP2;1 and interaction with AtPIP1;2

Previously, AtPIP2;1 has been shown to facilitate water permeability in proteoliposomes (Verdoucq et al. 2008), guard cell protoplasts and X.*laevis* oocytes (Grondin et al. 2015). We confirmed that AtPIP2;1 increased water permeability (P_{os}) in X. *laevis* oocytes and was localized to the plasma membrane (Fig.1 and Supporting Information Fig. S1). Various other Arabidopsis PIPs were examined for water permeation; AtPIP2;2, AtPIP2;6, AtPIP1;4, AtPIP1;5 and AtPIP1;2, of which only AtPIP2;2 and AtPIP2;6 increased P_{os} when expressed alone (Fig. 1a and Supporting Information Fig. S2). AtPIP1;2, AtPIP1;4 and AtPIP1;5 did not increase P_{os} above control levels when expressed alone, but they further increased P_{os} when co-expressed with AtPIP2;1, with AtPIP1;2 and AtPIP1;5 being the most effective at increasing P_{os} (Fig. 1b and Supporting Information Fig. S2).

AtPIP2;1 elicited currents in Xenopus *laevis* oocytes

A survey of some of the PIP aquaporins from Arabidopsis expressed in X.*laevis* oocytes revealed that AtPIP2;1 was not only a water channel but also was associated with ionic currents inND96bath saline (Fig.2and Supporting Information Fig. S3; at 100mV: I_m =795nA, SEM=65nA, n=28 oocytes combined from two frogs; controls at 100mV: I_m =355nA, SEM=33nA, n=32). AtPIP2;1 gave conductances of 10.3 and 11.4μS in batches of oocytes from two frogs (Fig. 2c,d), which were significantly higher than the control conductance (3 and 4.6μS). These conductances are measured as the slope of the linear portion of the current versus voltage cure through the reversal potential (crossing the x-axis). AtPIP1;2 and AtPIP2;2 expressing oocytes in ND96 saline did not display ionic conductances that were significantly different from those of water injected controls (Fig. 2a,b,c). When AtPIP2;1 was co-expressed with AtPIP1;2, the ionic conductance was not significantly different to that of water injected controls (Fig. 2d and Supporting Information Fig. S3); however, water permeability was significantly increased when these two PIPs were co-expressed (Fig. 1b). Additional experiments over a period of four years involving four different experimenters and two laboratories with different sets of cRNA and re-cloned AtPIP2;1 gave similar results for PIP2;1-induced ion conductance. Comparison of amplitudes of water permeabilities and ionic conductances measured in ND96 as a function of the amount cRNA injected showed saturation of both P_{os} and ionic conductance at higher concentrations of cRNA (Fig. 3a). The data were fitted to the Michaelis–Menten equation and indicated close similarity between the responses of ionic conductance and P_{os} with the amount of cRNA injected. This is reflected in the linear relationship between ionic conductance and P_{os} shown in Fig. 3b. Given that PIP2;1 induced a much higher water permeability

in oocytes compared to water injected controls (Fig. 1), we tested the possibility that a slight imbalance in bathing medium osmolality from isotonic may induce a swelling response in the PIP2;1 expressing oocytes that could have activated a native oocyte channel or transporter. For a 50mosmolkg^{1} reduction in osmolality (from 234 to 183mosmolkg^{1}) neither the controls nor PIP2;1 injected oocytes showed any change in current–voltage curve characteristic when bathed in 50мм NaCl or 50мм $NaNO_3$ solutions (Supporting Information Fig. S4). AtPIP2;1 water permeability and conductance were affected by a glycine to tryptophan mutation at residue 103 Previously, we showed that a naturally occurring PIP from grapevine (Vitis vinifera L. cv Cabernet Sauvignon) was nonfunctional as a water channel when expressed in X.l*aevis* (Shelden et al. 2009). This was due to a tryptophan substituting for a glycine in Loop B, which was suggested to block the water pore based on a homology model of SoPIP2;1 (Shelden et al. 2009). This mutation (G100W in VvPIP2;1 corresponding to G103W in AtPIP2;1) was previously tested for AtPIP2;1 to explore CO_2 permeation induced by AtPIP2;1 in X. *laevis* oocytes (Wang et al. 2016). We tested the effect of the G103W mutation on water permeation using oocyte swelling assays. The AtPIP2;1 G103W mutant did not induce an increase in water permeability when expressed alone (Fig. 4a,c), but when co-expressed with AtPIP1;2 there was an increase in P_{os}, however, not to the level observed for AtPIP2;1 alone or AtPIP1;2: AtPIP2;1 WT (Fig. 4b,c). This G103W mutation was also tested for effects on the ionic conduction through AtPIP2;1. Current–voltage curves for water injected controls, AtPIP2;1 and AtPIP2;1 G103W expressing X. *laevis* oocytes in a series of solutions were compared to explore the selectivity of the ionic current (Fig. 5). The Na^+ concentration was held

approximately constant while Cl concentration was varied using MES as a substitute anion. With this sequence of solutions there was no change in conductance of the water injected controls and no significant change in reversal potential (Fig. 5a). AtPIP2;1-expressing oocytes showed increasing conductance as MES was substituted by Cl with the inward current increasing more so than the outward current (Fig. 5b). All the curves intersected the control current–voltage curve at approximately 13mVas an estimate of the reversal potential after subtraction of control current– voltage curves. These results are best explained by the current being predominately carried by Na^+ because there was no substantial shift in reversal potential; however, conductance increased with increasing Cl concentration, suggesting potential allosteric modulation. The AtPIP2;1 G103W mutant showed a similar response to controls indicating that it did not induce an ionic conductance.

AtPIP2;1 ion currents in Xenopus *laevis* oocytes were carried by Na^+

We further explored the selectivity of the ionic currents by examining changes in reversal potentials (controls subtracted) with changes in NaCl concentrations. Increasing NaCl concentration while keeping the solution isotonic with sorbitol caused a positive shift in the reversal potential (Fig. 6). Four separate experiments are shown in Fig. 6 from four separate frogs and three different experimenters. In every case, the reversal potential shifted positive when NaCl concentration was increased at the higher NaCl concentrations. This indicates that the AtPIP2;1 induced currents were predominately carried by Na^+ in these solutions. The reversal potentials were compared with calculated Nernst potentials for Na^+ and Cl taking either literature values for internal oocyte concentrations (Weber 1999), or those that we measured for our oocytes after incubation in ND96 during expression of AtPIP2;1. For all experiments, the measured reversal potentials at 10mM external NaCl were similar to predicted Nernst potentials for Na^+, while at high NaCl concentrations the reversal potentials were sometimes closer to the Cl Nernst potential. The Nernst potential for K^+ was 100mV, using published values for internal K^+ concentration, and 86mV for our measured internal K^+ concentrations for all solutions used in Fig. 6.

Exploring the selectivity of the AtPIP2;1-induced currents further, we measured the concentration of K^+, Na^+ and Cl in oocytes that were incubated in ND96 for 3days after either injection with water, un-injected or injected with AtPIP2;1 cRNA (10ng). The internal Na^+ concentration was significantly elevated in AtPIP2;1-injected oocytes compared to both un-injected and water-injected oocytes (Fig. 7a). There was a reduction in K^+ concentration in AtPIP2;1 injected oocytes when compared with un-injected oocytes but not compared to water injected oocytes (Fig. 7b). There were no

significant differences observed in Cl concentrations (Fig. 7c). The Na^+/K^+ ratio was significantly lower for AtPIP2;1 injected oocytes relative to controls because of both the increase in Na^+ and decrease in K^+ concentrations (Fig. 7d). It should be noted that the volume of oocytes used to calculate these concentrations was on average 1.21$mm^{3,}$ and the mean volume did not differ between water injected and AtPIP2;1 injected oocytes (Supporting Information Fig. S5).

Given that AtPIP2;1 appeared to induce an increase in Na^+ permeability, we examined the net fluxes of Na^+ after a sudden reduction in external NaCl concentration using the microelectrode ion flux estimation (MIFE) technique. This technique works best at low external concentrations of the measured ions, so measurements of Na^+ efflux were performed after reducing the Na^+ concentration from 96мм to 5мм while maintaining a constant osmolality. Initial net Na^+ efflux after reducing the NaCl concentration was significantly larger for AtPIP2;1 expressing oocytes compared to controls (two-way repeated measures ANOVA, $P<0.05$) (Fig. 8a and Supporting Information Fig. S6). There was no significant difference between PIP1;2+PIP2;1 and controls (Fig. 8b), or PIP1;2 and controls ($P>0.05$) (Fig. 8b) consistent with the TEVC results indicating that co-expression of PIP1;2 with PIP2;1 abolishes the ionic conductance (Fig. 2).

AtPIP2;1 was permeable to Na^+ when expressed in Saccharomyces cerevisiae

Saccharomyces cerevisiae was used as an alternative heterologous system to explore whether expression of AtPIP2;1 caused increased accumulation of Na^+ as compared with yeast containing empty vectors. Yeast expressing AtPIP2;1 accumulated more Na^+ than yeast containing empty vectors when incubated for 24h

in growth media containing 0.1м or 0.5м NaCl (Fig. 9a). At low external Na^+ concentrations, yeast K^+ concentration tended to be lower than empty vector controls (Fig. 9b), consistent with the Xenopus oocyte results; however, at 0.5м external NaCl the K^+ concentrations were significantly elevated in the PIP2;1 expressing cells.

AtPIP2;1 ionic conductance was inhibited by divalent cations and protons

As noted above, the AtPIP2;1 conductances we observed were relatively small under the solution conditions initially used and compared to other transporters expressed in Xenopus oocytes, such as High-affinity Potassium (K^+) Transporters (HKTs) (Munns et al. 2012; Byrt et al. 2014). It has previously been shown that AtPIP2;1 water permeation is strongly inhibited by Ca^{2+}, other divalent metals including Cd^{2+} and protons (Verdoucq et al. 2008), and that non-selective cation channels in roots have been found to be inhibited by high Ca^{2+} and low pH (Demidchik & Tester 2002). With this information in mind, we tested the possibility that AtPIP2;1-induced conductances may be inhibited by the standard Ca^{2+} concentration (1.8мм; free Ca^{2+} =0.6мм) in ND96 saline, as used in the experiments described above. We measured ionic conductances of water injected controls and AtPIP2;1 injected oocytes in Ca^{2+} and Cd^{2+} free conditions, and in conditions with various concentrations of Ca^{2+} or 1мм Cd^{2+} in a modified ND96 solution (96мм NaCl, 2мм KCl, 5мм HEPES (4-(2-hydroxyethyl)-1-piperazineethanesulfonic acid), pH7.6 with various EGTA buffered Ca^{2+} or Cd^{2+} concentrations as indicated). Ca^{2+} and Cd^{2+} inhibited AtPIP2;1 ionic conductance (Fig. 10 and Supporting Information Figs S7 and S8). A small reduction in conductance is associated with changing external solutions (Fig. 10a). A significant reduction in conductance was observed with the addition of just 50 µм free Ca^{2+} (Fig. 10b). Further

increase in free Ca^{2+} to 0.4mM gave more substantial inhibition (Fig. 10c). We observed that the inward current was more inhibited by Ca^{2+} than the outward current (Supporting Information Fig. S9). External Cd^{2+} at 1mM inhibited the conductance similarly to high external free Ca^{2+} concentration (Fig. 10d). Examples of the current versus time traces are shown in the Supporting Information Fig. S7. We consistently observed higher conductances (slope of the current versus voltage curve through the reversal potential) for AtPIP2;1 injected oocytes when bathed in the lower Ca^{2+} concentrations. At close to zero Ca^{2+} concentration, the mean conductance was 33.3+/2.1μS (SEM) while water injected controls under these conditions had conductances of 3.96+/ 0.46μS SEM. Conductances of individual oocytes in the initial 'zero' Ca^{2+} concentration and then when the bath saline was perfused with the higher concentration of Ca^{2+} or Cd^{2+} are included in the Supporting Information Fig. S8. These experiments were used to construct a dose–response curve for the AtPIP2;1 induced ionic conductance expressed as values relative to the initial conductance in the near zero external Ca^{2+} concentration (Fig. 11a). Complex responses were obtained and were best fitted by a biphasic dose–response curve where about 50% of the conductance was inhibited by very low external Ca^{2+} (IC_{50} =5.7 μM free Ca^{2+}), and the remainder inhibited by a higher concentration (IC_{50} =0.32mM free Ca^{2+}). It should be noted that inhibition was not complete at higher external Ca^{2+} because even at 0.6mM free external Ca^{2+} (in ND96), there was still a conductance that was significantly higher than that of the water injected controls as was also evidenced by the experiments reported in Figs 2, 3 and 5. We also investigated the effect of external pH on the PIP2;1 induced current relative to control water-injected oocytes. The conductance of PIP2;1 expressing oocytes relative

to that of the water injected controls in the same solution was inhibited by low pH (Fig. 11b). The fitted dose–response curve shown gives an IC_{50} of pH6.8.

Discussion

The Arabidopsis plasma membrane aquaporin, PIP2;1, conducted both water and ions when expressed in X. *laevis* oocytes (Figs 2, 3, 5 & 10). There was a close correlation between the water permeability induced by PIP2;1 and the ionic conductance when variable amounts of cRNA were injected (Fig. 3). This ionic conductance was not associated with higher water permeability in of itself because it was specifically associated with the expression of AtPIP2;1, that is, in similar conditions AtPIP2;2, a protein 93.4% identical to AtPIP2;1, also conducted water but did not induce an ionic conductance. A hypo-osmotic gradient induced by reducing the osmolality of the bathing medium did not alter the ionic currents in PIP2;1 injected oocytes or water injected controls. This result indicates that the ionic currents induced by PIP2;1 expression were not as a consequence of a higher water permeability or a swelling response activating native oocyte channels. Furthermore, an AtPIP2;1 mutant with a single amino acid substitution in the pore (G103W) did not induce an ionic current (Figs 4 & 5) but was expressed in the oocyte membrane based on the positive interaction with AtPIP1;2. This indicates that the ionic conductance observed for AtPIP2;1 is unlikely to be an artefact of aquaporin associated expression or swelling in X.*laevis* oocytes and that the AtPIP2;1 protein is unlikely to be interacting with a native oocyte ion transporter to induce the conductance based on the AtPIP2;1 G103W results.

Co-expression of AtPIP2;1 with AtPIP1;2 increased water permeability relative to AtPIP2;1 expression alone, yet abolished ionic conductance and higher Na^+ efflux

when associated with AtPIP2;1 (Figs 1, 2 & 8). This provides further evidence that the ionic conductance and Na^+ flux associated with AtPIP2;1 were not an artefact. Interestingly CO_2 permeability induced by NtAQP1 (a PIP1) also seems to be abolished by interaction with NtPIP2;1, and this has been used as an argument for the homotetrameric structure being critical for CO_2 permeation (Otto et al. 2010). AtPIP2;1 is abundant in all Arabidopsis tissues and was reported to be present in the homomeric form in roots (Prak et al. 2008; Li et al. 2015), but we lack information about the relative proportions of AtPIP2;1 in homo- and heteromeric forms, and involvement of the subunits in complexes with other proteins such as AtPIP1;2 in different plant tissues and in varying environmental conditions (Yaneff et al. 2014; Yaneff et al. 2015). Xenopus *laevis* oocytes expressing AtPIP2;1 consistently displayed greater ionic conductance than controls in the presence of NaCl. In response to an increase in external NaCl we observed, a positive shift in reversal potential compatible with Na^+ transport through AtPIP2;1 channels (Figs 5b & 6). There was no evidence of a negative shift in reversal potential associated with increased external Cl, but increased conductance of Na^+ in the presence of Cl rather than MES indicates that conductance by AtPIP2;1 might require the presence of Cl. We also observed that X.*laevis* oocytes and S. cerevisiae expressing AtPIP2;1 accumulated more Na^+ than control cells in the presence of relatively high external NaCl (Figs 7 & 9). However, the reversal potentials measured in voltage clamp recordings indicated the current is most likely to be a non-selective cation conductance rather than a strictly Na^+ selective conductance. Our data showed that both K^+ and Na^+ concentrations were altered in oocytes and yeast expressing AtPIP2;1. Further research is needed to examine whether AtPIP2;1

conducts other physiologically important monovalent cations such as K^+, NH^+_4 or anions such as NO_3 or H_2CO_3 . Of central importance will be determining whether AtPIP2;1 conducts ions and the nature of the ion selectivity in planta. There is a precedent for dual water and ion conducting aquaporins functioning as non-selective monovalent cation channels. The human AQP1 is a water channel that functions as a non-selective monovalent cation channel when activated by secondary messengers (Anthony et al. 2000; Yool & Campbell 2012) and AQP6 has been shown to be a NO_3 selective channel (Ikeda et al. 2002). We know from previous studies that AtPIP2;1 water permeability is gated by divalent cations such as Ca^{2+} and Cd^{2+} (Verdoucq et al. 2008), and here we demonstrate that AtPIP2;1 ionic conductance is also inhibited by Ca^{2+} and Cd^{2+} (Figs 10 & 11). These observations are reminiscent of the Ca^{2+} block observed for the Drosophila dual ion and water conducting aquaporin Big Brain (BIB) (Yanochko & Yool 2002, 2004). The signalling role for Ca^{2+} in regulating BIB conductance is likely to be physiologically important in neuronal cell fate determination (Yanochko & Yool 2004). In plants, where changes in free Ca^{2+} have important signalling roles particularly in response to stress (Sanders et al. 2002; Choi et al. 2014), the inhibition of AtPIP2;1 ionic conductance by Ca^{2+} may be physiologically important.

The biphasic dose–response curve that we observed for external Ca^{2+} inhibition of the ionic conductance in X.*laevis* oocytes is reminiscent of the biphasic curve observed for water permeation through aquaporins in Beta vulgaris where a high affinity (IC_{50} =5nM) and a lower affinity component (IC_{50} =200μM) of Ca^{2+} inhibition on the cytoplasmic face of the membrane was observed (Alleva et al. 2006). A Cd^{2+}

binding site (presumed to bind Ca^{2+} in vivo) of SoPIP2;1 is located on the N-terminus that stabilizes the closed state of the channel by interaction with loop D and loop B (Törnroth-Horsefield et al. 2006). A second Cd^{2+} binding site (also presumed to mediate Ca^{2+} binding in vivo) has been identified on the C-terminus interacting with loop D (Frick et al. 2013). Both of these sites are located on the cytoplasmic side and thought to be important in gating the channel. Although it would be tempting to suggest that the biphasic dose–response we observed for ionic conductance here could be linked to these two binding sites, it is difficult to reconcile the sidedness of the extracellular effect in our experiments with the intracellular location of the sites identified in prior work. One possibility is that Ca^{2+} and Cd^{2+} may gain access via the ion conducting pore to interact with potentially intracellular sites. The prospect that ions could permeate AtPIP2;1 in planta brings to mind three key particularly interesting physiological implications. The first is a function for AtPIP2;1 in regulating coupled ion and water flow that could drive rapid shrinking responses as occurs during guard cell closing (Macrobbie 2006; Grondin et al. 2015) or hypoosmotic turgor regulation (Findlay 2001). The second is at the root epidermis where AtPIP2;1 is highly expressed and could be considered as a candidate for facilitating the Na^+ currents associated with non-selective cation channels observed in protoplasts from Arabidopsis root cells —which are blocked by H^+ (pK~6) and Ca^{2+} (IC_{50} ~0.1мм), voltage independent, and weakly selective for monovalent cations (Demidchik & Tester 2002). These characteristics are remarkably similar to the Ca^{2+} and pH sensitivity we have shown for AtPIP2;1 expressed in X. *laevis* oocytes and investigations of the pharmacological profile of the AtPIP2;1 ionic currents may further

test this link. The third implication is that AtPIP2;1 becomes a candidate for having a role in the water and ion co-transport into the xylem that sustains water flow in plants in the absence of water potential differences (Wegner 2014; Fricke 2015; Wegner 2015).

Phosphorylation regulates water permeability through AtPIP2;1 (Pradoet al. 2013; Grondinet al. 2015)and protein localization (Prak et al. 2008). This indicates that we need to explore relationships between the AtPIP2;1 phosphorylation state and the ionic conductance via AtPIP2;1. In a previous study, variation in Na^+ sensitivity of yeast expressing CsPIP2;1 was associated with phosphorylation at Ser273 (Jang et al. 2014), and kinase activity regulated HsAQP1 ion channel activity (Zhang et al. 2007). The phosphorylation of tyrosine Y253 in the carboxyl terminal domain of AQP1 is described as a master switch for regulating the responsiveness of AQP1 ion channels to cyclic nucleotide activators (Campbell et al. 2012; Yool & Campbell 2012). Testing of whether similar secondary messengers influence dual ion and water aquaporin function in plants and animals may be warranted, as links have been reported between (1) cyclic nucleotide levels in roots and phosphorylation of root proteins including aquaporins (Maurel et al. 1995; Isner et al. 2012), and Na^+ uptake (Maathuis & Sanders 2001); and (2) between cyclic nucleotide levels and Ca^{2+} and abscisic signalling (Sanders et al. 2002; Dubovskaya et al. 2011).

We have demonstrated that AtPIP2;1 expression induces an ionic conductance in X.*laevis* oocytes that can be carried at least in part by Na^+ and that this can explain the changes in Na^+ concentration in both oocytes and yeast expression systems. The AtPIP2;1-induced ionic conductance is inhibited by Ca^{2+}, Cd^{2+} and protons. This finding

necessitates further research to establish whether AtPIP2;1 is part of a subset of plant aquaporins with dual ion and water conducting roles in plants, which may function to couple ion and water flow across key membranes.

ACKNOWLEDGMENTS

We thank Wendy Sullivan for expert technical assistance and preparation of oocytes. Funding for this research was supported by the Australian Research Council (ARC) in the form of a DECRA for CB (ARC DE150100837). The ARC Centre of Excellence supported the salaries of J.B., S.H., J.Q. and S.R. through the ARC Centre of Excellence in Plant Energy Biology (CE140100008). The ARC supported A.Y. through ARC DP160104641 and M.G. through ARC FT130100709.

REFERENCES

Alexandersson, E., Fraysse, L., Sjövall-Larsen, S., Gustavsson, S., Fellert, M., Karlsson, M., Johanson, U. and Kjellbom, P., (2005) Whole gene family expression and drought stress regulation of aquaporins. Plant molecular biology, 59, 469–484.

Alleva K., Niemietz C.M., Sutka M., Maurel C., Parisi M., Tyerman S.D. & Amodeo G. (2006) Plasma membrane of Beta vulgaris storage root shows high water channel activity regulated by cytoplasmic pH and a dual range of calcium concentrations. Journal of Experimental Botany 57, 609–621.

Anthony T.L., Brooks H.L., Boassa D., Leonov S., Yanochko G.M., Regan J.W. & YoolA.J. (2000)Clonedhuman aquaporin-1 is a cyclic GMP-gated ion channel. Molecular Pharmacology 57, 576–588.

Bose J., Xie Y., Shen W. & Shabala S. (2013) Haem oxygenase modifies salinity tolerance in Arabidopsis by controlling K^+ retention via regulation of the plasma membrane H^+-ATPase and by altering SOS1 transcript levels in roots. Journal of Experimental Botany 64, 471–481.

BoursiacY.,ChenS., Luu D.T.,Sorieul M., VanDen Dries N.& MaurelC.(2005) Early effects of salinity on water transport in Arabidopsis roots. Molecular and cellular features of aquaporin expression. Plant Physiology 139, 790–805.

Byrt C.S., Xu B., Krishnan M., Lightfoot D.J., Athman A., Jacobs A.K., Tester M. (2014) The Na^+ transporter, TaHKT1; 5-D, limits shoot Na^+ accumulation in bread wheat. The Plant Journal 80, 516–526.

Campbell E.M., Birdsell D.N. & Yool A.J. (2012) The activity of human aquaporin 1 as a cGMP-gated cation channel is regulated by tyrosine phosphorylation in the carboxyl-terminal domain. Molecular Pharmacology 81, 97–105.

Choi W.-G., Toyota M., Kim S.-H., Hilleary R. & Gilroy S. (2014) Salt stressinduced Ca2+ waves are associated with rapid, long-distance root-to-shoot signaling in plants. Proceedings of the National Academy of Sciences 111, 6497–6502.

Demidchik V. & Tester M. (2002) Sodium fluxes through nonselective cation channels in the plasma membrane of protoplasts from Arabidopsis roots. Plant Physiology 128, 379–387.

Dubovskaya L.V., Bakakina Y.S., Kolesneva E.V., Sodel D.L., Mcainsh M.R., Hetherington A.M. & Volotovski I.D. (2011) cGMP-dependent ABAinduced stomatal closure in the ABA-insensitive Arabidopsis mutant abi1-1. New Phytologist 191, 57–69.

Dynowski M., Mayer M., Moran O. & Ludewig U. (2008) Molecular determinants of ammonia and urea conductance in plant aquaporin homologs. FEBS Letters 582, 2458–2462.

Findlay G.P. (2001) Membranes and the electrophysiology of turgor regulation. Functional Plant Biology 28, 619–636.

Frick A., JarvaM., EkvallM., UzdavinysP.,Nyblom M.& Tornroth-Horsefield S. (2013) Mercury increases water permeability of a plant aquaporin through a non-cysteine-related mechanism. Biochemical Journal 454, 491–499.

Fricke W. (2015) The significance of water co-transport for sustaining transpirational water flow in plants: a quantitative approach. Journal of Experimental Botany 66, 731–739.

Gerbeau P., Amodeo G., Henzler T., Santoni V., Ripoche P. & Maurel C. (2002) The water permeability of Arabidopsis plasma membrane is regulated by divalent cations and pH. The Plant Journal 30, 71–81.

Grondin A., Rodrigues O., Verdoucq L., Merlot S., Leonhardt N. & Maurel C. (2015) Aquaporins contribute to ABA-triggered stomatal closure through OST1-mediated phosphorylation. Plant Cell 27, 1945–1954.

Holm L.M., Jahn T.P., Moller A.L.B., Schjoerring J.K., Ferri D., Klaerke D.A. & Zeuthen T. (2005) NH3 and NH4+ permeability in aquaporin-expressing *Xenopus* oocytes. Pflugers Archiv-European Journal of Physiology 450, 415–428.

Ikeda M., Beitz E., Kozono D., Guggino W.B., Agre P. & Yasui M. (2002) Characterization of aquaporin-6 as a nitrate channel in mammalian cells requirement of pore-lining residue threonine 63. Journal of Biological Chemistry 277, 39873–39879.

Isner J.C., Nühse T. & Maathuis F.J. (2012) The cyclic nucleotide cGMP is involved in plant hormone signalling and alters phosphorylation of Arabidopsis thaliana root proteins. Journal of Experimental Botany 63, 3199–3205.

Jang H.-Y., Rhee J., Carlson J.E. & Ahn S.-J. (2014) The Camelina aquaporin CsPIP2; 1 is regulated by phosphorylation at Ser273, but not at Ser277, of the C-terminus and is involved in salt- and drought-stress responses. Journal of Plant Physiology 171, 1401–1412.

Jayakannan M., Babourina O. & Rengel Z. (2011) Improved measurements of Na+ fluxes in plants using calixarene-based microelectrodes. Journal of Plant Physiology 168, 1045–1051.

Kamiya T., Tanaka M., Mitani N., Ma J.F., Maeshima M. & Fujiwara T. (2009) NIP1; 1, an aquaporin homolog, determines the arsenite sensitivity of Arabidopsis thaliana. Journal of Biological Chemistry 284, 2114–2120.

Li G., Boudsocq M., Hem S., Vialaret J., Rossignol M., Maurel C. & Santoni V. (2015) The calcium-dependent protein kinase CPK7 acts on root hydraulic conductivity. Plant, Cell & Environment 38, 1312–1320.

Loqué D., Ludewig U., Yuan L. & Von Wirén N. (2005) Tonoplast intrinsic proteins AtTIP2; 1 and AtTIP2; 3 facilitate NH_3 transport into the vacuole. Plant Physiology 137, 671–680.

Ma J.F., Tamai K., Yamaji N., Mitani N., Konishi S., Katsuhara M., … Yano M. (2006) A silicon transporter in rice. Nature 440, 688–691.

Maathuis F.J. & Sanders D. (2001) Sodium uptake in Arabidopsis roots is regulated by cyclic nucleotides. Plant Physiology 127, 1617–1625. Macrobbie E.A. (2006) Control of volume and turgor in stomatal guard cells. The Journal of Membrane Biology 210, 131–142.

Maurel C., Kado R.T., Guern J. & Chrispeels M.J. (1995) Phosphorylation regulates the water channel activity of the seed-specific aquaporin alpha-tip.

Embo Journal 14, 3028–3035.

Munns R., James R.A., Xu B., Athman A., Conn S.J., Jordans C., Tester M. (2012) Wheat grain yield on saline soils is improved by an ancestral Na+ transporter gene. Nature Biotechnology 30, 360–364.

Nelson B.K., Cai X. & Nebenführ A. (2007) A multicolored set of in vivo organelle markers for co-localization studies in Arabidopsis and other plants. The Plant Journal 51, 1126–1136.

Newman I. (2001) Ion transport in roots: measurement of fluxes using ion selective microelectrodes to characterize transporter function. Plant, Cell & Environment 24, 1–14.

Otto B., Uehlein N., Sdorra S., Fischer M., Ayaz M., Belastegui-Macadam X., Kaldenhoff R. (2010) Aquaporin tetramer composition modifies the function of tobacco aquaporins. Journal of Biological Chemistry 285, 31253–31260.

Prado K., Boursiac Y., Tournaire-Roux C., Monneuse J.M., Postaire O., Da Ines O., Maurel C. (2013) Regulation of *arabidopsis* leaf hydraulics involves light-dependent phosphorylation of aquaporins in veins. Plant Cell 25, 1029–1039.

Prak S., Hem S., Boudet J., Viennois G., Sommerer N., Rossignol M., Maurel C. & Santoni V. (2008) Multiple phosphorylations in the C-terminal tail of plant plasma membrane aquaporins. Molecular & Cellular Proteomics 7, 1019–1030.

Preuss C.P., Huang C.Y. & Tyerman S.D. (2011) Proton-coupled high-affinity phosphate transport revealed from heterologous characterization in *Xenopus* of barley-root plasma membrane transporter, HvPHT1; 1. Plant, Cell & Environment 34, 681–689.

Rivers R.L., Dean R.M., Chandy G., Hall J.E., Roberts D.M. & Zeidel M.L. (1997) Functional analysis of nodulin 26, an aquaporin in soybean root nodule symbiosomes. Journal of Biological Chemistry 272, 16256–16261.

Sanders D., Pelloux J., Brownlee C. & Harper J.F. (2002) Calcium at the crossroads of signaling. The Plant Cell 14, S401–S417.

Shabala S., Shabala L., Bose J., Cuin T. & Newman I. (2013) Ion flux measurements using the MIFE technique. Plant Mineral Nutrients: Methods and Protocols 953, 171–183.

Shelden M.C., Howitt S.M., Kaiser B.N. & Tyerman S.D. (2009) Identification and functional characterisation of aquaporins in the grapevine, Vitis vinifera. Functional Plant Biology 36, 1065–1078.

Sorieul M., Santoni V., Maurel C. & Luu D.T. (2011) Mechanisms and effects of retention of over-expressed aquaporin AtPIP2; 1 inthe endoplasmic reticulum. Traffic 12, 473–482.

Sutka M., LiG.W.,BoudetJ.,Boursiac Y.,DoumasP. & Maurel C.(2011)Natural variation of root hydraulics in *arabidopsis* grown in normal and salt-stressed conditions. Plant Physiology 155, 1264–1276.

Takano J., Wada M., Ludewig U., Schaaf G., Von Wirén N. & Fujiwara T. (2006) The Arabidopsis major intrinsic protein NIP5; 1 is essential for efficient boron uptake and plant development under boron limitation. The Plant Cell 18, 1498–1509.

Törnroth-Horsefield S., Wang Y., Hedfalk K., Johanson U., Karlsson M., Tajkhorshid E., Neutze R. & Kjellbom P. (2006) Structural mechanism of plant aquaporin gating. Nature 439, 688–694.

Tournaire-Roux C., Sutka M., Javot H., Gout E., Gerbeau P., Luu D.-T., Bligny R. & Maurel C. (2003) Cytosolic pH regulates root water transport during anoxic stress through gating of aquaporins. Nature 425, 393–397.

Uehlein N., Lovisolo C., Siefritz F. & Kaldenhoff R. (2003) The tobacco aquaporin NtAQP1 is a membrane CO_2 pore with physiological functions. Nature 425, 734–737.

Verdoucq L., GrondinA.& Maurel C.(2008) Structure–function analysis of plant aquaporin AtPIP2; 1 gating by divalent cations and protons. Biochemical Journal 415, 409–416.

Verdoucq L., Rodrigues O., Martiniere A., Luu D.T. & Maurel C. (2014) Plant aquaporins on the move: reversible phosphorylation, lateral motion and cycling. Current Opinion in Plant Biology 22, 101–107.

Wang, C., Hu, H., Qin, X., Zeise, B., Xu, D., Rappel, W.-J., Boron, W.F., and Schroeder, J.I. (2016). Reconstitution of CO_2 regulation of SLAC1 anion channel and function of CO_2-permeable PIP2; 1 aquaporin as carbonic anhydrase 4 interactor. The Plant Cell, TPC2015-00637-RA.

Weaver C.D., Shomer N.H., Louis C.F. & Roberts D.M. (1994) *Nodulin 26*, a nodule-specific symbiosome membrane protein from soybean, is an ion channel. Journal of Biological Chemistry 269, 17858–17862.

Weber W.-M. (1999) Ion currents of *Xenopus laevis* oocytes: state of the art. Biochimica et Biophysica Acta (BBA)-Biomembranes 1421, 213–233.

Wegner L.H. (2014) Root pressure and beyond: energetically uphill water transport into xylem vessels? Journal of Experimental Botany 65, 381–393.

Wegner L.H. (2015) A thermodynamic analysis of the feasibility of water secretion intoxylem vessels against a water potential gradient. Functional Plant Biology 42, 828–835.

Yaneff A., Sigaut L., Marquez M., Alleva K., Pietrasanta L.I. & Amodeo G. (2014) Heteromerization of PIP aquaporins affects their intrinsic permeability. Proceedings of the National Academy of Sciences of the United States of America 111, 231–236.

Yaneff A., Vitali V. & Amodeo G. (2015) PIP1 aquaporins: intrinsic water channels or PIP2 aquaporin modulators? FEBS Letters 589, 3508–3515.

Yanochko G.M. & Yool A.J. (2002) Regulated cationic channel function in *Xenopus* oocytes expressing *Drosophila big brain*. The Journal of Neuroscience 22, 2530–2540.

Yanochko G.M. & Yool A.J. (2004) Block by extracellular divalent cations of *Drosophila big brain* channels expressed in *Xenopus* oocytes. Biophysical Journal 86, 1470–1478.

Yool A.J. & Campbell E.M. (2012) Structure, function and translational relevance of aquaporin dual water and ion channels. Molecular Aspects of Medicine 33, 553–561.

Zhang W., Zitron E., Hömme M., Kihm L., Morath C., Scherer D., … Zeier M. (2007) Aquaporin-1 channel function is positively regulated by protein kinase C. Journal of Biological Chemistry 282, 20933–20940.

Received 6 July 2016; received in revised form 8 September 2016; accepted for publication 10 September 2016

SUPPORTING INFORMATION

Additional Supporting Information may be found in the online version of this article at the publisher's web-site:

Table S1. Primers used in the study

Figure S1. Fluorescence of the plasma membrane of Xenopus *laevis* oocytes injected with cRNA encoding AtPIP2;1mCherry or water.

Figure S2. Water permeability of Xenopus *laevis* induced by different Arabidopsis PIP1s and interactions with PIP2;1 and PIP2;6 compared to water injected controls.

Figure S3. Example current versus time traces of cRNA injected Xenopus *laevis* oocytes for: AtPIP2;1, AtPIP1;2 : AtPIP2;1 co-injected, AtPIP1;2, and water injected controls. Figure S4. Hyposomotic conditions did not alter ionic conductance in PIP2;1 expressing or water injected Xenopus *laevis* oocytes.

Figure S5. Oocyte volumes in ND96 of PIP2;1 expressing or water injected Xenopus *laevis* oocytes.

Figure S6. Sodium efflux measured after transition to low bath Na^+ concentration with the microelectrode ion flux estimation technique (MIFE) comparing PIP2;1 expressing and water injected Xenopus *laevis* oocytes.

Figure S7. Examples of current versus time traces of PIP2;1 expressing Xenopus *laevis* oocytes in different free Ca^{2+} concentrations in the bath.

Figure S8. Initial and final conductances of AtPIP2;1 expressing and water injected Xenopus *laevis* oocytes before and after addition of different free Ca^{2+} concentrations in the bath and in response to 1mM Cd^{2+}.

Figure S9. Rectification of currents for AtPIP2;1 expressing Xenopus *laevis* oocytes as a function of free Ca^{2+} concentration in the bath.

Figure Legends

Figure 1: PIP-induced swelling of Xenopus *laevis* oocytes is dependent on PIP-isoform and the amount of cRNA injected. Osmotic water permeabilities (P_{os}) from oocyte swelling experiments comparingAtPIP2;1, AtPIP2;2, AtPIP1;2, andco-expressed AtPIP1;2 and AtPIP2;1, compared with water injected controls. (a) AtPIP2;1 and AtPIP2;2 (11.5ng cRNA each). (b) AtPIP2;1 and AtPIP1;2, and co-expression with cRNA amounts indicated. Significant differences ($P < 0.05$) are indicated by different letters using one way ANOVAwith Holm–Sidak's multiple comparisons test. Individual data points and mean+/ SEM, n=5 to 20 oocytes from two frogs are shown.

Figure 2: AtPIP2;1 elicits ionic currents when heterologously expressed in Xenopus *laevis* oocytes. Steady-state current–voltage curves of X.*laevis* oocytes injected with (a) AtPIP1;2, (b) AtPIP2;2, (c) AtPIP2;1 and (d) AtPIP1;2 and AtPIP2;1 cRNA in ND96 (pH7.5). Currents are from oocytes injected with water or cRNA (6ng per oocyte) from the same batch. Conductances are indicated for the linear part of the curves across the reversal potential. Mean +/ SEM. (a) n =17 for controls, n= 13 for PIP1;2 (b) n= 5 for controls, n =5 for PIP2;2 (c) Same controls as (a), n=7 for PIP2;1 (d) n= 15 for controls, n=21 for PIP2;1 and n=20 for PIP2;1 co-expressed with PIP1;2. For AtPIP2;1 expressing oocytes, at 100 mV: I_m =795nA, SEM =65nA, n =28 oocytes combined from two frogs; controls at 100mV: I_m =355nA, SEM =33nA, n=32.

Figure 3: Water and ion transport of oocytes display similar dependence on the amount of AtPIP2;1 cRNA injected. (a) Ionic conductance (left y-axis, solid triangles) for Xenopus *laevis* oocytes expressingAtPIP2;1in ND96pH7.5comparedwithP_{os} (swelling in 1/5 ND96 pH 7.5) (right y-axis, open circles) as a function of cRNA injected (n =11–17 oocytes for swelling assays, n=6–15 oocytes for conductance in same batch of oocytes). The data were fitted with a Michaelis–Menten curve (R^2 =0.92 for conductance and R^2 =0.59 for P_{os}), and fitted parameters were conductance K_m =2.75ng, V_{max} =17.7μS; P_{os} K_m =1.71ng, V_{max} =0.019cms^1. (b) The linear relationship between ionic conductance and P_{os} taken from the data in (a) (linear regression+/ 95% confidence intervals, ^{R2} =0.97). Mean +/ SEM.

Figure 4: G103W mutation of AtPIP2;1 reduces water permeability. P_{os} comparing AtPIP1;2, AtPIP2;1 and AtPIP2;1 G103W from three separate experiments (frogs); 10ng of cRNAwas injected. (a) Comparing AtPIP2;1 with AtPIP2;1 G103Wand water injected controls. (b) Comparing AtPIP1;2, AtPIP2;1, AtPIP1;2:AtPIP2;1 co-injected, AtPIP1;2:AtPIP2;1 G103Wand water injected controls. (c) Comparing AtPIP1;2, AtPIP2;1, AtPIP2;1 G103W, AtPIP1;2: AtPIP21 G103Wand water injected controls. Significant differences (P< 0.05) are indicated by different letters using one-way ANOVAwith Holm–Sidak's multiple comparisons test. Individual data points and mean+/ SEM are shown.

Figure 5: AtPIP2;1 Na^+ conductance is Cl dependent and abolished by G103W substitution. Current–voltage curves (steady state) for (a) water injected controls

(n=4, mean conductance shown for all solutions at the left of the curve), (b) AtPIP2;1 (n= 18) and (c) AtPIP2;1 G103W (n =10, common conductance shown) in a range of Cl concentrations with constant Na^+ concentration, pH7.5. Conductances shown are for the linear part of curve through the reversal potential. Mean +/ SEM.

Figure 6: Reversal potentials from a series of two-electrode voltage clamp experiments where the NaCl concentration in the bathing solution was changed. Reversal potentials are plotted against the Na^+ concentration (log scale) because Cl concentration was slightly higher from other salts in the buffer. The reversal potentials were taken as the intersection with control current–voltage curves. Same symbols connected by dotted lines indicate the same oocytes (n =3–8 oocytes) from the same frog. Additionally shown are Nernst potentials for Na^+ (dashed lines, red shade) and Cl (solid lines, blue shade) based on literature values for internal oocyte concentrations (red lines) and those calculated from our measurements of internal concentration (blue lines). Error bars, where indicated, are 95% confidence intervals of the reversal potential based on linear regressions through the linear part of the current–voltage curves that cross the voltage axis (controls subtracted).

Figure 7: Expression of AtPIP2;1 alters the internal Na^+ concentration of Xenopus *laevis* oocytes. Internal oocyte ion concentrations measured on oocytes after incubation in 96mM Na^+ for three days for un-injected oocytes, water injected oocytes and AtPIP2;1 cRNA injected (10ng) oocytes. (a) Na^+ concentrations, (b) K^+ concentrations, (c) Cl concentrations, (d) Na^+/K^+ ratio. In each case, the error bars

indicate the range of the data, while the box indicates the SEM of the mean (horizontal internal bar) for n =21 (uninjected), n =17 (water injected), n =29 (cRNA injected). Significant differences were determined by one-way ANOVA; significant differences ($P < 0.05$) are indicated by different letters using one-way ANOVA with Holm–Sidak's multiple comparisons test. Individual data points and mean+/ SEM are shown.

Figure 8: Decreasing external NaCl concentration resultedin a larger Na^+ efflux from AtPIP2;1 expressing oocytes compared with controls. Larger Na^+ efflux was observed for AtPIP2;1 expressing oocytes relative to water injected oocytes (a), AtPIP2;1+AtPIP1;2 co-injected (b) and AtPIP1;2 injected oocytes (c). Na^+ efflux (indicated as a negative flux) as a function of time after transferring oocytes from ND96 (containing 96 mM NaCl) to a solution consisting of 5mM NaCl, 2mM KCl, 50μM $CaCl_2$, 5mM HEPES pH7.5 which was isotonic, with ND96 (mannitol, 231mosmol kg^1). In (a), (b) and (c), the water injected control oocytes are the same data and shown for comparison with gene-injected oocytes. The fluxes were obtained using the microelectrode ion flux estimation (MIFE) technique; electrodes were placed adjacent to the animal pole of the oocyte. Mean+/ SEM, n=7–8 oocytes.

Figure 9: Expression of AtPIP2.1 changes the Na^+/K^+ ratio of yeast cells. Na^+ (a) and K^+ (b) concentrations in yeast empty vector controls or AtPIP2;1 expressing cells at three external Na^+ concentrations. Individual data points and mean+/ SEM are shown. Significant differences between empty vector and PIP2;1 are indicated for each

external Na^+ concentration from two-way ANOVAwith Sidak's multiple comparison (*P < 0.05; **P < 0.01; ***P < 0.001) for three replicate batches of cells.

Figure10: AtPIP2.1 ion currents in Xenopus *laevis* oocytes are inhibited by divalent cations. Examples of current–voltage curves from single oocytes illustrating the effect of external Ca^{2+} and Cd^{2+} on AtPIP2;1 induced currents. In each case, the currents are relative (Relative I_m) to the initial current at 60mVand do not have the water injected control currents subtracted. Zero (effectively) Ca^{2+} and Cd^{2+} concentration is the initial current–voltage curve (square symbol) and the treatment current–voltage curves are after solution replacement with (a) 0μм external Ca^{2+}; (b) 50μм external Ca^{2+}; (c) 400μM external Ca^{2+}; (d) 1mм external Cd^{2+}.

Figure 11: External Ca^{2+} (a) and pH (b) dose–response relationships for the ionic conductance induced by AtPIP2;1 expressed in Xenopus *laevis* oocytes. (a) The data are expressed relative to the initial conductance from experiments such as those shown in Fig. 10 and Supporting Information Fig. S7. The mean relative conductance in the very low external Ca^{2+} concentration is less than 100%, but not significantly so, because sometimes when substituting with the same solution the conductance decreased slightly. The data have been fitted by a single-component dose–response to all the data from very low Ca^{2+} (dotted line) and to the data for higher Ca^{2+}(solid line, R =0.75, IC_{50} =0.321mм). Mean+/ SEM, n=3–6 oocytes for each point. (b) Ionic conductance for AtPIP2;1 expressing oocytes relative to that of controls in solutions

of 10mM NaMES at pH 5.5, 6.5, 7.5 and 8.5. pH adjusted with Tris-base/MES, free Ca^{2+} approximately 0.6mM; mean +/ SEM n= 6. Dose–response curve fitted to the data gives IC_{50} of pH6.8.

Figures

Figure 1

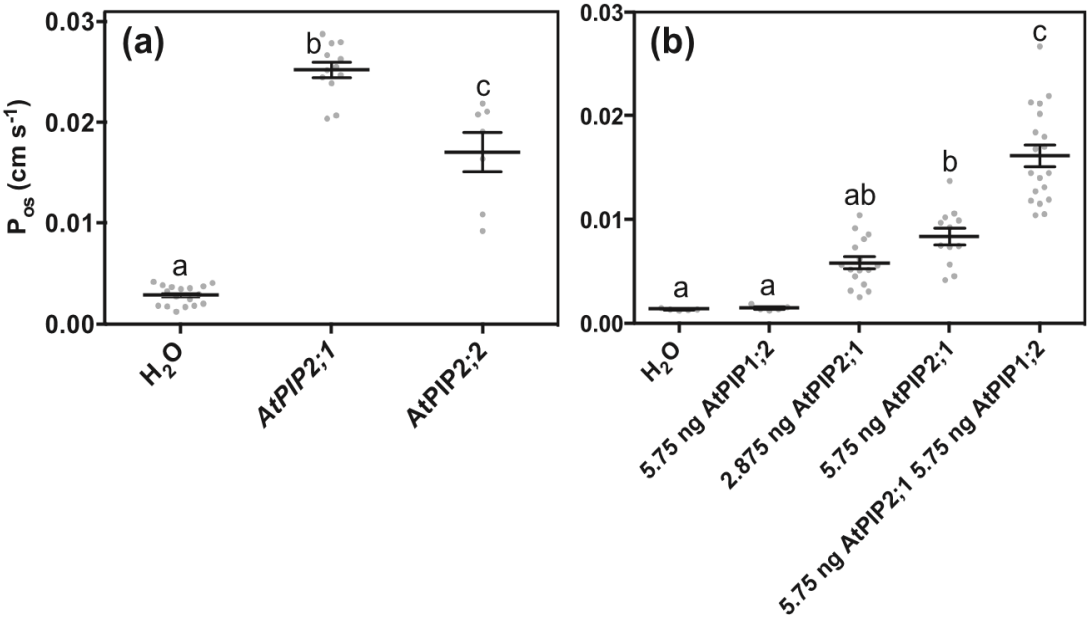

Figure 2

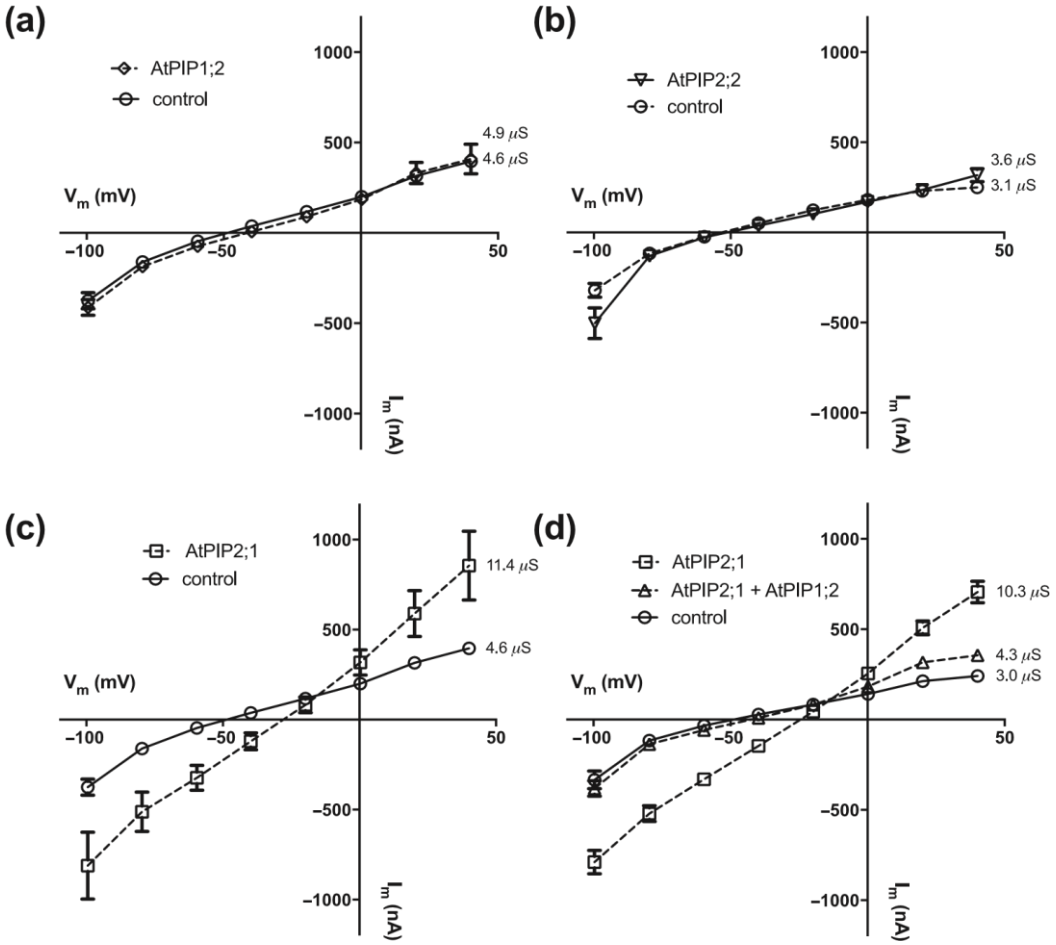
(a)
AtPIP1;2
control
4.9 μS
4.6 μS
(b)
AtPIP2;2
control
3.6 μS
3.1 μS
(c)
AtPIP2;1
control
11.4 μS
4.6 μS
(d)
AtPIP2;1
AtPIP2;1 + AtPIP1;2
control
10.3 μS
4.3 μS
3.0 μS
V_m (mV)
I_m (nA)
1000
500
−500
−1000
−100
−50
50

Figure 3

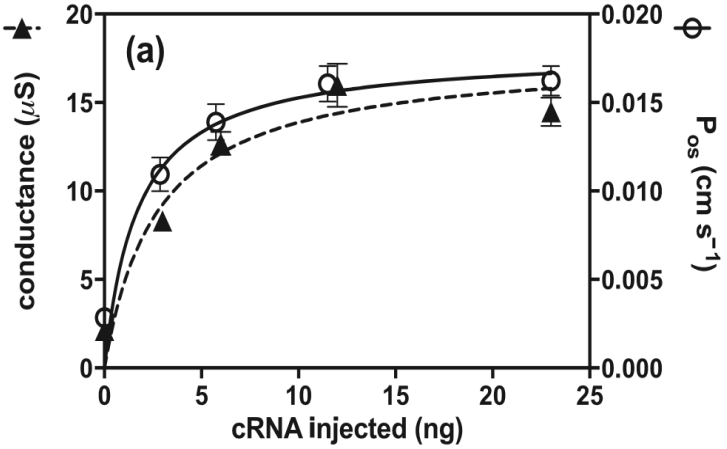
(a)
conductance (μS)
P os (cm s−1)
cRNA injected (ng)
0
5
10
15
20
25
0.000
0.005
0.010
0.015
0.020

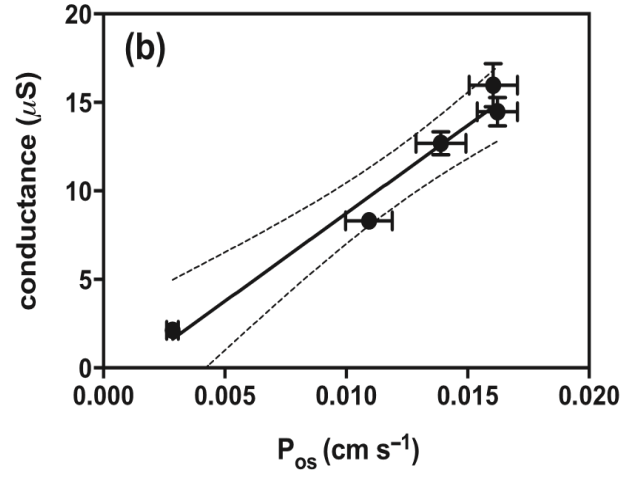
(b)
conductance (μS)
P os (cm s−1)
0
5
10
15
20
0.000
0.005
0.010
0.015
0.020

Figures 4

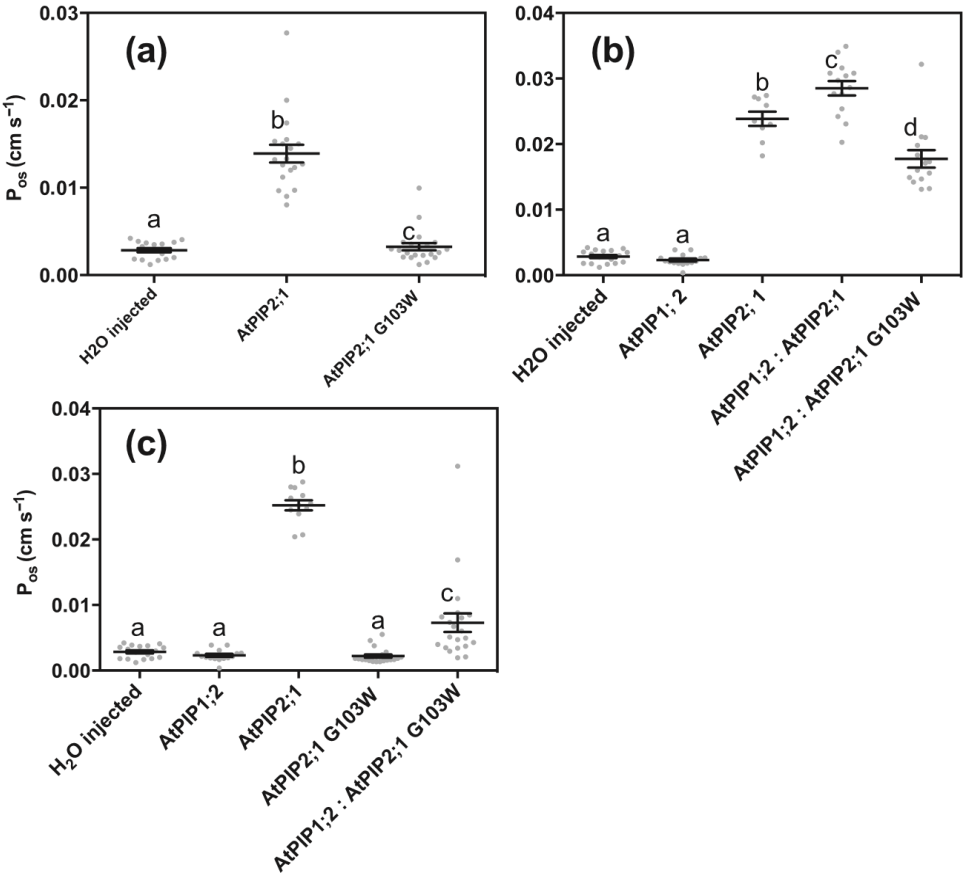
(a)
(b)
(c)
P_{os} (cm s^{-1})
H2O injected
AtPIP2;1
AtPIP2;1 G103W
AtPIP1;2
AtPIP2; 1
AtPIP1;2 : AtPIP2;1
AtPIP1;2 : AtPIP2;1 G103W
H_2O injected

Figure 5

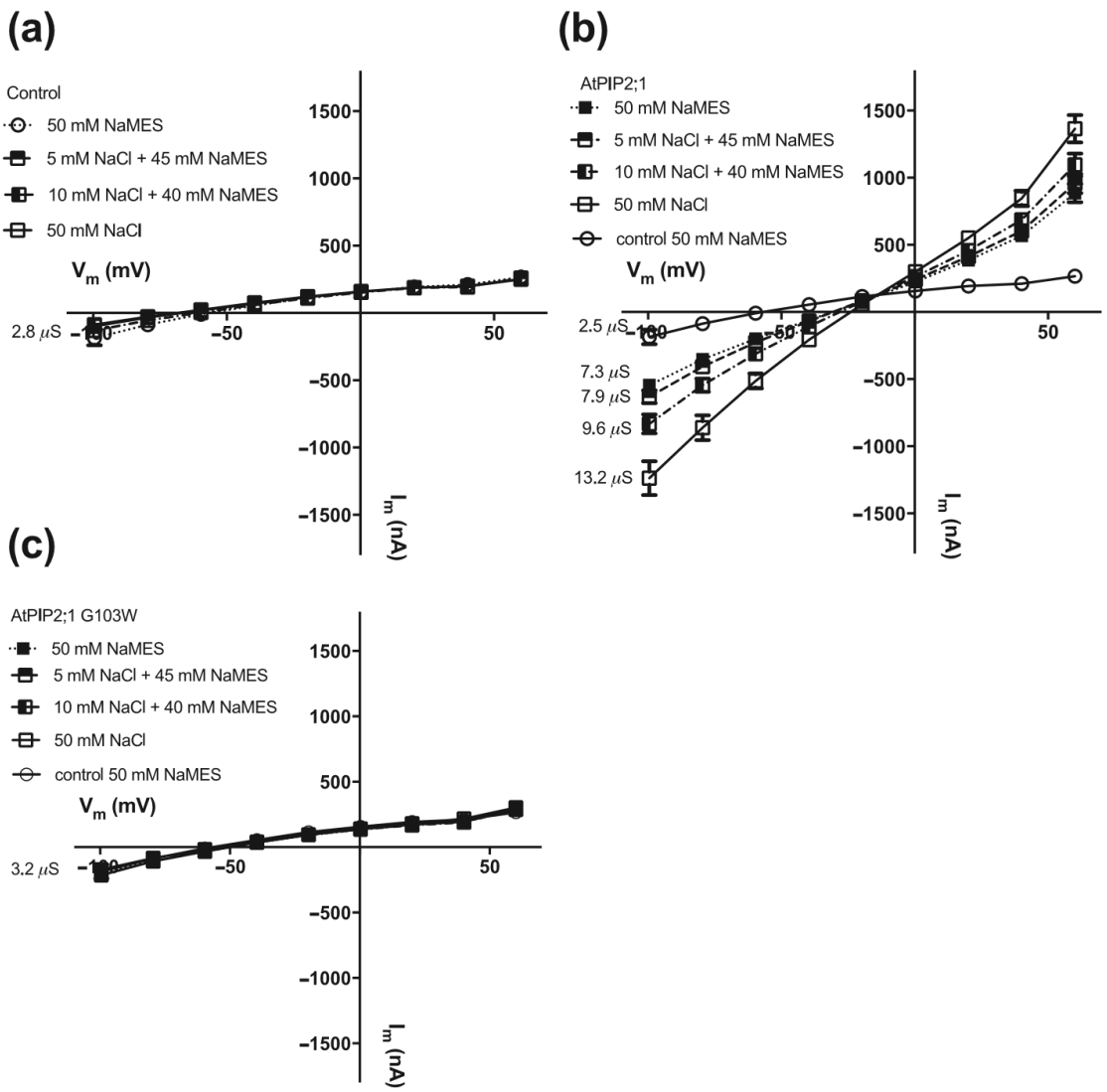
(a)
Control
50 mM NaMES
5 mM NaCl + 45 mM NaMES
10 mM NaCl + 40 mM NaMES
50 mM NaCl
V_m (mV)
2.8 μS
1500
1000
500
−500
−1000
−1500
−50
50
I_m (nA)
(b)
AtPIP2;1
50 mM NaMES
5 mM NaCl + 45 mM NaMES
10 mM NaCl + 40 mM NaMES
50 mM NaCl
control 50 mM NaMES
V_m (mV)
2.5 μS
7.3 μS
7.9 μS
9.6 μS
13.2 μS
1500
1000
500
−500
−1000
−1500
50
I_m (nA)
(c)
AtPIP2;1 G103W
50 mM NaMES
5 mM NaCl + 45 mM NaMES
10 mM NaCl + 40 mM NaMES
50 mM NaCl
control 50 mM NaMES
V_m (mV)
3.2 μS
1500
1000
500
−500
−1000
−1500
−50
50
I_m (nA)

Figure 6

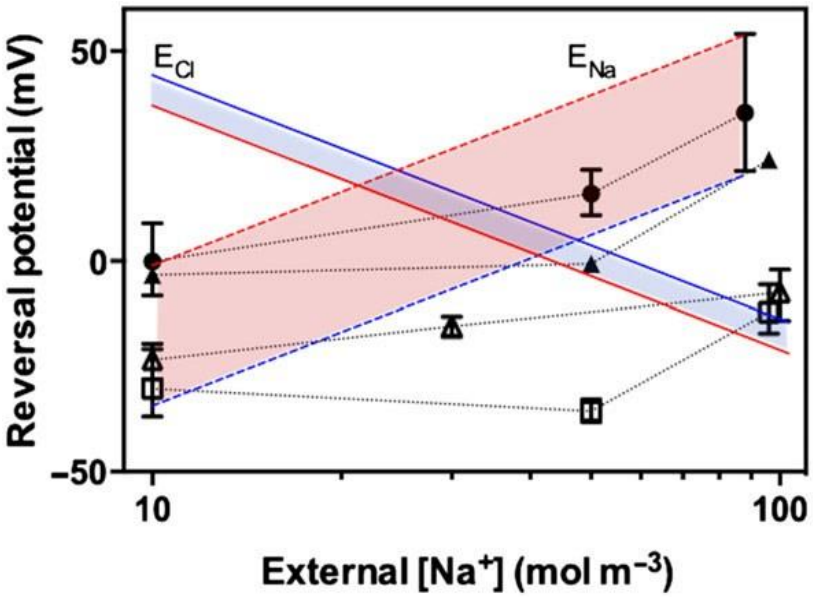
50
0
−50
10
100
Reversal potential (mV)
External [Na+] (mol m−3)
ECl
ENa

Figure 7

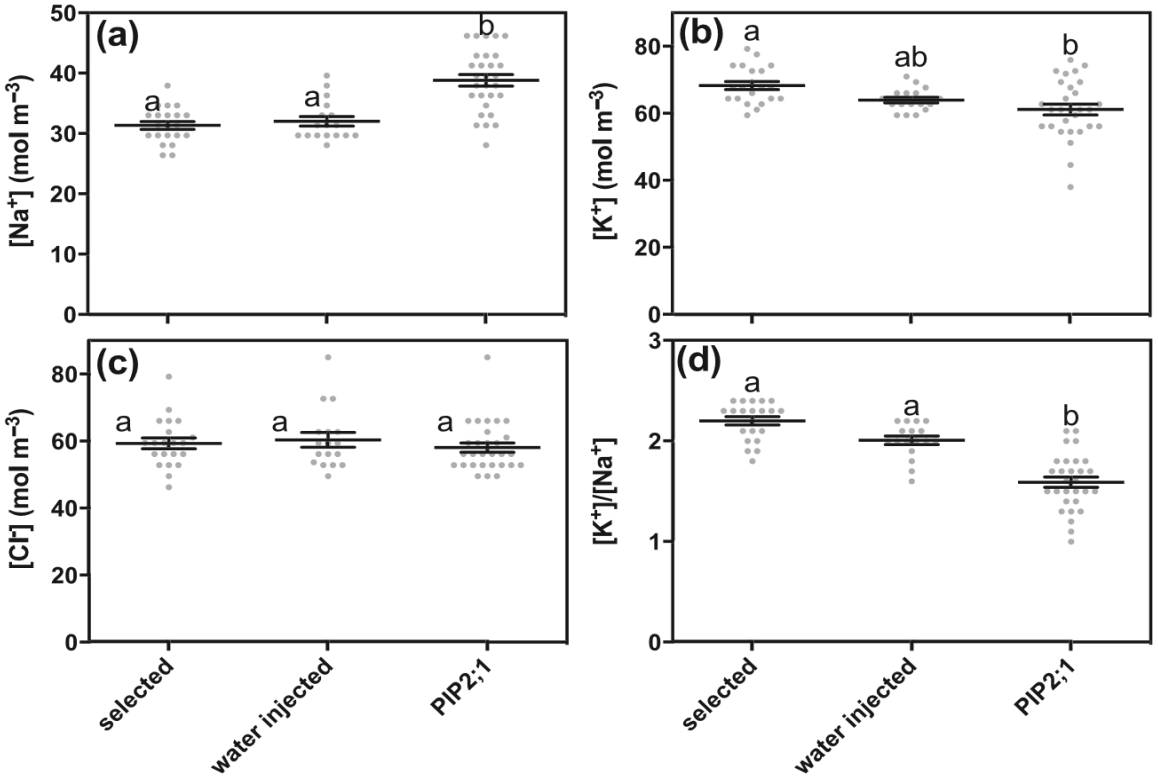
(a)
[Na+] (mol m−3)
50
40
30
20
10
0
a
a
b
(b)
[K+] (mol m−3)
80
60
40
20
0
a
ab
b
(c)
[Cl-] (mol m−3)
80
60
40
20
0
a
a
a
(d)
[K+]/[Na+]
3
2
1
0
a
a
b
selected
water injected
PIP2;1
selected
water injected
PIP2;1

Figure 8

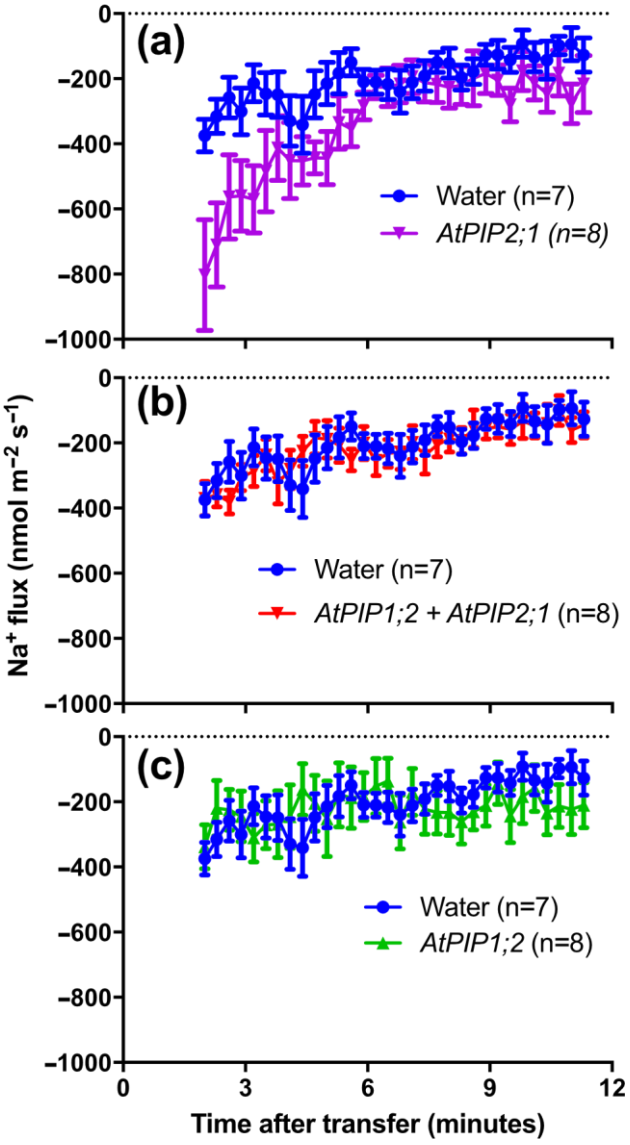
(a)
Water (n=7)
AtPIP2;1 (n=8)
(b)
Water (n=7)
AtPIP1;2 + AtPIP2;1 (n=8)
(c)
Water (n=7)
AtPIP1;2 (n=8)
Na+ flux (nmol m−2 s−1)
0
−200
−400
−600
−800
−1000
0
3
6
9
12
Time after transfer (minutes)

Figure 9

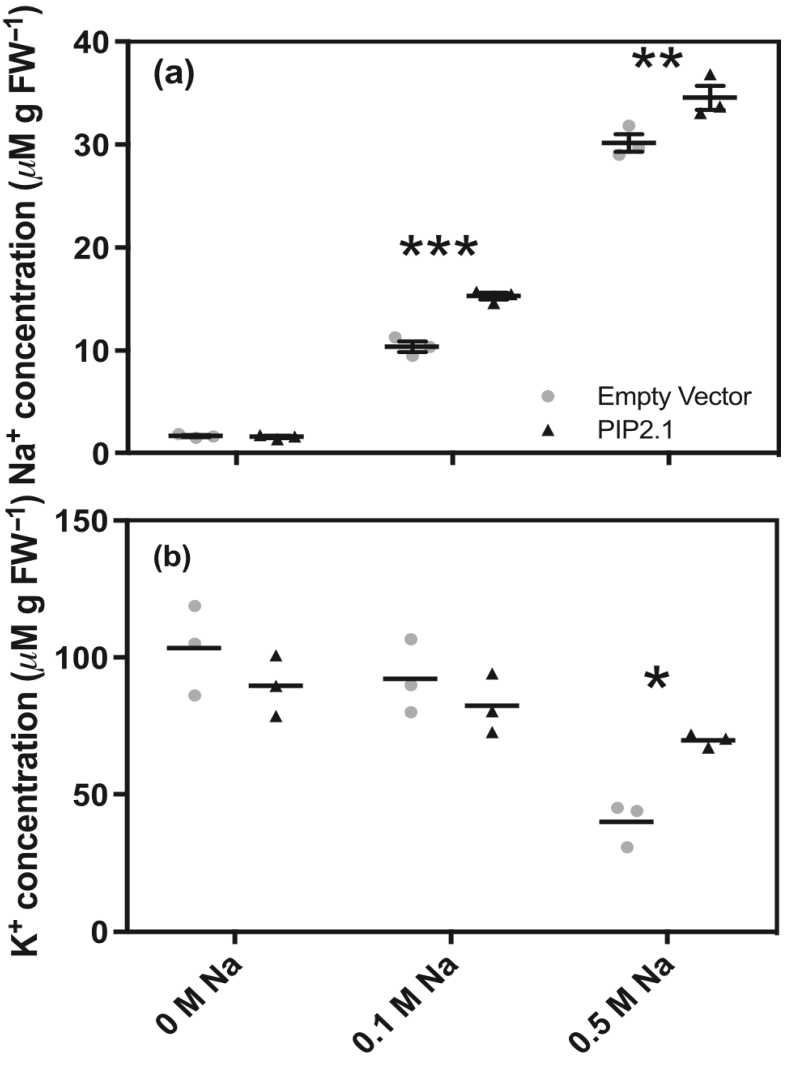
(a)
(b)
Empty Vector
PIP2.1
***
**
*
0 M Na
0.1 M Na
0.5 M Na
K+ concentration (μM g FW−1) Na+ concentration (μM g FW−1)

Figure 10

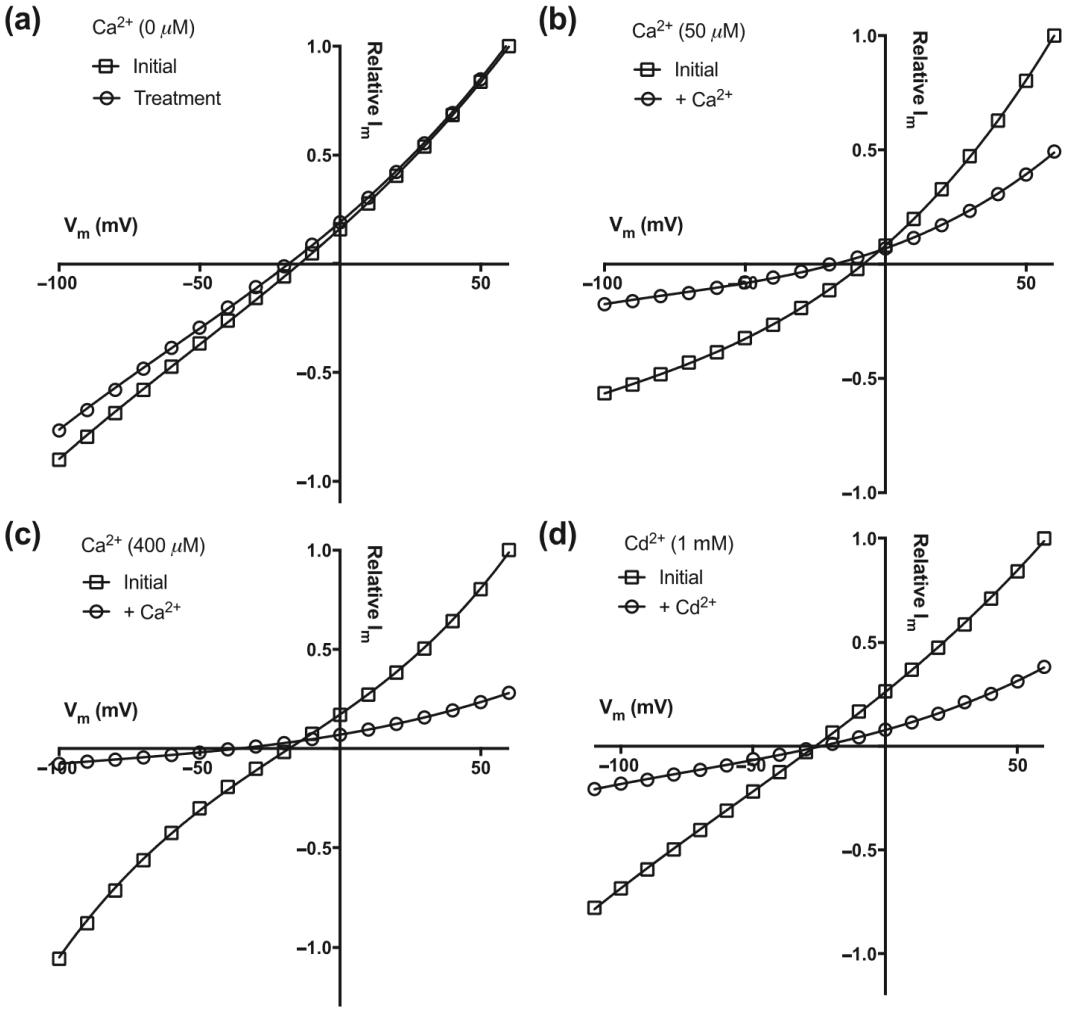
(a)
Ca2+ (0 μM)
Initial
Treatment
Relative Im
Vm (mV)
1.0
0.5
−0.5
−1.0
−100
−50
50
(b)
Ca2+ (50 μM)
Initial
+ Ca2+
Relative Im
Vm (mV)
(c)
Ca2+ (400 μM)
Initial
+ Ca2+
Relative Im
Vm (mV)
(d)
Cd2+ (1 mM)
Initial
+ Cd2+
Relative Im
Vm (mV)

Figure 11

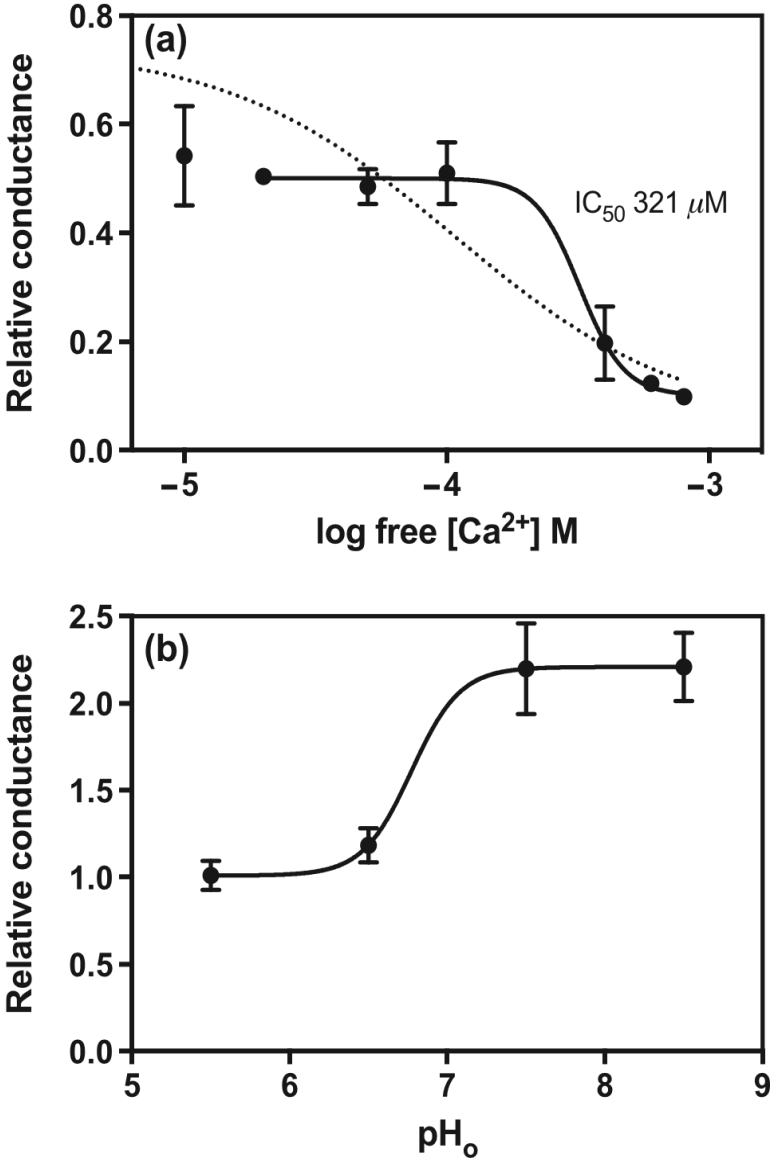
(a)
Relative conductance
0.8
0.6
0.4
0.2
0.0
−5
−4
−3
log free [Ca2+] M
IC50 321 μM
(b)
Relative conductance
2.5
2.0
1.5
1.0
0.5
0.0
5
6
7
8
9
pHo

Statement of Authorship

Title of Paper	Chapter 7: Comparison of the functional and pharmacological properties of Aquaporin cation-conducting channels from plant, vertebrate and invertebrate species
Publication Status	☐ Published ☐ Accepted for Publication ☐ Submitted for Publication ☑ Unpublished and Unsubmitted w ork w ritten in manuscript style
Publication Details	

Principal Author

Name of Principal Author (Candidate)	Mohamad Kourghi
Contribution to the Paper	Contributed to electrophysiology and imaging experiments. Wrote the manuscript. Analysed and contributed to preparing figures 1, 2, 3, 4, 5 and 7.
Overall percentage (%)	65%
Certification:	This paper reports on original research I conducted during the period of my Higher Degree by Research candidature and is not subject to any obligations or contractual agreements with a third party ~~that would constrain~~ its inclusion in this thesis. I am the primary author of this paper.
Signature	Date 6/09/2017

Co-Author Contributions

By signing the Statement of Authorship, each author certifies that:

i. the candidate's stated contribution to the publication is accurate (as detailed above);

ii. permission is granted for the candidate in include the publication in the thesis; and

iii. the sum of all co-author contributions is equal to 100% less the candidate's stated contribution.

Name of Co-Author	Saeed Nourmohammadi
Contribution to the Paper	Contributed with writing the discussion section, helped in preparing data and analyses for figure 6.
Agree contribution (%)	15%
Signature	Date 6/9/2017

Please cut and paste additional co-author panels here as required.

Name of Co-Author	Jinxin Pei		
Contribution to the Paper	Contributed to writing the manuscript. Generated figure 6 and wrote the figure legend.		
Agreed contribution percentage (%)	10%		
Signature		Date	6/9/17

Name of Co-Author	Caitlin Byrt		
Contribution to the Paper	Contributed to reviewing and editing the manuscript.		
Agreed contribution percentage (%)	5%		
Signature		Date	11/10/2017

Name of Co-Author	Stephen D Tyerman		
Contribution to the Paper	Contributed with experimental design, reviewing and editing the manuscript.		
Agreed contribution percentage (%)	10%		
Signature		Date	11/10/2017

Name of Co-Author	Andrea J. Yool		
Contribution to the Paper	Contributed to experimental design, reviewing and editing the manuscript.		
Agreed contribution percentage (%)	10%		
Signature		Date	5/9/2012

Chapter 7: Comparison of the functional and pharmacological properties of Aquaporin cation-conducting channels from plant, vertebrate and invertebrate species.

Mohamad Kourghi, Saeed Nourmohammadi, Jinxin V. Pei, Caitlin Byrt, Stephen Tyerman, and Andrea J. Yool

Abstract

Aquaporins (AQPs) facilitate water fluxes across barrier membranes and enable dynamic adjustment of volume in living cells across all forms of life. A subset of AQPs also serve as monovalent non-selective cation or anion-conducting channels. Recent work by Byrt and colleagues identified block by Ca^{2+} as a key mechanism of regulation for a newly described plant aquaporin ion channel, AtPIP2;1. Results here show that AQP ion channel block by divalent cations is a general mechanism, evident across diverse species. Work here also identifies a new plant AQP ion channel, AtPIP2:2, previously missed because of its high sensitivity to block by Ca^{2+}. Electrophysiological recordings in the Xenopus oocyte expression system in EGTA-buffered salines were used to evaluate the effects of divalent cations (Ca^{2+}, Mg^{2+}, Ba^{2+} and Cd^{2+}) on ionic conductances in oocytes expressing human HsAQP1, Arabidopsis thaliana AtPIP2;1, AtPIP2;2, and Drosophila melanogaster big brain (DmBIB) channels. The classes of AQP ion channels showed differential sensitivity to block by different divalent ions, as well as voltage-sensitive rectification. The order of sensitivity to block by Ca^{2+} ion was AtPIP2;2 (10 μM) > AtPIP2;1 (100 μM) > HsAQP1 (1000 μM) > DmBIB. Though less effective, Mg^{2+} showed the same order of potency. Block by Ba^{2+} was associated with strong outward rectification and voltage-dependent relief of block, with AtPIP2;2 > AtPIP2:1 > HsAQP1. Conversely, DmBIB channels showed enhanced outward current

with Ba^{2+}, suggesting competitive unblocking of the channel from chronic inhibition. Similarly, the channels with highest sensitivity to Ca^{2+}, AtPIP2;1 and AtPIP2;2, both showed relief of Ca^{2+} block by co-application of Ba^{2+}. The plant AtPIP2;7 showed no ionic conductance under any of the conditions tested. AQP1, AtPIP2;2, AtPIP2;1 and BIB ion channels were blocked uniformly by Cd^{2+} (1 mM). The plant AQP channels were not blocked by the bumetanide derivative AqB011 characterized previously as a blocker of the HsAQP1 ion channel, consistent with the observation that the plant aquaporins lack the arginine sequence proposed as the intracellular docking site for AqB011 in the human AQP1 channel. Understanding the properties and modulation of AQP ion channels could be important in improving salinity tolerance in plants, reducing cancer metastasis, or controlling angiogenesis, hypertension and cerebral ischemia.

Introduction

Water is an essential element of life, therefore maintaining water homeostasis in living organisms is fundamental to survival. The major intrinsic proteins (MIPs), referred to as aquaporins facilitate the transport of water and other solutes across biological membranes and play important roles in physiological functions (Anthony, Brooks et al. 2000, Holm, Jahn et al. 2005, Hibuse, Maeda et al. 2006, Zhao, Bankir et al. 2006, Herrera and Garvin 2011).

AQPs are comprised of six membrane spanning helices and 5 loops (loops A to E). (Jung et al., 1994), and are distinguished by the conserved asparagine-proline-alanine (NPA) signature motif located in loops B and E. AQPs organize as tetrameric pores in cell membranes that are found across all forms of life from prokaryotes to eukaryotes

(Agre, Preston et al. 1993, Jung, Preston et al. 1994, Murata, Mitsuoka et al. 2000, Sui, Han et al. 2001).

Up to date 15 different aquaporin genes have been identified in various mammalian tissues (AQP0- AQP14) (Ishibashi 2009, Finn, Chauvigne et al. 2014). Plants appear to have more diversity with between 20–60 different AQP loci occurring within single species of flowering plants (Zhang, Ali et al. 2013).

One of the five sub-families of plant aquaporins, referred to as Plasma membrane Intrinsic Proteins (PIPs) has been classified into two groups, PIP1 and PIP2, forming a group of 5 and 8 members respectively out of a total of 35 different aquaporins in the model plant *Arabidopsis thaliana (Soto, Alleva et al. 2012)*. Osmotic water permeability assays conducted on *Xenopus* oocytes have shown that the PIP2 channels have high water channel activity, whereas PIP1 proteins show little or no response in Xenopus (Daniels, Mirkov et al. 1994, Kammerloher, Fischer et al. 1994, Yamada, Katsuhara et al. 1995). This observation could in part be due to lack of targeting pf PIP1 channels to the *Xenopus* oocyte membranes, as the coexpression of a PIP1 with a PIP2 can increase water permeability in a synergistic fashion indicating that PIP1 can transport water but requires PIP2 for membrane targeting and function (Fetter, Van Wilder et al. 2004).

Despite the similarities between the amino acid sequence of the PIP1 and PIP2 aquaporins, they differ in the length of N and C terminal ends (Yaneff, Sigaut et al. 2014). AtPIP2;1 and AtPIP2;2 are widely and highly expressed in the plasma membranes of *Arabidopsis* and are prominent in roots. They generally play important roles in maintaining water homeostasis in several “gatekeeper” cells including

stomatal guard cells (Grondin et al. 2015). Studies conducted on suspensions of *Arabidopsis* cells revealed that the plasma membrane water permeability is regulated by Ca^{2+} and pH. Studies revealed that Ca^{2+} was able to reduce the water permeability by up to 60%, whereas other divalent cations such as Ba^{2+}, Sr^{2+}, and Mg^{2+} caused a decrease in permeability only by 25-30%. Lowering the pH was also shown to inhibit water transport in vesicles expressing the water channels (Gerbeau, Amodeo et al. 2002).

AQP1, previously known as CHIP28, was the first discovered water channel protein and is widely expressed in epithelial and endothelial tissues. In addition to facilitating the transport of water molecules through the tetrameric pores, AQP1 allows the passage of cations through the central pore (Yool and Weinstein 2002, Yu, Yool et al. 2006). The ion channel function of AQP1 depends on cGMP for activation (Anthony, Brooks et al. 2000). AQP1 expression has been associated with migration and metastasis in in sub-types of aggressive cancers including colon, melanoma, mammary, astrocytoma and glioma cancer cell lines (Hu and Verkman 2006, Jiang 2009, El Hindy, Bankfalvi et al. 2013, El Hindy, Rump et al. 2013, Yoshida, Hojo et al. 2013). Early work on characterizing AQP blockers showed that AQP1 water permeability is blocked by mercury ions (Hg^{2+}) (Preston, Jung et al. 1993) while the central ion pore is blocked by cadmium ions (Cd^{2+}) (Boassa, Stamer et al. 2006). However both blockers are toxic and lack specificity. An arylsulfonamide, AqB013, has been shown to block water permeability in AQP1 and AQP4 channels (Migliati, Meurice et al. 2009). In contrast, a bumetanide, AqB011, is a potent inhibitor of the AQP1 ion channel permeability while sparing water permeability (Kourghi, Pei et al. 2016). More

recently bacopaside I and bacopaside II, two structurally related compounds from the medicinal plant *Bacopa monnieri,* have been identified as efficient AQP1 water channel blockers. Bacopaside I however, also blocks the ionic permeation at high doses (Pei, Kourghi et al. 2016). These newly identified AQP1 modulators could serve as powerful tools in unravelling the diverse physiological roles of AQP1 and their importance in pathology such as in cancer metastasis.

Ion channel function has been demonstrated for other members of the MIP family. Lens MIP AQP 0 has been shown to be anion selective and regulated by pH (Zampighi, Hall et al. 1985, Ehring and Hall 1988, Ehring, Zampighi et al. 1990). Patch clamp recordings have shown that mammalian AQP6, an intracellular vesicle water channel has an anion permeability activated by low pH or $HgCl_2$ (Yasui, Kwon et al. 1999). More recently the plant AQP, AtPIP2;1 shows monovalent cation transport when expressed in *Xenopus laevis* oocytes and yeast (Byrt, Zhao et al. 2016). The cation function of AtPIP2;1 is blocked by Ca^{2+}, Cd^{2+} and low pH (Byrt, Zhao et al. 2016) as is the water permeation (Gerbeau, Amodeo et al. 2002). The modulation of AtPIP2;1 by Ca^{2+} and pH could be physiologically important in guard cell closing in response to stress, or in control of volume and turgor in other cell types (Findlay 2001, MacRobbie 2006, Grondin, Rodrigues et al. 2015). Non Selective Cation Channels (NSCC) of *Arabidopsis thaliana* roots expressed in epidermal protoplast membranes are voltage independent and are inhibited by Ca^{2+} and pH (Demidchik and Tester 2002) and it is hypothesised that AtPIP2;1 may be a candidate for these channels (Byrt, Zhao et al.

2016). Calcium is important in plant signalling, volume regulation, development, maintaining structure and growth (Rudd and Franklin-Tong 2001).

The insect AQP, Drosophila Big Brain (BIB), is an important protein in early development of the fly nervous system and has been demonstrated to have cationic permeability when expressed in the *Xenopus* oocyte system, activated by pricking the membrane (Yanochko and Yool 2002). The cationic permeation of wild type BIB is blocked by divalent cations Ca^{2+} and Ba^{2+}, but not with Mg^{2+} (Yanochko and Yool 2004). Interestingly a mutation in the conserved glutamate residue at position 71 (Glu^{71}) makes the BIB channel sensitive to block by Mg^{2+} (Yanochko and Yool 2004). Block by divalent cations in ion channels is physiologically important in signal transduction, feedback regulation and voltage dependence.

Other channels such as the voltage gated Na^{+} channels are also regulated by Ca^{2+} ions. The binding of Ca^{2+} not only blocks Na^{+} channels but it also shortens the time course of closure of the activation gates (Armstrong and Cota 1999). Similarly *Shaker* potassium channels are also blocked by extracellular calcium ions (Gomez-Lagunas, Melishchuk et al. 2003).

Store Operated Calcium Channels (SOCs) of non-excitable cells are regulated by Ca^{2+}. These channels are voltage independent Ca^{2+} channels and are activated when endoplasmic reticulum Ca^{2+} stores are depleted. SOC channels play important roles in Ca^{2+} oscillations and Ca^{2+} homeostasis (Parekh and Penner 1997), and are highly selective for Ca^{2+} (Hoth and Penner 1993). Interestingly in Arabidopsis, the root plasma membrane AtPIP2;1 water permeability is blocked by Ca^{2+}, Cd^{2+}, Mn^{2+} and H^{+}

(Verdoucq, Grondin et al. 2008), and the ionic permeation similarly is blocked by Ca^{2+}, Cd^{2+} and H^{+} (Byrt, Zhao et al. 2016).

In the current study we compare and contrast the effects of divalent cations on AQP ion channels from different phyla. Understanding the regulation of AQP ion channels and their different properties is essential in determining their diverse physiological roles and their value in pathological conditions.

Methods

Preparation and injection of *Xenopus laevis* oocytes

The use of animals in this study has been carried out in accordance with the Guide for the Care and Use of Laboratory Animals, licensed under the South Australian Animal Welfare Act 1985, under protocols approved by the University of Adelaide Animal Ethics Committee. Oocytes used in this study were obtained from adult female *Xenopus laevis* frogs kept at the University of Adelaide Animal Laboratory Services. Oocytes were defoliculated through incubation in collagenase (type 1A, 1 mg/ml; Sigma-Aldrich, St. Louis, MO) and trypsin inhibitor (0.05 mg/ml; Sigma-Aldrich, St. Louis, MO) in calcium free OR-2 saline containing 96 mM NaCl, 2 mM KCl, 5 mM $MgCl_2$, penicillin 100 units/ml streptomycin 0.1 mg/ml, and 5 mM HEPES at pH7.6 for 1 to 1.5 hours. After collagenase treatment oocytes were kept at 16°C in Frog Ringer saline consisting of 96 mM NaCl, 2mM KCl, 5 mM $MgCl_2$, 0.6 mM $CaCl_2$, 5mM HEPES buffer, horse serum (5%; Sigma-Aldrich, St. Louis, MO), penicillin 100 units/ml streptomycin 0.1 mg/ml, and tetracycline 0.5 mg/ml, pH 7.6. Stage V-VI oocytes were

selected and injected slowly (over 5-10s) with 50 nl of RNAse-free water containing 1 ng of *HsAQP1* cRNA or 12 ng of *AtPIP2;7*, *AtPIP2;2* and *AtPIP2;1* CRNA, or 20ng of drosophila big brain (*bib)* cRNA using a micro injector (manual oocyte microinjection pipette, Drummond Scientific). RNAase-free Water injected oocytes served as controls in this experiment. AQP1 and BIB expressing oocytes were incubated in Frog Ringer saline while oocytes injected with *AtPIP2;7*, *AtPIP2;2* and *AtPIP2;1* CRNA were incubated at 16°C in high potassium Frog Ringer saline (62 mM NaCl, 36 mM KCl, 5 mM $MgCl_2$, 0.6 mM $CaCl_2$, 5mM HEPES buffer, horse serum 5%, penicillin 100 units/ml, streptomycin 0.1mg/ml, and tetracycline 0.5mg/ml, pH 7.6) for 1 to 1.5 days and a minimum of 2-5 days for oocytes injected with AQP1 or *bib* cRNA in the same saline to allow sufficient time for expression prior to electrophysiology. Swelling assays were used to test for successful expression in which oocytes expressing *AtPIP2;7, AtPIP2;2 AtPIP2;1* and *HsAQP1* swelled and burst within 3-5 minutes after emersion in distilled water. Water injected control oocytes remained intact and unchanged for up to 10 minutes. Experiments were conducted at the University of Adelaide, Medical School North.

Two electrode voltage clamp recordings

Two electrode voltage clamp (TEVC) recordings were used to investigate the functional properties and modulation of AQP ion channels on *Xenopus* oocytes between 24 to 48 hours after injection with water with or without cRNA. Capillary glass electrodes were pulled to achieve 1-3MΩ of resistance in ND96 solution and were filled with 1M KCl. Recordings were performed in EGTA (ethylene glycol-bis(β-aminoethyl

ether)-N,N,N',N'-tetraacetic acid)-buffered divalent free saline containing 100 mM NaCl, 2 mM KCl, and 5 mM HEPES, pH 7.6 at room temperature. The total concentration of Ca^{2+} required to achieve the desired free Ca^{2+} concentration in 20mM EGTA was calculated using http://maxchelator.stanford.edu/CaEGTA-NIST.htm.

Two electrode recording pipettes were used conventionally to control voltage and deliver current. Membrane permeable analogue of cGMP, CPT-cGMP (*R*p)-8-(*para*-chlorophenylthio)-cGMP (8-CPT-cGMP; 10 µM; Sigma-Aldrich) was applied to the recording saline to initiate ionic conductance in AQP1 expressing oocytes. Ionic conductance was monitored throughout the experiments by repeated steps to +40mV (800-ms duration) every 6 s from a holding potential of -40mV. Recordings were made using a GeneClamp amplifier and Clampex 9.0 software (pClamp 9.0 Molecular Devices, Sunnyvale, CA, USA). Data were filtered at 2 kHz, digitized at 2 kHz, and stored to hard disk for analysis. Quantitative values of the magnitude of relative outward rectification were calculated by standardizing outward current amplitude (at +60 mV) to inward current amplitude (at -80 mV). Statistical analyses were done with one-way ANOVA with Bonferroni post-hoc tests; p values are indicated in the figure legends.

Bath application of divalent cations

The effects of divalent cations Ca^{2+}, Mg^{2+}, Ba^{2+} and Cd^{2+} were tested in oocytes expressing AQP1, AtPIP2;7, AtIP2;2, AtPIP2,1 and BIB channels. Oocytes were placed in EGTA-buffered divalent free saline for initial electrophysiological recordings. After recording the initial conductance, the current flow was monitored over 30 minutes

for oocytes expressing AQP1 to reach maximal activation, and 2 to 3 minutes for oocytes expressing BIB, AtPIP2;1 and AtPIP2;2 since these channels showed activation from the time the recording electrodes were placed in the oocyte membrane. After recording the initial activated responses, the bath saline was perfused with test salines containing Ca^{2+}, Mg^{2+} or Ba^{2+}. New steady state response levels was achieved rapidly within 1 to 2 mins. Each divalent cation was added after washing away the effect of the previous cation using the perfusion system. The final conductance values were measured at 6 minutes after achieving a steady state response to the cation.

Osmotic swelling assays

Immediately before the swelling assays, control and AQP-expressing oocytes were rinsed in calcium free saline for 10 minutes. Swelling assays were performed in 50% hypotonic saline (calcium free saline diluted with equal volume of water). Oocytes were placed in 50% hypotonic saline and changes in cross-sectional area of oocytes membranes were imaged using a grayscale camera device (Cohu, San Diego, CA) fixed on a dissecting microscope (Olympus SZ-PT; Olympus, Macquarie Park, Australia). Images were captured at 0.5 per second for 60 s. Swelling rates of the oocytes were assessed with Image J software from National Institutes of Health (http://rsbweb.nih.gov/ij/), and measured as the slopes of the linear regression fits of relative volume as a function of time using Prism (GraphPad Software Inc.,San Diego, CA).

Results

Expression of AQP channels on oocyte membranes

To confirm the expression of functional AQP channels in the *Xenopus* oocytes, swelling assays were performed for *AtPIP2;7, AtPIP2;2, AtPIP2;1 and HsAQP1* cRNA injected oocytes. Prior to experiments water injected controls and AQP expressing oocytes were rinsed in divalent free saline for 10 minutes. The increase in volume recorded over 60s was not significantly different between oocytes expressing AtPIP2;7, AtPIP2;2, AtPIP2;1 and HsAQP1 channels injected with the same quantity of cRNA, but was significantly greater than water-injected controls, confirming the expression of the channels on the oocyte membrane (Figure 1A). Figure 1B is box plot summary of data presented in A. BIB channels have not been found to mediate osmotic water permeability (Yanochko and Yool 2002). The expression of BIB channels on oocyte plasma membranes was previously confirmed by (Yanochko and Yool 2002) using immunocytochemistry and confocal microscopy.

Differential sensitivity of AQP ion currents to block by Ca^{2+}

Two electrode voltage clamp recording were used to measure AQP ion channel currents in *Xenopus* oocytes (Figure 2). Water injected control oocytes and oocytes expressing AtPIP2;7 channels did not show any ionic activation 30 minutes after recording the ionic conductance, and were unresponsive to Ca^{2+} or Mg^{2+} applications . AQP1 expressing oocytes were activated after bath application of 10μM CPT-cGMP. Maximum activation was achieved approximately 30 minutes after CPT-cGMP application. Ionic conductance in AtPIP2;1, AtPIP2;2 and *Drosophila* big brain (BIB) expressing oocytes were evident upon the insertion of recording electrodes

showing that these channels were already active in the expression system (Figure 2A). Current traces were recorded for control and AQP-expressing oocytes after maximal activation in divalent-free saline; after perfusion of bath saline with Mg^{2+}; and after washout and application of EGTA-buffered Ca^{2+} saline for the same oocytes (Figure 2A). AtPIP2;2 and AtPIP2;1 currents were reduced by Mg^{2+} at 1 mM, however both channels are very sensitive to Ca^{2+}. Maximum block can be achieved at 100 μM $CaCl_2$ concentration in oocytes expressing AtPIP2;1, and 10 μM $CaCl_2$ in AtPIP2;2 expressing oocytes. While AQP1 ion channel was not sensitive to Mg^{2+}, it was blocked by Ca^{2+} cations at a concentration of 1 mM. Similar to AQP1 ion conductance, BIB channels were not blocked by Mg^{2+}; however a block in conductance was observed with 1 mM Ca^{2+} added to the saline. Figure 2B shows a summary box plot for data presented in Figure 2A. Figure 2C illustrates current-voltage relationships for the oocytes shown in Figure 2A.

Voltage-sensitive block of AQP ion channels by Ba^{2+}

In subsequent experiments we tested the effect of $BaCl_2$ on ion channel function of each AQP. After recording the initial or activated conductance, 1 mM $BaCl_2$ was applied to the bath saline followed by recording the different responses (Figure 3A). Wild type AtPIP2;1, AtPIP2;2, AQP1 and BIB channels have an approximately linear current-voltage relationship in response to Mg^{2+} application (Figure 2C). However when 1mM $BaCl_2$ was applied to the recording saline, oocytes expressing AtPIP2;1, AtPIP2;2, AQP1 and BIB channels display outward rectification by Ba^{2+} suggesting that there is an apparent unblocking by Ba^{2+}. AtPIP2;2 ion channels showed more

sensitivity to block by Ba^{2+} ions as compared to AtPIP2;1, AQP1 and BIB channels (Figure 3B) as seem for data is summarized in a box plot. Figure 3C illustrates the current-voltage relationship for current versus time for traces shown in A. Figure 3D shows compiled data for current ratios (I_{+60}/ I_{-80}) for wildtype AQP1, BIB, AtPIP2;1 and AtPIP2;2 channels at initial (before Ba^{2+} application) and after external application of 1 mM Ba^{2+}. For all channels the magnitude of outward rectification current ratio was significantly greater in saline with Ba^{2+} as compared to without Ba^{2+}, ($p<0.001$, one-way ANOVA).

Inhibition of AQP ion channel by Cd^{2+}

The effect of 1 mM Cd^{2+} was tested on non-AQP expressing control oocytes and on oocytes expressing AQP1, AQP4, AQP5, AtPIP2;1 and AtPIP2;2. After full activation in Ca^{2+} free saline, 1 mM $CdCl_2$ was perfused into the recording saline and the response was recorded (Figure 4A). Oocytes expressing, AQP1, AtPIP2;1 and AtPIP2;2 showed block after the application of 1 mM Cd^{2+}. Figure 4B illustrates the current voltage relationships for oocytes presented in Figure 4A. Reversal potentials in salines with Cd^{2+} were not different between AQP1, AtPIP2;1 and AtPIP2;2 expressing oocytes. Wildtype AQP1, AtPIP2;1 and AtPIP2;2 have an approximately linear current-voltage relationship in the recording saline, but show outward rectification with the addition of Cd^{2+}, indicating a relief of block by Cd^{2+} at depolarized membrane potentials. Figure 4D shows the compiled data for the effect of 1 mM $CdCl_2$ on AQP1, AtPIP2;1 and AtPIP2;2 expressing oocytes. The block is significant for AQP1, AtPIP2;1, and AtPIP2;2 treated with Cd^{2+}. Figure 4E shows

compiled data for current ratios (I_{+60} / I_{-80}) for wildtype AQP1, BIB, AtPIP2;1 and AtPIP2;2 at initial (before Cd^{2+} application) and after bath application of 1 mM Cd^{2+}. For all channels the magnitude of outward rectification was significantly greater in saline with Cd^{2+} as compared to without Cd^{2+}, ($p<0.001$, one-way ANOVA).

Relief of Ca^{2+} block by the addition of Ba^{2+}

Combined application of Ca^{2+} followed by Ba^{2+} was used to investigate possible competitive interactions between divalent cation blockers (Figure 5). After recording the initial traces in Ca^{2+} free solution (Figure 5A), $CaCl_2$ was applied to the recording chamber. 1 mM $CaCl_2$ was added to the recording saline of oocytes expressing AQP1 and BIB channels, 100 μM to AtPIP2;1 and 10 μM to AtPIP2;2 expressing oocytes. The response to $CaCl_2$ was recorded for each oocyte. This was followed by application of 1mM $BaCl_2$ in addition to the $CaCl_2$. The subsequent application of 1mM $BaCl_2$ to the presence of the $CaCl_2$ resulted in unblocking of the outward rectification current in oocytes expressing AtPIP2;1 and AtPIP2;2 channels. Oocytes expressing AQP1 and BIB channels did not show a similar recovery (Figure 5A right) Figure 5B shows box plots of data shown in Figure 5A. Figure 5C illustrates the current voltage relationship for traces shown in A.

Analysis of other AQP ion conducting properties with AqB011

The bumetanide derivative AqB011 was previously shown to block the human AQP1 ion Channel function. In the subsequent experiment we investigated the possible blocking effect of AqB011 on AtPIP2;1 and AtPIP2;2 channels (Figure 6). Oocytes

expressing HsAQP1 were activated by CPT-cGMP, then incubated 2 h in divalent free saline with or without 20 μM AqB011, and re-tested for activation by CPT-cGMP. Results here confirm the inhibition of the HsAQP1 ion channel by AqB011 (Figure 6A). AtPIP2;1 and AtPIP;2 expressing oocytes were recorded in initial normal saline, then incubated 2 hours with 100μM AqB011, and recorded again. In comparison with HsAQP1, AqB011 treatment had no effect on AtPIP2;1 and AtPIP2;2 expressing oocytes (Figure 6A). This suggests that AQP1 is a selective blocker for mammalian AQP1. Non-AQP expressing control oocytes displayed minimal basal baseline conductance and 2 h incubation in 100 μM AqB011 had no effect on the oocytes.

Discussion

AQP ion channels carry different functional properties and are regulated differently among different species. HsAQP1 is activated via cGMP interaction with poly arginine residues on the loop D domain (Anthony, Brooks et al. 2000). The activation is influenced by tyrosine phosphorylation at position 253 (Y253) at the carboxyl terminal domain (Campbell, Birdsell et al. 2012). Ionic conductance is not a feature of all AQPs since no ionic conductance was observed in oocytes expressing HsAQP4, HsAQP5 or AtPIP2;7 aquaporins. The bath application of 10 μM CPT-cGMP failed to trigger an ionic response in oocytes expressing HsAQP4 and HsAQP 5 channels. This observation is important since it rejects the possibility that the ionic conductances observed in AtPIP2;2, AtPIP2;1, HsAQP1 and DmBIB channels is simply due to other indirect mechanisms such as activation of native oocyte channels, or removal of extracellular divalent cations during recording sessions. AtPIP2;1, AtPIP2;2 and BIB channels moreover showed ionic conductance upon the insertion of recording electrodes into the oocyte membrane, thus it is possible that the activation observed in AtPIP2;1, AtPIP2;2 and BIB channels could have been constitutively on in the oocyte system, or rapidly triggered via intracellular signalling cascades (Yanochko and Yool 2002, Byrt, Zhao et al. 2016). External ion sensitive electrodes also demonstrated that AtPIP2;1 was functioning to transport Na^+ independently of any “pricking” response (Byrt, Zhao et al. 2016). Possible contributions of the native oocyte Cl^- current activated by intracellular Ca^{2+} were

minimized by using a holding potential of -40 mV for the voltage-clamp recordings, which results in inactivation of the native voltage-gated Ca2+ channels.

Results here are the first to show that the plant AQP AtPIP2;2 from *Arabidopsis* functions to conduct ionic current when expressed in *Xenopus* oocytes in Ca^{2+}-free saline. The ionic conductance recorded for these ion-conducting AQPs was not observed in non-AQP expressing oocytes treated in the same experimental conditions nor in AtPIP2;7 expressing oocytes, reducing the possibility that the ionic conductance observed is as an artefact, due to the exclusion of external Ca^{2+}, or as a result of recruiting or activating a native oocyte cation channel by the exogenous expression of the aquaporins.

The expression of the AQPs on oocyte membranes was confirmed using swelling assays, where oocytes expressing the HsAQP1, HsAQP4, HaAQP5, AtPIP2;7, AtPIP2;2 and AtPIP2;1 channels were placed in 50% hypotonic saline and the expansion of the oocyte membrane was recorded using a camera connected to a computer. The rates of oocyte swelling were significantly higher in oocytes expressing HsAQP1, AtPIP2;7, AtPIP2;2 and AtPIP2;1 channels as compared to non-AQP controls, confirming the expression of the channels on the membrane. Since BIB channels do not show osmotic permeability, the expression of BIB channels on oocyte membranes was previously confirmed using western blot and immunocytochemistry as described by (Yanochko and Yool 2002).

Effect of divalent cations on the ionic conductance

We have demonstrated that both AtPIP2;1, and AtPIP2;2 ion channels are blocked by Ca^{2+} cations. In comparison with AtPIP2;1, the AtPIP2;2 channels are more sensitive to Ca^{2+}, while both channels show less sensitivity to Mg^{2+}. Previous studies have shown that AtPIP2;1 and AtPIP2;2 water permeability are inhibited by Ca^{2+} (Verdoucq, Grondin et al. 2008). In this study we show that the ionic component is also blocked by Ca^{2+}. This property could be physiologically important, especially in response to stress, or during shrinking (Gerbeau, Amodeo et al. 2002). AQP1 and BIB channels on the other hand show no sensitivity to Mg^{2+} ions, but both channels are blocked by Ca^{2+} at 1 mM (Figure 2). HsAQP1, BIB, AtPIP2;1, and AtPIP2;2 channels are also blocked by Ba^{2+} cations, and show a voltage dependent unblocking of the outward rectification current in response to Ba^{2+} application (Figure 3).

Oocytes expressing HsAQP1, BIB, AtPIP2;1 and AtPIP2;2 also show block of ionic conductance by Cd^{2+}. Moreover the application of Cd^{2+} to the bath saline causes an outward rectification in oocytes expressing HsAQP1, BIB, AtPIP2;1 and AtPIP2;2 channels (Figure 4). It is interesting to mention that Cd^{2+} directly interacts with Asp^{28} and Glu^{31} residues of spinach SoPIP2;1 (*Spinacia oleracea* PIP2;1) channel (Tornroth-Horsefield, Wang et al. 2006). The equivalent residues are present in AtPIP2;1 and AtPIP2;2 channels, at positions Asp^{28} and Glu^{31} for AtPIP2;1 channels, and Asp^{26} and Glu^{29} for AtPIP2;2 channels. Therefore the equivalent site might serve as a Cd^{2+} binding site in AtPIP2;1 and AtPIP2;2 channels. When comparing AtPIP2;1 and AtPIP2;2 with HsAQP1 channels, AtPIP2;1 and AtPIP2;2 are more sensitive to block by Ca^{2+} as compared to Cd^{2+}, on the other hand HsAQP1 ion conductance is more

sensitive to block by Cd^{2+} as compared to Ca^{2+}. This difference in sensitivity to Ca^{2+} and Cd^{2+} between AQP1, AtPIP2;1 and AtPIP2;2 channels could be due to the difference in the amino acid sequences between the AQP1 and the AtPIP2;1, AtPIP2;2 channels, such as in extracellular loop A region, as illustrated in Figure 7. AtPIP2;1 channels also have aspartic acid residues at positions 67 and 74, ($Asp^{67, 74}$), which in AtPIP2;2 are located at positions 65 and 72 ($Asp^{65, 72}$). HsAQP1channels have a single Aspartic acid residue at position 48 (Asp^{48}), while BIB channels do not have any negatively charged residues in loop A. The difference in sensitivity to Ca^{2+} could be that Ca^{2+} is binding to Asp residues in loop A, therefore AtPIP2;1 and AtPIP2;2 channels are more sensitive to Ca^{2+} compared to HsAQP1 due to more negatively charged residues in loop A.

We were interested in testing the dual effect of Ca^{2+} and Ba^{2+} in oocytes expressing HsAQP1, BIB, AtPIP2;1 and AtPIP2;2 channels. The application of Ca^{2+} caused a block in AQP1, BIB, AtPIP2;1 and AtPIP2;2 ionic conductance, while AtPIP2;1 and AtPIP2;2 channels are more sensitive to Ca^{2+} ions as shown in this work. The application of Ba^{2+} in addition to Ca^{2+} in the saline caused an outward rectification at positive membrane potentials in oocytes expressing AtPIP2;1 and AtPIP2;2 (Figure 5). This suggests that both Ca^{2+} and Ba^{2+} are competing for the same binding site in AtPIP2;1 and AtPIP2;2 channels, while Ba^{2+} has lower binding affinity for the site. Another possibility is Ca^{2+} and Ba^{2+} are competing for binding to a double Aspartic acid resides on positions 244 and 245 ($Asp^{244, 245}$) of AtPIP2;2, equivalent to $Asp^{246, 247}$ of AtPIP2;1 on extracellular loop E domain between the 5^{th} and 6^{th} region. This negatively charged resides are not present in AQP1 nor BIB channels (Figure 7). The loop E

domain is demonstrated as the interaction site with mercury and TEA in HsAQP1 channels (Preston, Jung et al. 1993, Brooks, Regan et al. 2000).

AqB011 block

In this study we confirmed the Inhibition of ion HsAQP1 ion channel function by AqB011, which was not observed in oocytes expressing AtPIP2;1 or AtPIP2;2 channels. AqB011 previously was predicted to interact with the loop D gating domain at the intracellular side of the AQP1 channel (Kourghi, Pei et al. 2016), precisely with the first two arginine residues within a series of four arginines that is highly conserved among vertebrate AQP1 channels, and is also suggested as the cGMP-mediated activation site of the ionic conductance in AQP1 (Yu, Yool et al. 2006). Interestingly, this pair of arginine residues are absent in AtPIP2;1 or AtPIP2;2 sequences, instead have a proline residue as the first residue in the series (Figure 7). These results are in agreement with the hypothesis that the loop D domain of AQP1 functions as the interaction site of AqB011, and support the idea that AQP pharmacological agents can have differential effects based on differences in amino acid sequences between the AQP channels.

Further research is needed to validate the possible interaction sites between the divalent cation blockers and the AQP channels, and further investigation is needed to study if the ionic pathway in AtPIP2;1 and AtPIP2;2 channels is through the central pore, or through the individual water pores of the monomers. In HsAQP1 evidence indicates that ions pass through the central channel, distinct from the water pores (Yool

and Weinstein 2002, Yu, Yool et al. 2006), while in BIB it is proposed that the individual monomer pores might serve as the permeation pathway for anions (Yool 2007).

In this study we have demonstrated that AQP ion channel channels respond differently to the same pharmacological agents and have different sensitivities to block by divalent cations. Understanding the regulation of AQP ion channels using pharmacology and divalent cations is an important step in unravelling their different properties, which will help us in understanding their diverse physiological roles such as in cancer metastasis, and improving salinity tolerance in plants.

References

Agre, P., G. M. Preston, B. L. Smith, J. S. Jung, S. Raina, C. Moon, W. B. Guggino and S. Nielsen (1993). "Aquaporin CHIP: the archetypal molecular water channel." Am J Physiol **265**(4 Pt 2): F463-476.

Anthony, T. L., H. L. Brooks, D. Boassa, S. Leonov, G. M. Yanochko, J. W. Regan and A. J. Yool (2000). "Cloned human aquaporin-1 is a cyclic GMP-gated ion channel." Molecular Pharmacology **57**(3): 576-588.

Anthony, T. L., H. L. Brooks, D. Boassa, S. Leonov, G. M. Yanochko, J. W. Regan and A. J. Yool (2000). "Cloned human aquaporin-1 is a cyclic GMP-gated ion channel." Mol Pharmacol **57**(3): 576-588.

Armstrong, C. M. and G. Cota (1999). "Calcium block of Na^+ channels and its effect on closing rate." Proc Natl Acad Sci U S A **96**(7): 4154-4157.

Boassa, D., W. D. Stamer and A. J. Yool (2006). "Ion channel function of aquaporin-1 natively expressed in choroid plexus." J Neurosci **26**(30): 7811-7819.

Brooks, H. L., J. W. Regan and A. J. Yool (2000). "Inhibition of aquaporin-1 water permeability by tetraethylammonium: involvement of the loop E pore region." Mol Pharmacol **57**(5): 1021-1026.

Byrt, C. S., M. Zhao, M. Kourghi, J. Bose, S. W. Henderson, J. Qiu, M. Gilliham, C. Schultz, M. Schwarz, S. A. Ramesh, A. Yool and S. Tyerman (2016). "Non-selective cation channel activity of aquaporin AtPIP2;1 regulated by Ca^{2+} and pH." Plant Cell Environ.

Campbell, E. M., D. N. Birdsell and A. J. Yool (2012). "The activity of human aquaporin 1 as a cGMP-gated cation channel is regulated by tyrosine phosphorylation in the carboxyl-terminal domain." Mol Pharmacol **81**(1): 97-105.

Daniels, M. J., T. E. Mirkov and M. J. Chrispeels (1994). "The plasma membrane of Arabidopsis thaliana contains a mercury-insensitive aquaporin that is a homolog of the tonoplast water channel protein TIP." Plant Physiol **106**(4): 1325-1333.

Demidchik, V. and M. Tester (2002). "Sodium fluxes through nonselective cation channels in the plasma membrane of protoplasts from Arabidopsis roots." Plant Physiology **128**(2): 379-387.

Ehring, G. R. and J. E. Hall (1988). "Single channel properties of lens MIP 28 reconstituted into planar lipid bilayers." Proc West Pharmacol Soc **31**: 251-253.

Ehring, G. R., G. Zampighi, J. Horwitz, D. Bok and J. E. Hall (1990). "Properties of channels reconstituted from the major intrinsic protein of lens fiber membranes." J Gen Physiol **96**(3): 631-664.

El Hindy, N., A. Bankfalvi, A. Herring, M. Adamzik, N. Lambertz, Y. Zhu, W. Siffert, U. Sure and I. E. Sandalcioglu (2013). "Correlation of Aquaporin-1 Water Channel Protein Expression with Tumor Angiogenesis in Human Astrocytoma." Anticancer Research **33**(2): 609-613.

El Hindy, N., K. Rump, N. Lambertz, Y. Zhu, U. H. Frey, A. Bankfalvi, W. Siffert, U. Sure, J. Peters, M. Adamzik and I. E. Sandalcioglu (2013). "The Functional Aquaporin 1-783G/C-Polymorphism Is Associated With Survival in Patients With Glioblastoma Multiforme." Journal of Surgical Oncology **108**(7): 492-498.

Fetter, K., V. Van Wilder, M. Moshelion and F. Chaumont (2004). "Interactions between plasma membrane aquaporins modulate their water channel activity." Plant Cell **16**(1): 215-228.

Findlay, G. P. (2001). "Membranes and the electrophysiology of turgor regulation." Australian Journal of Plant Physiology **28**(7): 617-634.

Finn, R. N., F. Chauvigne, J. B. Hlidberg, C. P. Cutler and J. Cerda (2014). "The lineage-specific evolution of aquaporin gene clusters facilitated tetrapod terrestrial adaptation." PLoS One **9**(11): e113686.

Gerbeau, P., G. Amodeo, T. Henzler, V. Santoni, P. Ripoche and C. Maurel (2002). "The water permeability of Arabidopsis plasma membrane is regulated by divalent cations and pH." Plant Journal **30**(1): 71-81.

Gomez-Lagunas, F., A. Melishchuk and C. M. Armstrong (2003). "Block of Shaker potassium channels by external calcium ions." Proc Natl Acad Sci U S A **100**(1): 347-351.

Grondin, A., O. Rodrigues, L. Verdoucq, S. Merlot, N. Leonhardt and C. Maurel (2015). "Aquaporins Contribute to ABA-Triggered Stomatal Closure through OST1-Mediated Phosphorylation." Plant Cell **27**(7): 1945-1954.

Herrera, M. and J. L. Garvin (2011). "Aquaporins as gas channels." Pflugers Arch **462**(4): 623-630.

Hibuse, T., N. Maeda, A. Nagasawa and T. Funahashi (2006). "Aquaporins and glycerol metabolism." Biochim Biophys Acta **1758**(8): 1004-1011.

Holm, L. M., T. P. Jahn, A. L. Moller, J. K. Schjoerring, D. Ferri, D. A. Klaerke and T. Zeuthen (2005). "NH_3 and NH_4 permeability in aquaporin-expressing *Xenopus* oocytes." Pflugers Arch **450**(6): 415-428.

Hoth, M. and R. Penner (1993). "Calcium release-activated calcium current in rat mast cells." J Physiol **465**: 359-386.

Hu, J. and A. S. Verkman (2006). "Increased migration and metastatic potential of tumor cells expressing aquaporin water channels." FASEB J **20**(11): 1892-1894.

Ishibashi, K. (2009). "New members of mammalian aquaporins: AQP10-AQP12." Handb Exp Pharmacol(190): 251-262.

Jiang, Y. (2009). "Aquaporin-1 activity of plasma membrane affects HT20 colon cancer cell migration." IUBMB Life **61**(10): 1001-1009.

Jung, J. S., G. M. Preston, B. L. Smith, W. B. Guggino and P. Agre (1994). "Molecular-Structure of the Water Channel through Aquaporin Chip - the Hourglass Model." Journal of Biological Chemistry **269**(20): 14648-14654.

Kammerloher, W., U. Fischer, G. P. Piechottka and A. R. Schaffner (1994). "Water channels in the plant plasma membrane cloned by immunoselection from a mammalian expression system." Plant J **6**(2): 187-199.

Kourghi, M., J. V. Pei, M. L. De Ieso, G. Flynn and A. J. Yool (2016). "Bumetanide Derivatives AqB007 and AqB011 Selectively Block the Aquaporin-1 Ion Channel Conductance and Slow Cancer Cell Migration." Mol Pharmacol **89**(1): 133-140.

MacRobbie, E. A. (2006). "Control of volume and turgor in stomatal guard cells." J Membr Biol **210**(2): 131-142.

Migliati, E., N. Meurice, P. DuBois, J. S. Fang, S. Somasekharan, E. Beckett, G. Flynn and A. J. Yool (2009). "Inhibition of aquaporin-1 and aquaporin-4 water permeability

by a derivative of the loop diuretic bumetanide acting at an internal pore-occluding binding site." Mol Pharmacol **76**(1): 105-112.

Murata, K., K. Mitsuoka, T. Hirai, T. Walz, P. Agre, J. B. Heymann, A. Engel and Y. Fujiyoshi (2000). "Structural determinants of water permeation through aquaporin-1." Nature **407**(6804): 599-605.

Parekh, A. B. and R. Penner (1997). "Store depletion and calcium influx." Physiol Rev **77**(4): 901-930.

Pei, J. V., M. Kourghi, M. L. De Ieso, E. M. Campbell, H. S. Dorward, J. E. Hardingham and A. J. Yool (2016). "Differential Inhibition of Water and Ion Channel Activities of Mammalian Aquaporin-1 by Two Structurally Related Bacopaside Compounds Derived from the Medicinal Plant Bacopa monnieri." Mol Pharmacol **90**(4): 496-507.

Preston, G. M., J. S. Jung, W. B. Guggino and P. Agre (1993). "The Mercury-Sensitive Residue at Cysteine-189 in the Chip28 Water Channel." Journal of Biological Chemistry **268**(1): 17-20.

Rudd, J. J. and V. E. Franklin-Tong (2001). "Unravelling response-specificity in Ca^{2+} signalling pathways in plant cells." New Phytologist **151**(1): 7-33.

Soto, G., K. Alleva, G. Amodeo, J. Muschietti and N. D. Ayub (2012). "New insight into the evolution of aquaporins from flowering plants and vertebrates: orthologous identification and functional transfer is possible." Gene **503**(1): 165-176.

Sui, H. X., B. G. Han, J. K. Lee, P. Walian and B. K. Jap (2001). "Structural basis of water-specific transport through the AQP1 water channel." Nature **414**(6866): 872-878.

Tornroth-Horsefield, S., Y. Wang, K. Hedfalk, U. Johanson, M. Karlsson, E. Tajkhorshid, R. Neutze and P. Kjellbom (2006). "Structural mechanism of plant aquaporin gating." Nature **439**(7077): 688-694.

Verdoucq, L., A. Grondin and C. Maurel (2008). "Structure-function analysis of plant aquaporin AtPIP2;1 gating by divalent cations and protons." Biochemical Journal **415**: 409-416.

Yamada, S., M. Katsuhara, W. B. Kelly, C. B. Michalowski and H. J. Bohnert (1995). "A family of transcripts encoding water channel proteins: tissue-specific expression in the common ice plant." Plant Cell **7**(8): 1129-1142.

Yaneff, A., L. Sigaut, M. Marquez, K. Alleva, L. I. Pietrasanta and G. Amodeo (2014). "Heteromerization of PIP aquaporins affects their intrinsic permeability." Proc Natl Acad Sci U S A **111**(1): 231-236.

Yanochko, G. M. and A. J. Yool (2002). "Regulated cationic channel function in Xenopus oocytes expressing Drosophila big brain." J Neurosci **22**(7): 2530-2540.

Yanochko, G. M. and A. J. Yool (2004). "Block by extracellular divalent cations of *Drosophila big brain* channels expressed in *Xenopus* oocytes." Biophys J **86**(3): 1470-1478.

Yasui, M., T. H. Kwon, M. A. Knepper, S. Nielsen and P. Agre (1999). "Aquaporin-6: An intracellular vesicle water channel protein in renal epithelia." Proc Natl Acad Sci U S A **96**(10): 5808-5813.

Yool, A. J. (2007). "Dominant-negative suppression of big brain ion channel activity by mutation of a conserved glutamate in the first transmembrane domain." Gene Expr **13**(6): 329-337.

Yool, A. J. and A. M. Weinstein (2002). "New roles for old holes: ion channel function in aquaporin-1." News Physiol Sci **17**: 68-72.

Yoshida, T., S. Hojo, S. Sekine, S. Sawada, T. Okumura, T. Nagata, Y. Shimada and K. Tsukada (2013). "Expression of aquaporin-1 is a poor prognostic factor for stage II and III colon cancer." Mol Clin Oncol **1**(6): 953-958.

Yu, J., A. J. Yool, K. Schulten and E. Tajkhorshid (2006). "Mechanism of gating and ion conductivity of a possible tetrameric pore in aquaporin-1." Structure **14**(9): 1411-1423.

Zampighi, G. A., J. E. Hall and M. Kreman (1985). "Purified Lens Junctional Protein Forms Channels in Planar Lipid Films." Proceedings of the National Academy of Sciences of the United States of America **82**(24): 8468-8472.

Zhang, D. Y., Z. Ali, C. B. Wang, L. Xu, J. X. Yi, Z. L. Xu, X. Q. Liu, X. L. He, Y. H. Huang, I. A. Khan, R. M. Trethowan and H. X. Ma (2013). "Genome-wide sequence characterization and expression analysis of major intrinsic proteins in soybean (Glycine max L.)." PLoS One **8**(2): e56312.

Zhao, D., L. Bankir, L. M. Qian, D. Y. Yang and B. X. Yang (2006). "Urea and urine concentrating ability in mice lacking AQP1 and AQP3." American Journal of Physiology-Renal Physiology **291**(2): F429-F438.

Figure legends

Figure 1: Osmotic water permeability assays confirm the expression of AQP1, AQP4, AQP5, AtPIP2;7, AtPIP2;2, and AtPIP2;1 channels on xenopus oocyte membranes. (A) Mean of swelling responses as a function of time of HsAQP1, AtPIP2;7, AtPIP2;2, and AtPIP2;1 expressing oocytes in 50% hypotonic saline. Water injected oocytes showed significantly lower changes in volume. Data are mean values for all oocytes assessed from different batches; error bars are S.E.M.; n = 6 per treatment group. (B) Box plots of swelling rates calculated from the data in A.

Figure 2: Effects of Mg^{2+} and Ca^{2+} divalent cations on ionic current responses in oocytes expressing different classes of AQPs. (A) Superimposed currents as a function of time measured by voltage clamp steps from -110 to +60 mV, from a holding potential of -40 mV at maximal activation in divalent free saline (left), after application of Mg2+ (middle), and after application of Ca^{2+} (right). Control and AtPIP2;7-expressing oocytes lacked appreciable ionic conductances. (B) Current voltage relationships for the traces illustrated in A. (D) Box plot summary of the ionic conductance responses compiled for AQP types and treatments. **** ($p<0.0001$); ** ($p < 0.01$); * ($p < 0.05$); NS (not significant). n values are in italics above the x-axis. The data presented in A is summarized as box plots of ionic conductance in B. (C) Standardized current-voltage relationships for the traces illustrated in A.

Figure 3: AtPIP2;1, AtPIP2;2 AQP1 and BIB ion channels display a voltage dependent unblocking of the outward current in response to $BaCl_2$ treatment (A) Electrophysiology

traces recorded at initial or after activation (before treatment) and after bath application of 1 mM $BaCl_2$. (B) Ionic conductance as box plots of the data presented in A. (C) Current-voltage relationships for data presented in A. (D) Diagram of relative rectification for HsAQP1, AtPIP2;1 and AtPIP2;2 and BIB channels recorded before and after Ba^{2+} application. Rectification values are the ratios of currents at +60 to that at -80 mV. Asterisks indicate significance (*p < 0.01, ** p <0.001, one-way ANOVA, Bonferroni post-hoc test).

Figure 4: HsAQP1, BIB, AtPIP2;1 and AtPIP2;2 channels are sensitive to block by cadmium. (A) Superimposed current as a function of time for each clamped membrane potential illustrating the effect of $CdCl_2$ on HsAQP1, HsAQP4, HsAQP5, AtPIP2;1 and AtPIP2;2 channels recorded in divalent free saline initially and after the bath application of 1 mM $CdCl_2$. (B) Current voltage relationship for traces illustrated in A. (C) Decrease in current amplitude with time after bath application of 1 mM $CdCl_2$ in recording saline monitored with repeated steps to +40 mV. (D) Summary box plots of the ionic conductance illustrating the effect of 1 mM $CdCl_2$ on HsAQP1, AtPIP2;1 and AtPIP2;2 ion channels. (E) Summary of outward rectification for HsAQP1, AtPIP2;1 and AtPIP2;2 and BIB channels recorded at initial (before $CdCl_2$ application) and after bath application of 1 mM $CdCl_2$. Rectification values are the ratio of current measured at +60 to that at -80 mV. Asterisks indicate significance (*p < 0.01, ** p <0.001, one-way ANOVA, Bonferroni post-hoc test).

Figure 5: Accumulative effect of subsequent application of Ca^{2+} followed by Ba^{2+} on different classes of AQP channels. (A) Superimposed traces showing the accumulative effect of Ca^{2+} followed by Ba^{2} application on AtPIP2;2, AtPIP2;1, HsAQP1 and BIB expressing oocytes recorded in divalent-free saline (left), after perfusion of saline containing the indicated amount of free Ca2+ (middle), and after application of Ba2+ in the continuing presence of the same concentration of Ca^{2+} (right) (B) Summary box plots of the ionic conductance in AtPIP2;2, AtPIP2;1, HsAQP1 and BIB expressing oocytes in different divalent salines. **** ($p<0.0001$); ** ($p < 0.01$);* ($p < 0.05$); NS (not significant); n values are above the x-axis (C) Current-voltage relationships for traces shown in A.

Figure 6: AqB011 blocks the HsAQP1 ionic conductance but not that carried by AtPIP2;1 and AtPIP2;2. (A) Traces recorded initially for AtPIP2;1 and AtPIP2;2 or after cGMP activation of HsAQP1, and after incubation in AqB011. HsAQP1 expressing oocytes were incubated in 20 μM AqB011 for 2 h and did not reactivate in response to a second cGMP application. AtPIP2;1 and AtPIP2;2 expressing oocytes were incubated in 100 μM AqB011 and remained unblocked after 2 h of incubation. (B) Box plot summary of the conductance levels before and after treatment with AqB011. **** ($p<0.0001$); NS (not significant); n values are below the x-axis.

Figure 7: Amino acid sequence alignment of HsAQP1, HsAQP4, HsAQP5, AtPIP2;1, AtPIP2;2, AtPIP2;7 and DmBIB. Subunit topology domains were assigned by structural prediction software (http://www.cbs.dtu.dk/services/TMHMM/) and visual inspection.

Amino acid sequences from the Protein Data Bank (PDB) were aligned using Clustal Omega (http://www.ebi.ac.uk/Tools/msa/clustalo/). Symbols: asterisk (*) identical residues across all sequences; colon (:) conserved substitutions; period (.) semi-conserved substitutions. Colors illustrate physiochemical properties: basic (magenta), acidic (blue), amine or sulfhydryl groups (green), small hydrophobic (red). Highlighted in yellow is the NPA (Asn-Pro-Ala) signature motif located in loops B and E, conserved in most aquaporins.

Figures

Figure 1

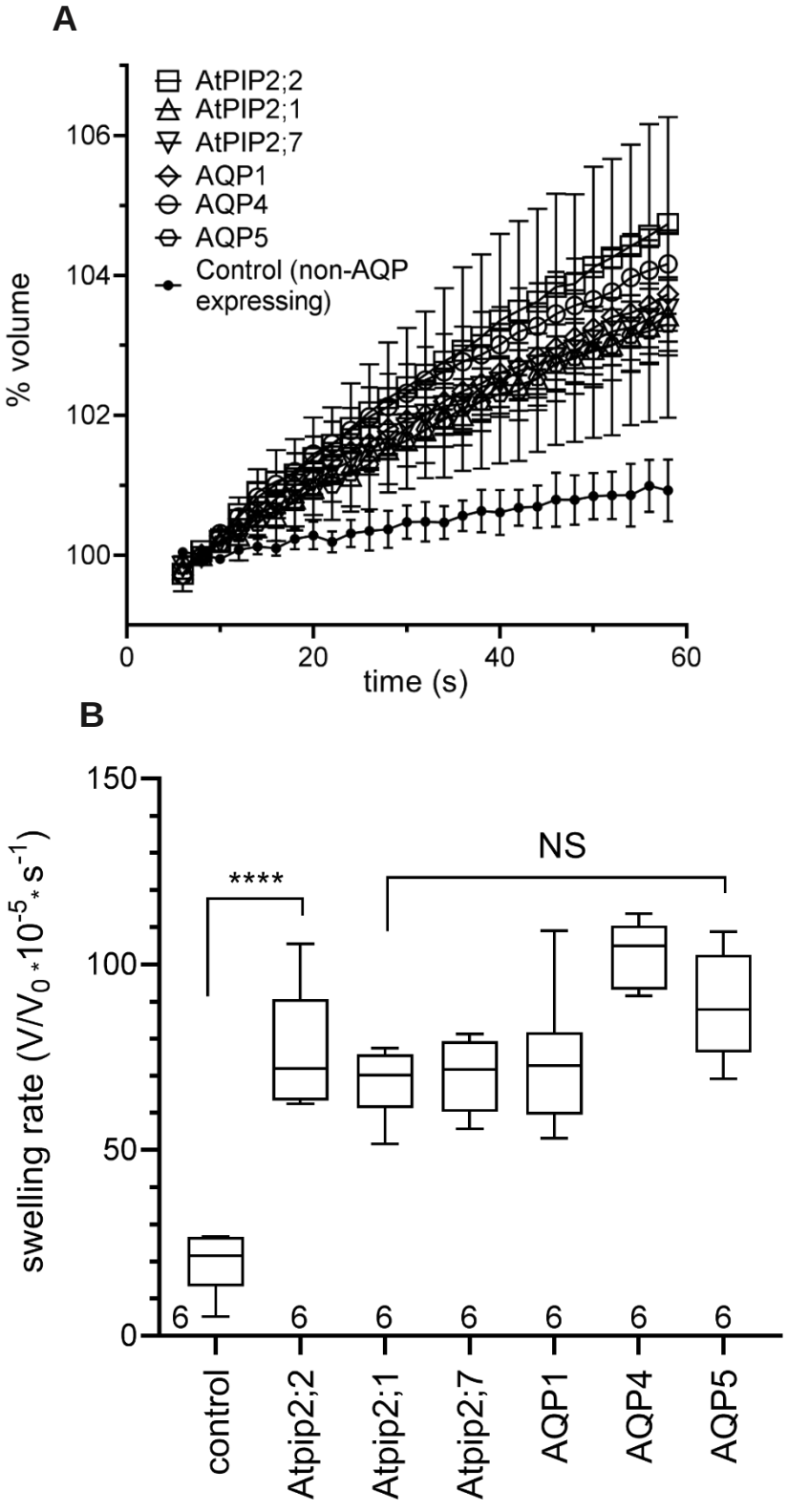

Figure 2

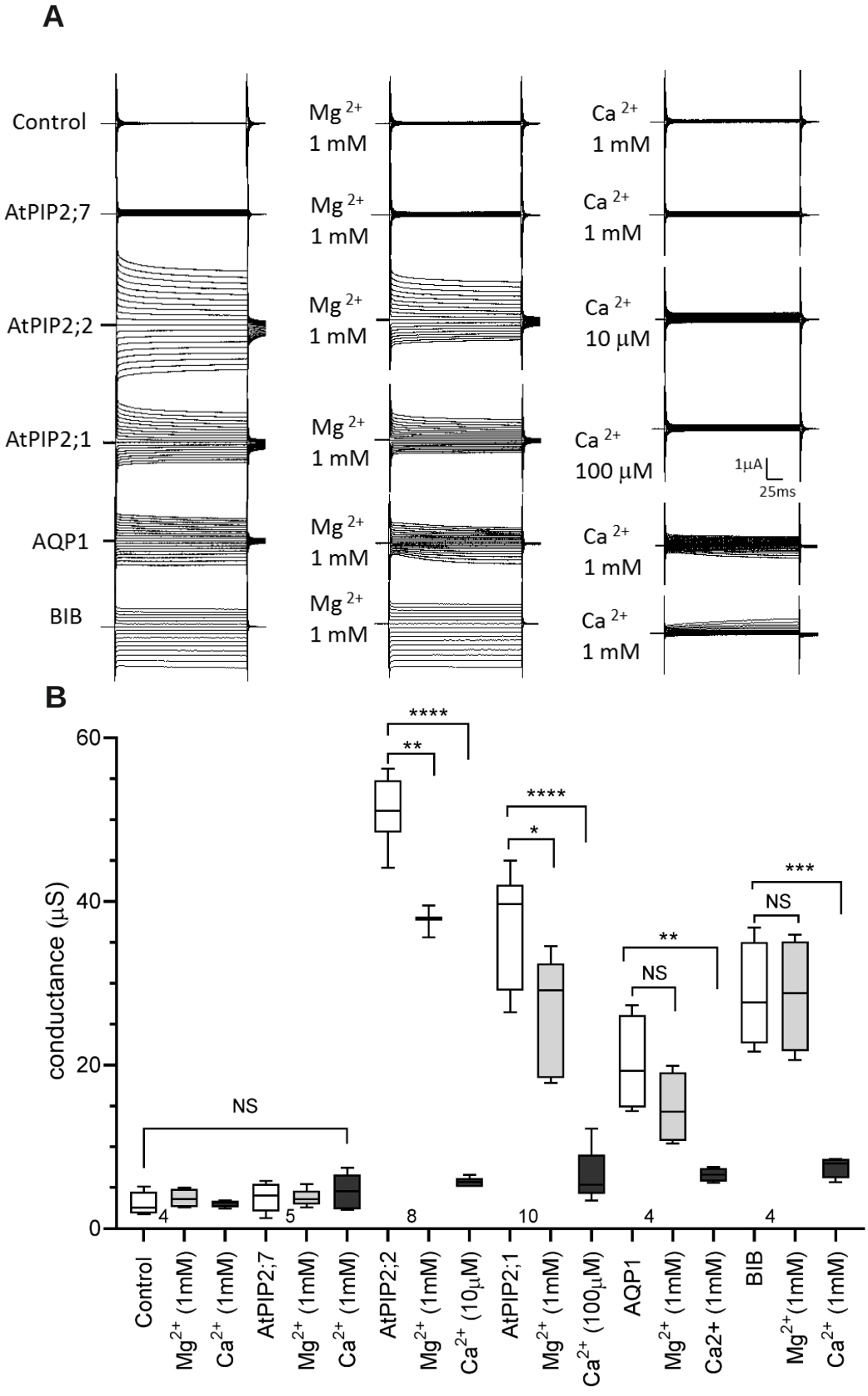
A
Control
AtPIP2;7
AtPIP2;2
AtPIP2;1
AQP1
BIB
Mg 2+ 1 mM
Ca 2+ 1 mM
Ca 2+ 10 µM
Ca 2+ 100 µM
1µA
25ms
B
conductance (µS)
0
20
40
60
NS
**
****
*
***
4
5
8
10
4
4
Control
Mg2+ (1mM)
Ca2+ (1mM)
AtPIP2;7
Mg2+ (1mM)
Ca2+ (1mM)
AtPIP2;2
Mg2+ (1mM)
Ca2+ (10µM)
AtPIP2;1
Mg2+ (1mM)
Ca2+ (100µM)
AQP1
Mg2+ (1mM)
Ca2+ (1mM)
BIB
Mg2+(1mM)
Ca2+ (1mM)

C

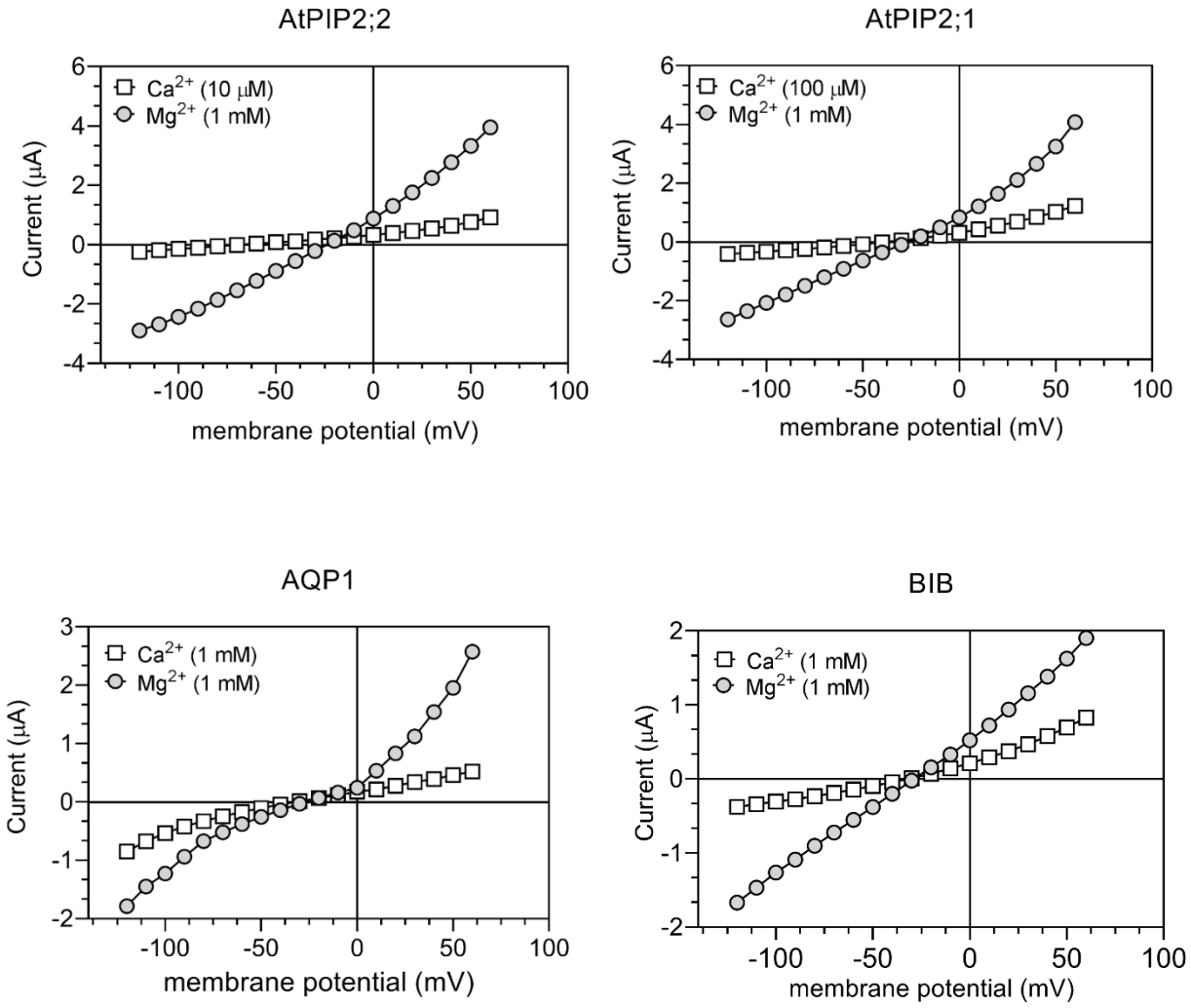
AtPIP2;2
Ca2+ (10 μM)
Mg2+ (1 mM)
Current (μA)
membrane potential (mV)
AtPIP2;1
Ca2+ (100 μM)
Mg2+ (1 mM)
Current (μA)
membrane potential (mV)
AQP1
Ca2+ (1 mM)
Mg2+ (1 mM)
Current (μA)
membrane potential (mV)
BIB
Ca2+ (1 mM)
Mg2+ (1 mM)
Current (μA)
membrane potential (mV)

Figure 3

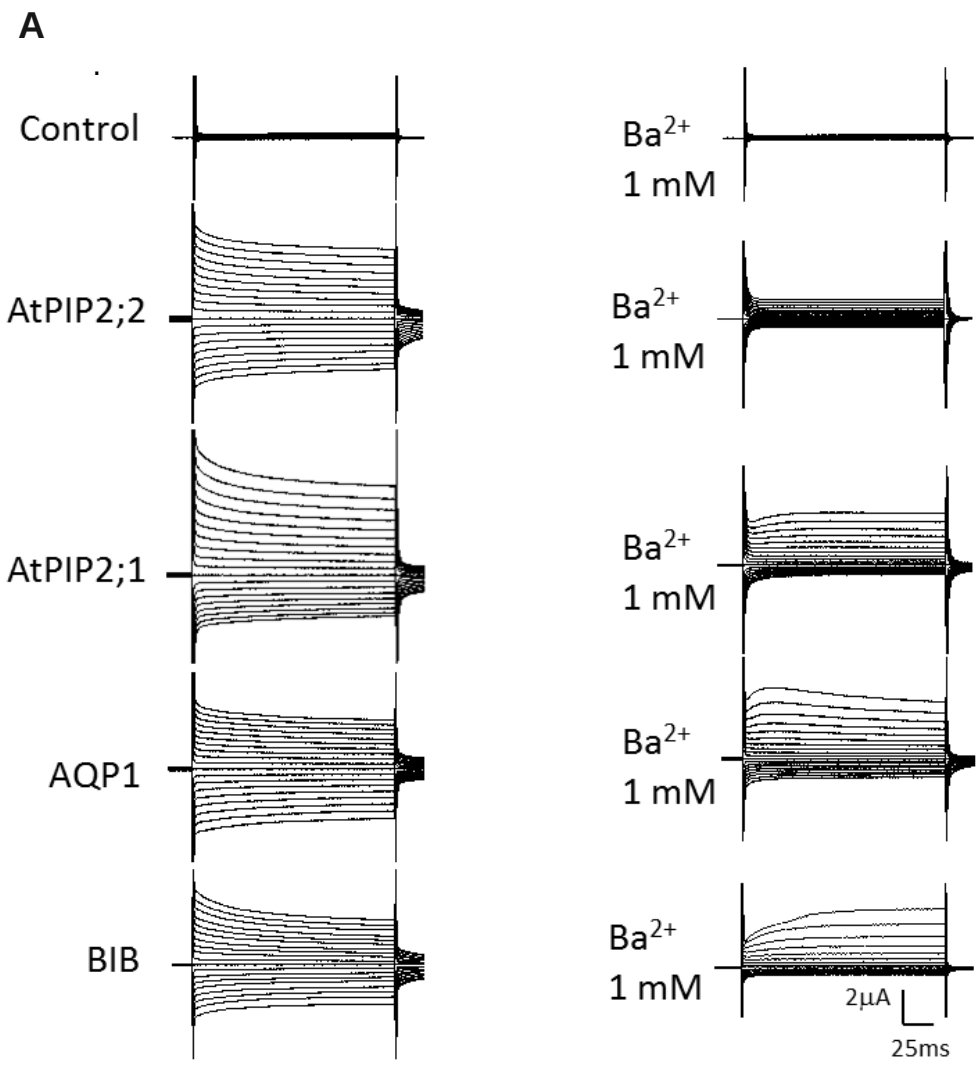
A
Control
AtPIP2;2
AtPIP2;1
AQP1
BIB
Ba2+
1 mM
Ba2+
1 mM
Ba2+
1 mM
Ba2+
1 mM
Ba2+
1 mM
2µA
25ms

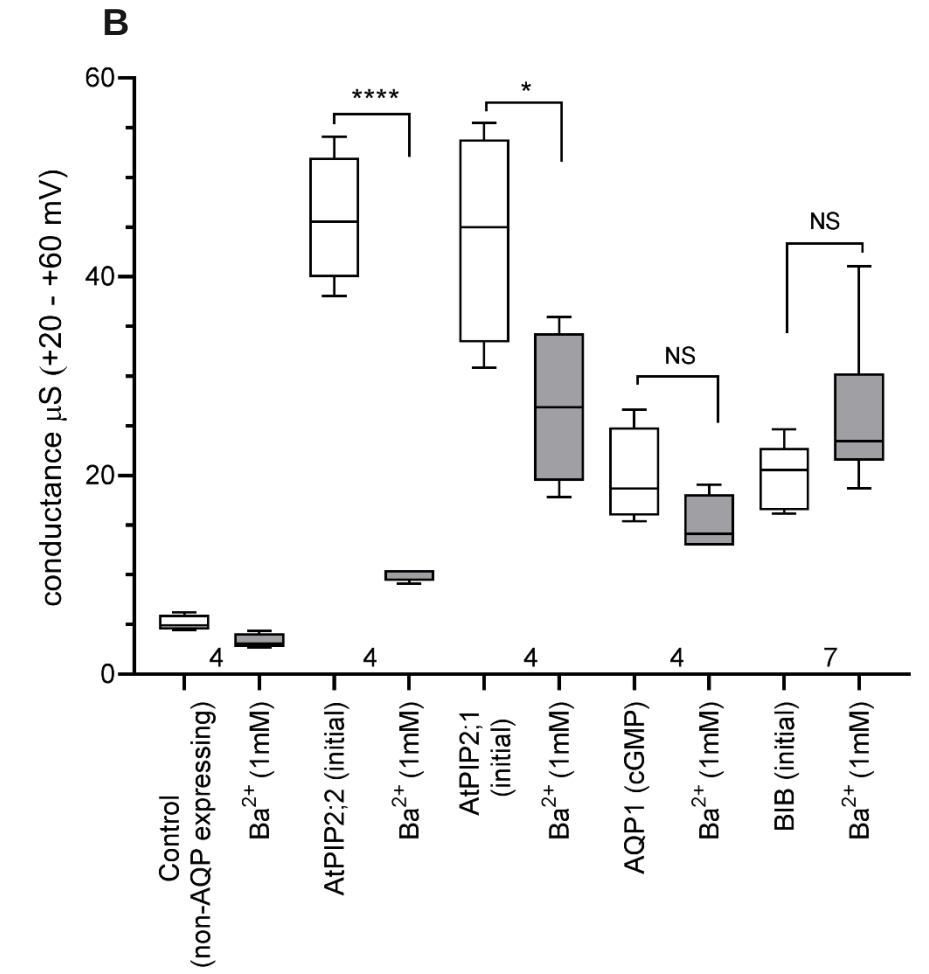
B
conductance µS (+20 - +60 mV)
60
40
20
0
****
*
NS
NS
4
4
4
4
7
Control (non-AQP expressing)
Ba2+ (1mM)
AtPIP2;2 (initial)
Ba2+ (1mM)
AtPIP2;1 (initial)
Ba2+ (1mM)
AQP1 (cGMP)
Ba2+ (1mM)
BIB (initial)
Ba2+ (1mM)

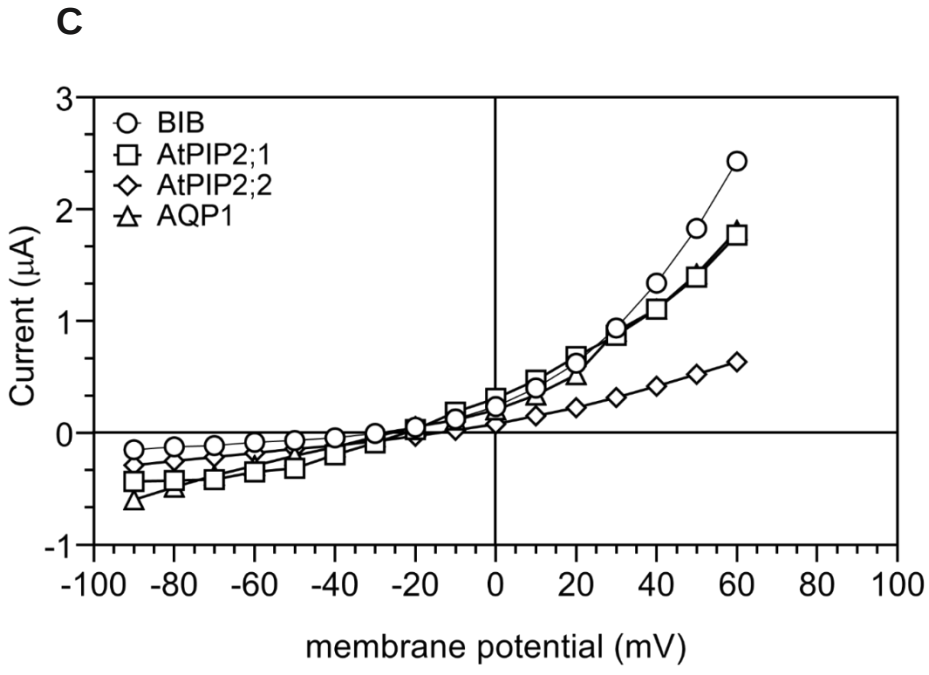
C
BIB
AtPIP2;1
AtPIP2;2
AQP1
Current (µA)
3
2
1
0
-1
-100
-80
-60
-40
-20
0
20
40
60
80
100
membrane potential (mV)

D

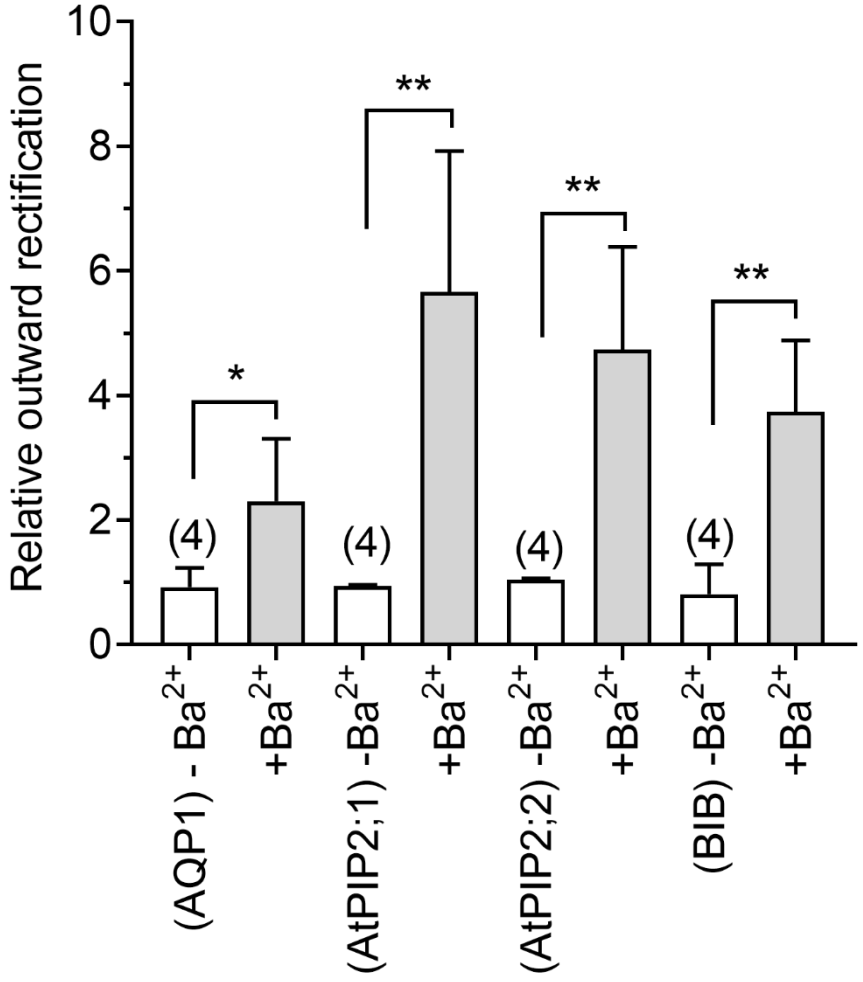
Relative outward rectification
10
8
6
4
2
0
*
**
**
**
(4)
(4)
(4)
(4)
(AQP1) - Ba2+
+Ba2+
(AtPIP2;1) -Ba2+
+Ba2+
(AtPIP2;2) -Ba2+
+Ba2+
(BIB) -Ba2+
+Ba2+

Figure 4

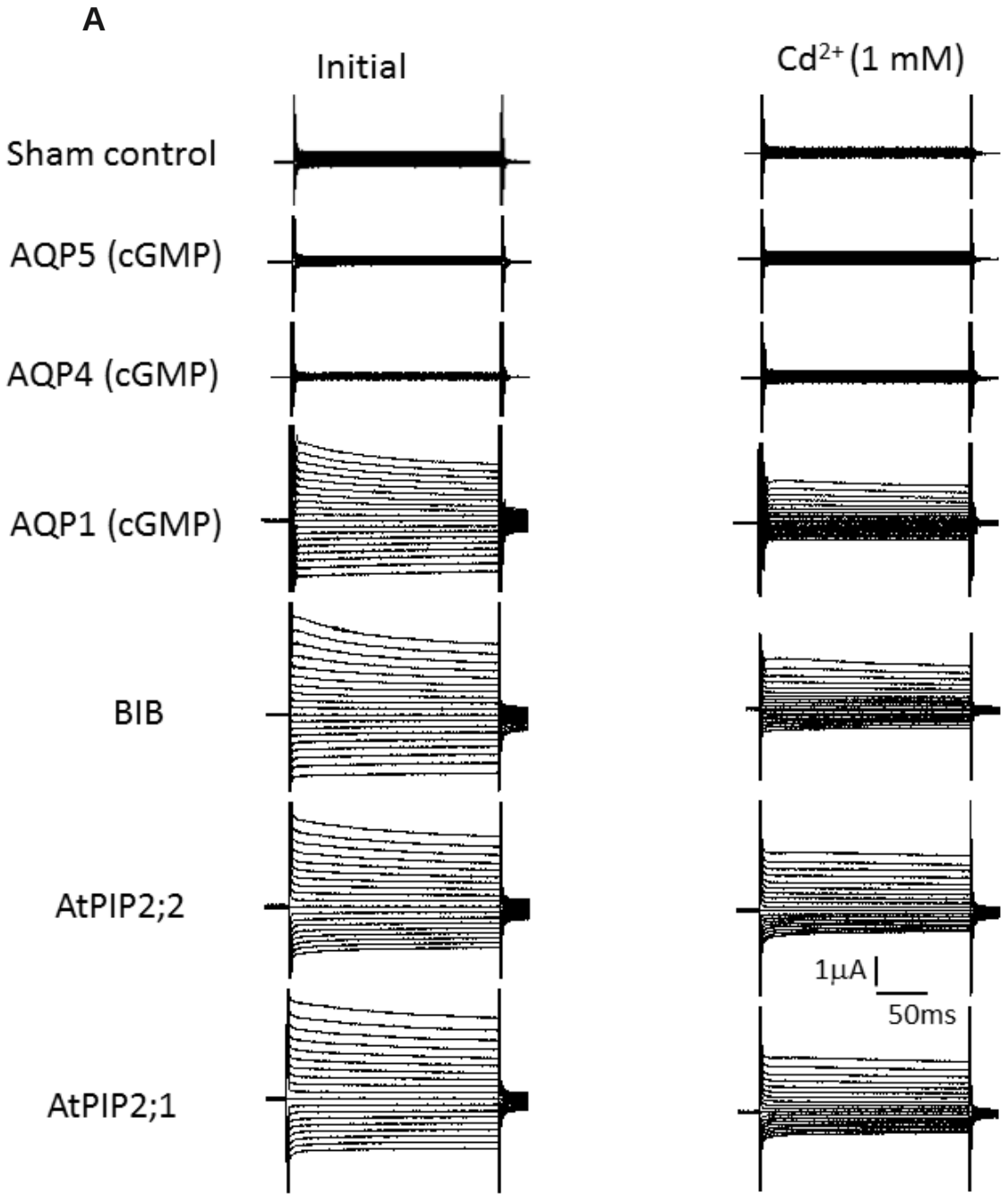
A
Initial
Cd2+ (1 mM)
Sham control
AQP5 (cGMP)
AQP4 (cGMP)
AQP1 (cGMP)
BIB
AtPIP2;2
AtPIP2;1
1μA
50ms

B

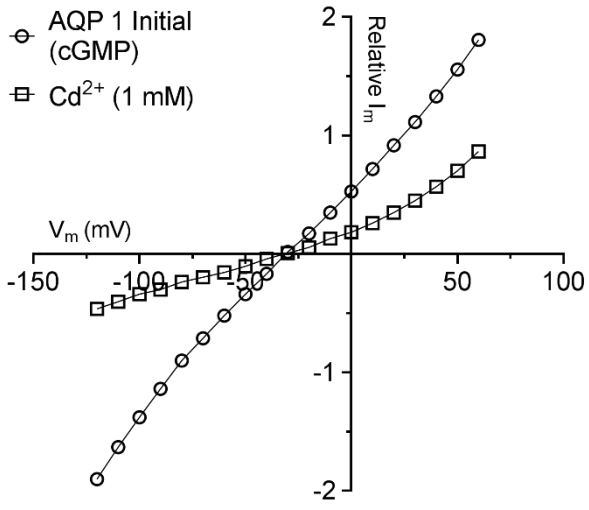
AQP 1 Initial
(cGMP)
Cd2+ (1 mM)
Relative Im
Vm (mV)
-150
-100
-50
50
100
2
1
-1
-2

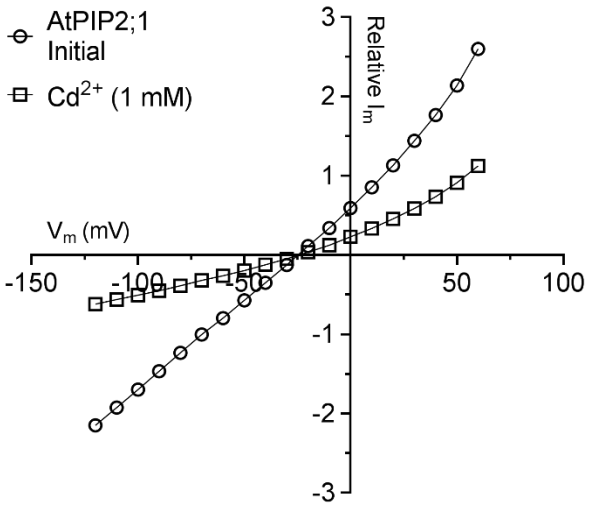
AtPIP2;1
Initial
Cd2+ (1 mM)
Relative Im
Vm (mV)
-150
-100
-50
50
100
3
2
1
-1
-2
-3

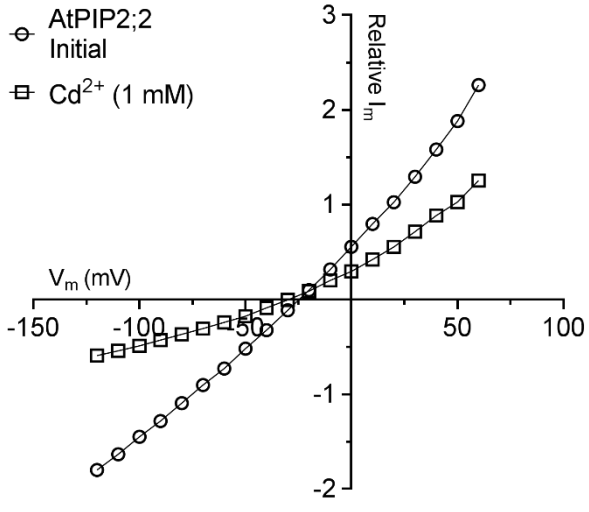
AtPIP2;2
Initial
Cd2+ (1 mM)
Relative Im
Vm (mV)
-150
-100
-50
50
100
3
2
1
-1
-2

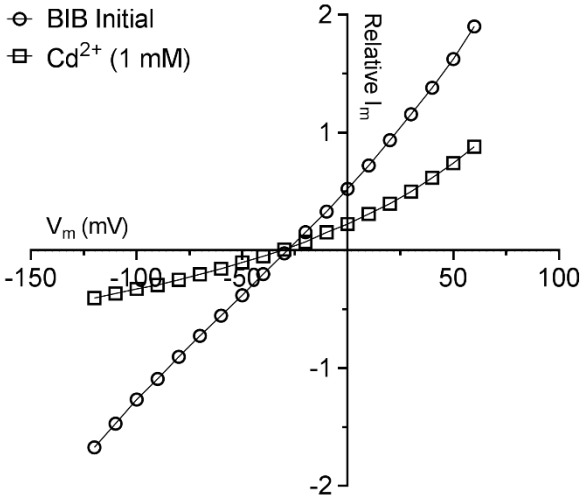
BIB Initial
Cd2+ (1 mM)
Relative Im
Vm (mV)
-150
-100
-50
50
100
2
1
-1
-2

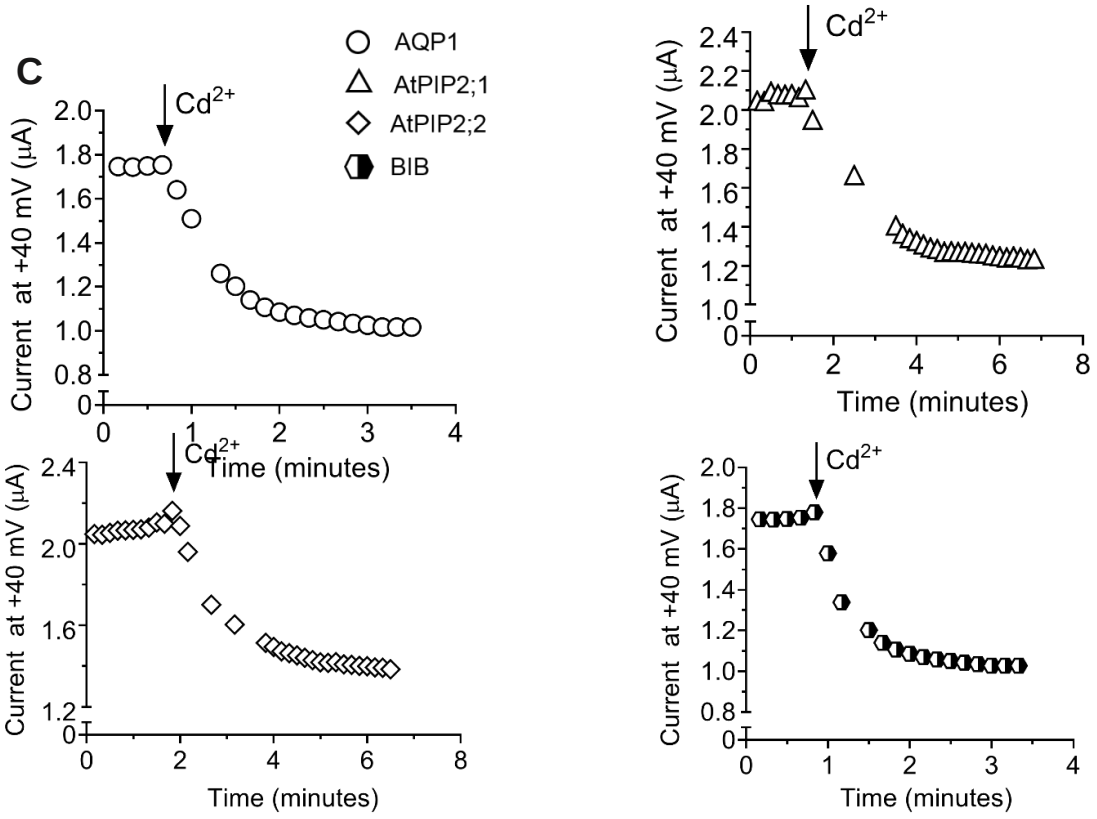
C
AQP1
AtPIP2;1
AtPIP2;2
BIB
Cd2+
Current at +40 mV (μA)
Time (minutes)

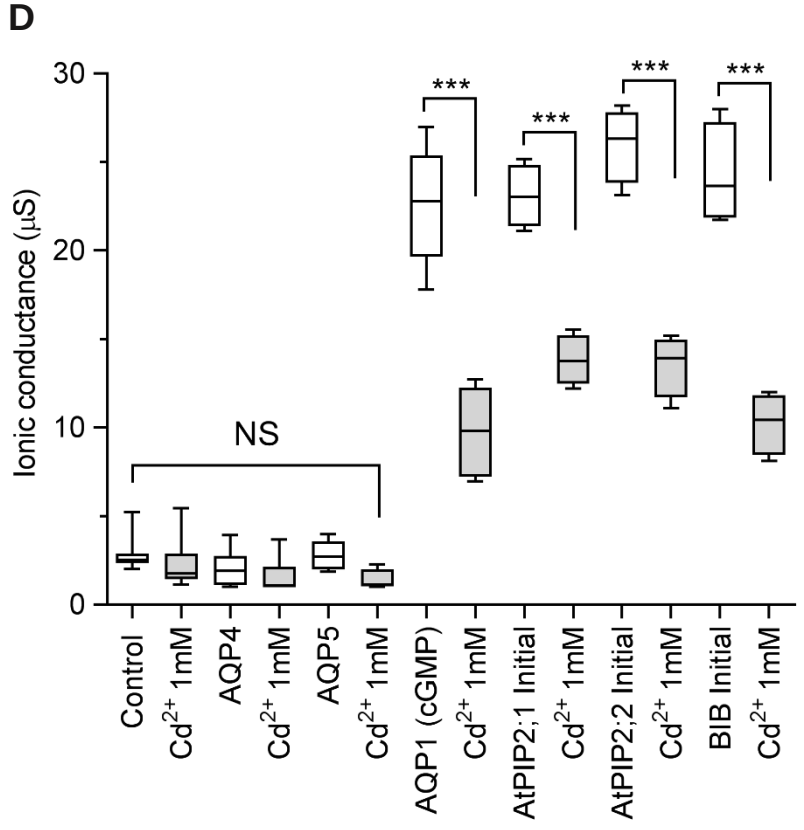
D
Ionic conductance (μS)
NS
***
Control
Cd2+ 1mM
AQP4
AQP5
AQP1 (cGMP)
AtPIP2;1 Initial
AtPIP2;2 Initial
BIB Initial

E

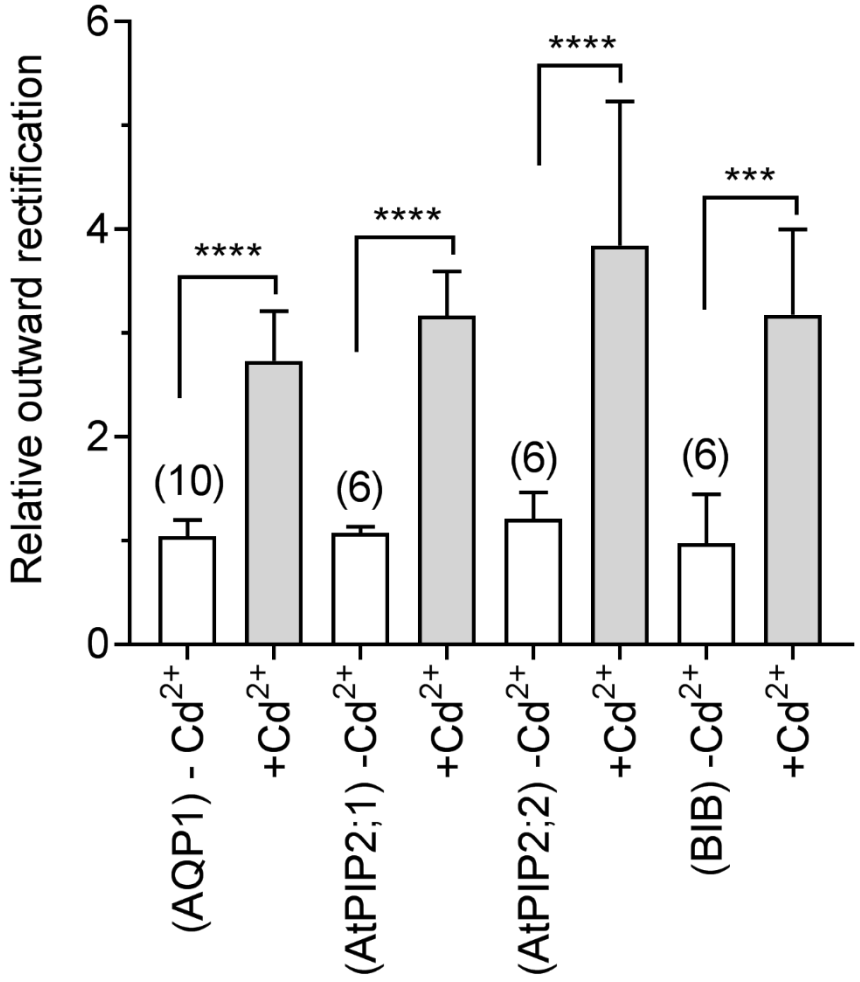
Relative outward rectification
6
4
2
0
****
****
****
***
(10)
(6)
(6)
(6)
(AQP1) - Cd2+
+Cd2+
(AtPIP2;1) -Cd2+
+Cd2+
(AtPIP2;2) -Cd2+
+Cd2+
(BIB) -Cd2+
+Cd2+

Figure 5

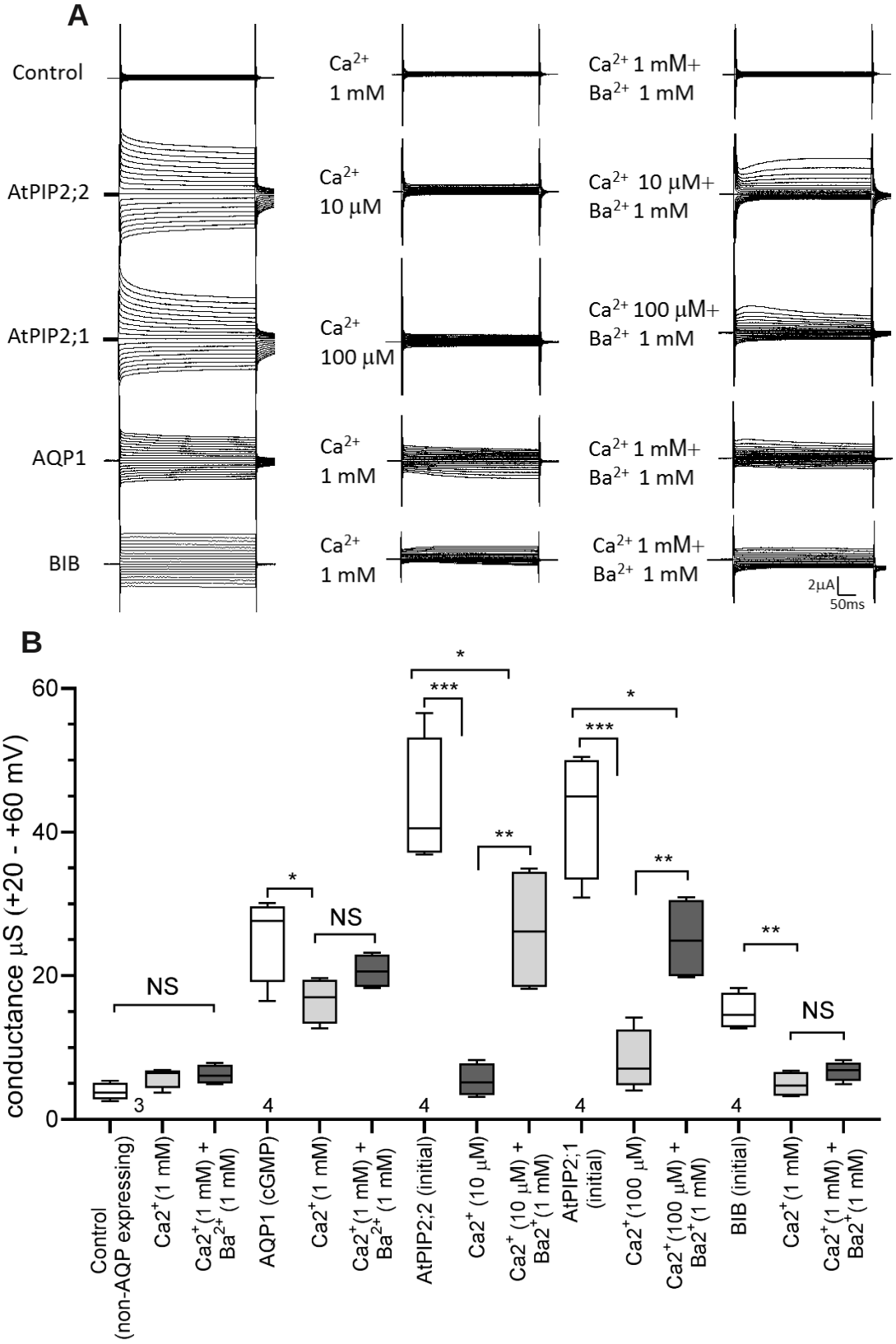
A
Control
AtPIP2;2
AtPIP2;1
AQP1
BIB
Ca2+ 1 mM
Ca2+ 10 µM
Ca2+ 100 µM
Ca2+ 1 mM
Ca2+ 1 mM
Ca2+ 1 mM+ Ba2+ 1 mM
Ca2+ 10 µM+ Ba2+ 1 mM
Ca2+ 100 µM+ Ba2+ 1 mM
Ca2+ 1 mM+ Ba2+ 1 mM
Ca2+ 1 mM+ Ba2+ 1 mM
2µA
50ms
B
conductance µS (+20 - +60 mV)
60
40
20
0
NS
NS
NS
*
*
*
***
**
*
***
**
**
3
4
4
4
4
Control (non-AQP expressing)
Ca2+(1 mM)
Ca2+(1 mM) + Ba2+(1 mM)
AQP1 (cGMP)
Ca2+(1 mM)
Ca2+(1 mM) + Ba2+(1 mM)
AtPIP2;2 (initial)
Ca2+ (10 µM)
Ca2+ (10 µM) + Ba2+(1 mM)
AtPIP2;1 (initial)
Ca2+(100 µM)
Ca2+(100 µM) + Ba2+(1 mM)
BIB (initial)
Ca2+(1 mM)
Ca2+(1 mM) + Ba2+(1 mM)

C

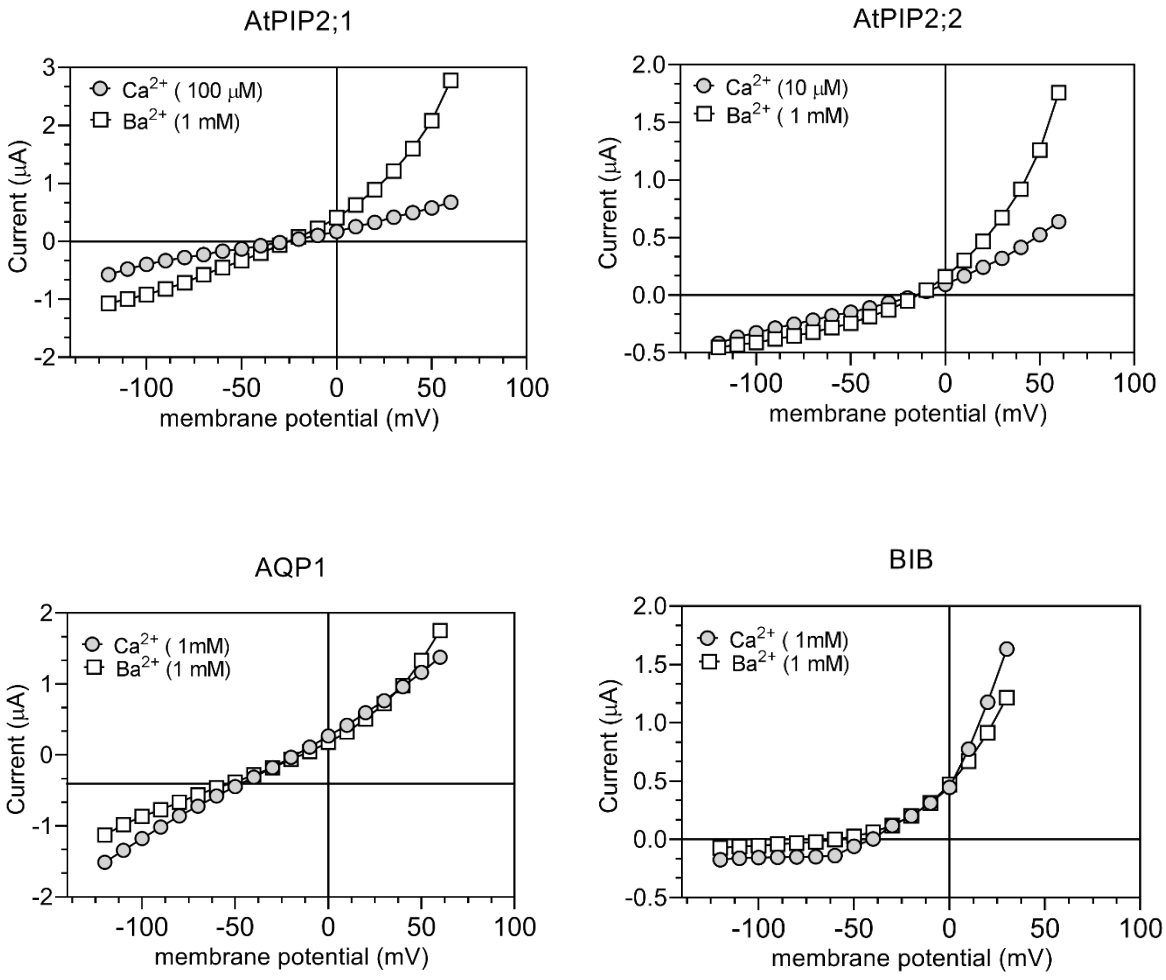
AtPIP2;1
Ca2+ (100 μM)
Ba2+ (1 mM)
Current (μA)
membrane potential (mV)
AtPIP2;2
Ca2+ (10 μM)
Ba2+ (1 mM)
Current (μA)
membrane potential (mV)
AQP1
Ca2+ (1mM)
Ba2+ (1 mM)
Current (μA)
membrane potential (mV)
BIB
Ca2+ (1mM)
Ba2+ (1 mM)
Current (μA)
membrane potential (mV)

Figure 6

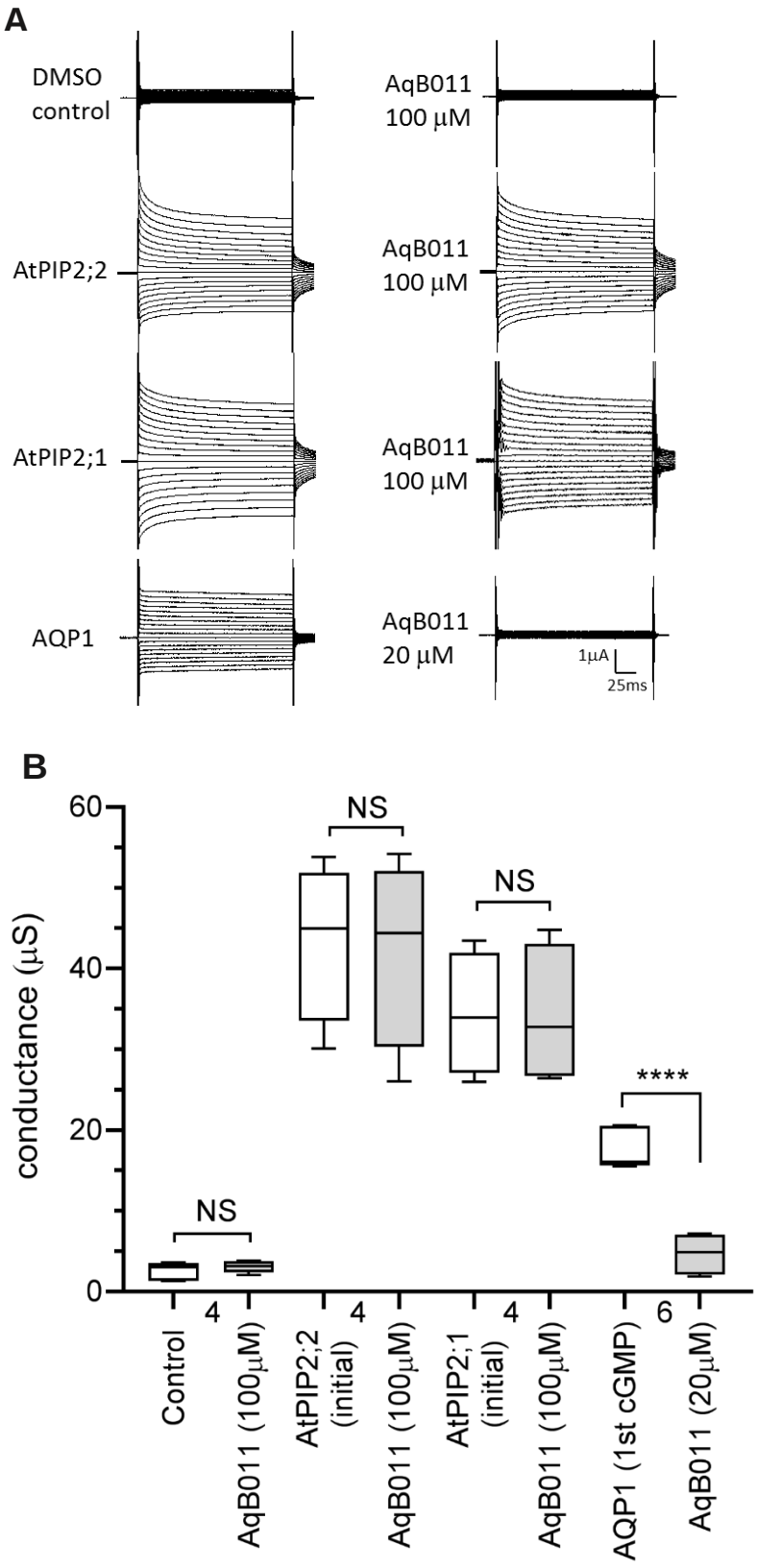
A
DMSO control
AtPIP2;2
AtPIP2;1
AQP1
AqB011 100 µM
AqB011 100 µM
AqB011 100 µM
AqB011 20 µM
1µA
25ms
B
conductance (µS)
60
40
20
0
NS
NS
NS
****
4
4
4
6
Control
AqB011 (100µM)
AtPIP2;2 (initial)
AqB011 (100µM)
AtPIP2;1 (initial)
AqB011 (100µM)
AQP1 (1st cGMP)
AqB011 (20µM)

Figure 7

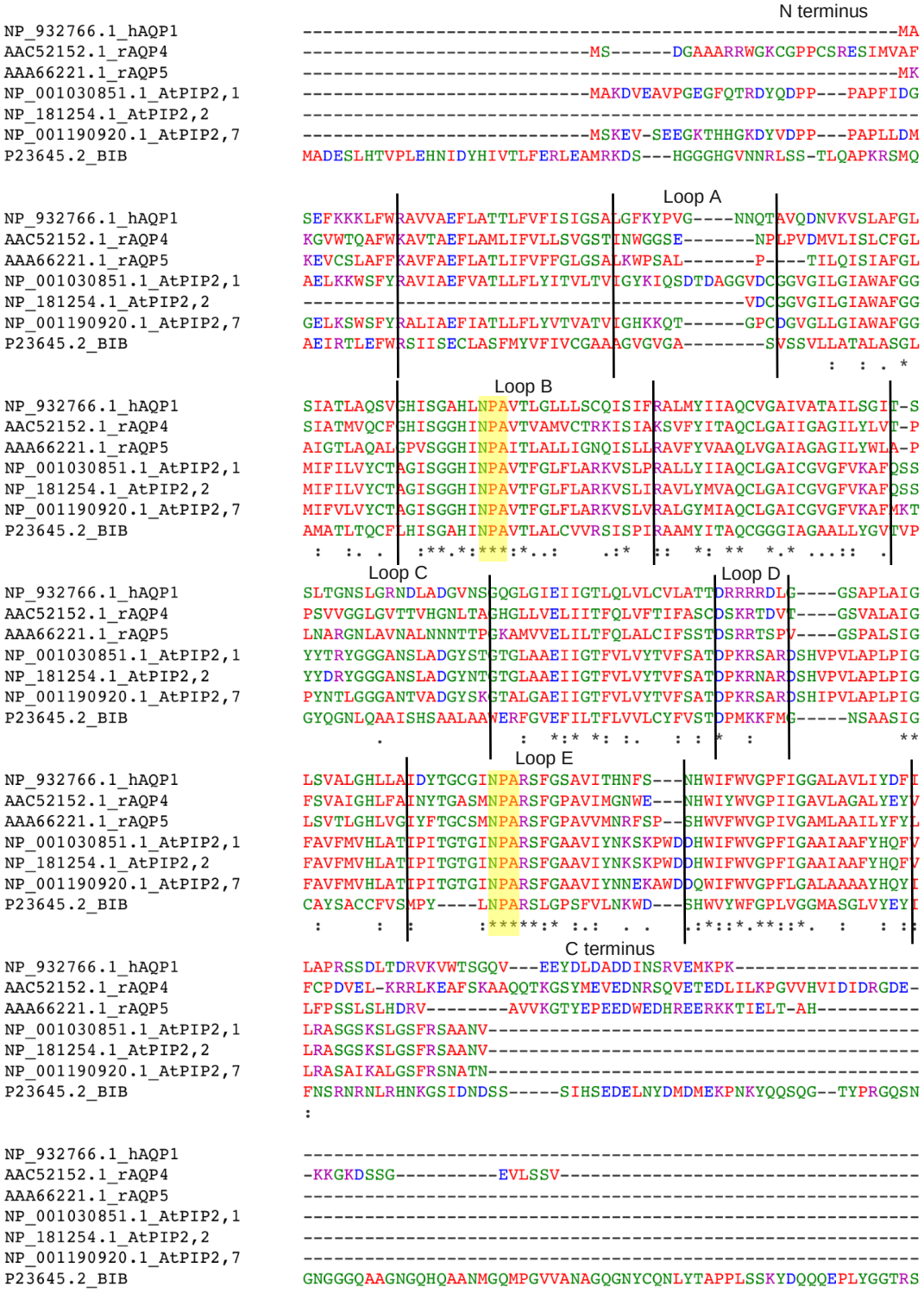
N terminus
Loop A
Loop B
Loop C
Loop D
Loop E
C terminus
NP_932766.1_hAQP1
AAC52152.1_rAQP4
AAA66221.1_rAQP5
NP_001030851.1_AtPIP2,1
NP_181254.1_AtPIP2,2
NP_001190920.1_AtPIP2,7
P23645.2_BIB

CONCLUSION

Mohamad Kourghi

Water is an essential compound for survival. Its homeostasis is mediated by a group of Membrane Intrinsic Proteins (MIP) known as Aquaporins (AQPs) found in all kingdoms of life. Not only do AQPs maintain water homeostasis, they also allow pathways for ion transport in a subset of AQPs. The mammalian AQPs 0, 1, and 6, the insect Drosophila big brain (BIB), and the plant nodulin 26, AtPIP2;1 and AtPIP2;2 channels have been shown to have ionic activity (Yool and Campbell 2012, Byrt, Zhao et al. 2016). AQP1 might be an unusual member of the mammalian AQP family, given its ability to allow water permeability through the individual pores of the tetramer and cationic transport at the central pore gated via cGMP (Anthony, Brooks et al. 2000, Yu, Yool et al. 2006), however other classed of AQPs might yet be found to act as ion channels when the correct array of stimuli are identified. Whether the ionic transport through AQP1 was of physiological relevance was an area of debate (Saparov, Kozono et al. 2001). Recent evidence supporting a functional role of the AQP1 ion channel in processes such as cancer cell migration (Kourghi, Pei et al. 2016, Pei, Kourghi et al. 2016) has opened the door for new research opportunities. AQP1 plays an important role in migration and metastasis of subtypes of aggressive cancers such as mammary, melanoma, astrocytoma and glioblastoma (Hu and Verkman 2006, McCoy and Sontheimer 2007, El Hindy, Bankfalvi et al. 2013). Therefore it is possible that if we can impair water transport by blocking AQP1 channels, we can slow down the rate of cancer cell migration.

Results gained using newly developed pharmacological inhibitors of the ion channel and the water channels of AQP1 (Kourghi, Pei et al. 2016, Pei, Kourghi et al. 2016)

have shown that both play a significant role in the migration of cancer cells. Two AQP1 ion channel blockers AqB007 and AqB011, from a custom library of bumetanide derivatives synthesised by collaborator Dr Gary Flynn (Spacefill Enterprises; Montana USA), are specific blockers of the AQP1 central pore, without inhibiting the water permeability of AQP1 (Kourghi, Pei et al. 2016). Results have shown that AqB011 is the more potent blocker with an IC_{50} value of 14 μM. AqB007 and AqB011 were tested in two colon cancer cell lines: HT29 with high AQP1 expression, and SW480 with high AQP5 expression, evaluating effects on migration rate using wound closure assay. Both compounds, AqB007 and AqB011 slowed down the rate of wound closure in HT29 cancer cells, without appreciable effects on SW480 cells, indicating that the inhibitory effects of the compounds are likely to be selective for AQP1. AqB011 caused a greater block of migration as compared to AqB007, as predicted from the relative order of potency observed in electrophysiology analyses or AQP1 channels recorded in the Xenopus oocyte expression system (Kourghi, Pei et al. 2016).

Molecular docking analysis predicted a pair of arginine residues located in positions 159 and 160 in loop of D domain of human AQP1 to be the interaction site for the blocker AqB011 (Chapter 3 in this thesis). This prediction was tested using voltage clamp recordings of a double arginine mutant construct AQP1 R159A+R160A, which showed no sensitivity to block. These data supported the in silico model, showing that the gating loop D domain is necessary for AqB011-mediated block of the AQP1 central pore. Taken together our findings have demonstrated that AQP1 ion channel function is physiologically important in facilitating migration of cancer cells, and blocking AQP1 ionic conductance can significantly reduce migration in cancer cells expressing AQP1.

Further research in the field has led to the discovery of two additional AQP1 water channel inhibitors, bacopaside I and bacopaside II, derived from the medicinal plant *Bacopa monnieri*. Results showed that bacopaside II is a potent blocker with an IC_{50} value of 14 μM compared to bacopaside I (IC_{50} 48 μM). Wound closure experiments conducted on HT29 cancer cell lines revealed that both bacopaside I and bacopaside II slowed down the rate of migration in HT29 cell lines (Pei, Kourghi et al. 2016). It will be interesting to test whether combined block of ionic conductance with AqB011 and water flux with Bacopaside II could have synergistic effect in blocking cancer cell migration in cell lines expressing AQP1. The newly identified AQP1 water and ion channel blockers open the opportunity for in vitro and in vivo experiments to test these AQP1 water and ion channel functions in vivo, and possibly in future clinical trials.

AQP1 is also highly expressed in cell membrane of red blood cells (RBCs). Sickle cell anaemia is a genetic disorder that affects RBCs, caused by inherited mutations in the oxygen-carrying haemoglobin (Hb) molecule. Dehydration of the affected RBCs leads to aggregation of HbS, forming long polymers that induce the sickling morphology characteristic of sickle cell anaemia.. This change in morphology of RBC follows the activation of a leak pathway known as the P_{sickle} current; loss of cations from the cell causes dehydration, promoting the sickle state of RBC. 5-hydroxymethyl furfural (5HMF) is an agent used to reduce the severity of the disease, however the target site is not well understood. We have shown that 5HMF is a blocker of AQP1 ion channel. Therefore it is possible that 5HMF is preventing the leak current and promoting the hydration state of RBC via targeting AQP1 ion channels. Therefore it is possible to further enhance the hydration state of RBC and reduce the sickling via a more potent blocker such as AqB011, yet to be validated by in vivo experiments.

Our research has led to the discovery of two new AQP ion channels, AtPIP2;1 and AtPIP2;2 from the plant AQP family. Based on experimental recordings it's suggested that they may function as a non-selective cation channel through the central pore, much like the AQP1 channel. Both AtPIP2;1 and AtPIP2;2 are highly sensitive to calcium, and this could be an important physiological role, particularly in response to stress. This finding has opened new research opportunities to investigate the physiological implications of AtPIP2;1 and AtPIP2;2 ion channels. One possible suggestion could be improving salt tolerance in plants (Byrt, Zhao et al. 2016).

These findings helps to reform our perception of AQPs as just simple water channels and opens new exciting opportunities to further investigate the importance and the diverse roles that AQP ion channels can play in physiology and pathology.

References

Anthony, T. L., H. L. Brooks, D. Boassa, S. Leonov, G. M. Yanochko, J. W. Regan and A. J. Yool (2000). "Cloned human aquaporin-1 is a cyclic GMP-gated ion channel." Mol Pharmacol **57**(3): 576-588.

Byrt, C. S., M. Zhao, M. Kourghi, J. Bose, S. W. Henderson, J. Qiu, M. Gilliham, C. Schultz, M. Schwarz, S. A. Ramesh, A. Yool and S. Tyerman (2016). "Non-selective cation channel activity of aquaporin AtPIP2;1 regulated by Ca2+ and pH." Plant Cell Environ.

El Hindy, N., A. Bankfalvi, A. Herring, M. Adamzik, N. Lambertz, Y. Zhu, W. Siffert, U. Sure and I. E. Sandalcioglu (2013). "Correlation of aquaporin-1 water channel protein expression with tumor angiogenesis in human astrocytoma." Anticancer Res **33**(2): 609-613.

Hu, J. and A. S. Verkman (2006). "Increased migration and metastatic potential of tumor cells expressing aquaporin water channels." FASEB J **20**(11): 1892-1894.

Kourghi, M., J. V. Pei, M. L. De Ieso, G. Flynn and A. J. Yool (2016). "Bumetanide Derivatives AqB007 and AqB011 Selectively Block the Aquaporin-1 Ion Channel Conductance and Slow Cancer Cell Migration." Mol Pharmacol **89**(1): 133-140.

McCoy, E. and H. Sontheimer (2007). "Expression and function of water channels (aquaporins) in migrating malignant astrocytes." Glia **55**(10): 1034-1043.

Pei, J. V., M. Kourghi, M. L. De Ieso, E. M. Campbell, H. S. Dorward, J. E. Hardingham and A. J. Yool (2016). "Differential Inhibition of Water and Ion Channel Activities of Mammalian Aquaporin-1 by Two Structurally Related Bacopaside Compounds Derived from the Medicinal Plant Bacopa monnieri." Mol Pharmacol **90**(4): 496-507.

Saparov, S. M., D. Kozono, U. Rothe, P. Agre and P. Pohl (2001). "Water and ion permeation of aquaporin-1 in planar lipid bilayers. Major differences in structural determinants and stoichiometry." J Biol Chem **276**(34): 31515-31520.

Yool, A. J. and E. M. Campbell (2012). "Structure, function and translational relevance of aquaporin dual water and ion channels." Mol Aspects Med **33**(5-6): 553-561.

Yu, J., A. J. Yool, K. Schulten and E. Tajkhorshid (2006). "Mechanism of gating and ion conductivity of a possible tetrameric pore in aquaporin-1." Structure **14**(9): 1411-1423.